

**Gating of water channels (aquaporins) in
plants: effects of osmotic and oxidative stresses
and the role of unstirred layers**

**Inaugural-Dissertation
zur Erlangung des Doktorgrades
der Fakultät Biologie, Chemie und Geowissenschaften
der Universität Bayreuth**

von

Qing Ye

aus Jiangxi, China

Bayreuth, im November 2005

Die vorliegende Arbeit wurde am Lehrstuhl für Pflanzenökologie der Universität Bayreuth unter der Leitung von Prof. Dr. Ernst Steudle durchgeführt und entstand im Zeitraum von September 2001 bis November 2005.

1. Berichterstatter: Prof. Dr. E. Steudle

2. Berichterstatter: Prof. Dr. E. Komor

Tag der Einreichung: 16.11.2005

Tag der mündlichen Prüfung: 01.03.2006

Prüfungsausschuss:

Prof. Dr. K.H. Hoffmann (Vorsitz)

Prof. Dr. E. Steudle

Prof. Dr. E. Komor

Prof. Dr. E. Beck

Prof. Dr. B. Westermann

Vollständiger Abdruck der von der Fakultät für Biologie, Chemie und Geowissenschaften der Universität Bayreuth genehmigten Dissertation zur Erlangung des Grades eines Doktors der Naturwissenschaften (Dr. rer. Nat.).

To my beloved parents, my wife and son
给我亲爱的父母，妻子和儿子

This dissertation is submitted as a “Cumulative Thesis” that covers six (6) publications: four (4) printed articles, and two (2) articles are in press. In order to clarify the publications, they are listed below.

Printed articles:

1. **Ye Q., Wiera B. & Steudle E.** (2004) A cohesion/tension mechanism explains the gating of water channels (aquaporins) in *Chara* internodes by high concentration. **Journal of Experimental Botany** 55, 449–461 (Chapter 2).
2. **Ye Q., Muhr J. & Steudle E.** (2005) A cohesion/tension model for the gating of aquaporins allows estimation of water channel pore volumes in *Chara*. **Plant Cell and Environment** 28, 525–535 (Chapter 3).
3. **Henzler T., Ye Q. & Steudle E.** (2004) Oxidative gating of water channels (aquaporins) in *Chara* by hydroxyl radicals. **Plant Cell and Environment** 27, 1184–1195 (Chapter 4).
4. **Zhao C.X., Deng X.P., Zhang S.Q., Ye Q., Steudle E. & Shan L.** (2005) Advances in the studies on water uptake by plant roots. **Acta Botanica Sinica** 46, 505–514 (Chapter 7).

Articles in press:

5. **Ye Q. & Steudle E.** (2006) Oxidative gating of water channels (aquaporins) in corn roots. **Plant Cell and Environment** (in press, doi: 10.1111/j.1365-3040.2005.01423) (Chapter 5).
6. **Ye Q., Kim Y.M. & Steudle E.** (2006) A quantitative re-examination of the role of unstirred layers (USLs) during the measurement of transport coefficients for water and solutes with the cell pressure probe: minor role of USLs. **Plant Cell and Environment** (in press, manuscript number PC&E 05-417) (Chapter 6).

Declaration of the self-contribution of research articles

This thesis contains five research articles and one review paper. Most of the research work in the thesis was carried out by myself independently at the Department of Plant Ecology, University of Bayreuth, under the supervision of Prof. Dr. Ernst Steudle.

In Chapter 2, most of the research experiments were done by myself in addition to drafting the manuscript. My contribution in this chapter was about 80 %. Mr. Boguslaw Weira from Katowice, Poland, joined some experiments, while mainly focused on learning pressure probe techniques during his stay in the lab as an ERASMUS student.

My contribution in Chapter 3 was about 80 % in that I did most of the research experiments and drafted the manuscript. Mr. Jan Muhr was in the lab during a Praktikum for about one month. After learning pressure probe techniques, he carried out some experimental work and was involved in discussion of the manuscript.

The discovery of hydroxyl radicals (*OH) as a novel inhibitor of aquaporins started by Dr. Tobias Henzler, a former PhD student in the lab. A substantial part of experiments and the draft of the manuscript were done by myself. My contribution to the paper in Chapter 4 was about 50 %.

In Chapter 5, all the research experiments were done by myself in addition to drafting the manuscript. My contribution in this article was about 85 %.

For the paper in Chapter 6, I did most of the experimental work and drafted the manuscript. My contribution in this chapter was about 70 %. Miss Yangmin Kim, currently a PhD student in the lab, joined part of experiments and did substantially contribution to the discussion and draft of the manuscript.

The review paper in Chapter 7 is an outcome of a CSC/DAAD program between Chinese Academic Sciences and University of Bayreuth. As a member of the program, I joined some revision work of the manuscript. My contribution in this article was about 20 %.

All published articles can be downloaded from the worldwide web:
<http://www.homepage.steudle.uni-bayreuth.de>.

Acknowledgements

First of all, I would like to express my deepest gratitude to my supervisor, **Prof. Dr. Ernst Steudle**, Department of Plant Ecology, University of Bayreuth, Germany. Without his perceptiveness, ideas, patience, criticism and ‘cracking-of-the-whip’, I would never have accomplished this thesis. I would never forget those discussions of revising manuscripts usually occurred in ‘Sunday morning’ over years during my study in Bayreuth, from which I benefit a lot. I could not have imagined having a better advisor and mentor for my PhD.

I especially thank **Burkhard Stumpf**, not only for his outstanding technical assistance throughout all my experiments, but also for his innumerable important helps of daily life during my stay in Bayreuth. I will cherish our great friendship forever.

I am grateful to **Prof. Carol Peterson** (University of Waterloo, Canada) for her excellent teaching in plant anatomy and correcting manuscripts during her visit Bayreuth. I would like to thank **Prof. Jack Dainty** (University of Norwich, UK), **Prof. David Clarkson** (University of Bristol, UK), **Prof. Steve Tyerman** (University of Adelaide, Australia) and **Dr. Wieland Fricke** (University of Paisley, UK) for their valuable suggestion and discussion of my experiments.

Thanks go to co-workers Dr. Tobias Henzler, Boguslaw Wiera, Jan Muhr, and Yangmin Kim for their excellent joined experimental work and preparation of manuscripts. Thanks especially go to Hagen Reinhardt for his great help in German translation.

I would like to thank all the lab members and friends especially to Changxing, Chris, Ewa, Kosala, Liying, Lukasz, Marcella, Ola, Seonghee, Suiqi, Thorsten, Yangmin and others, who build up a friendly and relaxed atmosphere during my stay in Bayreuth.

Finally, I am forever indebted to my beloved parents and my wife Lifan for their understanding, support, and encouragement when it was most required.

Content

I	Detailed Summary	1
1	Introduction	3
1.1	Water and solute flows	9
1.1.1	Elastic modulus.....	12
1.1.2	Hydrostatic pressure relaxations.....	13
1.1.3	Osmotic pressure relaxations.....	14
1.1.3.1	Monophasic osmotic pressure relaxation	14
1.1.3.2	Biphasic osmotic pressure relaxations	16
1.2	Composite transport model	18
1.2.1	Composite transport model at the cell level	18
1.2.2	Composite transport model at the tissue (root) level.....	20
1.3	Single file water transport in water channels (aquaporins): p_f/p_d ratios	
	determine the number of water molecules in a pore	22
1.3.1	Bulk flow of water (p_f) across a single-file pore.....	23
1.3.2	Diffusive (isotopic) flow of water (p_d) across a single-file pore.....	24
1.3.3	Restrictions to this procedure.....	27
1.4	Unstirred layers (USLs)	27
1.4.1	Sweep away effect.....	27
1.4.2	Gradient dissipation effect.....	29
1.5	Materials and methods	33
1.5.1	Growth of <i>Chara corallina</i>	33
1.5.2	Growth of corn seedlings	33
1.5.3	Pressure probe for <i>Chara</i> internodes	33
1.5.4	Pressure probe for higher plant cells	34
1.5.5	Pressure probe for roots	35
1.6	Results and Discussions	37
1.6.1	Gating of aquaporins by high concentration –	

a cohesion/tension mechanism.....	37
1.6.2 Estimation of water channel pore volumes in the plasma membrane of <i>Chara corallina</i>	37
1.6.3 Oxidative gating of water channels (aquaporins) in <i>Chara corallina</i>	39
1.6.4 Oxidative gating of water channels (aquaporins) in corn roots	40
1.6.5 Quantitatively re-examining the role of unstirred layers during measurements of transport parameters of water and solute.....	41
1.7 Short Summary.....	42
1.8 Literature cited.....	46
II Publications.....	55
2 A cohesion/tension mechanism explains the gating of water channels (aquaporins) in <i>Chara</i> internodes by high concentration.....	57
3 A cohesion/tension model for the gating of aquaporins allows estimation of water channel pore volumes in <i>Chara</i>.....	91
4 Oxidative gating of water channels (aquaporins) in <i>Chara</i> by hydroxyl radicals.....	123
5 Oxidative gating of water channels (aquaporins) in corn roots.....	153
6 A re-examination of the role of unstirred layers (USLs) during the measurement of transport coefficients of <i>Chara</i> internodes with the cell pressure probe: minor role of USLs.....	185
7 Advances in the studies on water uptake by plant roots.....	229
8 Summary	253
9 Zusammenfassung	259
10 Erklärung.....	265

I

Detailed Summary

1 General introduction

The existence of life is based on the existence of water. Water is not only used in metabolic processes during growth and development of organisms, it also plays a critical role as a solvent and transport vehicle for nutrients and metabolites. Water transport across cell membranes (osmosis) still is a hot research topic as indicated by the delivery of the Nobel prize in chemistry to Peter Agre in 2003 for the discovery of aquaporins (water channels, AQPs) in the early 1990s. Before the discovery of AQPs, water movement across cell membranes has been thought to be *via* simple diffusion through the lipid bilayer (e.g. Lüttge, Kluge & Bauer 2002). However, this could not explain that membrane water permeability of some cells, such as erythrocytes and renal epithelia, is extremely high (Macey 1984). Actually, even earlier than that, scientists started to discuss that pores or channels could exist in biological membranes, and that water may also transport across water-filled pores. The selectivity of these pores has been discussed as well at that time (Koefoed-Johnsen & Ussing 1953; Dainty 1963; House 1974; Stein 1986; Finkelstein 1987).

The discovery of the proteinaceous AQPs started in the late 1980ies. The first AQP gene – CHIP28 of erythrocytes (‘channel forming integral membrane protein’; MW = 28 kDa; now called AQP1) – was cloned by Denker *et al.* (1988). The expression of CHIP28 in *Xenopus* oocytes subsequently enhanced the swelling rate of the cells in hypotonic buffer indicating that CHIP28 facilitated water transport across the membrane. The process was reversibly inhibited by mercurials such as HgCl₂ which is now accepted as a common inhibitor of AQP activity (Preston *et al.* 1992; 1993). γ -TIP from the tonoplast of *Arabidopsis* was the first AQP gene which was identified in plants. It was functionally expressed in *Xenopus* eggs by Maurel *et al.* (1993). Later, AQP activity was also shown for homologues residing in the plant plasma membrane (e.g., Daniels, Mirkov & Chrispeels 1994; Kammerloher *et al.* 1994).

AQPs are membrane proteins that belong to the major intrinsic protein (MIP) family, with members found in nearly all-living organisms (Agre, Bonhivers & Borgnia 1998). AQPs have six membrane-spanning alpha helices with cytoplasmically oriented N- and

C- termini (Fig. 1). The cytosolic loop (loop B) between the second and third trans-membrane domain and the extra-cytosolic loop (loop E) between the fifth and sixth trans-membrane domain form short helices that are relatively hydrophobic and insert into the membrane from opposite sides. These two loops contain highly conserved Asn-Pro-Ala (NPA) motifs and form an aqueous channel at its narrowest, and hence, the selective point (Murata *et al.* 2000). Studies of the transport properties of AQP pores demonstrated that, in accordance with their small internal diameter, AQPs are highly selective for water largely by excluding bigger molecules and charged ions. AQPs just allow the passage of one water molecule after the other in a single file. Actually, MIPs that specifically transport water are named AQPs. To date, 35 MIPs have been identified in plants, which can be classified into four different subfamilies based on their sequence similarity: PIPs (plasma membrane intrinsic proteins); TIPs (tonoplast intrinsic proteins); NIPs (nodulin26-like intrinsic proteins) and SIPs (small basic intrinsic proteins) (Weig, Deswarte & Chrispeels 1997; Chaumont *et al.* 2001; Johanson *et al.* 2001; Javot & Maurel 2002).

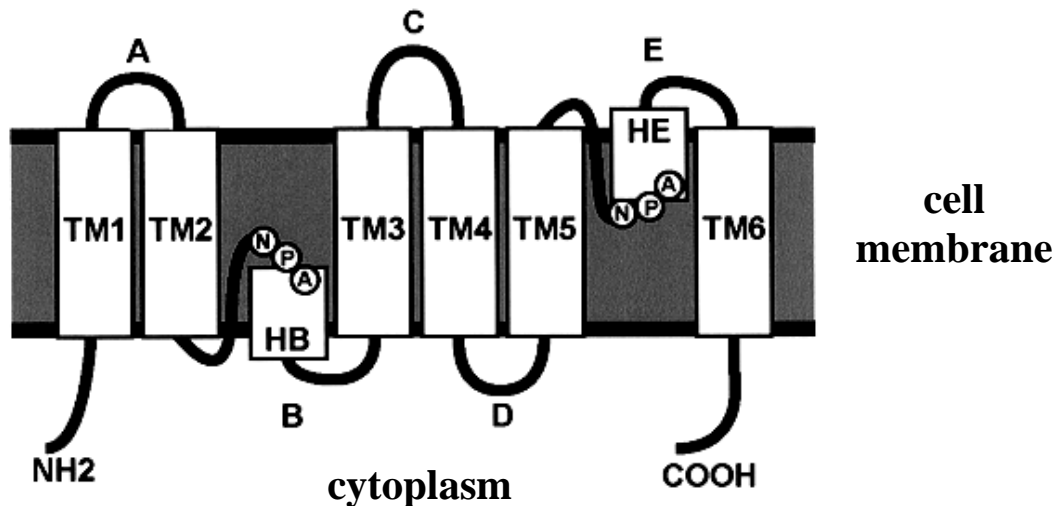


Figure 1. Schematic model of the structure of an AQP showing the principal features of the protein. Alpha helices are represented as rectangles. There are six trans-membrane domains (TM1-TM6) with N and C termini sitting in the cytosol connected by five loops (A-E). Two helical domains (HB and HE) in different loops dip halfway into the membrane from opposite sides and form the ‘single file’ aqueous pore. Loops B and E contain the highly conserved NPA motifs which should be positioned one above the other in the three-dimensional structure (modified after Chaumont *et al.* 2001)

Although water transport across membrane pores has been proposed before (Dainty 1963; House 1974; Finkelstein 1987), the discovery of the molecular structure of AQPs and detailed studies of their function did bring a revolution into investigations of plant water relations, at least where membranes are involved (Steudle & Henzler 1995; Maurel 1997; Kjellbom *et al.* 1999; Tyerman *et al.* 1999; Steudle 2000, 2001; Maurel & Chrispeels 2001; Javot & Maurel 2002; Tyerman, Niemietz & Bramley 2002; Chaumont, Moshelion & Daniels 2005; Luu & Maurel 2005). There is accumulating evidence that AQPs play an important role in plant water relations at the levels of cells, tissues, organs, and whole plants. AQPs facilitate the rapid, passive exchange of water across cell membranes. Most (75% – 95%) of the water permeability of plasma membranes is due to AQP activity (Henzler, Ye & Steudle 2004).

As during the transport of ions across ion channels, the flow of water is always downhill (passive) across AQPs. However, the open/closed state of AQPs may be ‘gated’ in order to regulate water relations. Quite a bit of current research on plant water channels is focusing on this gating of AQPs; i.e. on opening or closing mechanisms which are thought to play a key role in the adaptation of plants to different kinds of factors or stresses and, perhaps, in the cross-linking of events such as between water relations and plant nutrition or oxidative and osmotic stresses (Clarkson *et al.* 2000; Javot & Maurel 2002; Tyerman *et al.* 2002; Pastori & Foyer 2002). Many internal (metabolic) factors or external (environmental) stresses have been found to cause a gating of AQPs (switches between open and closed states) as following:

(i) Metabolic control of AQP activity:

- pH and pCa: both H⁺ and Ca²⁺ contributed to switch membrane AQPs from an active to an inactive state (Gerbeau *et al.* 2002; Tournaire-Roux *et al.* 2003).
- Protein phosphorylation: provided a metabolic control of AQP activity which could be activated by protein phosphorylation (Johannson *et al.* 1996).

(ii) Environmental control of AQP activity:

- Osmotic stress or salinity: cell or root hydraulic conductivity decreased with increasing medium concentration or salinity (Steudle & Tyerman 1983; Azaizeh, Gunse & Steudle 1992).
- Temperature: cell hydraulic conductivity increased as increasing temperature (Hertel & Steudle 1997; Lee, Chung & Steudle 2005 a, b).
- Heavy metals: mercurials (HgCl_2) bind to SH-groups of cysteine residues of AQPs changing the conformation of AQPs. The subsequent closure of AQPs could be recovered by scavengers such as 2-mercaptoethanol (Henzler & Steudle 1995; Tazawa, Asai & Iwasaki 1996; Zhang & Tyerman 1999; Niemietz & Tyerman 2002; Virkki *et al.* 2002).
- Nutrient deprivation: lowered root hydraulic conductivity (Carvajal, Cooke & Clarkson 1996; Clarkson *et al.* 2000).
- Drought: decreased root hydraulic conductivity (Martre, North & Nobel 2001).
- Hypoxia: reduced hydraulic conductivity of cortical cells of wheat roots (Zhang & Tyerman 1999).
- Development of plant: a higher level of cell membrane AQP gene expression in younger (elongating) regions than older (mature) regions (Hukin *et al.* 2002; Eisenbarth & Weig 2005).
- Diurnal rhythm: related to diurnal synthesis and degradation of channel proteins (Henzler *et al.* 1999).
- Mechanical stimuli (energy-input model): big pressure pulses resulted in the input of kinetic energy to the channel constriction (NPA motif of AQPs) which may cause a conformational change of the channel protein (Wan, Steudle & Hartung 2004; Lee *et al.* 2005b).

- Plant stress hormone ABA: had a positive effect on AQP activity to re-open closed channels induced by pressure pulses or low temperature (Freundl, Steudle & Hartung 1998, 2000; Hose, Steudle & Hartung 2000; Wan *et al.* 2004; Lee *et al.* 2005b).

This list may get longer in the future. In most of the examples presented, precise mechanisms by which stresses or other factors actually gate the open/closed states of AQPs are not yet known. Intense research is underway in different labs to clarify mechanisms. Eventually, we may end up with a picture analogous to that available for ion channels (Khakh & Lester 1999).

The studies referred to in this dissertation focused on two new gating mechanisms of AQPs in plants by different stresses.

- One is called ‘**cohesion/tension (C/T) mechanism**’ for the gating of AQPs at high external concentration/salinity. Internodes of *Chara corallina*, have been used in these studies to work out the concentration dependence of cell hydraulic conductivity (L_p) during osmotic stress (Ye, Wiera & Steudle 2004). A cohesion/tension model has been developed which explains the osmotic dehydration of AQPs. The model proposes an exponential decrease of the cell membrane permeability to water (hydraulic conductivity; the cell L_p) with increasing osmolyte concentration. Pore volumes of AQPs (V_c) in the plasma membrane of *Chara* internodes have been estimated from the ‘dehydration curves’ (Ye, Muhr & Steudle 2005). Alternatively, pore volumes were estimated from ratios between osmotic ($P_f = L_p \cdot RT / \bar{V}_w$) and diffusional (P_d) water flow. P_f/P_d ratios should represent the number of water molecules (N) in a single-file water channel pore (Levitt 1974), which refers to the pore volume. Since P_d could have been underestimated due to effects of unstirred layers (USLs), which in turn, affect calculations of the N values and pore volumes, a quantitative re-examination of the role of USLs during measurements of transport parameters of water and solutes has been performed with internodal cells of *Chara corallina* (Ye, Kim & Steudle 2006).
- The other mechanism studied the ‘**oxidative gating**’ of AQPs which was first found in experiments with *Chara corallina* (Henzler, Ye & Steudle 2004). Besides the *Chara* system, this mechanism was also tested in a higher plant in experiments with roots of young corn seedlings (Ye & Steudle 2006). Oxidative gating caused a dramatic decrease of AQP activity both in *Chara* and root cells. Cell L_p reversibly decreased by a factor of 10 or more in the presence of reactive oxygen species (ROS) members. Hydroxyl radicals (*OH) appeared to be the most effective inhibitor of AQPs. Inhibition recovered after removal of ROS from the medium. Oxidative gating of AQP in the presence of ROS may indicate an interaction between the redox status (oxidative stress) and water relations (water stress) in plants.

1.1 Water and solute flows

Water and solute transport processes ('flows') across cell membranes or more complex barriers separating different compartments such as internal and external environment of a cell are particular irreversible processes (Kedem & Katchalsky 1958; 1963 a, b). The study of water and solute flows using pressure probe techniques has a theoretical background, which is derived from principles of irreversible thermodynamics, sometimes referred to as the "KK theory". In general terms, this theory considers flows (J_i) which are driven by certain forces (X_i), and the entropy production in the system (sum of $J_i \times X_i$). If the system is operating close to thermodynamic equilibrium, relationships between flows and forces are usually linear, i.e., flow = conductance \times force holds. For an ideal osmometer, it holds for the water (volume) flow (J_v in $\text{m}^3 \cdot \text{m}^{-2} \cdot \text{s}^{-1}$) that

$$J_v = L_p \cdot \Delta\Psi, \quad (1)$$

where L_p is the hydraulic conductivity (in $\text{m} \cdot \text{s}^{-1} \cdot \text{MPa}^{-1}$); $\Delta\Psi$ (in MPa) is the difference of water potential in both sides of the membrane or barrier which is the driving force of J_v . In the presence of just a passive, diffusional solute flow (J_s in $\text{mol} \cdot \text{m}^{-2} \cdot \text{s}^{-1}$), we have:

$$J_s = P_s \cdot \Delta C_s, \quad (2)$$

where P_s ($\text{m} \cdot \text{s}^{-1}$) is the permeability coefficient and ΔC_s the concentration difference which is the driving force of J_s . However, Eqns (1) and (2) are not complete because they neglect interactions or couplings between flows, which are more realistic and provided by the theory. For example, when water and solutes move through pores (such as water channels), they may interact with each other.

The KK theory provides a correct and complete quantitative description of transports across a membrane (barrier). For the sake of simplicity, the theory is applied here to a single cell in a medium to work out cell water relations and interactions between water and solute flows. If (i) the cell interior (superscript 'i') and the medium (superscript 'o') are treated as a two-compartment system; (ii) only the water (volume) flow (J_v) and the flow of a single solute (J_s) are considered; (iii) flows out of the cell are defined as positive and flows in to the cell as negative, we get for the flows (Steudle 1993):

$$J_v = -\frac{1}{A} \cdot \frac{dV}{dt} = \underbrace{Lp \cdot P}_{\text{hydraulic flow}} - \underbrace{Lp \cdot [\sigma_s \cdot RT(C_s^i - C_s^o)]}_{\text{osmotic flow}}, \quad (3)$$

and

$$J_s = -\frac{1}{A} \cdot \frac{dn_s^i}{dt} = \underbrace{P_s(C_s^i - C_s^o)}_{\text{diffusion flow}} + \underbrace{(1 - \sigma_s) \cdot \overline{C}_s \cdot J_v}_{\text{solvent drag}} + \underbrace{J_s^*}_{\text{active transport}}, \quad (4)$$

respectively. Here, J_v [$\text{m} \cdot \text{s}^{-1}$] water (volume) flow

V [m^3] cell volume

A [m^2] cell surface area

t [s] time

Lp [$\text{m} \cdot (\text{s} \cdot \text{MPa})^{-1}$] hydraulic conductivity

P [MPa] hydrostatic pressure (turgor) of the cell as referred the reference of atmospheric pressure

σ_s [1] reflection coefficient

R [$\text{J} \cdot (\text{mol} \cdot \text{K})^{-1}$] gas constant (≈ 8.314)

T [K] absolute temperature

C_s [$\text{mol} \cdot \text{m}^{-3}$] osmotic concentration

J_s [$\text{mol} \cdot \text{m}^{-2} \cdot \text{s}^{-1}$] solute flow

n [mol] number of molecule in mol

P_s [$\text{m} \cdot \text{s}^{-1}$] permeability coefficient

\overline{C}_s [$\text{mol} \cdot \text{m}^{-3}$] mean concentration in both sides of the membrane

J_s^* [$\text{mol} \cdot \text{m}^{-2} \cdot \text{s}^{-1}$] active transport flow

In Eqn (3), volume flow J_v is shown as a change of cell volume with time, which is referred to unit area of cell surface (A). Hence, J_v has the dimensions of a velocity and denotes the speed by which water molecules pass the membrane. The water (volume) flow has two components: (i) a hydraulic flow ($Lp \cdot P$) driven by the hydrostatic pressure gradient, Lp is the hydraulic conductivity of the cell membrane; and (ii) an osmotic water flow driven by the difference in osmotic pressure ($Lp \cdot \sigma_s \cdot \Delta\pi_s$; $\Delta\pi_s = RT \cdot (C_s^i - C_s^o)$, van't Hoff's law). The osmotic term is modified by another coefficient, the

reflection coefficient σ_s . The physiological meaning of σ_s is that of ‘passive selectivity’ of the membrane for a given solute. It is evident that σ_s is a quantitative measure of the deviation of the osmotic cell from being ideally semipermeable. It denotes the interaction between water and solutes as they cross the membrane. In the case of an ideal osmometer which has a semipermeable membrane, just the solvent (water), but no solute can pass through ($P_s = 0$; $\sigma_s = 1$). In this case, the osmotic force driving the water will be identical with the water potential difference, i.e. $\Delta\Psi = -\Delta\pi_s = -RT \cdot (C_s^i - C_s^o)$:

$$J_v = -\frac{1}{A} \cdot \frac{dV}{dt} = Lp \cdot P - Lp \cdot RT(C_s^i - C_s^o) = Lp \cdot \Delta\Psi, \quad (5)$$

which is identical with Eqn (1). On the other hand, when $\sigma_s = 0$, the membrane does not distinguish between the solute and water; both pass at the same rate. The reflection coefficient can also be interpreted as a measurement of the interaction between solute and water molecules as they cross the membrane (see above). Usually, σ_s ranges between zero and unity. For most of the solutes naturally present in the cell sap of plant cells (ions, sugars, metabolites etc.), reflection coefficients will be close to unity. There are also exotic cases, when $\sigma_s < 0$. This phenomenon that can be observed in plant cells is called anomalous or negative osmosis. As shown in this thesis, anomalous osmosis takes place during the closure of water channels, when rapidly permeating solutes move across the membrane at a rate which is higher than that of the water (Steudle & Henzler 1995; Henzler, Ye & Steudle 2004; Ye & Steudle 2005).

Eqn (4) contains three different components of the solute flow (J_s). A diffusional component, $P_s \cdot (C_s^i - C_s^o)$, relates concentration gradients to the flow according to Fick’s first law of diffusion by the permeability coefficient, P_s . The second term is called ‘solvent drag’. It quantifies the interaction between solute and water as they cross the membrane, or the amount of solute dragged along with the water flow, e.g. in membrane pore such as AQPs. This term is zero, when the solutes are completely excluded from the membrane and $\sigma_s = 1$. The last term on the right side (J_s^*) is the active component of the solute flow. It represents the interaction of solute flow with metabolic reaction, like splitting of ATP into the ATPase. This component is usually neglected during solute flow, but determines the absolute level of cell turgor which, for example, refers to the active pumping of ions (Steudle 2001; Gaxiola *et al.* 2001). There

is no equivalent for a primary active pumping of water in Eqn (4), because there is no evidence for such a direct coupling between water flow and the degradation metabolic energy (i.e., for an ATP-driven water pump; Steudle 2001). The existence H₂O-ATPases is highly unlikely, because such water pumps would be short-circuited by the high water permeability (L_p) of cell membranes.

1.1.1 Elastic modulus

The elastic modulus (ε) is an important physiological parameter that relates volume and pressure of the cell. It characterizes elastic properties of the cell wall, i.e. its mechanical rigidity. The definition of ε is the change in cell turgor (dP) caused by a given change of the relative cell volume (dV/V):

$$\varepsilon = V \frac{dP}{dV} \approx V \frac{\Delta P}{\Delta V}. \quad (6)$$

High values of elastic moduli refer to a low extensibility or a rigid cell wall, i.e., big changes in pressure cause small changes of cell volume. Low values of ε , on the other hand, mean a highly extensible cell wall. Different from plastic (viscous) properties of the walls, elastic properties refer to reversible changes in cell volume, which are typical for mature cells. The plastic (viscous) properties, on the other hand, dominate extension growth (Cosgrove 1998; Fricke 2002). The elastic modulus can be directly measured with the aid of a pressure probe by producing defined changes in cell volume (ΔV) and measuring the responses in cell turgor. According to Eqn (6), the elastic modulus has the dimensions of a pressure and is usually given in MPa. In Eqns (9) and (11), ε relates the volume of the cell (or of changes thereof) to the cell turgor pressure. Hence, it allows to work out the cell hydraulic conductivity, L_p (the osmotic water permeability P_f) from P(t) curves. Typically, L_p is worked out from the ‘half time of pressure relaxations’.

1.1.2 Hydrostatic pressure relaxations

In hydrostatic experiments, cell turgor pressure is rapidly increased or decreased in response to an imposed change in cell volume with the aid of a pressure probe (Fig. 2). The difference in turgor pressure, ΔP , causes water flow out of or into the cell.

When cell turgor pressure is ‘relaxing’ back in such an experiment to a value close to the original, the resulting exponential $P(t)$ curve is called ‘relaxation’:

$$P(t) = P_E + (P_A - P_E) \cdot \exp(-k_w \cdot t). \quad (7)$$

Here, P_0 is the original value of turgor pressure (P); P_A is the maximum value of P ; P_E is the end value of P ; k_w is the rate constant of the water flow process, which is the inverse of time constant (τ) of the process:

$$k_w = \frac{1}{\tau}. \quad (8)$$

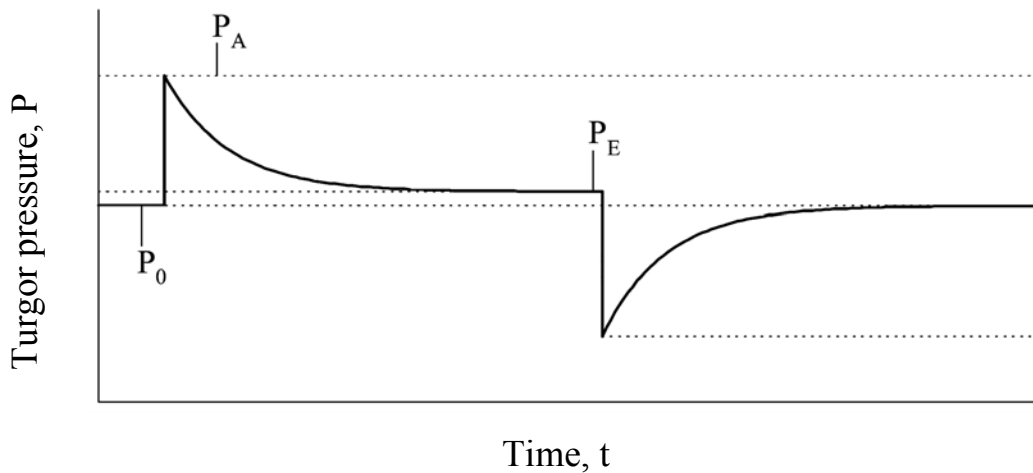


Figure 2. Schematic graph of ex- and endosmotic hydrostatic pressure relaxations. When the turgor pressure (P) is increased from P_0 to P_A , water flows out, P exponentially relaxes back to P_E which may slightly differ from P_0 due to small changes in osmotic concentration of the cell sap.

Time constant for water flow (τ) is the time required for 63 % ($1/e$) of the change in turgor pressure from the maximum (or minimum) value (P_A) to the end value (P_E). It is given by the product of the resistance of water permeability and the cell capacitance:

$$\tau = \frac{1}{Lp} \cdot \frac{V}{A \cdot (\varepsilon + \pi^i)}. \quad (9)$$

Here, $Lp \cdot A$ is the hydraulic conductance (inverse of a hydraulic resistance) and $V \cdot (\varepsilon + \pi^i)$ the storage capacity of a cell for water; π^i = osmotic pressure of cell sap. Usually, half time ($T_{1/2}^w$) rather than time constant is given, which refer to the time required for half (50 %) of a change in turgor or volume from P_A to P_E , i.e., to $[(P_A - P_E)/2]$. Half time $T_{1/2}^w$ is related to time constants by:

$$T_{1/2}^w = \tau \cdot \ln(2). \quad (10)$$

By combining Eqns (7) to (10), we get the equation for calculating hydraulic conductivity (Lp) which is usually given in units of $m \cdot s^{-1} \cdot MPa^{-1}$:

$$Lp = \frac{V}{A} \cdot \frac{\ln(2)}{T_{1/2}^w (\varepsilon + \pi^i)}. \quad (11)$$

This equation is used to work out Lp from hydrostatic relaxations of turgor by measuring $T_{1/2}^w$ and determining cell shape dimensions (V and A) such as for a cylindrical internode of *Chara* or of cortical cells of corn roots (see Chapters 2 and 5). The osmotic pressure of the cell (π^i) is estimated from the steady-state cell turgor (P_o) and from the π^o of the medium by $P_o = \pi^i - \pi^o$.

1.1.3 Osmotic pressure relaxations

1.1.3.1 Monophasic osmotic pressure relaxation in the absence of a solute flow ($J_s = 0$).

In osmotic experiments, the concentration of the medium is changed by addition or removal of solutes to induce water flows. In the absence of a solute flow ($P_s = 0$ and $\sigma_s = 1$), the response is monophasic. Theory shows that the half time of the osmotic response (k_w) should be the same as during the hydrostatically induced water flows. A typical response curve can be seen in Fig. 3.

The basic theory (see section 1.1) shows that in the absence of solute flow, changes in turgor will be given by:

$$-\frac{dP}{dt} = \frac{Lp \cdot A \cdot (\varepsilon + \pi_0^i)}{V} \left[P - P_0 + \left(\frac{\varepsilon}{\varepsilon + \pi_0^i} \right) \cdot \Delta\pi_{imp}^o \right] = k_w \cdot (P - P_E). \quad (12)$$

Here $\Delta\pi_{imp}^o$ is external change in osmotic pressure which provides the force driving the process. The coefficient in front of the brackets on the right side of Eqn (12) is the rate constant of water exchange (k_w , see Eqn (8)). The term $[\varepsilon/(\varepsilon + \pi_0^i)]$ denotes for changes in concentration in the cell during shrinking or swelling. As $\varepsilon \gg \pi^i$ holds, this term is close to unity.

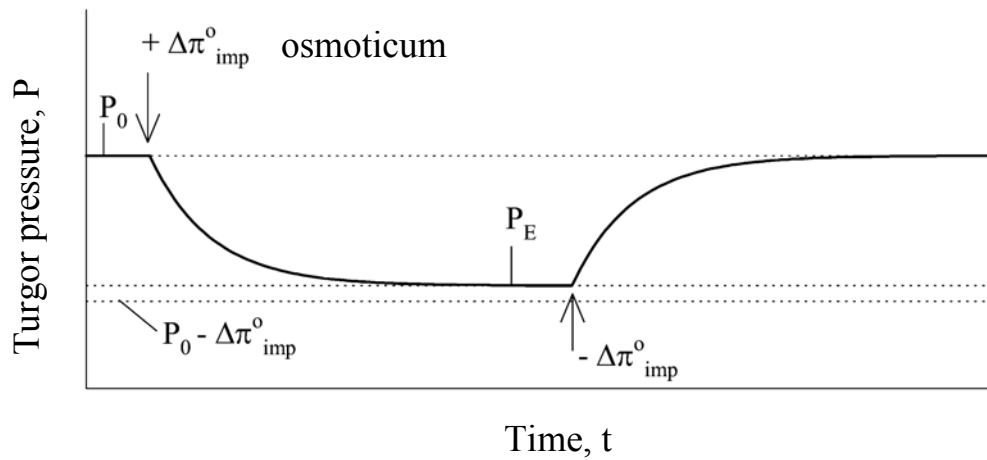


Figure 3. Schematic graph of monophasic osmotic pressure relaxations. There is only the water transport in the presence changes of osmotic pressure of the medium, when a non-permeating solute is added to or removed from the medium. Pressure changes are symmetric in both cases and half times of responses are the same as during hydrostatic relaxations (Fig. 2).

Overall, the changes in turgor ($P_0 - P_E$) in response to changes of osmotic concentration at equilibrium are given by:

$$P_E = P_0 - \left(\frac{\varepsilon}{\varepsilon + \pi_0^i} \right) \cdot \Delta\pi_{imp}^o. \quad (13)$$

This means that changes in turgor should exactly be identical with those in osmotic pressure.

1.1.3.2 Biphasic osmotic pressure relaxations in the presence of a permeating solute ($J_s \neq 0$; $\sigma_s < 1$; Steudle & Tyerman 1983)

This case was met in many experiments in this thesis, for example, when testing effects of high concentration on the open/closed state of AQPs.

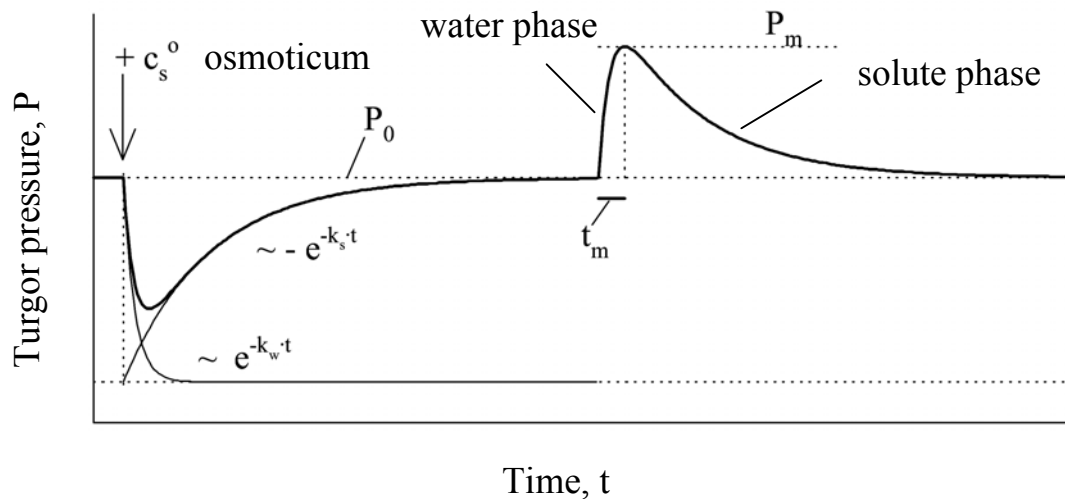


Figure 4. Schematic graph of biphasic osmotic pressure relaxations. When a permeating solute is added to the medium, water is sucked out in response to difference in osmotic concentration and turgor pressure decreases. This is called water phase. In solute phase, turgor pressure increases back to the original value, because water follows the solute resulting in a new equilibrium on both sides of the membrane. Removal of the solute causes a symmetric change in pressure, but in another direction.

In the presence of permeating solutes, osmotic response curves are biphasic as can be seen in Fig. 4. There is a first rapid phase during which turgor pressure rapidly decreases or increases due to an exosmotic/endosmotic water flow. The ‘water phase’ is rapid because of the high permeability of the cell membrane to water. It is followed by a ‘solute phase’. The second phase is due to the permeation of water into or out of the cell tending to equilibrate the concentration gradient across the cell membrane, turgor subsequently increases or decreases as the osmotic gradient changes. Eventually, equilibrium is attained, when the concentration within the cell and in the medium is the same. It should be noted that, what is seen during a pressure probe experiment, are water movements rather than solute movements. However, the latter cause the water flow and, therefore, the rate constant ($k_s \propto P_s$) just depends on the solute (P_s) rather than

on the water permeability (L_p). Rates of solute phases strongly depend on the nature of solutes used. Solute which are soluble in the lipid phase of the membrane cause short half times ($T_{1/2}^s$); those which are polar (ions, hydrophilic solutes), have long half times (Henzler & Steudle 1995; Hertel & Steudle 1997).

The solute permeability (P_s) is obtained from the rate/time constant of the solute phase (k_s ; τ_s):

$$k_s = \frac{\ln(2)}{T_{1/2}^s} = P_s \cdot \frac{A}{V} \quad \Rightarrow \quad P_s = \frac{V \cdot \ln(2)}{A \cdot T_{1/2}^s}. \quad (14)$$

Here, $T_{1/2}^s$ is the half time of the solute phase; permeability coefficient (P_s) of the solute is determined by measuring k_s and the geometry of the cell (volume, V ; surface area, A). P_s has unit of $\text{m} \cdot \text{s}^{-1}$. It is a measure of the speed by which solutes move across the membrane.

In the presence of a permeating solute added to the medium at $t = 0$, the $P(t)$ or $V(t)$ curves are calculated according to the Steudle/Tyerman theory (Steudle & Tyerman 1983; see also: Steudle & Henzler 1995; Ye & Steudle 2005):

$$\frac{V(t) - V_0}{V_0} = \frac{P(t) - P_0}{\varepsilon} = \frac{\sigma_s \cdot \Delta\pi_s^o \cdot Lp}{(\varepsilon + \pi^i)Lp - P_s} [\exp(-k_w \cdot t) - \exp(-k_s \cdot t)]. \quad (15)$$

Eqn (15) describes a biphasic pressure response as schematically depicted in Fig. 4. When the osmotic solute is added, there is a rapid decrease in turgor (volume) due to a rapid water efflux (mainly determined by the first term in the brackets on the right side of Eqn (15)). Then, water is again taken up because of the equilibration of permeating solutes across the membrane (solute phase; see above). The theory assumes that both the internal and the external compartments are stirred, i.e., USLs can be either excluded or incorporated into k_w (L_p) or k_s (P_s) (see Ye *et al.* 2005). The other assumption is that the permeability of the tonoplast for both water and solute is much bigger than that of the plasma membrane (Kiyosawa & Tazawa 1977; Maurel *et al.* 1997; Ye *et al.* 2005).

The reflection coefficient (σ_s) is obtained from biphasic response curves at $J_v = 0$, i.e., by considering the minima or maxima of pressure in Fig. 4 (Steudle & Tyerman 1983).

However, it has to be noted that there is some solute flow during the first (water) phase.

We have:

$$\sigma_s = \frac{P_0 - P_{\min(\max)}}{\Delta\pi_s^o} \cdot \frac{\varepsilon + \pi^i}{\varepsilon} \cdot \exp(k_s \cdot t_{\min(\max)}). \quad (16)$$

The second term on the right side corrects σ_s for shrinking or swelling of the cell during osmotic process (see Eqn 12). The third exponential term corrects the uptake of solute during the time ($t_{\min(\max)}$) required to reach the minimum or maximum value of the pressure in the first (water) phase.

It should be noted that the Steudle/Tyerman theory neglects the drag of solutes by the water flow (middle term on the right side of Eqn 4). However, it has been readily shown by numerical simulation that effects of solvent drag are usually small even in the presence of rapidly permeating solutes with a small σ_s (Steudle & Brinckmann 1989).

1.2 Composite transport model

1.2.1 Composite transport model at the cell level

Usually, the transport properties of membranes are described assuming a homogenous membrane structure. Homogeneity has been also assumed in Eqns (7) to (16). However, a closer look to the transport pattern shows that it is more realistic to treat membrane as composite structures. This takes into account that there are arrays in the membrane which would allow the passage of water (such as AQPs) and other which would allow a preferred passage of solutes such as special solute transporters or the bilayer. In the simplest case, we may treat the cell membrane being composite of two arrays to describe water and solutes trans-membrane movement: water channels (aquaporins) array (superscript ‘a’) and lipid bilayer array or the rest of the membrane (superscript ‘b’). The latter array would largely allow the passage of solutes. According to the KK theory, transport properties of both arrays may be characterized by different sets of transport coefficients (Lp^a, P_s^a, σ_s^a and Lp^b, P_s^b, σ_s^b).

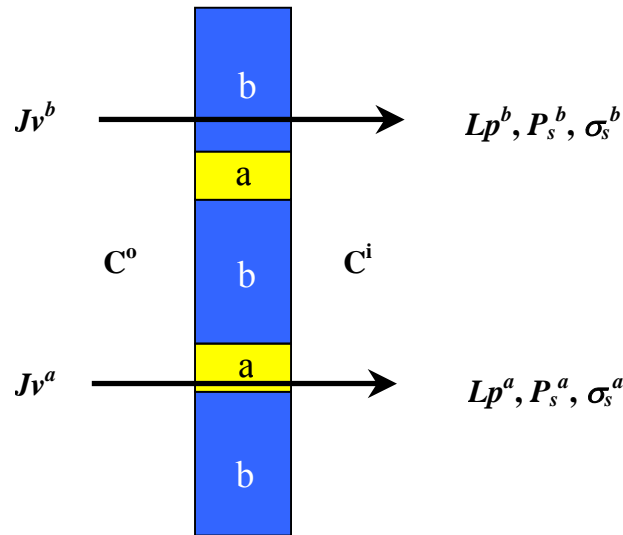
In such a system, the overall volume (water) flow is then given by:

$$J_v = \gamma^a \cdot J_v^a + \gamma^b \cdot J_v^b. \quad (17)$$

Here, γ^a and γ^b represent the fractional area of both arrays, which separated form the overall area (A) of membrane ($\gamma^a = A^a/A$; $\gamma^b = A^b/A$; $\gamma^a + \gamma^b = 1$). $\gamma^a \cdot Lp^a$ and $\gamma^b \cdot Lp^b$ are the hydraulic conductances of the two arrays (referred to unit area). They are arranged in parallel, and it holds that:

$$Lp = \gamma^a Lp^a + \gamma^b Lp^b. \quad (18)$$

This means that the elements of composite membrane will contribute to the overall Lp according to their hydraulic conductance.



a: aquaporin arrays

b: lipid bilayer or the rest of the membrane

Figure 5. Schematic graph of a composite membrane model, where two arrays are arranged in parallel according to the KK theory (Kedem & Katchalsky 1963a): water channels (aquaporins) array (a) and lipid bilayer or the rest of the membrane array (b). Transport properties of arrays are characterized by two different sets of transport coefficients (for detailed explanation see text).

The overall reflection coefficient (σ_s) is expressed in terms of a weighted mean of the two different arrays (water channel array, ' σ_s^a ', and the rest of the membrane, ' σ_s^b '). According to basic irreversible thermodynamics (Kedem & Katchalsky 1963a; House 1974), the overall σ_s is given by:

$$\sigma_s = \frac{\gamma^a Lp^a}{Lp} \sigma_s^a + \frac{\gamma^b Lp^b}{Lp} \sigma_s^b. \quad (19)$$

The overall solute permeability (P_s) will be larger than expected from the contribution of the arrays to the absolute surface area. The difference is due to a solvent drag effect, as expressed the last term on the right side of the equation:

$$P_s = \gamma^a P_s^a + \gamma^b P_s^b + (\sigma_s^a - \sigma_s^b)^2 \cdot RT \frac{Lp^a \cdot Lp^b}{Lp} \cdot \overline{C_s}. \quad (20)$$

Here, $\overline{C_s}$ is the mean concentration of solute in the membrane ($\approx (C_s^i - C_s^o)/2$). It can be seen from Eqn (20) that the solvent drag will vanish, if reflection coefficients of the two paths are equal, or one of arrays is blocked for water flow, i.e., when either $Lp^a = 0$ or $Lp^b = 0$.

There is also a composite transport when two different membranes are arranged in series (Kedem & Katchalsky 1963b; House 1974). Plant cells contain a double-membrane system, i.e., the plasma membrane and the tonoplast (vacuolar membrane), which is in principle, a series composite structure for the transport of water and solute. It has been shown, however, in the literature that the permeability of tonoplast is far higher than that of the plasma membrane, i.e., by a factor of two orders of magnitude (see above; Maurel *et al.* 1997; Niemietz & Tyerman 1997).

1.2.2 Composite transport model at the tissue (root) level

In principal, the concept of composite transport should also apply to plant tissue. It should be most relevant to roots (Steudle 2000; 2001). In the root (as in other tissue), there are three different pathways for radial water flow. The first is the apoplastic path around protoplasts, which including cell walls, intercellular spaces and the lumens of tracheary elements of xylem. The second is the symplastic path, which transport water and solutes across plasmodesmata within the cytoplasmic continuum (excluding the vacuoles). The third is the transcellular or vacuolar path in which water moves from one cell to the next across membranes. Due to the high permeability of membranes to water, the latter route is special for water. Experimentally, symplastic and transcellular components of water flow cannot yet be separated. Therefore, they are summarized as a cell-to-cell or protoplasmic pathway (Fig. 6). There could be, of course, combinations of

pathways in that water may travel within the symplast for some distance and may then cross the plasma membrane and move within the cell walls. In the root, the Casparian bands of the endo- and exodermis should more or less interrupt the apoplastic passage. According to the basic principles outlined above for the membrane, this should have been remarkable effect on the overall transport coefficients of roots (L_{pr} , P_{sr} , σ_{sr}), as measured with root pressure probes (Steudle & Frensch 1989; Steudle & Peterson 1998; Ye & Steudle 2005).

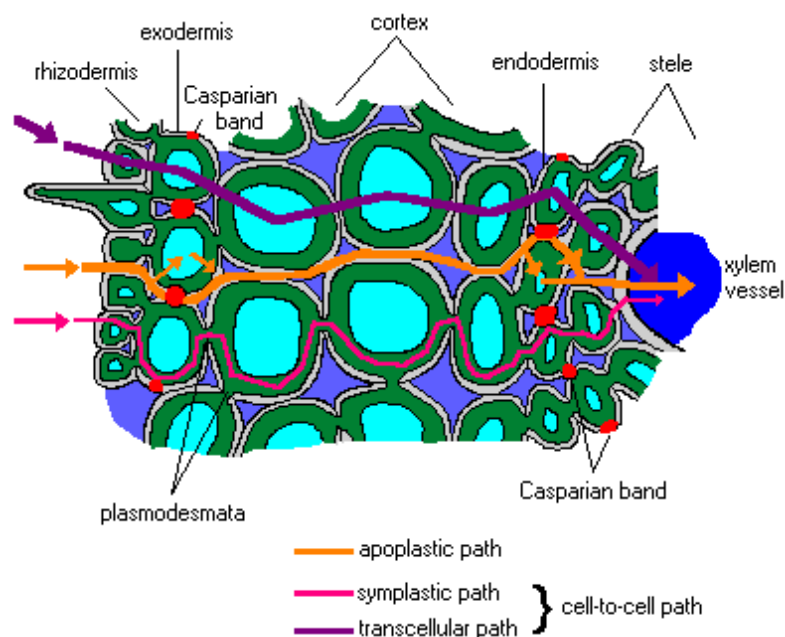


Figure 6. Composite transport model in tissue (root). Three pathways for the movement of water and solutes are indicated. The apoplast provides a porous path to water, solutes and even for nutrient ions, but may be interrupted by Casparian bands in the endo- and exo-dermis. The symplastic path is through plasmodesmata and the cytosol of cells. For the transcellular path, water and solutes have to cross many membranes (two for each cell layer). Since the symplastic and transcellular pathways cannot be separated experimentally, they are summarized as a cell-to-cell path (for detailed explanation see text).

Water flow across the root cortex should be largely apoplastic. This changes at the endodermis because of the Casparian band, which interrupts the apoplastic path. There is a protoplasmic transport step at the endodermis, which is thought to be the rate-limit of water transport across roots. In the stele, the situation is similar to that in the cortex. However, the relative contribution of pathways to overall water uptake or root hydraulic

conductivity may be highly variable depending on the conditions, namely the development of apoplastic barriers, which depends on growth conditions (Steudle & Peterson 1998). This has been explained by establishing a composite transport model according to the root structure (Steudle & Frensch 1989; Steudle 2000). The model shows that the different pathways may be used with different intensity, which results in the plasticity of water uptake as observed. Besides the intensity of water flow, the physical nature of driving forces is important. In the presence of hydrostatic pressure gradients, water flow is largely around protoplasts (apoplastic) because this path represents a low hydraulic resistance. Steudle & Peterson (1998) showed that there should also be some apoplastic flow across the endodermis, i.e., Casparian bands appear to be somehow permeable to water too. Ranathunge, Steudle & Lafitte (2005) provide experimental evidence for some permeability of Casparian bands even for ions in roots of rice and corn. The existence of a permeability of Casparian bands to water may result in a high overall hydraulic conductivity of the root (root L_{p_r}). On the other hand, water flow in the presence of osmotic gradients is rather low as observed in the absence of transpiration (for instance during draught condition or at night) and during phenomena such as root exudation. Osmotic driving forces only cause a water movement in the presence of membranes. Provided that osmotic gradients applied do not create hydrostatic forces within the root, an osmotic water flow across the root has to pass many layers of membranes which results in a low overall root L_{p_r} (Zimmerman & Steudle 1998). The composite transport provides some kind of ‘coarse’ regulation of water flow across root, which is a consequence of the composite root structure. The composite transport model readily explains the variability of root hydraulic properties in terms of changes in driving forces which cause a switching between the pathways used.

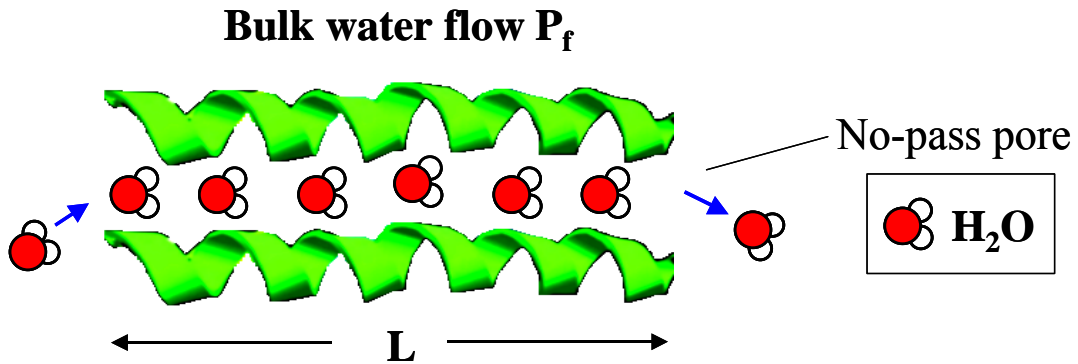
1.3 Single file water transport in water channels (aquaporins): p_f/p_d ratios determine the number of water molecules (N) in a pore

In this section, we consider water flows across individual pores such as AQPs, in which flow is only in a single file. This means that water (and solute) molecules cannot pass each other while moving through (‘no-pass pore’). We consider both a bulk flow of

water, which is either driven by a hydrostatic or by an osmotic pressure difference, and a diffusional water flow in the absence pressure gradients. The latter type transport can be only measured using isotopic water, i.e., heavy or tritiated water. The approach is based on Levitt's (1974) basic paper, who adopted the famous theory of diffusion developed in Einstein's PhD thesis (1906) just one hundred years ago (Einstein 1905). P_f/P_d ratios play an important role in research on the transport properties of AQPs (e.g. Finkelstein 1987; Henzler & Steudle 1995; Mathai *et al.* 1996; Hertel & Steudle 1997; Niemietz & Tyerman 1997; Zhu, Tajkhorshid & Schulten 2004).

1.3.1 Bulk flow of water (p_f) across a single-file pore

We consider a single-file or no-pass pore of a length of L in which N water molecules are aligned. For the derivation of the bulk (osmotic) permeability coefficient of the pore (p_f) we use an osmotic gradient ($\Delta\pi_s$) in the following.



When N water molecules cross the membrane, the volume work, W_V , done during this process is:

$$W_V = \overline{V}_w \cdot N \cdot \Delta\pi_s. \quad (21)$$

Here $\overline{V}_w = V_w / N_L =$ volume of an individual water molecule ($N_L =$ Avogadro's (Loschmidt) number). Since work is force multiplied by length, we also have:

$$W_V = F_{\Delta\pi} \cdot L. \quad (22)$$

Hence, we have for the osmotic force acting across the pore:

$$F_{\Delta\pi} = \frac{\overline{V}_W \cdot N \cdot \Delta\pi_s}{L} = \frac{\overline{V}_W \cdot N \cdot kT \cdot \Delta n_s}{L} \left[\frac{\text{Newton}}{\text{pore}} \right]. \quad (23)$$

Here, Δn_s is the concentration difference in molecules of solute per unit volume ($kT \cdot \Delta n_s = RT \cdot \Delta C_s$). When the water molecules in the pore move at a certain steady, v , this causes a frictional drag, F_{drag} , also in Newton per pore. The velocity is related to F_{drag} by the frictional coefficient of the pore, γ :

$$F_{\text{drag}} = -\gamma \cdot N \cdot v. \quad (24)$$

At steady flow, $F_{\Delta\pi} = -F_{\text{drag}}$ holds. By combining Eqns (23) and (24), we obtain for the velocity:

$$v = \frac{\overline{v}_W \cdot kT \cdot \Delta n_s}{L \cdot \gamma}. \quad (25)$$

The osmotic water flow, Φ_w , in molecules of water per second & pore can be then written as:

$$\Phi_w = \frac{N \cdot v}{L} = \frac{-\overline{v}_W \cdot kT \cdot N}{\gamma \cdot L^2} \cdot \Delta n_s. \quad (26)$$

By definition, we have then for the bulk flow across a single pore:

$$\Phi_w = -p_f \cdot \Delta n_s. \quad (27)$$

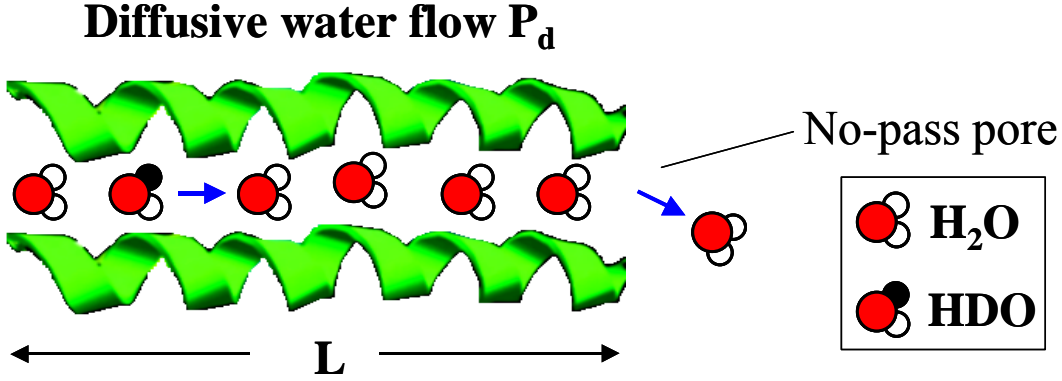
Hence, we arrive at an expression for the osmotic permeability of a single pore of:

$$p_f = \frac{\overline{v}_W \cdot kT \cdot N}{\gamma \cdot L^2} = \frac{\overline{v}_W \cdot D_w \cdot N}{L^2}. \quad (28)$$

According to the Einstein/Stokes relationship, kT/γ represents the diffusion coefficient of water within the pore (D_w). It can be seen that p_f is proportional to the diffusive mobility of water and the number of molecules in a pore. It is inversely proportional to the square of pore length.

1.3.2 Diffusive (isotopic) flow of water (p_d) across a single-file pore

We consider the same single-file pore as above, except that it now contains a tracer molecule (e.g., heavy water) besides the normal water. First, we consider the force acting on that tracer molecule as it moves down a gradient in tracer concentration set up across the membrane.



As during bulk flow, a tracer molecule moving across the pore at a steady velocity of ' v ' will experience a frictional force, F . Analogous to Eqn (24), we have:

$$F = N \cdot \gamma \cdot v. \quad (29)$$

The tracer flux as related to friction would be:

$$\vec{\Phi}^* = \frac{N^* \cdot v}{L} = \frac{N^* \cdot F}{N \cdot \gamma \cdot L}. \quad (30)$$

N^* denotes the mean number of tracer molecules in the pore. If there is no force counteracting the downhill diffusion of tracer, there will be a steady diffusive flux of tracer from the concentrated to the less concentrated solution across the membrane given by:

$$\Phi^* = -p_d \cdot \Delta n_s^*, \quad (31)$$

where p_d is the diffusional permeability coefficient of the pore for water. Δn_s^* denotes the difference in concentration of tracer between the left and right compartments separated by the membrane ($\Delta n_s^* = n_l^* - n_r^*$). At equilibrium, it should hold that:

$$\Phi^* = -\vec{\Phi}^*, \quad (32)$$

therefore,

$$p_d \cdot \Delta n^* = \frac{N^* \cdot F}{N \cdot \gamma \cdot L}. \quad (33)$$

In the experimental situation, the differences in tracer concentration refer to differences in free energy. At equilibrium, the ratio of n_l^*/n_r^* must satisfy the Boltzmann distribution, which exactly defines the equilibrium in terms of the difference in energy between left and right. The latter energy is given by $F \cdot L$. We get for the ratio:

$$n_l^* / n_r^* = e^{-FL/kT}. \quad (34)$$

From this we work out the difference in concentration between right and left side as:

$$-\Delta n_s^* \equiv (n_r^* - n_l^*) = n_r^* \cdot (1 - e^{-FL/kT}). \quad (35)$$

During tracer experiments, Δn_s^* is usually rather small. Hence, the balancing force (pressure) should be small, too. Eqn (35) may be written as ($e^{-F \cdot L/kT} \gg 1 - F \cdot L/kT$):

$$-\Delta n_s^* = \frac{FL}{kT} \cdot n^*. \quad (36)$$

where n^* is the average concentration of tracer in the two compartments, i.e., $n^* = (n_r^* + n_l^*)/2$. When we combine Eqns (33) and (36), we obtain for p_d :

$$p_d = \frac{\overline{v_w} \cdot kT \cdot N^*}{\gamma \cdot L^2 \cdot N \cdot n^* \cdot \overline{v_w}}. \quad (37)$$

Here, the numerator and denominator have been multiplied by the volume of a water molecule ($\overline{v_w}$). $n^* \cdot \overline{v_w}$ represents the fraction of heavy water in the bulk solution. This should equal N^*/N . Eqn (37) simplifies to:

$$p_d = \frac{\overline{v_w} \cdot kT}{\gamma \cdot L^2} = \frac{\overline{v_w} \cdot D_w}{L^2}. \quad (38)$$

By comparing Eqns 28 and 38, we arrive at the simple result that:

$$\boxed{\frac{p_f}{p_d} = \frac{P_f}{P_d} = N}. \quad (39)$$

As indicated, this relation should also hold for the cell or overall membrane level (P_f and P_d in units of $\text{m} \cdot \text{s}^{-1}$ instead of $\text{m}^3 \cdot \text{s}^{-1} \cdot \text{molecule}^{-1}$ for p_f and p_d). This, however, is only true when the membrane pores rather than the bilayer dominate the overall P_f or P_d . When there is a substantial contribution of the bilayer, this may be accounted for if the contribution of the bilayer is known (Finkelstein 1987; Hertel & Steudle 1997). During water movement across the bilayer in the absence of pores, $P_f/P_d = 1$ should hold. Equation (39) was used in this thesis to work out numbers of molecules in membrane pores (see Chapter 3). The diffusional water permeability was measured in a tracer experiment using heavy water. The bulk flow water permeability was derived from L_p ($P_f = L_p \cdot RT / \overline{V_w}$). In both cases, the cell pressure probe was employed for the measurements.

1.3.3 Restrictions to this procedure

- (i) Experimentally, P_f (L_p) can be measured with high accuracy and rather free of effects of unstirred layers (USLs). This is not true for P_d , namely in big cells (see below and Chapter 6). So, N may be overestimated.
- (ii) When aiming at p_f/p_d ratios of water channels (aquaporins), these may not be directly accessible by the P_f/P_d ratios of cell membranes because of the effects of the bilayer (rest of the membrane, see above).

1.4 Unstirred layers (USLs)

Due to effects of unstirred layers, solute concentrations that govern the permeation of solutes and water across cell membranes, i.e., the concentrations adjacent to the membrane/solution interfaces differ from the concentration in the bulk solutions. When bulk concentrations are used to quantify the driving forces such as an osmotic pressure difference driving a water flow (J_v) or a concentration difference driving a solute flow (J_s), the ‘real’ forces may be overestimated because of the existence of USLs. As a consequence, transport parameters such as the hydraulic conductivity (L_p), the permeability (P_s) and reflection (σ_s) coefficient are underestimated. For uncharged substances like organic solutes and water, there are two different types of USLs. One is the ‘sweep away effect’ which occurs in the presence of a water flow across cell membrane (measurement of L_p ; Dainty 1963). The other one is the ‘gradient dissipation effect’ which exists in the presence of a solute flow across the membrane (measurements of P_s or σ_s ; Barry & Diamond 1984).

1.4.1 Sweep away effect

Water flow (J_v) across the membrane tends to ‘sweep away’ or dilute the solution on one side of the membrane, while increasing the local concentration on the other side. Solutes are moved to the membrane surface with the water (but do not permeate as fast as the water and they are swept away). Overall, this reduces the osmotic driving force at

the membrane surface reducing a water flow induced by a change in cell turgor or external osmotic concentration. The hydraulic conductivity is reduced. In the presence of a steady water flow, the concentration right at the membrane surface, C_s^m , should be given by (Dainty 1963):

$$C_s^m = C_s^b \cdot \exp\left(-\frac{J_v \cdot \delta}{D_s}\right). \quad (40)$$

Here, C_s^b is the concentration in the bulk solution; δ is the thickness of the unstirred layer and D_s the diffusion coefficient of the solute. The effect increases with an increasing J_v as well as with the increasing thickness of the unstirred layer δ , but decreases with an increasing mobility of the solute (increasing diffusion coefficient D_s). Often, thicknesses of USLs are hard to access experimentally. They are subject to external stirring of the medium, but this cannot completely remove the layers. During hydrostatic experiments with the pressure probe, an upper limit of USLs may be worked out. According to the definition of the cell elasticity (elastic modulus, ε), we have:

$$\varepsilon = V \frac{dP}{dV} \approx V \frac{\Delta P}{\Delta V}. \quad (41)$$

Here V is volume of the cell; ΔP and ΔV are changes of turgor pressure and volume of the cell. Assuming that all of the water is extruded instantaneously during a relaxation building up an unstirred layer, the maximum value of δ_{\max} can be given as:

$$\delta_{\max} = \frac{\Delta V}{A} = \frac{V \cdot \Delta P}{A \cdot \varepsilon} = \frac{r}{2} \cdot \frac{\Delta P}{\varepsilon}. \quad (42)$$

This refers to a cylindrical cell such as a *Chara* internode. A is the surface area and r is radius of the cell and, neglecting the contribution of cell ends, $V/A = \pi \cdot r^2 \cdot l / 2\pi \cdot r \cdot l = r/2$.

However, this procedure to work out effects of USLs may underestimate the effect of sweep-away during hydrostatic experiments of pressure probes, because it assumes that water flow is even throughout the entire cell surface, which may not be true. Due to the composite structure of cell membranes, water flow should be largely confined to certain arrays in the membrane such as aquaporins (AQPs). Effects of flow constriction should result in higher water flow density in these arrays than in the rest of the membrane

tending to increase effects of sweep-away, also by an increase of δ_{\max} . Hence, one would expect a rather large effect of USLs during hydrostatic experiments using the pressure probe (for a detailed discussion, see Chapter 6).

1.4.2 Gradient dissipation effect

The ‘gradient dissipation effect’ is due to the permeation of solutes across cell membrane (Barry and Diamond, 1984). The effect denotes the tendency gradients of the solute concentration adjacent to the membrane to level off. Gradient dissipation is important in the presence of rapidly permeating solutes during passive solute flows. Since concentration differences represent the driving forces, the ‘gradient dissipation effect’ is of interest for osmotic water transport besides the solute flow. The solutes exhibit a high permeability to cell membrane so that on one side of the membrane a depletion of solutes takes place while on the other side the local concentration increases. In the presence of rapidly permeating solutes such as HDO or acetone, gradient dissipation should contribute to the absolute values of P_s and σ_s as measured with the pressure probe from biphasic pressure relaxations. The overall measured ‘permeation resistance’ per unit area of the solute ($1/P_s^{meas}$) contains the true diffusional resistances for the membrane ($1/P_s$) and that of the two USLs on both side of the membrane δ^o/D_s^o and δ^i/D_s^i , respectively (δ^o and δ^i = equivalent thicknesses of USLs on the two sides of the membrane; D_s^o and D_s^i = diffusion coefficients of the solute which may be different on both sides):

$$\frac{1}{P_s^{meas}} = \frac{1}{P_s} + \frac{\delta^o}{D_s^o} + \frac{\delta^i}{D_s^i}. \quad (43)$$

This assumes steady state, a planar, homogenous membrane, and linear concentration profiles within the layers. For the cylindrical *Chara* internodes used in this thesis, we may denote the radial distances from the center of the cell to the boundaries of USLs by ‘a’ (internal) and ‘b’ (external). (Fig 1A in Chapter 6). In the steady state, assuming $D_s^o = D_s^i = D_s$, the overall measured permeation resistance $1/P_s^{meas}$ can be written as:

$$\frac{1}{P_s^{meas}} = \frac{1}{P_s} + \frac{R}{D_s} \cdot \ln \frac{b}{a}. \quad (44)$$

It should be noted that, Eqns (43) and (44) relate to linear concentration profiles within the USLs. In the presence of USLs at both sides of the plasma membrane of a *Chara* cell, for $D_s^o = D_s^i = D_s$, the measured value of reflection coefficient (σ_s^{meas}) would be given as (Steudle & Frensch 1989):

$$\sigma_s^{meas} = \frac{1/P_s}{1/P_s + R/D_s \cdot (\ln(b/a))} \cdot \sigma_s. \quad (45)$$

By the first factor on the right side of Eqn (45), the measured coefficient would be smaller than the true one (σ_s). If D_s would be different in the medium/cell wall from that in the cytoplasm, a more extended expression may be used (Steudle & Frensch 1989). Eqn (44) may be re-written to separate external from internal USLs, i.e.:

$$\underbrace{\frac{1}{P_s^{meas}}}_{\text{measured resistance}} = \underbrace{\frac{1}{P_s}}_{\text{true membrane resistance}} + \underbrace{\frac{R}{D_s} \cdot \ln \frac{b}{R}}_{\text{resistance of external USL}} + \underbrace{\frac{R}{D_s} \cdot \ln \frac{R}{a}}_{\text{resistance of internal USL}}. \quad (46)$$

For the unsteady state which is closer to reality, an analytical solution lacking or in the presence of a membrane surrounding a cylindrical *Chara* cell may be used to work out the ‘equivalent thicknesses’ of USLs. Hence, a quantitative examination of the role of USLs, i.e., the contribution of USLs to the overall permeability of solutes used, becomes possible (for details see Chapter 6 and Fig. 8 of the chapter).

Any permeation of water and solutes is inevitably suffering from the effects of USLs. The question is how large the contributions of USLs to the overall permeability are. Recently, Tyree, Koh & Sands (2005) argued that USLs play a substantial or even dominating role in measurements of transport coefficients with pressure probe in *Chara corallina*. These authors neither had own results nor experience with pressure probes, and were supplied with original data from this thesis. They employed a simple simulation model to support their view. However, they erroneously (i) assumed too high values of external and internal USLs; (ii) neglected the vigorous external stirring situation in the experimental set-up, and (iii) overlooked the sensitivity of pressure

transducer used in the experiments. Based on experiments results and theoretical analyses, a re-examination of the role of USLs showed that the conclusions of Tyree *et al.* (2005) have neither an experimental nor a theoretical basis (for details see Chapter 6).

This dissertation can be divided into following sub-sections:

- I A cohesion/tension mechanism explains the gating of water channels (aquaporins) in *Chara* internodes by high concentration (Ye, Wiera & Steudle 2004).
- II A cohesion/tension model for the gating of aquaporins allows estimation of water channel pore volumes in *Chara* (Ye, Muhr & Steudle 2005)
- III Oxidative gating of water channels (aquaporins) in *Chara* by hydroxyl radicals (Henzler, Ye & Steudle 2004).
- IV Oxidative gating of water channels (aquaporins) in corn roots (Ye & Steudle 2005).
- V A re-examination of the role of unstirred layers (USLs) during the measurement of transport coefficients of *Chara* internodes with the cell pressure probe: minor role of USLs (Ye, Kim & Steudle 2005).
- VI Advances in the studies on water uptake by plant roots (Zhao, Deng, Zhang, Ye, Steudle & Shan 2005).

1.5 Material and Methods

1.5.1 Growth of *Chara corallina*

Mature internodal cells of *Chara corallina* (50 to 120 mm long and 0.8 to 1.0 mm in diameter) were used in experiments. *Chara* had been grown in artificial pond water (APW) in tanks that contained layers of autoclaved mud from a natural pond. Compositions of APW were 1.0 mM NaCl, 0.1 mM KCl, 0.1 mM CaCl₂ and 0.1 mM MgCl₂. Tanks were placed in the laboratory and illuminated for 24 h a day with a 15 W fluorescent lamp (Electronic, Germany) positioned 0.2 m over the water surface.

1.5.2 Growth of corn seedlings

Seeds of corn (*Zea mays* L. cv. Helix, Kleinwanzlebener Saatzucht AG, Einbeck, Germany) were germinated on filter paper soaked in 0.5 mM CaSO₄ for 3 d at 25 °C in the dark. When seminal roots were 30 to 50 mm long, seedlings were transferred to 7-L containers which accommodated 20 seedlings each. Compositions of the growing solution were in mM: KH₂PO₄ 1.5, KNO₃ 2.0, CaCl₂ 1.0, MgSO₄ 1.0 and in μM: FeNaEDTA 18, H₃BO₃ 8.1, MnCl₂ 1.5. The growing condition was day/night 12 h photoperiod with 300 mmol·m⁻²·s⁻¹ photosynthetically active radiation, and 24/19 °C day/night temperature. Roots (250 to 400 mm long) of 8 to 10 days old seedlings (including time required for germination) were used in the experiments.

1.5.3 Pressure probe for *Chara* internodes

As shown in Fig. 7, a cell pressure probe (completely filled with silicone oil) was introduced through the protruding node adjacent to a *Chara* internode which had been placed in a glass tube with an inner diameter of 3 mm and fixed by a clamp. APW or test solutions were pumped through the other end of the glass tube along the cell (flow rates were 0.2 – 0.3 m·s⁻¹), so that the solution around the cell was vigorously stirred. This minimized the thickness of external unstirred layers (USLs). Cell turgor pressure was measured by an electronic pressure transducer and was recorded by a computer

connected to the output of the transducer. Two types of experiment can be performed with the aid of the probe. (i) In the hydrostatic experiments, the oil/cell sap meniscus forming in the tip of the capillary was moved forward or backward and was then kept stable after each move until termination of a pressure relaxation; (ii) osmotic experiments were conducted by changing the osmotic pressure (concentration) of the medium while keeping the position of meniscus constant throughout.

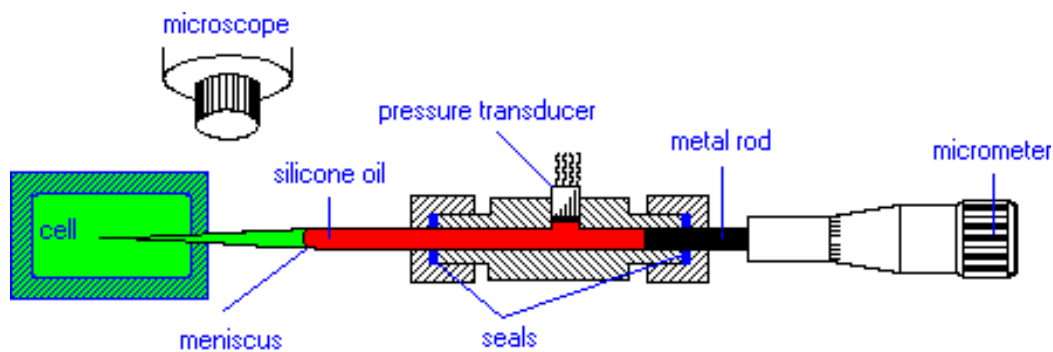


Figure 7. Schematic drawing of a cell pressure probe for giant single cells (*Chara corallina*). An oil/cell sap meniscus was forming in the tip of the capillary. The position of this meniscus was used as a point of reference during the measurements. Water flows were induced either by changing the pressure in the system using a metal rod (hydrostatic experiments) or by changing the osmotic pressure (concentration) of the medium (for a detailed explanation see text).

1.5.4 Pressure probe for higher plant cells

A root segment was fixed by magnetic bars on a metal sledge which was arranged at an angle of 45° . It was covered by one layer of paper tissue at the top and at the bottom to keep the root wet. The center part of the root was lying open at a length of ≈ 10 mm, and solution was running down along the root and at the edges of the metal plate. An average rate of solution flow along the root was around $0.2 \text{ m}\cdot\text{s}^{-1}$. The measuring principle of this type of pressure probe was identical with that for giant *Chara* cells. However, due to the tiny size of higher plant cells, the measurement required a precise adjustment of the meniscus to follow and measure the small volume changes produced by shifting the meniscus. Compared with the equipment used during the *Chara* experiments, there were three modifications: (i) the diameter of the glass capillary was

reduced to 5 ~ 10 μm ; (ii) the volume of the pressure chamber of the probe was substantially reduced as compared with the other type, and (iii) meniscus movements were performed with the aid of a little motor, which allowed a sufficiently fine adjustment of the position of the meniscus and tending to avoid vibrations which would cause leakages around the tip inserted in a cell.

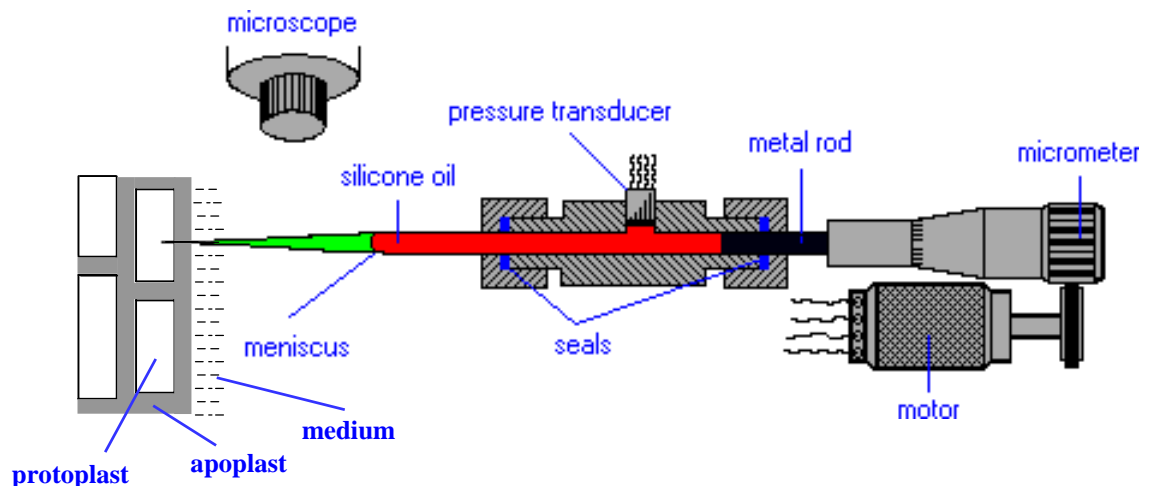


Figure 8. Schematic drawing of a cell pressure probe for higher plant tissue cells. The oil/cell sap meniscus in the tip of the glass capillary was used as a reference point. The meniscus was adjusted and water flows induced with a motor driving a metal rod into or out of the probe (for detailed explanation, see text).

1.5.5 Pressure probe for roots

End segments of roots were placed in a glass tube (inner diameter: 6 mm) with the basal cut end protruding, which was connected to a root pressure probe. Segments were fixed to the probe by silicone seals (Zhu & Steudle 1991). Root medium was flowing along the roots by gravity from a reservoir sitting about 0.5 m above the glass tube at a rate of $0.3 - 0.5 \text{ m}\cdot\text{s}^{-1}$, and circulated back to the reservoir by a peristaltic pump. After tightening the silicone seals in steps with the aid of a screw, root pressure (P_r) began to increase and became steady within 1 to 3 h (Hose *et al.* 2000). In hydrostatic experiments, pressure relaxations were induced by changing the volume of the system i.e., changing the position of the meniscus with the aid of the probe. The osmotic experiments were performed by changing the osmotic pressure (concentration) of the

medium. After experiments with a given root, it was cut at a position close to the seal. When root pressure decreased immediately to close to zero following the cut, and half times of pressure relaxations became much shorter as compared with the original values (less than 1.0 s), this indicated that root xylem within the seal remained open. If there was no or a delayed effect upon cutting, this indicated that root xylem was interrupted during tightening or later. Results from these experiments were discarded (Peterson & Steudle 1993).

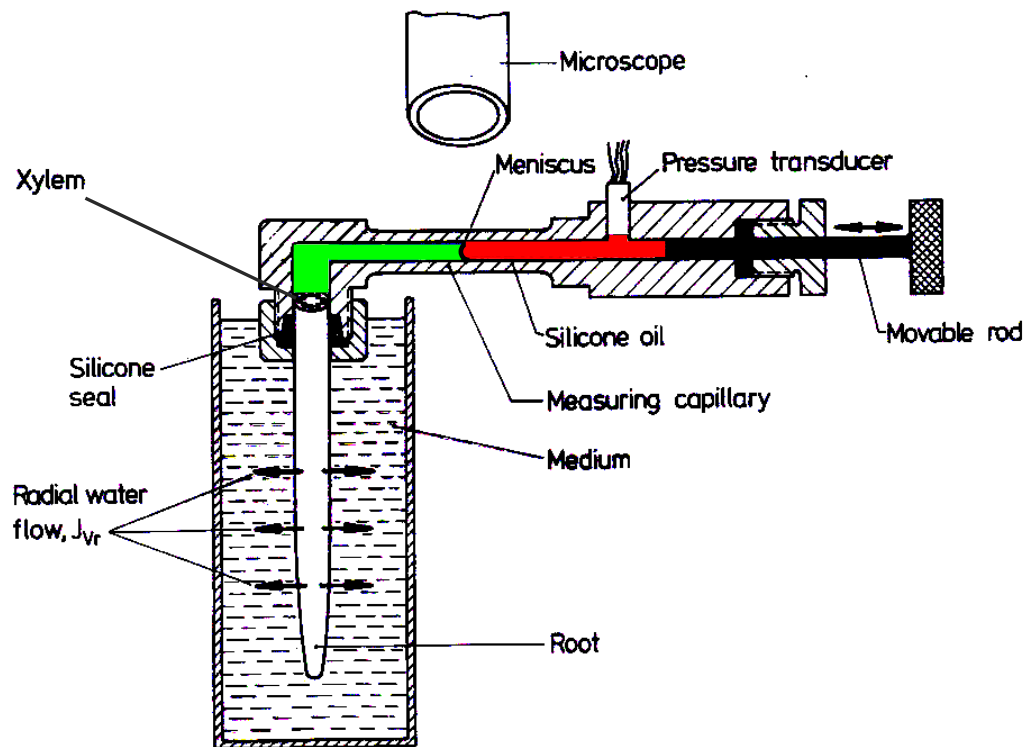


Figure 9. Schematic drawing of a root pressure probe for measuring water and solute transport across roots. A root segment is tightly connected to the probe by silicone seals. Part of the glass capillary is filled with silicone oil and the other by water so that a meniscus forms in the capillary. Water flows can be induced either by changing the pressure in the system using a metal rod (hydrostatic experiments) or by changing the osmotic pressure (concentration) of the medium (for detailed explanation, see text).

1.6 Results and Discussion

1.6.1 Gating of aquaporins by high concentration – cohesion/tension mechanism

An inhibition of cell membrane L_p by high concentration is known for a long time, but the mechanism is not well understood (Kiyosawa & Tazawa 1972; Steudle & Tyerman 1983). Isolated internodes of *Chara corallina* have been used to study the gating of aquaporins (water channels) in the presence of high concentrations of osmolytes of different size (molecular weight). The ‘osmotic gating efficiency’ of osmolytes was quite different, i.e., inhibition of aquaporin activity increased with increasing both concentration and size of osmolytes (reflection coefficients). As cell L_p decreased, P_s increased indicating that water and solutes used different passages across the plasma membrane. Similar to earlier findings of an osmotic gating of ion channels (Zimmerberg & Parsegian 1986), results from long term and reversible experiments with *Chara* internodes support the view that osmotic dehydration in terms of a cohesion/tension mechanism is an important trigger of water channel activity in *Chara* and, perhaps, in higher plants, too. According to the cohesion/tension model, osmotic solutes are excluded from water channels. This, in turn, results in a reversible deformation or even a collapse of channel protein as tensions (negative pressures) develop within aquaporins. According to theory, the effect of osmotic gating of AQPs decreased exponentially with increasing concentration. The ‘osmotic efficiency’ of osmolytes increased with increasing size (molecular weight) of the substances used, as one would expect (see Chapter 2).

1.6.2 Estimation of water channel pore volumes in the plasma membrane of *Chara corallina*

The cohesion/tension model of the gating (osmotic dehydration) of aquaporins predicted that, the water permeability (hydraulic conductivity; L_p) of turgid, intact internodes of *Chara corallina* decreased exponentially as the concentration of osmolytes applied in the medium increased (Ye, Wiera & Steudle 2004). The change in the activity of AQPs was measured by a pressure probe for concentration series of osmolytes which were

applied on both sides of the membrane. Because the larger the molecular size of the osmolyte, the more efficient it was in reducing cell L_p at a given concentration, osmolyte of different molecular size (molecular weight; MW) and reflection coefficients (σ_s) were used in the experiments. Pore volumes were calculated from 'dehydration curves', which required the measurement of responses over large ranges of concentration. Since the osmolytes had to be applied in the medium and in the cell at the same concentration, the selection of big osmolytes was limited to those which were sufficiently permeating. In the thesis, I used different glycol ethers of different MW such as: ethylene glycol monomethyl ether (EGMME), diethylene glycol monomethyl ether (DEGMME), and triethylene glycol monoethyl ether (TEGMEE). Small osmolytes were: heavy water (HDO), hydrogen peroxide (H_2O_2), acetone, and 2-propanol.

These compounds were applied in concentrations of up to 2000 mM, whereby the concentration was changed in steps to avoid plasmolysis. In order to check for reversibility, concentrations were then lowered in steps again until the original medium was obtained. The procedure showed that changes in L_p , P_s and σ_s were reversible within 90 - 95 %. Furthermore, it showed that turgor pressure (and, hence, the osmotic concentration of cells) was constant within 5 % of the original value of above 0.55 MPa.

In the presence of the big osmolytes DEGMME and TEGMEE, dehydration curves were best described by the sum of two exponentials (as predicted from the theory in the presence of two different types of AQPs with differing pore diameters and volumes). AQPs with big diameters could not be closed in the presence of the smallest osmolyte acetone, even at very high concentrations. The cohesion/tension theory allowed pore volumes of AQPs to be evaluated, which was $2.3 \pm 0.2 \text{ nm}^3$ for the narrow pore and between 5.5 ± 0.8 and $6.1 \pm 0.8 \text{ nm}^3$ for the wider pores. The existence of different types of pores was also evident from differences in the residual L_p , i.e., the residual cell L_p decreased with increasing size of osmolytes.

Alternative to the procedure just described for the osmotic treatment, pore volumes were estimated from ratios between osmotic (P_f) and diffusional (P_d) water flow.

According to Levitt's (1974) theory, ratios of P_f/P_d should directly yield the number of water molecules (N) in an AQP, which is related to pore volume (see section 1.3). N values ranged between 35 and 60, which referred to volumes of 0.51 and 0.88 nm³/pore. Values of pore volumes obtained by either method were bigger than those reported in the literature for other AQPs. This may be due to reasons that either the water channels in *Chara* are somewhat wider than just the diameter of a water molecule, or that the mouth parts of channels contributed to the calculated overall pore volume in the presence of osmolytes, or both (see Chapter 3).

1.6.3 Oxidative gating of water channels (aquaporins) in *Chara*

Hydroxyl radicals (*OH) as produced in the Fenton reaction ($\text{Fe}^{2+} + \text{H}_2\text{O}_2 = \text{Fe}^{3+} + \text{OH}^- + *OH$) have been used to reversibly inhibit water channel activity in the plasma membrane of internodes of *Chara corallina*. Compared to conventional agents such as HgCl_2 , *OH turned out to be more effective in blocking water channels and was less toxic for the cell. When internodes were treated for 30 min, cell hydraulic conductivity (L_p) decreased by 90 % or even more. This effect was reversed within a few minutes after removing the radicals from the medium. Unlike HgCl_2 , *OH reduced the permeability of small unchanged solutes indicating some transport of these solutes across the pores in addition to water. For rapidly permeating lipophilic solutes, the blockage of water channels with *OH resulted in negative reflection coefficients and anomalous osmosis. This as expected from the composite transport model. Two possible mechanisms by which *OH acts on water channels were speculated. One is that aquaporins were oxidized by *OH attacking the channel from inside the pore to cause conformational changes of the proteins and its closure. The other alternative is that C = C double bonds of the plasma membrane were attacked by *OH, resulting in the formation of aggressive radicals which attacked aquaporins from outside (see Chapter 4).

1.6.4 Oxidative gating of water channels (aquaporins) in corn roots

An oxidative gating of water channels (aquaporins: AQPs) was observed in experiments with young roots of corn (*Zea mays* L.) as already found in experiments with the green alga *Chara corallina* (see above and Chapter 4). In the presence of 35 mM hydrogen peroxide (H_2O_2) in the root medium, half times of water flows (as measured with the aid of pressure probes) increased at the level of both entire roots and individual cortical cells by factors of 3 and 9, respectively. In the presence of H_2O_2 , channel closure caused anomalous (negative) osmosis at both the root and cell level, when using the rapidly permeating solute acetone. This was interpreted by the composite transport structures of both the root and cell. In the presence of the lipophilic solute acetone, channel closure caused a situation in which the solute moved faster than the water and the reflection coefficient (σ_s) reversed its sign. As during the experiments with *Chara* internodes, effects were reversible at both the root and cell level, when H_2O_2 was removed from the medium. Unlike the gating by mechanical stimuli (Wan *et al.* 2004) or by low temperature (Lee *et al.* 2005 a, b), the stress hormone ABA had no ameliorative effect on restoring the original conformation of channel proteins and re-opening closed channels, possibly, because the oxidative gating in the presence of H_2O_2 or $\cdot\text{OH}$ radicals caused a chemical modification of AQPs. The precise mechanism of the oxidative gating of AQPs in the presence of the ROS ($\cdot\text{OH}$ or H_2O_2) is not yet understood. Three alternatives may be possible: AQPs were (i) directly attacked (oxidized) by $\cdot\text{OH}$, or (ii) oxidized by other aggressive radicals which were subsequently produced by $\cdot\text{OH}$. (iii) Alternatively, H_2O_2 may have elicited changes in cytoplasmic Ca^{2+} concentration *via* cell signaling cascades resulting in channel closure. In either case, AQP activity could be regulated by an oxidative gating or signaling initiated by the presence of H_2O_2 or $\cdot\text{OH}$ radicals. There may be a common interaction between the redox state (oxidative stress) and water relations (water stress) during the life of plants (see Chapter 5).

1.6.5 Quantitatively re-examination of the role of unstirred layers during measurements of transport parameters of water and solutes

Using rapidly permeating solutes (acetone, 2-propanol, dimethylformamide (DMF)), effects of unstirred layers (USLs) on measurements of water and solutes transport (L_p , P_s and σ_s) across cell membranes of isolated *Chara* internodes were rigorously re-examined. There are two types of USL effects, i.e., sweep-away effect and gradient-dissipation effect (see Section 1.4). In order to test effects of USLs due to sweep-away, half times of water flow across cell membrane ($T_{1/2}^w$) were measured with small ($\Delta P \approx \pm 0.04$ MPa) or big ($\Delta P \approx \pm 0.4$ MPa) peak size of pressure pulses. Water flow induced by big pulses should have been larger by an order of magnitude than that in the presence of small pulses. The thickness of USLs built up by sweep-away during big pulses should have had a bigger effect on $T_{1/2}^w$ than during the small ones. However, there was no significant difference in $T_{1/2}^w$. The reason was due to the fact that maximum thicknesses of USLs induced by water flow were too small to cause a significant effect (Eqn (42)), even in the presence of effects of a flow constriction due to the existence of aquaporin array in cell membranes. Pressure clamp experiments should have induced a larger amount of water flow as compared with pressure pulses. The results indicated that sweep-away effect in the presence of a pressure clamp caused transient increases of $T_{1/2}^w$ (decreases of hydrostatic L_{ph}) by about 20 %, which could have been affected by the flow constriction or concentration polarization effects, or both.

Effects of stirring of the external solution around the internodes were measured for the osmotic hydraulic conductivity (L_{p_o}), permeability (P_s) and reflection (σ_s) coefficients by varying flow rates (v_{med}) of between 0.02 and 55 $m \cdot s^{-1}$. Measured parameters (L_{p_o} , P_s and σ_s) increased as increasing of flow rates for the three different osmolytes of different permeability: acetone, 2-propanol and DMF. L_{p_o} tended to saturate at values close to L_{ph} at rates of $v_{med} \approx 0.20$ $m \cdot s^{-1}$, while smaller values of v_{med} were required to saturate P_s and σ_s ($v_{med} \approx 0.10$ $m \cdot s^{-1}$). There was no further increase of L_{p_o} , P_s and σ_s , when the vigorous external stirring was increased by flushing air bubbles through the tube at high rates. Taking the cell wall tortuosity into account, an upper limit of the thickness of external USLs of 30 μm at high stirring rates was estimated. Comparison of

calculated values for solutes diffusion into a cylinder lacking or containing a membrane with experimental data of solute uptake by the same diameter intact *Chara* internodes showed significant differences. When used acetone as test solute, from the calculations, upper limits of the equivalent thickness of diffusive internal USLs were estimated to be 117 and 97 μm for a cylindrical cell ($R = 0.4 \text{ mm}$) lacking or with a membrane, respectively. For less permeating solutes like DMF, the up limits were 108 and 95 μm , respectively. Results indicated that the real equivalent thickness of internal USLs should have been smaller by a factor of 2 to 3 than the upper limits. Overall, it was concluded that measurement of L_p was free of effects of USLs during hydrostatic experiments. For P_s and σ_s , the effects of USLs may not be negligible, but even for the most rapidly permeating solutes like heavy water (HDO) and acetone, USLs should have resulted in an underestimation of P_s and σ_s by less than 25 ~ 30 %.

1.7 Short summary

- The concentration dependence of cell hydraulic conductivity (L_p) can be explained in terms of a **cohesion/tension (C/T) mechanism for the gating of water channels** in the plasma membrane of *Chara* internodes. Osmolytes in the presence of both sides of the membrane, i.e., excluded from water channels, caused a **reversible deformation or even collapse of the channel protein as tensions (negative pressures)** develop within the pores. Inhibition of water channel activity **increased with both concentration and size of osmolytes (reflection coefficients)**, i.e., the bigger the osmolytes, the lower was the concentration which induced a reversible closure of aquaporins (AQPs). The C/T mechanism may be relevant for higher plant L_p , too, e.g. in the presence of high salinity.
- As theoretically expected according to the C/T mechanism, the cell L_p of turgid, intact internodes of *Chara corallina* **decreased exponentially** as the concentration of osmolytes applied in the medium increased due to a C/T mechanism of the gating aquaporins. Pore volumes of water channels estimated

from the ‘**dehydration curves**’ using different osmolytes with different molecular sizes over large ranges of concentrations indicated that, there may be **populations of AQPs with differing pore diameters and volumes** existing in the plasma membrane instead of just one type. AQPs with bigger volumes just responded to big osmolytes and were not affected by solute of low MW.

- **Pore volumes** obtained both from the ‘dehydration curves’ and from ratios between osmotic (P_f) and diffusional (P_d) water flow ($P_f/P_d =$ the number of water molecules (N) in an AQP) **were bigger** than those reported in the literature for other AQPs. This may be due to reasons that either water channels in *Chara* are somewhat **wider than just the diameter of a water molecule**, or that the **mouth parts** of channels contributed to the calculated overall pore volume, or both.
- An ‘**oxidative gating**’ of aquaporins had been proposed both in *Chara* internodes and in corn root. In the presence of **hydroxyl radicals (*OH) or hydrogen peroxide (H₂O₂)**, hydraulic conductivity was reduced by a factor of more than 10 for *Chara* and by factors of 9 and 3 for root cortical cells and entire roots, respectively. Effects were largely recovered after removal of *OH or H₂O₂ from the medium. Three alternative mechanisms of the ‘oxidative gating’ were speculated that, AQPs were (i) **directly attacked (oxidized)** by *OH, (ii) **oxidized by other aggressive radicals which were subsequently produced** by *OH, or (iii) **closed due to changes in cytoplasmic Ca²⁺ concentration** elicited by H₂O₂ *via* cell signaling cascades. There may be an **interaction** between the **redox states** (oxidative stress) and **water relations** (water stress) in plants.
- In the presence of high concentration of osmolytes, cell L_p decreased, while solute permeability coefficients (P_s) increased suggesting that **water and solutes use different passages across the plasma membrane**, i.e., water mainly uses AQPs across cell membrane while solutes diffusing through the bilayer. However, *OH reduced the permeability of small uncharged solutes indicating

that **AQPs were not ideally selective for water**, some solutes may also partly transport across the pores.

- **Anomalous (negative) osmosis** has been demonstrated both at the cell level (*Chara* internodes and root cortical cells) and at the organ level (entire root in the presence of a rather complicated osmotic barrier). This has been interpreted by the **composite transport structures** of both the cell and root. In the presence of a rapidly permeating solute like acetone, channel closure caused a situation in which the **solute moved faster than the water, and the reflection coefficient (σ_s) reversed its sign**.
- Unlike other gating mechanisms such as mechanical stimuli or low temperature, the stress hormone **ABA had no ameliorative effect during the ‘oxidative gating’ of AQPs** (Wan *et al.* 2004; Lee *et al.* 2005b). This may indicate that the chemical modification of AQPs in the presence of oxidative stress required a **biochemical (reduction of oxidized AQPs)** rather than just a **physical action** (change of activation energy of transition between conformational states) to re-open closed channels.
- A rigorous re-examination of the role of **unstirred layers (USLs)** during pressure probe experiments with *Chara* internodes showed that USLs had **no measurable effect** on the **hydrostatic water permeability (L_{p_h})**, even when considering an effect of a **flow constriction** due to the composite structure of the cell membrane, i.e., the existence of AQP arrays. **Thickness of external USLs of 30 μm** at high external stirring rates was estimated including the cell wall (thickness: 5 to 10 μm). In osmotic experiments, USLs should have resulted in **an underestimation of P_s and σ_s by less than 25 ~ 30 %**, even for the most rapidly permeating solutes like heavy water (HDO) and acetone. Based on diffusion kinetic theory and using acetone as the test solute, upper limits of **equivalent thicknesses of diffusive internal USLs** were estimated to be **117 and 97 μm** for a cylindrical cell (**$R = 0.4 \text{ mm}$**) lacking or containing a membrane, respectively. Results indicated that **cell membrane** acts as the **rate-limiting resistance** allowing substantial time for an internal mixing by

diffusion. The **real equivalent thicknesses** of internal USLs should be **smaller** than the estimated upper limits which were calculated by assuming a **completely stagnant and homogenous** internal compartment. It may be safe to estimate the **equivalent thickness of internal USLs of 50 μm** .

1.8 Literature cited

- Agre P., Bonhivers M. & Borgnia M.J. (1998) The aquaporins, blueprints for cellular plumbing systems. *Journal of Biological Chemistry* **273**, 14659–14662.
- Azaizeh H., Gunse B., & Steudle E. (1992) Effects of NaCl and CaCl₂ on water transport across root cells of maize (*Zea mays* L.) seedlings. *Plant Physiology* **99**, 886–894.
- Barry P.H. & Diamond J.M. (1984) Effects of unstirred layers on membrane phenomena. *Physiological Reviews* **64**, 763–872.
- Carvajal M., Cooke D.T. & Clarkson D.T. (1996) Responses of wheat plants to nutrient deprivation may involve the regulation of water-channel function. *Planta* **199**, 372–381.
- Cosgrove D.J. (1998) Cell wall loosening by expansins. *Plant Physiology* **118**, 333–339.
- Chaumont F., Barrieu F., Wojcik E., Chrispeels M.J. & Jung R. (2001) Aquaporins constitute a large and highly divergent protein family in maize. *Plant Physiology* **125**, 1206–1215.
- Chaumont F., Moshelion M. & Daniels M.J. (2005) Regulation of plant aquaporin activity. *Biology of the Cell* **97**, (in press).
- Clarkson D.T., Carvajal M., Henzler T., Waterhouse R.N., Smyth A.J., Cooke D.T. & Steudle E. (2000) Root hydraulic conductance: diurnal aquaporin expression and the effects of nutrient stress. *Journal of Experimental Botany* **51**, 61–70.
- Dainty J. (1963) Water relations of plant cells. *Advances in Botanical Research* **1**, 279–326.
- Daniels M.J., Mirkov T.E. & Chrispeels M.J. (1994) The plasma membrane of *Arabidopsis thaliana* contains a mercury-insensitive aquaporin that is a homolog of the tonoplast water channel protein TIP. *Plant Physiology* **106**, 1325–1333.
- Denker B.M., Smith B.L., Kuhajda F.P. & Agre P. (1988) Identification, purification and partial characterization of a novel Mr 28,000 integral membrane protein from

- erythrocytes and renal tubules. *Journal of Biological Chemistry* **263**, 15634–15642.
- Einstein A. (1905) Eine neue Bestimmung der Moleküldimensionen. Dissertation, Universität Zürich, Schweiz, and *Annalen der Physik* (1906) **17**, 289–306.
- Eisenbarth D.A. & Weig A.R. (2005) Dynamics of aquaporins and water relations during hypocotyl elongation in *Ricinus communis* L. seedlings. *Journal of Experimental Botany* **56**, 1831–1842.
- Finkelstein A. (1987) Water movement through lipid bilayers, pores and plasma membranes. Theory and reality. Distinguished lecture series of the Society of General Physiologists. Vol. 4. Wiley, New York.
- Freundl E., Steudle E. & Hartung W. (1998) Water uptake by roots of maize and sunflower affects the radial transport of abscisic acid and the ABA concentration in the xylem. *Planta* **207**, 8–19.
- Freundl E., Steudle E. & Hartung W. (2000). Apoplastic transport of abscisic acid through roots of maize: effect of the exodermis. *Planta* **210**, 222–231.
- Fricke W. (2002) Biophysical limitation of cell elongation in cereal leaves. *Annals of Botany* **90**, 157–167.
- Gaxiola R.A., Li J., Undurraga S., Dang L.M., Allen G.J., Alper S.L. & Fink G.R. (2001) Drought- and salt-tolerant plants result from overexpression of the AVP1 H⁺-pump. *Proceedings of the National Academy of Sciences, USA* **98**, 11444–11449.
- Gerbeau P., Amodeo G., Henzler T., Santoni V., Ripoche P. & Maurel C. (2002) The water permeability of Arabidopsis plasma membrane is regulated by divalent cations and pH. *Plant Journal* **30**, 71–81.
- Henzler T. & Steudle E. (1995) Reversible closing of water channels in *Chara* internodes provides evidence for a composite transport model of the plasma membrane. *Journal of Experimental Botany* **46**, 199–209.

- Henzler T. (2001) Die Funktion von Wasserkanälen in der pflanzlichen Zellmembran und ihre Bedeutung für den Wassertransport in Wurzeln. Dissertation, University of Bayreuth, Germany.
- Henzler T., Waterhouse R.N., Smyth A.J., Carvajal M., Cooke D.T., Schäffner A.R., Steudle E. & Clarkson D.T. (1999) Diurnal variations in hydraulic conductivity and root pressure can be correlated with the expression of putative aquaporins in the roots of *Lotus Japonicus*. *Planta* **210**, 50–60.
- Henzler T., Ye Q. & Steudle E. (2004) Oxidative gating of water channels (aquaporins) in *Chara* by hydroxyl radicals. *Plant Cell and Environment* **27**, 1184–1195.
- Hertel A. & Steudle E. (1997) The function of water channels in *Chara*: the temperature dependence of water and solute flows provides evidence for composite membrane transport and for a slippage of small organic solutes across water channels. *Planta* **202**, 324–335.
- Hose E., Steudle E. & Hartung W. (2000) Abscisic acid and hydraulic conductivity of maize roots: a root cell- and pressure probe study. *Planta* **211**, 874–882.
- House C.R. (1974) Water transport in cells and tissues. London: Edward Arnold.
- Hukin D., Doering-Saad C., Thomas C.R. & Pritchard J. (2002) Sensitivity of cell hydraulic conductivity to mercury is coincident with symplasmic isolation and expression of plasmalemma aquaporin genes in growing maize roots. *Planta* **215**, 1047–1056.
- Javot H. & Maurel C. (2002) The role of aquaporins in root water uptake. *Annals of Botany* **90**, 301–313.
- Johansson I., Larsson C., Ek B. & Kjellbom P. (1996) The major integral proteins of spinach leaf plasma membranes are putative aquaporins and are phosphorylated in response to Ca^{2+} and apoplastic water potential. *The Plant Cell* **8**, 1181–1191.
- Johanson U., Karlsson M., Gustavsson S., Sjoval S., Fraysse L., Weig A.R. & Kjellbom P. (2001) The complete set of genes encoding Major Intrinsic Proteins in *Arabidopsis* provides a framework for a new nomenclature for Major Intrinsic Proteins in plants. *Plant Physiology* **126**, 1358–1369.

- Kalra, A. Garde S. & Hummer G. (2003) Osmotic water transport through carbon nanotube membranes. *Proceedings of the National Academy of Sciences USA* **100**, 10175–10180.
- Kammerloher W., Fischer U., Piechottka G.P. & Schäffner A.R. (1994) Water channels in the plant plasma membrane cloned by immunoselection from a mammalian expression system. *The Plant Journal* **6**, 187–199.
- Kedem O. & Katchalsky A. (1963a) Permeability of composite membranes. Part 2. Parallel arrays of elements. *Transactions of the Faraday Society (London)* **59**, 1931–1940.
- Kedem O. & Katchalsky A. (1963b) Permeability of composite membranes. Part 3. Series arrays of elements. *Transactions of the Faraday Society (London)* **59**, 1941–1953.
- Khakh B.S. & Lester H.A. (1999) Dynamic selectivity filters in ion channels. *Neuron* **23**, 653–658.
- Kiyosawa K. & Tazawa M. (1972) Influence of intracellular and extracellular tonicities on water permeability in characean cells. *Protoplasma* **74**, 257–270.
- Kiyosawa K. & Tazawa M. (1977) Hydraulic conductivity of tonoplast free *Chara* cells. *journal of membrane biology* **37**, 157–166.
- Kjellbom P., Larsson C., Johansson I., Karlsson M. & Johansson U. (1999) Aquaporins and water homeostasis in plants. *Trends in Plant Science* **4**, 308–314.
- Koefoed-Johnsen V. & Ussing H.H. (1953) The contributions of diffusion and flow to the passage of D₂O through living membranes. *Acta Physiology Scand* **28**, 60–76.
- Lee S.H., Chung G.C. & Steudle E. (2005a) Gating of aquaporins by low temperature in roots of chilling-sensitive cucumber and chilling-tolerant figleaf gourd. *Journal of Experimental Botany* **56**, 985–995.
- Lee S.H., Chung G.C. & Steudle E. (2005b) Low temperature and mechanical stresses differently gate aquaporins of root cortical cells of chilling-sensitive cucumber and chilling-resistant figleaf gourd. *Plant Cell and Environment* **28**, 1191–1202.
- Lüttge U., Kluge M. & Bauer G. (2002) Botanik (4th edition): Weinheim, Germany.

- Luu D.T. & Maurel C. (2005) Aquaporins in a challenging environment: molecular gears for adjusting plant water status. *Plant Cell and Environment* **28**, 85–96.
- Macey R.I. (1984) Transport of water and urea in red blood cells. *American Journal of Physiology* **246**, C195–C203.
- Martre P., North G.B. & Nobel P.S. (2001) Hydraulic conductance and mercury-sensitive water transport for roots of *Opuntia acanthocarpa* in relation to soil drying and rewetting. *Plant Physiology* **126**, 352–362.
- Mathai J.C., Mori S., Smith B.L., Preston G.M., Mohandas N., Collins M., van Zijl P.C., Zeidel M.L. & Agre P. (1996) Functional analysis of aquaporin-1 deficient red cells. The Colton-null phenotype. *Journal of Biological Chemistry* **271**, 1309–1313.
- Maurel C., Tacnet F., Güclü J., Guern J. & Ripoche P. (1997) Purified vesicles of tobacco cell vacuolar and plasma membranes exhibit dramatically different water permeability and water channel activity. *Proceedings of the National Academy of Sciences, USA* **94**, 7103–7108.
- Maurel C. & Chrispeels M.J. (2001) Aquaporins: a molecular entry into plant water relations. *Plant Physiology* **125**, 135–138.
- Maurel C. (1997) Aquaporins and the water permeability of plant cell membranes. *Annual Review of Plant Physiology and Plant Molecular Biology* **48**, 399–429.
- Murata K., Mitsuoka K., Hirai T., Walz T., Agre, P., Heymann J.B., Engel A. & Fujiyoshi Y. (2000) Structural determinants of water permeation through Aquaporin-1. *Nature* **407**, 599–605.
- Niemietz C.M. & Tyerman S.D. (1997) Characterization of water channels in wheat root membrane vesicles. *Plant Physiology* **115**, 561–567.
- Niemietz C.M. & Tyerman S.D. (2002) New potent inhibitors of aquaporins: silver and gold compounds inhibit aquaporins of plant and human origin. *FEBS Letters* **531**, 443–447.

- Pastori G. & Foyer C.H. (2002) Common components, networks, and pathways of cross-tolerance to stress: the central role of "redox" and abscissic acid mediated controls. *Plant Physiology* **129**, 460–468.
- Peterson C.A. & Steudle E. (1993) Lateral hydraulic conductivity of early metaxylem vessels in *Zea mays* L. roots. *Planta* **189**, 288–297.
- Preston G.M., Carroll T.P., Guggino W.B. & Agre P. (1992) Appearance of water channels in *Xenopus* oocytes expressing red cell CHIP28 protein. *Science* **256**, 385–387.
- Preston G.M., Jung J.S., Guggino, W.B. & Agre P. (1993) The mercury-sensitive residue at cysteine-189 in the CHIP28 water channel. *Journal of Biological Chemistry* **268**, 17–20.
- Ranathunge K., Steudle E. & Lafitte R. (2005) A new precipitation technique provides evidence for the permeability of Casparian bands to ions in young roots of corn (*Zea mays* L.) and rice (*Oryza sativa* L.). *Plant, Cell & Environment* **28**, 1450–1462.
- Stein W.D. (1986) Transport and diffusion across cell membranes. Academic Press, Orlando.
- Steudle E. & Brinckmann E. (1989) The osmometer model of the root: water and solute relations of *Phaseolus coccineus*. *Botanica Acta* **102**, 85–95.
- Steudle E. & Frensch J. (1989) Osmotic responses of maize roots. Water and solute relations. *Planta* **177**, 281–295.
- Steudle E. & Henzler T. (1995) Water channels in plants: do basic concepts of water transport change? *Journal of Experimental Botany* **46**, 1067–1076.
- Steudle E. & Peterson C.A. (1998) How does water get through roots? *Journal of Experimental Botany* **49**, 775–788.
- Steudle E. & Tyerman S.D. (1983) Determination of permeability coefficients, reflection coefficients and hydraulic conductivity of *Chara corallina* using the pressure probe: effects of solute concentrations. *Journal of Membrane Biology* **75**, 85–96.

- Steudle E. (2000) Water uptake by roots: effects of water deficit. *Journal of Experimental Botany* **51**, 1531–1542.
- Steudle E. (2001) The cohesion/tension mechanism and the acquisition of water by plant roots. *Annual Review Plant Physiology and Plant Molecular Biology* **52**, 847–875.
- Tazawa M., Asai K. & Iwasaki N. (1996) Characteristics of Hg- and Zn-sensitive water channels in the plasma membrane of *Chara corallina*. *Botanica Acta* **105**, 388–396.
- Tournaire-Roux C., Sutka M., Javot H., Gout E., Gerbeau P., Luu D.T., Bligny R. & Maurel C. (2003) Cytosolic pH regulates root water transport during anoxic stress through gating of aquaporins. *Nature (London)* **425**, 393–397
- Tyerman S.D., Bohnert H.J., Maurel C., Steudle E. & Smith J.A. (1999) Plant aquaporins: their molecular biology, biophysics and significance for plant water relations. *Journal of Experimental Botany* **25**, 1055–1071.
- Tyerman S.D., Niemietz C.M. & Bramley H. (2002). Plant aquaporins: multifunctional water and solute channels with expanding roles. *Plant, Cell and Environment* **25**, 173–194.
- Tyree M.T., Koh S. & Sands P. (2005) The determination of membrane transport parameters with the cell pressure probe: theory suggests that unstirred layers have significant impact. *Plant Cell and Environment* **28**, (in press). doi: 10.1111/j.1365-3040.2005.01384.x
- Virkki L.V., Franke C., Somieski P. & Boron W.F. (2002). Cloning and functional characterization of a novel aquaporin from *Xenopus laevis* oocytes. *Journal of Biological Chemistry* **277**, 40610–40616.
- Wan X.C., Steudle E. & Hartung W. (2004) Gating of water channels (aquaporins) in cortical cells of young corn roots by mechanical stimuli (pressure pulses): effects of ABA and of HgCl₂. *Journal of Experimental Botany* **55**, 411–422.
- Weig A., Deswarte C. & Chrispeels M.J. (1997) The major intrinsic protein family of *Arabidopsis* has 23 members that form three distinct groups with functional aquaporins in each group. *Plant Physiology* **114**, 1347–1357.

- Ye Q., Kim Y.M. & Steudle E. (2006) A quantitative re-examination of the role of unstirred layers (USLs) during the measurement of transport coefficients for water and solutes with the cell pressure probe: minor role of USLs. *Plant Cell and Environment* (in press).
- Ye Q., Muhr J. & Steudle E. (2005) A cohesion/tension model for the gating of aquaporins allows estimation of water channel pore volumes in *Chara*. *Plant Cell and Environment* **28**, 525–535.
- Ye Q., Wiera B. & Steudle E. (2004) A cohesion/tension mechanism explains the gating of water channels (aquaporins) in *Chara* internodes by high concentration. *Journal of Experimental Botany* **55**, 449–461.
- Ye Q. & Steudle E. (2006) Oxidative gating of water channels (aquaporins) in corn roots. *Plant Cell and Environment* **28**, (in press) doi: 10.1111/j.1365-3040.2005.01423.
- Zhang W.H. & Tyerman S.D. (1991) Effect of low O₂ concentration and azide on hydraulic conductivity and osmotic volume of cortical cells of wheat roots. *Australian Journal of Plant Physiology* **18**, 603–613.
- Zhang W.H. & Tyerman S.D. (1999) Inhibition of water channels by HgCl₂ in intact wheat root cells. *Plant Physiology* **120**, 849–858.
- Zhu F.Q., Tajkhorshid E. & Schulten K. (2004) Theory and simulation of water permeation in aquaporin-1. *Biophysical Journal* **86**, 50–57.
- Zhu G.L. & Steudle E. (1991) Water transport across maize roots. *Plant Physiology* **95**, 305–315.
- Zimmerberg J. & Parsegian V.A. (1986) Polymer inaccessible volume changes during opening and closing of a voltage-dependent ionic channel. *Nature* **323**, 36–39.
- Zimmermann H.M. & Steudle E. (1998) Apoplastic transport across young maize roots: effect of the exodermis. *Planta* **206**, 7–19.

II

Publications

**2 A cohesion/tension mechanism explains the gating of
water channels (aquaporins) in *Chara* internodes by
high concentration**

Qing Ye, Boguslaw Wiera and Ernst Steudle*

Department of Plant Ecology, Bayreuth University, D-95440 Bayreuth, Germany

Received 3 April 2003; Accepted 17 October 2003

*To whom correspondence should be addressed.

Fax: +49 921 55 2564

E-mail: ernst.steudle@uni-bayreuth.de

Journal of Experimental Botany (2004) 55: 449-461

DOI: 10.1093/jxb/erh040

Abstract

Isolated internodes of *Chara corallina* have been used to study the gating of aquaporins (water channels) in the presence of high concentrations of osmotic solutes of different size (molecular weight). Osmolytes were acetone and three glycol ethers: ethylene glycol monomethyl ether (EGMME), diethylene glycol monomethyl ether (DEGMME), and triethylene glycol monoethyl ether (TEGMEE). The ‘osmotic efficiency’ of osmolytes was quite different. Their reflection coefficients ranged between 0.15 (acetone), 0.59 (EGMME), 0.78 (DEGMME), and 0.80 (TEGMEE). Bulk water permeability (L_p) and diffusive permeabilities (P_s) of heavy water (HDO), hydrogen peroxide (H_2O_2), acetone and glycol ethers (EGMME, DEGMME and TEGMEE) were measured using a cell pressure probe. Cells were treated with different concentrations of osmotic solutes of up to 800 mM (\approx 2.0 MPa of osmotic pressure). Inhibition of aquaporin activity increased with both concentration and size of solutes (reflection coefficients). As cell L_p decreased, P_s increased indicating that water and solutes used different passages across the plasma membrane. Similar to earlier findings of an osmotic gating of ion channels (Zimmerberg & Parsegian 1986), a cohesion/tension model of the gating water channels in *Chara* internodes by high concentration is proposed. According to the model, tensions (negative pressures) within water channels affected the open/closed state by changing the free energy between states and favour a distorted/collapsed rather than the open state. They should have differed depending on the concentration and size of solutes that are more or less excluded from aquaporins. The bigger the solute, the lower was the concentration which induced a reversible closure of aquaporins, as predicted by the model.

Key words: aquaporins, *Chara*, cohesion/tension, gating, hydraulic conductivity, reflection coefficient, water channels.

Introduction

For a long time, water movement across cell membranes has been thought to be either due to transport across non-selective pores or to diffusion through the lipid bilayer (Dainty 1963; House 1974; Stein 1986; Finkelstein 1987). Since the discovery of aquaporins or water channels, however, more and more studies demonstrated that water channels represent the main selective pathway for water to move through the membranes of both plant and animal cells (Macey 1984; Preston *et al.* 1992; Verkman 1992; Maurel 1997; Steudle & Henzler 1995; Tyerman *et al.* 1999; Kjellbom *et al.* 1999; Murata *et al.* 2000). As ion channels, at least a subset of water channels is thought to be gated, although much less is known about the precise mechanisms of the gating of water channels (Yasui *et al.* 1999; Nemeth-Cahalan & Hall 2000; Kozono *et al.* 2002). The gating of water channels could play an important role in regulating water transport across cell membranes (Tyerman *et al.* 1999; 2002; Steudle 2000a, b; 2001). The activity of water channels could be decreased by different stresses such as high osmotic pressure, salinity, anoxia, heavy metals, nutrient deprivation, pH, calcium, and oxidative stress (Steudle & Tyerman 1983; Zhang & Tyerman 1991; Azaizeh *et al.* 1992; Birner & Steudle 1993; Steudle & Henzler 1995; Tazawa *et al.* 1996; Carvajal *et al.* 1996; Martinez-Ballesta *et al.* 2000; Henzler 2001; Gerbeau *et al.* 2002). Direct phosphorylation activates the hydraulic conductivity of channels (Johansson *et al.* 1996). The stress hormone ABA may transiently open aquaporins (Hose *et al.* 2000).

In this paper, we concentrate on a cohesion/tension mechanism of the gating of water channels in the presence of high concentration of osmotic solutes. For characean internodes, an inhibition of cell membrane L_p by high concentration is known for a long time, but the mechanism is not well understood (Kiyosawa & Tazawa 1972; Steudle & Tyerman 1983). For ion channels, Zimmerberg & Parsegian (1986) suggested that the open/closed states might be gated by osmotic pressure. According to the model, osmolytes, excluded from channels, may cause tensions (negative pressures) in the interior of channels which affect the difference in free energy between states by a term due to volume work. This should result in a reversible deformation of the protein. The proposed cohesion/tension mechanism is different from that known for the xylem of

higher plants which has been much discussed in the past decade (Steudle 2001; Tyree & Zimmermann 2002). In the xylem, the closed state is represented by embolized vessels. In aquaporins, however, mechanically distorted or collapsed membrane pores (aquaporins) represent the closed state.

We test whether or not this mechanism may work for the aquaporins (water channels) of *Chara* which are known to be affected by osmotic pressure. We used isolated internodes of *Chara corallina* for these studies. The aquaporins of this species have not yet been characterized from a molecular point of view. However, there are already very detailed functional studies (see lit. cited above). The *Chara* system has the advantage that it represents an isolated intact plant cell; no vesicles, as used with the stopped-flow technique: It is very stable, even when cells are subjected to substantial stresses for long periods of time. As osmotic solutes, we used acetone (MW: 58 Da) and glycol ethers of different size (monomethyl ethers of ethylene glycol and diethylene glycol, monoethyl ether of triethylene glycol; MW: 76 to 178 Da). The *Chara* membrane was permeable to these osmolytes which could be, hence, applied on both sides of the membrane at the same concentration. Solutes were not harmful, even when treating cells for several days at concentrations of up to 800 mM (equivalent to 2.0 MPa of osmotic pressure). Depending on its size, solutes should be excluded from channels to a different extent. Hence, we expected characteristic differences in changes of the bulk permeability for water (hydraulic conductivity, L_p) and of the permeability of solutes which use water channels to cross membranes. We also expected characteristic changes in reflection coefficients as shown for other inhibitors of water channel activity (Steudle & Henzler 1995; Tazawa *et al.* 1996; Henzler 2001; Tyerman *et al.* 1999; 2002). Expectations with respect to a cohesion/tension model of aquaporins could be verified suggesting that the model may be correct. However, there were deviations from expectations suggesting that treatments with the glycol ethers did also affect transport properties of the bilayer.

Materials and methods

Plant material

Chara corallina was grown in artificial pond water (APW; composition in mole m⁻³: 1.0 NaCl, 0.1 KCl, 0.1 CaCl₂ and 0.1 MgCl₂) in tanks which contained a layer of natural pond mud (Henzler and Steudle, 2000). Temperature was kept at 23 – 25 °C. Tanks were placed on the ground of the laboratory, and were illuminated for 24 h a day with a 15 W fluorescent lamp (Electronic, Germany) positioned 0.2 m over the water surface. *Chara* internodes used in cell pressure probe experiments were 60 to 120 mm in length and 0.8 to 1.0 mm in diameter.

Calculation of transport parameters (L_p, P_s and σ_s)

Three parameters were calculated from ‘hydrostatic’ (hydraulic conductivity, L_p) and ‘osmotic’ experiments (permeability, P_s, and reflection coefficient, σ_s) as previously described (Steudle, 1993). In hydrostatic experiments, turgor pressure (P) was rapidly changed with the aid of a cell pressure probe to induce water flows across the cell membrane in both directions. Hydraulic conductivity (L_p) was calculated from hydrostatic pressure relaxations, in which the half time (T_{1/2}^w) of water exchange between cell interior and the medium was measured (Hertel & Steudle 1997):

$$L_p = \frac{V}{A} \times \frac{\ln(2)}{T_{1/2}^w (\varepsilon + \pi^i)} \quad (1)$$

Here, V = cell volume; A = cell surface area; πⁱ = osmotic pressure of cell sap; ε is the elastic coefficient of the cell (elastic modulus). A and V were obtained from measuring diameter and length of cylindrical internodes; πⁱ was calculated from the initial cell turgor (P_o) and the osmotic pressure of the medium (APW), as P_o = πⁱ - π^o (π^o = osmotic pressure of the medium as measured with an osmometer); elastic modulus ε = V x dP/dV ≈ V x ΔP/ΔV was determined from relative changes of cell volume (ΔV/V) and the instantaneous changes of turgor (ΔP) using the probe.

In osmotic experiments, permeating test solutes (HDO, H₂O₂, acetone, ethylene glycol monomethyl ether (EGMME), diethylene glycol monomethyl ether (DEGMME), triethylene glycol monoethyl ether (TEGMEE)) were added to the medium (APW). The osmotic pressure of the medium was changed in time intervals which were short compared to $T_{1/2}^w$. In the presence of permeating solutes, osmotic response curves were biphasic (Steudle & Tyerman 1983; Steudle 1993). There was a first phase during which turgor pressure rapidly decreased or increased due to an exosmotic/endosmotic water flow. The ‘water phase’ was rapid because of the high permeability of the cell membrane to water. It was followed by a ‘solute phase’. During the second phase, turgor increased/decreased again due to the passive flow of solute into or out of the cell tending to equilibrate the concentration of permeating solutes on both sides of the cell membrane. Rates of solute phases strongly depended on the nature of solutes used. Solutes which were soluble in the lipid phase of the membrane had short half-times ($T_{1/2}^s$); those which were polar (ions, hydrophilic solutes), had long half-times (Henzler & Steudle 1995). Permeability (P_s) and reflection (σ_s) coefficients were calculated from response curves using the following equations (Steudle & Tyerman 1983; Steudle 1993). For the solute permeability coefficient, we used:

$$P_s = \frac{V}{A} \times \frac{\ln(2)}{T_{1/2}^s} = \frac{V}{A} k_s \quad (2)$$

where k_s is the rate constant of solute exchange. For the reflection coefficient, we used:

$$\sigma_s = \frac{P_o - P_{\min(\max)}}{RT \cdot \Delta C_s^o} \times \frac{\varepsilon + \pi^i}{\varepsilon} \exp(k_s \cdot t_{\min(\max)}) \quad (3)$$

Here, $P_o - P_{\min(\max)}$ is the maximum change in cell turgor pressure; ΔC_s^o was the given change of osmotic pressure of the medium.

Measurement of transport parameters (L_p , P_s and σ_s)

As described previously, an internode was freed from adjacent internodes and branches and placed in a glass tube (inner diameter: 3 mm) with one node protruding at one end and was fixed by a clamp to make the cell secure and to avoid vibrations which may have induced leakages (sudden pressure drops) during the measurements (Henzler & Steudle 1995; Hertel & Steudle 1997). The probe was introduced through the protruding

node. Artificial pond water (APW) or test solutions were pumped through the other end of the glass tube along the cell so that the solution around the cell was vigorously stirred. This minimized the thickness of external unstirred layers (Steudle & Tyerman 1983). APW was rapidly exchanged by solutions with different osmotica and osmotic pressures in times which were much shorter than $T_{1/2}^w$ or $T_{1/2}^s$. During the experiments, cells were illuminated by an Osram halogen lamp through glass fiber optics.

When the pressure probe was inserted into the internode through the protruding node, an oil/cell sap meniscus was formed in the tip of the probe. This served as a point of reference during measurements. With the aid of the probe, the position of the meniscus was changed forward or backward and was kept stable after the change. This resulted in pressure relaxations. L_p was calculated from the $T_{1/2}^w$ of relaxations. Effects of external concentration on the activity of aquaporins or water channels were determined using concentration series of several osmotic solutes (acetone, EGMME, DEGMME, or TEGMEE). To avoid plasmolysis, concentration was increased in four steps of 200 mM. When turgor pressure was stable following a step change in concentration, four hydrostatic pressure relaxations were induced to measure L_p at that concentration. Small hydrophilic test solutes like HDO and H_2O_2 have been shown to use water channels to pass through the cell membrane (Henzler & Steudle 1995; 2000). Acetone largely uses the bilayer to move across the cell membrane. Solute were added to the medium to determine concentration effects on P_s and σ_s . Because of their big molecular size, solutes such as EGMME, DEGMME and TEGMEE were expected to not using water channels to pass the cell membrane (Table1).

Cell turgor was higher than 0.55 MPa. Within ± 0.02 MPa, turgor remained constant during the experiments with a given cell which lasted for 7 to 8 h. To remove solutes taken up by the internodes, the external concentration of the medium was reduced in steps of 200 mM until APW was reached again. L_p , P_s and σ_s were re-examined to ensure that effects were completely reversible.

Table 1. Name, reflection coefficient, molecular weight and molecular structure of the solutes used in experiments. Reflection coefficients (σ_s) were measured at concentrations of 3.55 M for HDO, 60 mM for H₂O₂, 160 mM for acetone and 60 mM, 40 mM, 25 mM for EGMME, DEGMME, TEGMEE, respectively. Values are means \pm SD (n = 6).

solute name	reflection coefficient(σ_s)	molecular weight(g/mol)	molecular structure
HDO	0.004 \pm 0.001	19	HDO
H ₂ O ₂	0.36 \pm 0.04	34	H ₂ O ₂
acetone	0.15 \pm 0.03	58	CH ₃ COCH ₃
EGMME	0.59 \pm 0.03	76	HOCH ₂ CH ₂ OCH ₃
DEGMME	0.78 \pm 0.05	120	HOCH ₂ CH ₂ OCH ₂ CH ₂ OCH ₃
TEGMEE	0.80 \pm 0.07	178	HOCH ₂ CH ₂ OCH ₂ CH ₂ OCH ₂ CH ₂ OCH ₂ CH ₃

EGMME: ethylene glycol monomethyl ether

DEGMME: diethylene glycol monomethyl ether

TEGMEE: triethylene glycol monoethyl ether

Results

In Figure 1, typical hydrostatic pressure relaxations and biphasic osmotic response curves are shown for two individual cells A and B. Cells were either treated by 820 mM acetone (Fig. 1A) or with the smallest glycol ether EGMME (Fig. 1B). Table 2 summarizes the results from all 32 cells treated either with 820 mM acetone or EGMME. It can be seen from the figure and table that treatment with high external concentrations increased half times of water exchange during hydrostatic pressure relaxations by a decrease of hydraulic conductivity (L_p ; Eq. (1)). In the presence of the bigger solute, effects on $T_{1/2}^w$ (L_p) were bigger than in the presence of acetone (see also Fig. 3).

Table 2. Half times of the exchange of water ($T_{1/2}^W \sim 1/Lp$) and of permeating solutes (HDO, H₂O₂ and acetone; $T_{1/2}^s \sim 1/P_s$) across the cell membrane of *Chara* internodes as measured in control medium (APW) and during high concentration treatments of 820 mM acetone or EGMME (see Fig. 1). $T_{1/2}^W$ and $T_{1/2}^s$ of HDO and H₂O₂ increased due to the closure of water channels in the presence of high concentration. Different from water, HDO and H₂O₂, acetone mainly used bilayer to pass through cell membrane, and its $T_{1/2}^s$ (P_s) did not change significantly. Mean values are given \pm SD.

Test solutes	No. of cells (n)	<u>820 mM acetone</u>		<u>820 mM EGMME</u>	
		control	treated	control	treated
		$T_{1/2}^W$ [s]	$T_{1/2}^s$ [s]	$T_{1/2}^W$ [s]	$T_{1/2}^s$ [s]
H ₂ O	16	2.1 \pm 0.3	3.0 \pm 0.4	2.0 \pm 0.3	3.6 \pm 0.6
HDO	16	22.8 \pm 2.3	29.1 \pm 2.8	24.2 \pm 3.8	30.5 \pm 4.8
H ₂ O ₂	16	39.6 \pm 4.3	51.6 \pm 8.5	39.8 \pm 5.3	55.2 \pm 8.3
acetone	16	36.9 \pm 4.4	38.2 \pm 3.9	36.0 \pm 4.1	38.6 \pm 5.9

It can be seen from Fig. 1A, B and Table 2 that the permeability of HDO and H₂O₂ decreased in the presence of acetone and EGMME ($T_{1/2}^s$ increased), but there were no significant differences in the effects of the osmolytes. HDO and H₂O₂ largely use water channels to cross the plasma membrane of *Chara* (Hertel & Steudle, 1997; Henzler & Steudle, 2000). The permeability of HDO is usually denoted as the diffusional permeability of water (P_d) which is smaller than the bulk water permeability (L_p or P_f) when compared in the same units. For *Chara*, Steudle & Henzler (1995) found a P_f/P_d ratio of around 25. High concentrations did not significantly affect the permeability of acetone.

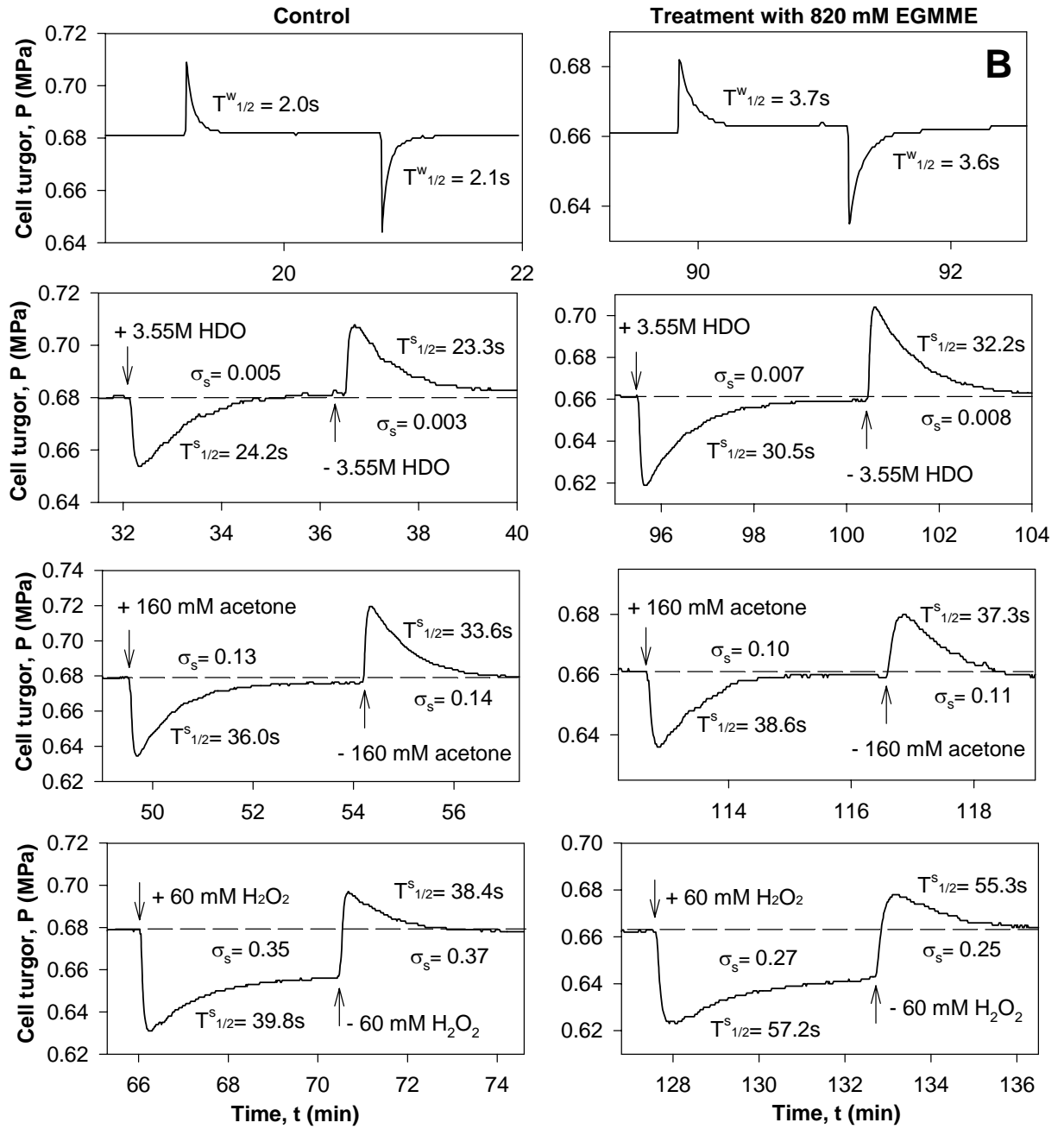


Fig. 1 Typical hydrostatic relaxations of cell turgor pressure (top) and biphasic osmotic response curves as measured by cell pressure probes in two *Chara* internodes, when water channels were partly closed by treatment with 820 mM acetone (A) or 820 mM EGMME (B). The control was artificial pond water (APW). There was an increase in the half time of water exchange, $T^w_{1/2}$, which corresponded to a

decrease in cell hydraulic conductivity, L_p ($1/L_p \sim T_{1/2}^W$; Eq. (1)). Half times for solutes, $T_{1/2}^s$ of HDO and H_2O_2 decreased as well. These solutes largely use water channels to cross the membrane. Different from HDO and H_2O_2 , acetone mainly used bilayer to pass through membrane, and its $T_{1/2}^s$ remained constant. In osmotic relaxations, solutes were first added at concentrations indicated, and then removed again from the medium. For H_2O_2 , final turgor pressures obtained in response curves were not identical with original values. This was due to the action of catalase in the cell which tended to keep the final concentration of H_2O_2 in the cell smaller than that outside. Average values of changes in $T_{1/2}^W$ and $T_{1/2}^s$ for all 32 cells used are given in Table 2.

Table 3. Reflection coefficient (σ_s) of H_2O_2 at control (APW) and at concentrations of high osmolarity (820 mM = 2.05 MPa of osmotic pressure) of either acetone or EGMME. There was a significant decrease of σ_s during treatments with EGMME (t-test; $p = 0.05$), but for treatments with acetone the decrease of σ_s was not significant (t-test; $p = 0.05$). In some of the cells (No. 9 and 10), the decrease in σ_s in the presence of EGMME was down to 60% of the original value. In these cases, the second phase was missing in biphasic responses (Fig. 2).

Cell No.	Reflection coefficients (σ_s) of H_2O_2 [1]			
	control	820mM acetone	control	820mM EGMME
1	0.38	0.36	0.33	0.31
2	0.33	0.32	0.33	0.25
3	0.38	0.30	0.27	0.20
4	0.31	0.25	0.36	0.35
5	0.44	0.37	0.40	0.30
6	0.33	0.33	0.35	0.29
7	0.40	0.39	0.31	0.23
8	0.40	0.33	0.36	0.32
9	-	-	0.37	0.21
10	-	-	0.31	0.19
Mean	0.37	0.33	0.34	0.27
\pm SD	0.04	0.05	0.04	0.06

For H_2O_2 , biphasic pressure relaxations looked somewhat different from those of the other solutes (bottoms of Figs. 1A, B). This is due to the fact that H_2O_2 was subject to metabolic degradation in the cells due to the presence of catalase (Henzler & Steudle

2000). Hence, a concentration difference between the medium and cell interior is maintained in the steady state. Effects due to the degradation of H_2O_2 were taken into account when calculating the P_s and σ_s of H_2O_2 from $T_{1/2}^s$. High concentration treatments caused reflection coefficients of H_2O_2 to decrease (Table 3).

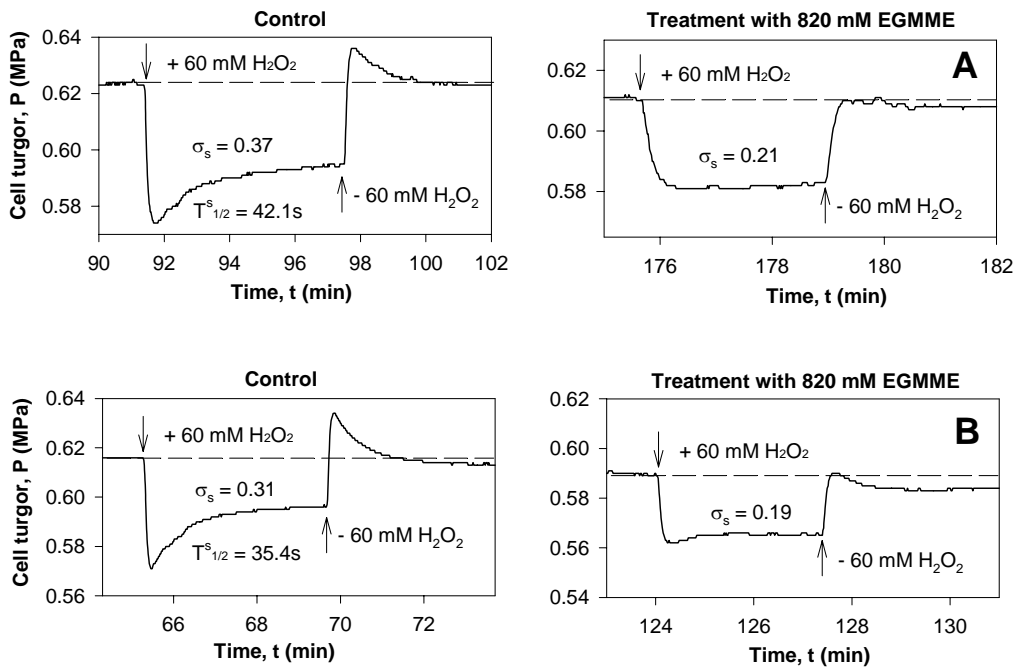


Fig. 2 In some cells (2 out of 10 cells), the inhibition of water channels by high concentration of osmotic solutes sitting in both sides of the membrane resulted in response curves in which the solute phase was completely missing (A) or nearly so (B). This was due to the fact that flow of H_2O_2 was strongly reduced. Hence, all the H_2O_2 entering the cell was immediately metabolized. In this case, reflection coefficients were reduced to 60% of the original value. For the cell shown in Fig. 2B, the turgor pressure slightly decreased during the experiment. This indicated that the cell was tending to become leaky in the presence of two stresses applied (osmotic and oxidative stresses). However, this case was fairly rare to happen.

Fig. 2 shows that in some cells (2 out of 10 cells), the inhibition of water channels resulted in response curves in which the solute phase was completely missing. This was due to the fact that flow of H_2O_2 was strongly interrupted. Hence, all the H_2O_2 entering the cell was immediately metabolized. Similar results have been obtained earlier, when

channels were closed by HgCl_2 (Henzler & Steudle 2000). In this case, reflection coefficients were much reduced as can be seen in Fig. 2.

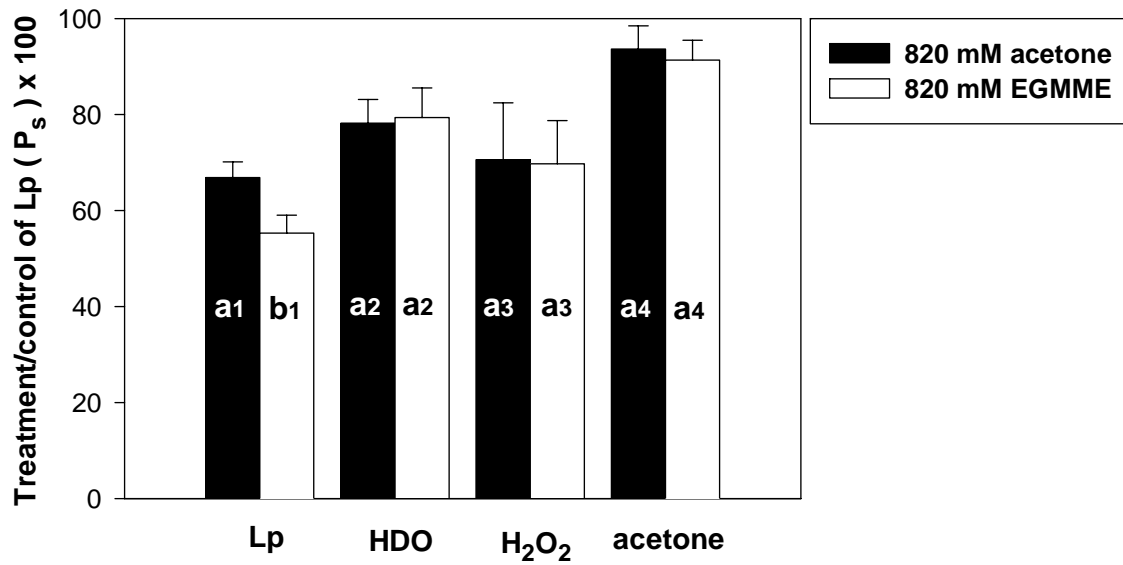


Fig. 3 Effects of high concentration (820 mM acetone and EGMME) on the hydraulic conductivity and the diffusive permeabilities of different solutes (HDO, H_2O_2 and acetone) across *Chara* internodes (means of $n = 16$ cells \pm SD). Relative changes are given rather than absolute values to avoid the variability between cells. It can be seen that osmolytes applied at high concentration reduced water and solute permeabilities. The permeability of acetone which moved across the bilayer, was not significantly affected (t-test; $p = 0.05$). Effects of the bulky EGMME on cell L_p significantly differed from those of acetone ($p = 0.05$), but there were no significant differences between osmolytes with respect to changes in the permeabilities of HDO, H_2O_2 and acetone as denoted by the symbols in the columns.

Fig. 3 summarizes effects of the small osmolyte acetone (820 mM) and the big osmolyte EGMME (820 mM) on the hydraulic conductivity and the permeabilities of HDO, H_2O_2 , and acetone. To avoid problems with differences in the absolute values of transport coefficients between cells, relative changes are given \pm SD. It can be seen from the figure that effects on L_p (bulk water flow) were largest. There was no significant effect on the permeability of acetone although it appeared that P_s was slightly reduced. The difference between the small osmolyte acetone and the bigger

osmolyte EGMME in the effect on the bulk water flow (L_p) was significant ($p = 0.05$). However, there were no differences in the effects of the two osmolytes on the diffusive water flow (HDO) or the permeability of H_2O_2 . Although HDO and H_2O_2 differ in size, there was no significant difference in the inhibition of permeability neither in the presence of high acetone nor EGMME. However, permeabilities of both solutes were significantly reduced as compared with that of acetone.

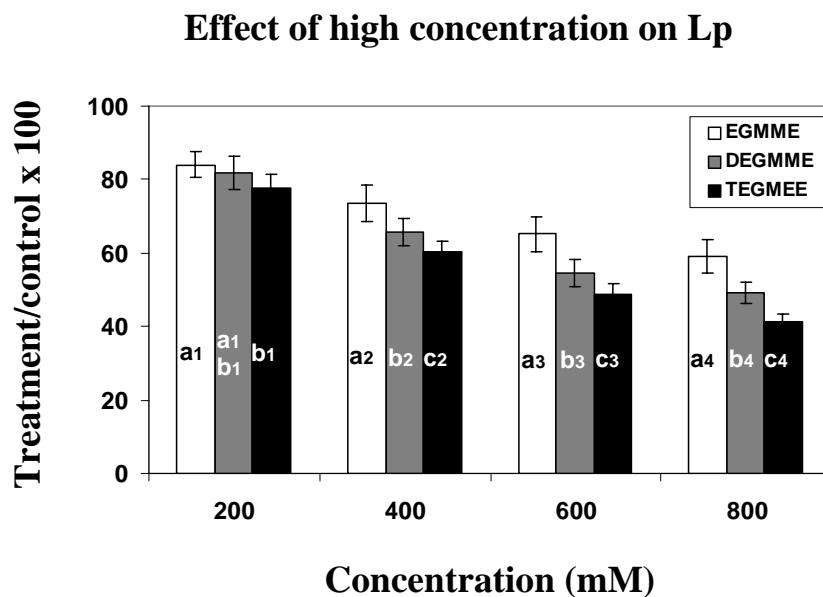


Fig. 4 Relative effect of concentration of the three big osmolytes (glycol ethers EGMME, DEGMME and TEGMEE) on bulk water permeability (L_p) of *Chara* internodes. Solutes were added in steps of 200 mM, and solute equilibration between medium and cell interior was waited for after each step. L_p decreased as the concentration on both sides of the membrane increased from 200 mM to 800 mM. The bigger the molecular size of the solute, the bigger was the effect on L_p ($n = 6$ cells for each type of measurement). As in Fig. 3, mean values of relative changes are given rather than absolute values to avoid differences in the absolute values of L_p between cells. Different symbols in columns denote significant differences between solutes at a given concentration (t-test; $p = 0.05$).

In Fig.4, effects on L_p are compared for the three big osmolytes EGMME, DEGMME and TEGMEE (Table 1) for four different concentrations (200, 400, 600, and 800 mM) which correspond to osmotic pressures of 0.5, 1.0, 1.5 and 2.0 MPa, respectively. There was a clear trend for L_p to decrease with increasing external concentrations of the three

osmotic solutes. Effects significantly increased with increasing molar weight of osmolytes ($p = 0.05$), except for the smallest concentration of 200 mM. At 200 mM, effects only differed significantly between the smallest (EGMME) and the biggest solute (TEGMEE). At the highest external concentration of 800 mM, reductions in cell L_p were as large as 41% to 59% depending on the solute.

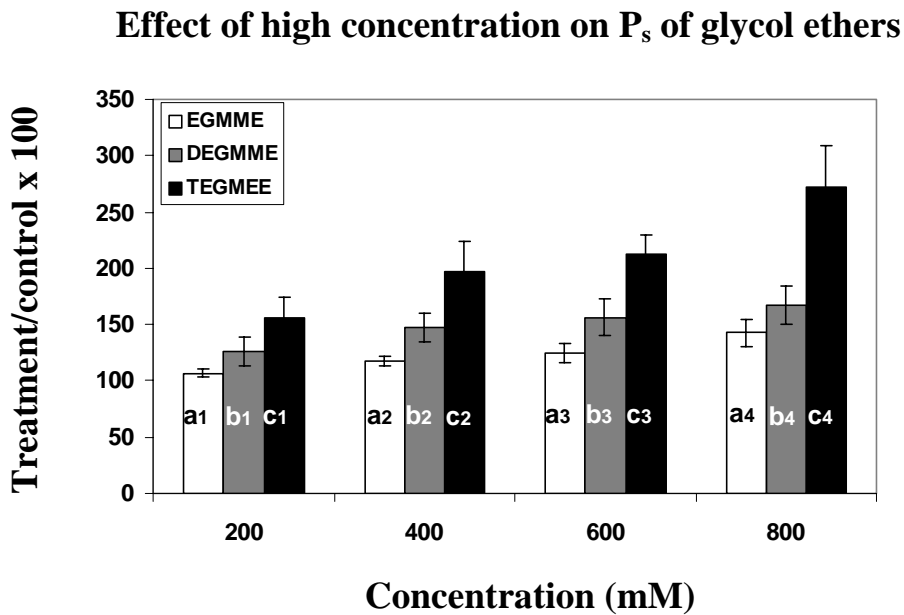


Fig. 5 Relative effect of concentration of the three ‘big’ osmotic solutes (glycol ethers EGMME, DEGMME and TEGMEE) on the permeability of these solutes (P_s). Different from the water (Fig. 4), P_s increased as the concentration around the cell membranes increased from 200 mM to 800 mM. The bigger the molecular size of the solute, the bigger was the increase of P_s ($n = 6$ cells for each type of measurement). As in Figs. 3 and 4, means of relative changes are given \pm SD. Different symbols in columns denote significant differences between solutes at a given concentration (t-test; $p = 0.05$).

The cell membrane was permeable to all three big osmolytes EGMME, DEGMME and TEGMEE. Permeability coefficients were obtained from biphasic pressure relaxations. Different from (bulk) water permeability (Figs. 1 to 3), permeability coefficients of big osmotic solutes increased with both increasing external concentration and size of osmolyte (Fig. 5). Compared to the control, P_s of EGMME, DEGMME and TEGMEE increased to 107%, 127% and 156% respectively, when the external concentration was

200 mM. At 800 mM, the P_s of EGMME, DEGMME and TEGMEE increased to 143%, 168% and 272% of the control, respectively. The opposite effect of high concentration on water than on solute permeability indicates that they use different pathways to cross the membrane.

Reflection coefficients of untreated cells increased with the size/molecular weight of osmolytes for EGMME, DEGMME and TEGMEE as one would expect (Table 1). Increase of high external concentration resulted in a decrease of σ_s (Fig. 6). However, the tendency was not as clear as that of L_p and P_s . At a first sight, this is surprising. For a homogeneous membrane, σ_s should be reduced with an increasing value of P_s/L_p . In the absence of an interaction between solute and water flow (i.e. in the absence of membrane pores used by both water and solutes), it should be valid that (Katchalsky & Curran, 1965; \bar{V}_s = molar volume of solute):

$$\sigma_s = 1 - \frac{\bar{V}_s \cdot P_s}{L_p \cdot RT} \quad (4)$$

As the effects of P_s/L_p ratios on σ_s in Fig.6 were much smaller than expected from Eq.(4), this simple model of the membrane does not apply.

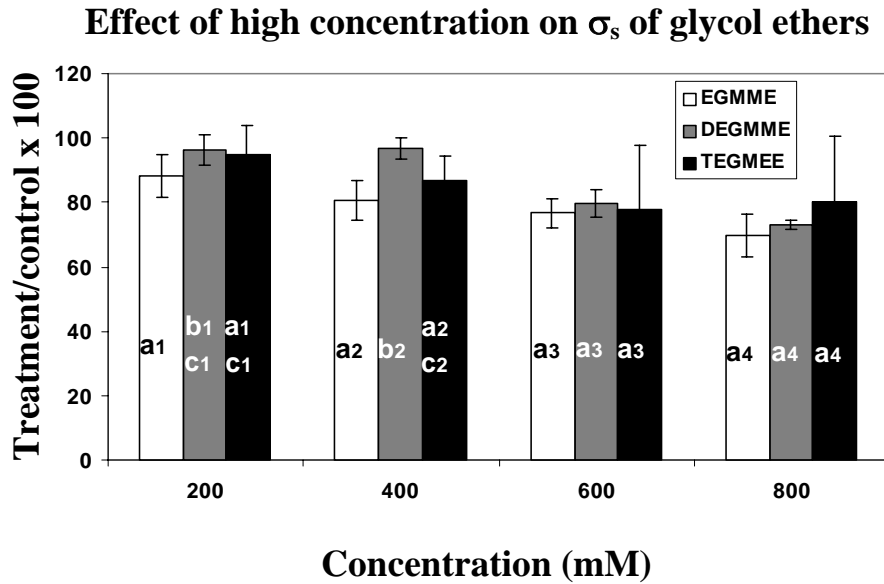
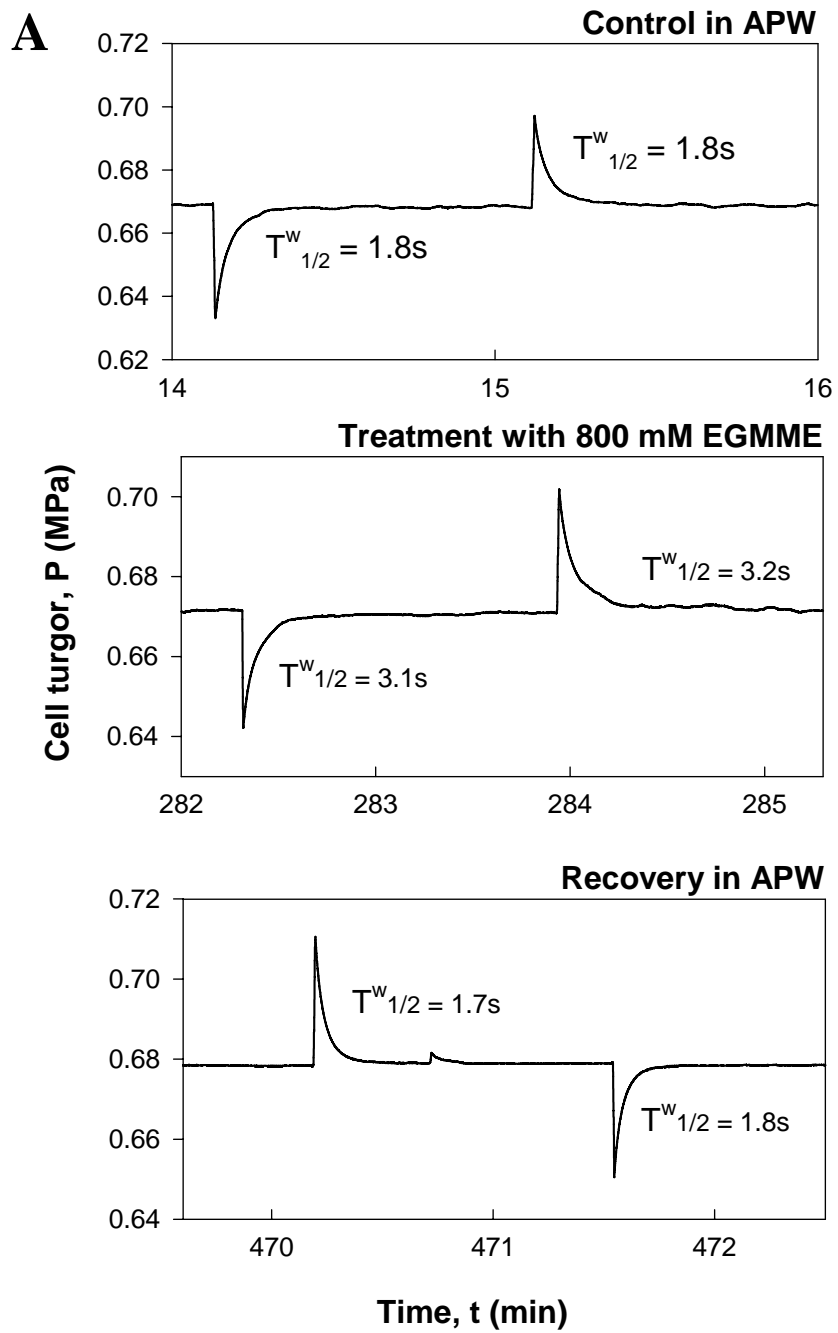
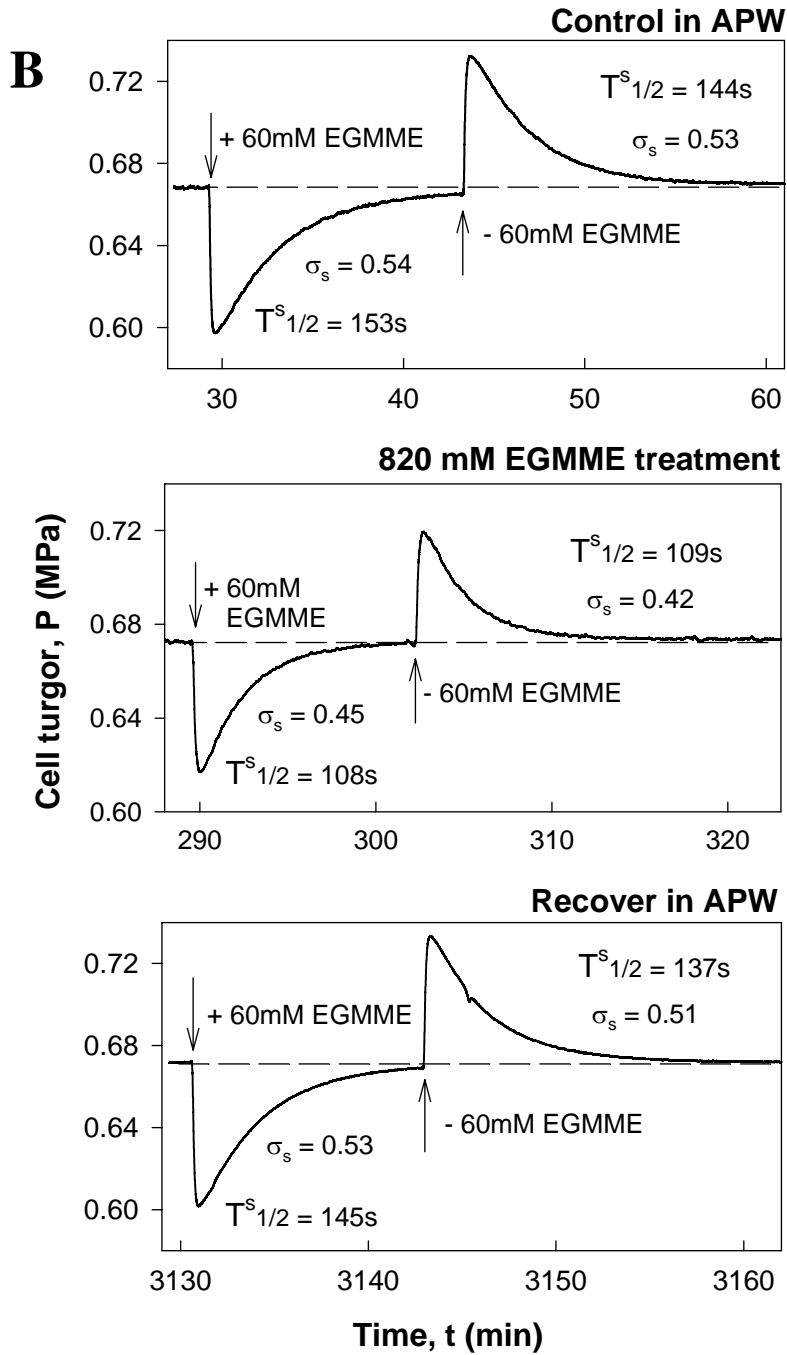


Fig. 6 Relative effect of concentration of the three ‘big’ osmotic solutes (glycol ethers EGMME, DEGMME and TEGMEE) on reflection coefficients of these solutes (σ_s). σ_s values tended to decrease as the concentration around the membrane increased from 200 mM to 800 mM. However, the tendency in the changes was not as clear as that of the L_p and P_s ($n = 6$ cells for each type of measurement). Absolute values of reflection coefficients in the presence of artificial pond water were: EGMME: $\sigma_s = 0.59$; DEGMME: $\sigma_s = 0.78$; TEGMEE: $\sigma_s = 0.80$ (measured at a concentration of 25 to 60 mM of solute in the medium, see Table 1). As in Figs. 3, 4 and 5, means of relative changes are given \pm SD. Different symbols in columns denote significant differences between solutes at a given concentration (t-test; $p = 0.05$).





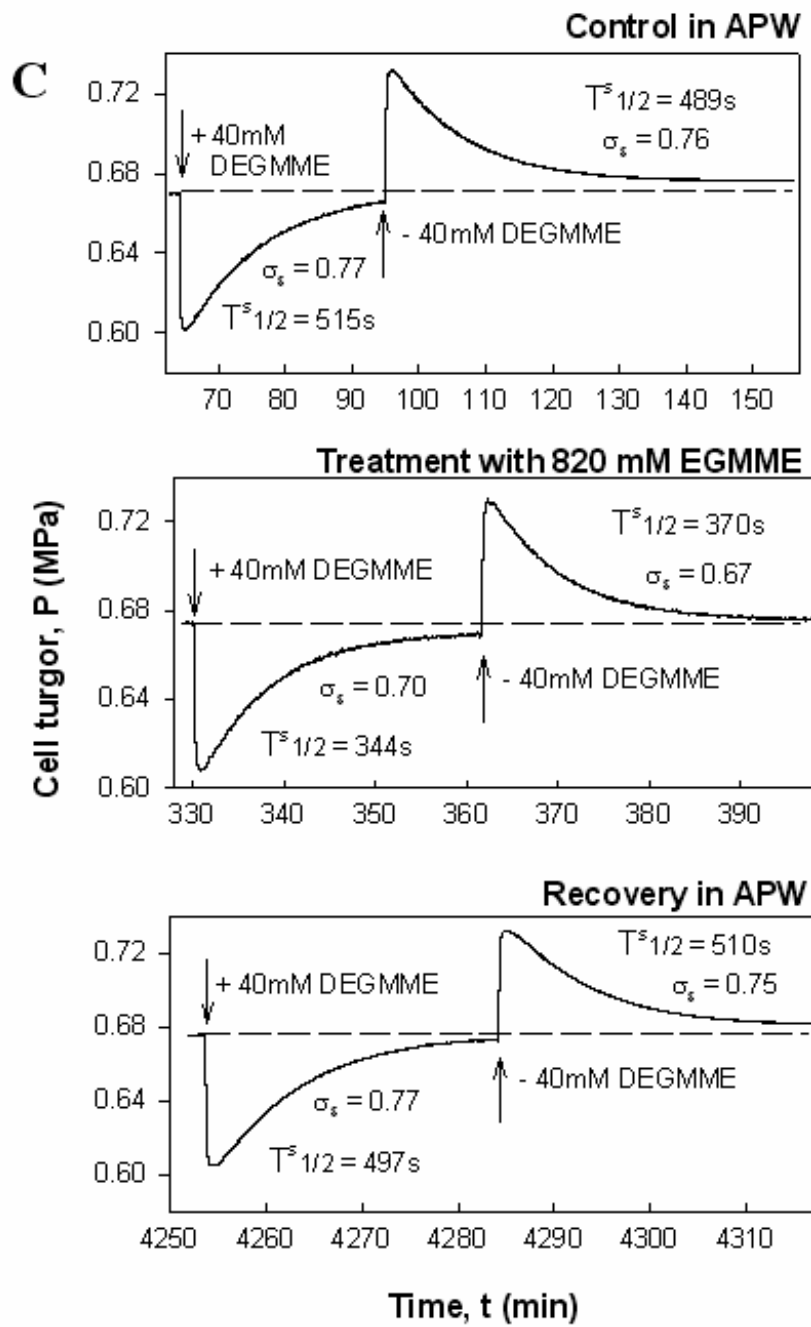


Fig. 7 (A) Recovery of hydraulic conductivity ($L_p \sim 1/T_{1/2}^w$) in a *Chara* internode following a treatment by 800 mM EGMME which increased half time of water exchange ($T_{1/2}^w$) by 75% and decreased L_p accordingly. The original $T_{1/2}^w$ (L_p) was re-attained when the external concentration was brought back in steps to that of the original medium (APW) and keeping the cell there for 2h. **(B)** Recovery of permeability of EGMEE ($P_s \sim 1/T_{1/2}^s$) in a *Chara* internode following a treatment of 800 mM EGMME. Osmotic treatment reduced half time ($T_{1/2}^s$) of solute permeability of EGMME by 27% and increased P_s accordingly. After changing the medium back to APW and incubating the cell in APW for 47h, the original value of $T_{1/2}^s$ (P_s) was re-attained. Changes in the reflection coefficient (σ_s) were completely reversed as well. **(C)** Recovery of permeability of DEGMME ($P_s \sim 1/T_{1/2}^s$) in a *Chara* internode following a treatment of 800 mM EGMME. Treatment reduced half time ($T_{1/2}^s$) of flow of DEGMME by 29% and increased P_s by accordingly. After changing back to APW and incubating the cell in APW for 65h, the original value of $T_{1/2}^s$ (P_s) was re-attained. Changes in the reflection coefficient (σ_s) were completely reversed as well.

Experiments with individual cells were performed over time intervals of as long as 7 to 8 h. Therefore, it was necessary to carefully check for reversibility. To do this, solutes were removed from internodes by lowering the external concentration in steps of 200 mM, and L_p , P_s and σ_s were again measured. A set of typical curves with 800 mM EGMME treatment in a single internode is shown in Fig. 7. Test solutes added or subtracted from the basic medium were ± 60 mM EGMME and ± 40 mM DEGMME, respectively. The half time of water flow increased by 75% during EGMME treatment (Fig. 7A), but $T_{1/2}^s$ of EGMME and DEGMME decreased by 27% (Fig. 7B) and 29% (Fig. 7C), respectively. It can be seen that the half time of water was completely recovered within less than 2h. However, for the solute permeability of EGMME and DEGMME, time intervals required to restore the original P_s were as long as 47 h and 65 h, respectively. Reflection coefficients of the test solutes were completely reversible after changing the medium back to APW (Fig. 7). Compared with original values of cell turgor of 0.55 to 0.70 MPa, changes in turgor were as small as ± 0.02 MPa at the end of the experiments.

Discussion

The data clearly demonstrate that the *Chara* system was remarkably stable and allowed reversible measurements with a single internode for time periods of as long as two to three days, depending on the osmotic stresses applied. It took a long time to remove the high molecular weight glycol ethers from *Chara* internodes (47 h and 65 h for EGMME and DEGMME, respectively). However, absolute values of transport coefficients (L_p , P_s , σ_s) were completely reversed even for these solutes, when the medium was changed back to APW. Cell turgor pressure remained constant within $\pm 4\%$ during long term experiments. Hence, the integrity of cell membranes was not affected. It appears that the osmotic treatment with glycol ethers was not harmful to the cells, even for concentrations of as high as 800 mM (equivalent to 2.0 MPa of osmotic pressure). Additional experiments showed that there was no significant effect on the cytoplasmic streaming of *Chara* internode under even higher concentration than used in the present study (concentration of glycol ethers of up to 1.2 M; data not shown). Obviously, there were much less side effects during the osmotic treatment than during treatment with HgCl_2 which caused drops in turgor when treatment was longer than about 10 or 20 min (Henzler & Steudle 1995). Hence, for *Chara* the gating by high concentration represents a procedure alternative to the standard use of mercurials to study effects of the closure of water channels on water permeability (L_p), but also on membrane selectivity (σ_s) and solute permeability (P_s). Appropriate solutes should be not harmful to cells and should exhibit a relatively high solute permeability at a relatively high σ_s to achieve high concentrations on both sides of the cell membrane within reasonable time intervals.

In the presence of high concentrations of glycol ethers applied to both sides of the membrane, both the bulk water permeability (L_p) and diffusional permeabilities of HDO and H_2O_2 were reduced. The chemical structures of the latter two solutes are similar to that of water. It has been shown that they largely use water channels to cross the membrane (Henzler & Steudle 1995; 2000). The permeability of acetone was not affected which should mainly use the bilayer, although there is some slippage across water channels for *Chara* (Hertel & Steudle 1997). The present results indicate a stronger effect of high external concentration on the bulk (hydraulic or osmotic) than on

the diffusional (heavy) water flow (P_d) across water channels. This may be interpreted by different mechanisms. For a macroscopic pore, the bulk water flow increases with r^4 (r = radius of the pore; Poiseuille's law), but diffusional water flow should increase with the cross-sectional area of the pore, i.e. with r^2 . Although the macroscopic picture may not exactly hold for narrow pores exhibiting a single-file transport of water, there could be, nevertheless, substantial differences (see discussion in Steudle & Tyerman 1983). It is interesting that besides the high P_f/P_d ratios found earlier for *Chara* (see Results), there was also a big difference in the temperature dependence of L_p and P_d in *Chara*. According to Hertel & Steudle (1997) the bulk water flow (L_p , P_f) was much more affected by changes in temperature than the diffusional water flow (P_d). This has been interpreted by differences in the mechanism as well.

According to Fig.1, there were big differences between reflection coefficients of hydrogen peroxide and heavy water, although both largely use water channels to cross the cell membrane (σ_s of HDO: 0.004; σ_s of H_2O_2 : 0.36). Differences in $T_{1/2}^s$ were much smaller indicating a P_s of H_2O_2 which was smaller by only a factor of less than two as compared with HDO. Henzler & Steudle (2000) reported similar findings during inhibition with $HgCl_2$. They interpreted the result assuming that there was a population of water channels present, part of which did not allow the passage of H_2O_2 because they were too narrow. When water channels were closed in the presence of 50 μM $HgCl_2$, this resulted in a decrease of the reflection coefficient for H_2O_2 and an increase of the half time of the solute phase. This was observed here, too, when channels were closed in the presence of high concentration (Fig. 1A, B). Compared with the mercury experiments, effects on the reflection coefficient were less pronounced, although for a few cells changes in the reflection coefficient were as large as a factor of two. This latter result is similar to the effects observed in the presence of $HgCl_2$. Overall, the present results do point into a direction similar to that discussed by Henzler & Steudle (2000). They favour the idea that there was a population of water channels of different diameter, some of them used as aquaporins whereas others were functioning as 'peroxoporins'.

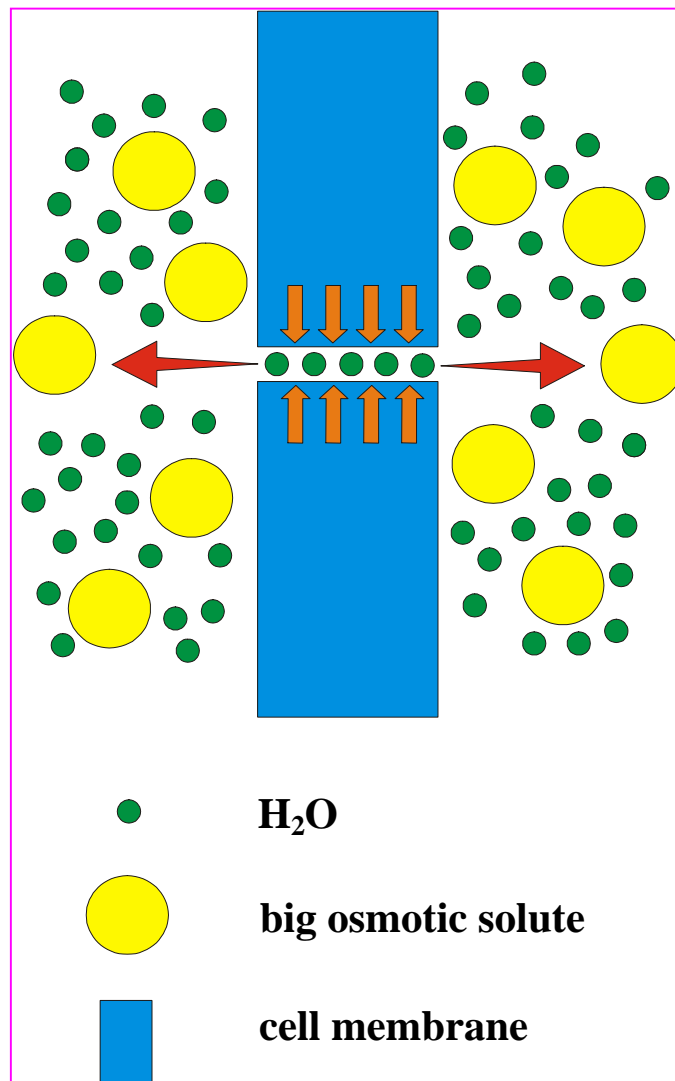


Fig. 8 Cohesion/tension model of the gating of water channels in membranes of *Chara* internodes by high concentration. The model does not include variations in the diameter of channels (see text). During the experiments, osmolytes were present on both sides of the membrane. Since solutes were excluded from aquaporins, tensions were set up in the pores which caused a reversible mechanical deformation of the protein as tensions (negative pressures) increased and a closure of the channel. The bigger the size of a solute, the higher its efficiency in exerting tensions within pores. Highest concentrations used in this study were 800 mM which was equivalent to 2 MPa or 20 bar of osmotic pressure. At a complete exclusion from pores, this refers to tensions of 20 bar or minus 20 bar of hydrostatic pressure in the pores.

Zimmerberg & Parsegian (1986) suggested that the open/closed states of ion channels might be gated by osmotic pressure. These authors used osmotic solutes which were much bigger than those used in the present paper and were completely excluded from channels (PEG, MW: 20,000; polyvinylpyrrolidone, MW: 40,000; dextran, MW: 500,000). Hence, they should have caused tensions (negative pressures) in the water in the channels to balance the water potential between pores and medium. A term for the volume work ($V_c \cdot \Delta P_c$) was added to the Boltzmann distribution of open and closed states by Zimmerberg & Parsegian (1986; see also Finkelstein 1987), i.e:

$$\frac{t_o}{t_c} = \exp \frac{-(\Delta G' - V_c \cdot \Delta P_c)}{RT} = \exp \frac{-\Delta G'}{RT} \cdot \exp \frac{V_c \cdot \Delta P_c}{RT} . \quad (5)$$

According to Eq. (5), the ratio of time (t_o) spent in the open state to time (t_c) spent in the closed state exponentially depends on the difference of free energy between states. In Eq. (5), $\Delta G'$ is the difference in free energy which does not include the volume work term ($V_c \cdot \Delta P_c$; V_c = volume of water channel, and ΔP_c = difference in hydrostatic pressure in the channel minus that in the surrounding medium). When the water in channel pores is under tension, ΔP_c is negative (Fig. 8). According to Eq. (5), there should be no critical tension (concentration), but a continuous decrease in L_p as found. In principle, the concentration dependence of L_p (Fig. 4) should allow to work out the channel volume, V_c . However, to work out reliable values of V_c , this would require to extend the range of concentrations to larger than 800 mM. This work is underway. It would be interesting to see if the volume depends on the size of osmotic solutes which could be more or less excluded from the mouth of channels tending to vary V_c . This effect would have to be separated from effects of reflection coefficients of smaller than unity for small solutes which should reduce ΔP_c at a given external concentration. The interpretation of results may be complicated by the fact, in *Chara*, there is a population of water channels of different size rather than just one channel (Henzler & Steudle 2000). If channel volume would vary depending on the accessibility of the entry of aquaporins, channels would have to be treated as mosaic structures with different arrays in series according to the theory of Kedem & Katchalsky (1963b; Ye & Steudle, in preparation).

The physical mechanism based on the tension in aquaporin pores may be questioned in favour of 'metabolic' models. For example, osmotic stresses may cause changes in cytoplasmic pH which, in turn, could affect aquaporins (Gerbeau *et al.* 2002). However, when employing such a model, one has to explain why the glycol ethers of different size had such a different effect. It is hard to imagine that cytoplasmic pH is regulated by the size (reflection coefficient) of osmolytes. With respect to pH, it is interesting to note that, in *Chara*, variation of external pH between pH = 7 and 11 had no effect on overall transport coefficients (L_p , P_s and σ_s ; Tyerman & Steudle 1984).

The cohesion/tension mechanism proposed here may well explain the known effect of external osmotic pressure on the L_p of Characean cells (Dainty & Ginzburg 1964; Kiyosawa & Tazawa 1972; Steudle & Tyerman 1983). Similar results have been reported for corn roots in the presence of high salinity (Azaizeh & Steudle 1991; Azaizeh *et al.* 1992). At an external concentration of NaCl of 100 mM, L_{p_r} of roots was reduced by a factor of 0.6, but L_p of root cells was reduced by a factor of as large as 4 to 6. For maize, differences between the cell and root level have been explained in terms of a dominating apoplastic transport in the presence of a hydrostatic pressure gradient.

In the model of Zimmerberg & Parsegian (1986), big osmolytes present on both sides of the membrane gate the open/closed state of channels. When solutes are not completely excluded from water channels, channels should have a reflection coefficient of less than unity. The tension caused at a given concentration should increase with increasing reflection coefficient of channels. The bigger the size of the solute, the stronger should be the effect, i.e. the reduction of L_p at a given concentration, as found. On the other hand, a solute like acetone which is known to slip across channels to some extent (Steudle & Henzler 1995; Hertel & Steudle 1997), should cause much smaller effects if any, as was also found. The findings provide strong evidence in favour of a cohesion/tension model of water channels (Fig. 8). They may indicate conformational changes of aquaporins which were reversible. When the medium was changed back to original, the original L_p was completely re-attained in less than 2 h. This time interval was short compared with that required for P_s (47 h and 65 h for EGMME and DEGMME, respectively). Different from the conventional cohesion/tension model as

used during long distance transport of water in higher plants (Steudle 2001), there are no problems of cavitation even when the water in the narrow pores is under tension. Diameters of water channels may be of an order of 0.2 to 0.4 nm (diameter of a water molecule). Formally, this is equivalent to a capillary pressure of as large as 730 to 1460 MPa, but, certainly, the meaning of capillary pressure has to be questioned in a single-file pore. However, considering the strong interactions (hydrogen bonding) between water and polar walls of channels, the tensions which could be sustained by such a pore should be enormous. Hence, it should be quite difficult to remove the water imbibing aquaporins.

The permeability coefficient (P_s) of glycol ethers increased as external concentration increased. As cell L_p decreased with increasing concentration, the opposite effect on solute permeability is strong evidence that water and solutes used different passages across the plasma membrane. Within the limits of accuracy, no slippage of solutes across water channels was detected as it was found with low molecular weight organic solutes such as alcohols, amides, H_2O_2 , or acetone (Hertel & Steudle 1997; Henzler & Steudle 2000). Increases in P_s were as large as 270%. The increase of P_s is not yet completely understood. It may be related to the chemical structure of the glycol ethers used. They are composed of a hydrophilic hydroxyl group and a rather long hydrophobic tail (Table 1). Hence, they may dissolve in the membrane bilayer at a relatively high concentration. The effect of a substantial partitioning of solutes between the water and the lipid phases may increase the permeability of the bilayer. It is, however, not affecting the function of water channels which quickly recover from the osmotic stress. Interestingly, the shorter ethylene glycol molecule with its two-hydroxyl groups is virtually impermeable and exhibits a reflection coefficient of close to unity (data not shown). Effects of partitioning should be bigger for the longer rather than for the shorter glycol ethers, as found. Equilibration between phases may take some time. This could explain the finding that reversal of solute treatment took as long as 47 to 65 h depending on the size of solutes. In the past, similar effects of relatively long times of recovery have never been observed with smaller solutes such as low molecular weight monohydric alcohols (methanol, ethanol, propanols etc.). With acetone, recovery was immediate as well.

Reflection coefficients (σ_s) had the tendency to decrease with increasing osmotic concentration of the different glycol ethers, but effects were not as clear as in the presence of HgCl_2 or low molecular weight solutes (Steudle & Tyerman 1983; Steudle and Henzler, 1995, 2000; Hertel and Steudle, 1997). Rather than using the simple model of a homogeneous membrane (Eq. (4)), the composite transport model has been employed to explain the effects of reduction in L_p and σ_s in the presence constant or rather small changes of P_s . In the composite transport model, the overall reflection coefficient is explained in terms of a weighted mean of two different arrays (water channel array, ‘a’, and bilayer array or rest of the membrane, ‘b’). Transport properties of arrays are characterized by different sets of transport coefficients (L_p^a , P_s^a , σ_s^a and L_p^b , P_s^b , σ_s^b). According to basic irreversible thermodynamics (Kedem & Katchalsky 1963 a, b), the overall σ_s is given by:

$$\sigma_s = \frac{\gamma^a \cdot L_p^a}{L_p} \cdot \sigma_s^a + \frac{\gamma^b \cdot L_p^b}{L_p} \cdot \sigma_s^b. \quad (6)$$

Here, γ^a and γ^b represent the fractional contribution of arrays ‘a’ and ‘b’, respectively ($\gamma^a + \gamma^b = 1$). Hence, $(\gamma^a \cdot L_p^a)/L_p$ and $(\gamma^b \cdot L_p^b)/L_p$ represent the relative contribution of arrays ‘a’ and ‘b’ to the overall hydraulic conductivity of the membrane. The model has been shown to apply during the inhibition of L_p by HgCl_2 or high concentrations of low molecular weight solutes (Steudle & Henzler 1995). In these applications, it was assumed that treatments just affected the open/closed state of water channels but not the transport properties of the bilayer. The fact that it does not apply here, may be then due to changes in the transport properties of the bilayer such as its hydraulic conductivity and the reflection coefficient. In part, changes may be compensating which may result in a moderate effect on the overall σ_s . A quantitative model (as during the inhibition by HgCl_2 and low molecular weight solutes) could be only made, when the changes in the transport properties of the bilayer would be known in detail. These data, however, are difficult to obtain experimentally.

In conclusion, our data from long term experiments with *Chara* internodes support the view that osmotic dehydration in terms of a cohesion/tension mechanism is an important trigger of water channel activity in *Chara* and, perhaps, in higher plants, too. Findings of a gating of water channel activity by high concentration are in line with

earlier findings for ion channels. The cohesion/tension model assumes that osmotic solutes are excluded from channels. This, in turn, results in a reversible deformation or even collapse of channel protein as tensions (negative pressures) develop within aquaporins. In accordance with the model, there was no critical tension (concentration) at which channels were blocked. Increasing size (molecular weight) of osmotic solutes made them more efficient to induce the deformation. The glycol ethers used in this study should have been largely excluded from aquaporins but moved across the bilayer. They may have been more or less accessible to the mouthpart of channels. Different pathways for water and solutes were demonstrated by the fact that increasing concentration decreased water permeability of the membrane (cell L_p) but increased solute permeability (P_s). The data show that changes in transport properties (L_p , P_s , σ_s) were completely reversible, even when experiments with a given internode lasted for 2 to 3 days.

Acknowledgements

We wish to thank Burkhard Stumpf (Department of Plant Ecology, Bayreuth University) for his expert technical assistance. BW thanks for a grant within the Erasmus/Socrates programme of the European Union.

References

- Azaizeh H, Gunse B, Steudle E.**1992. Effects of NaCl and CaCl₂ on water transport across root cells of maize (*Zea mays* L.) seedlings. *Plant Physiology* **99**, 886–894.
- Azaizeh H, Steudle E.**1991. Effects of salinity on water transport of excised maize (*Zea mays* L.) roots. *Plant Physiology* **97**, 1136–1145.
- Birner TP, Steudle E.** 1993. Effects of anaerobic conditions on water and solute relations and active transport in root of maize (*Zea mays* L.). *Planta* **190**, 474–483.
- Carvajal M, Cooke DT, Clarkson DT.** 1996. Response of wheat plants to nutrient deprivation may involve the regulation of water-channel function. *Planta* **25**, 372–381.
- Dainty J.** 1963. Water relations of plant cells. *Advances in Botanical Research* **1**, 279–326.
- Dainty J, Ginzburg BZ.** 1964. The measurement of the hydraulic conductivity (osmotic permeability to water) of internodal characean cells by means of transcellular osmosis. *Biochim. Biophys. Acta* **79**, 102–111.
- Finkelstein A.** 1987. Water movement through lipid bilayers, pores and plasma membranes. Theory and reality. Distinguished lecture series of the Society of General Physiologists, vol. 4. Wiley, New York.
- Gerbeau P, Amodeo G, Henzler T, Santoni V, Ripoche P, Maurel C.** 2002. The water permeability of *Arabidopsis* plasma membrane is regulated by divalent cations and pH. *Plant Journal* **30**, 71–81.
- Henzler T.** 2001. Die Funktion von Wasserkanälen in der pflanzlichen Zellmembran und ihre Bedeutung für den Wassertransport in Wurzeln. Dissertation, University of Bayreuth, Germany.
- Henzler T, Steudle E.**1995. Reversible closing of water channels in *Chara* internodes provides evidence for a composite transport model of the plasma membrane. *Journal of Experimental Botany* **46**, 199–209.
- Henzler T, Steudle E.** 2000. Transport and metabolic degradation of hydrogen peroxide in *Chara corallina*: model calculations and measurements with the pressure

probe suggest transport of H₂O₂ across water channels. *Journal of Experimental Botany* **51**, 2053–2066.

Hertel A, Steudle E. 1997. The function of water channels in *Chara*: the temperature dependence of water and solute flows provides evidence for composite membrane transport and for a slippage of small organic solutes across water channels. *Planta* **202**, 324–335.

Hose E, Steudle E, Hartung W. 2000. Abscisic acid and hydraulic conductivity of maize roots: a root cell- and pressure probe study. *Planta* **211**, 874–882.

House CR. 1974. Water transport in cells and tissues. Edward Arnold, London.

Johansson I, Larsson C, Ek B, Kjellbom P. 1996. The major integral proteins of spinach leaf plasma membranes are putative aquaporins and are phosphorylated in response to Ca²⁺ and apoplastic water potential. *The Plant Cell* **8**, 1181–1191.

Katchalsky A, Curran PF. 1965. Nonequilibrium thermodynamics in biophysics, Harvard University. Press, Cambridge, MA.

Kedem O, Katchalsky A. 1963a. Permeability of composite membranes. Part 2. Parallel arrays of elements. *Transactions of the Faraday Society* (London) **59**, 1931–1940.

Kedem O, Katchalsky A. 1963b. Permeability of composite membranes. Part 3. Series arrays of elements. *Transactions of the Faraday Society* (London) **59**, 1941–1953.

Kiyosawa K, Tazawa M. 1972. Influence of intracellular and extracellular tonicities on water permeability in characean cells. *Protoplasma* **74**, 257–270.

Kjellbom P, Larsson C, Johansson I, Karlsson M, Johanson U. 1999. Aquaporins and water homeostasis in plants. *Trends in Plant Science* **4**, 308–314.

Kozono, D, Yasui, M, King, LS, and Agre, P. 2002. Aquaporin water channels: atomic structure molecular dynamics meet clinical medicine. *Journal of Clinical Investigation* **109**, 1395–1399.

Macey RI. 1984. Transport of water and urea in red blood cells. *American Journal of Physiology* **246**, C195–C203.

Martinez-Ballesta MDC, Martinez V, Carvajal M. 2000. Regulation of water channel activity in whole roots and in protoplasts from roots of melon plants grown under saline conditions. *Australian Journal of Plant Physiology* **25**, 685–691.

Maurel C. 1997. Aquaporins and water permeability of plant membranes. *Annual Review of Plant Physiology Plant Molecular Biology* **48**, 399–429.

Murata K, Mitsuoka K, Hirai T, Walz T, Agre P, Heymann JB, Engel A, Fujiyoshi Y. 2000. Structural determinants of water permeation through aquaporin-1. *Nature* **407**, 599–605.

Nemeth-Cahalan KL, and Hall, JE. 2000. pH and calcium regulate the water permeability of aquaporin 0. *Journal of Biological Chemistry* **275**, 6777–6782.

Preston GM, Carroll TP, Guggino WB, Agre P. 1992. Appearance of water channels in *Xenopus* oocytes expressing red cell CHIP28 protein. *Science* **256**, 385–387.

Stein WD. 1986. Transport and diffusion across cell membranes. Academic Press, Orlando

Steudle E. 1993. Pressure probe techniques: basic principles and application to studies of water and solute relations at the cell, tissue and organ level. In: Smith JAC, Griffiths H, eds. Water deficits: plant responses from cell to community. Oxford: Bios Scientific Publishers, 5–36.

Steudle E. 2000a. Water uptake by plant roots: an integration of views. *Plant Soil* **226**, 45–56.

Steudle E. 2000b. Water uptake by roots: effects of water deficits. *Journal of Experimental Botany* **51**, 1531–1542.

Steudle E. 2001. The cohesion-tension mechanism and the acquisition of water by plant roots. *Annual Review of Plant Physiology Plant Molecular Biology* **52**, 847–875.

Steudle E, Henzler T. 1995. Water channels in plants: Do basic concepts of water transport change? *Journal of Experimental Botany* **46**, 1067–1076.

Steudle E, Tyerman SD. 1983. Determination of permeability coefficients, reflection coefficients, and hydraulic conductivity of *Chara corallina* using the pressure probe: effects of solute concentration. *Journal of Membrane Biology* **25**, 85–96.

Tazawa M, Asai K, Iwasaki N. 1996. Characteristics of Hg- and Zn-sensitive water channels in the plasma membrane of *Chara* cells. *Botanica. Acta* **109**, 388–396.

Tyerman SD, Bohnert HJ, Maurel C, Steudle E, Smith JA. 1999. Plant aquaporins: their molecular biology, biophysics and significance for plant water relations. *Journal of Experimental Botany* **25**, 1055–1071.

Tyerman SD, Niemietz CM, Bramley H. 2002. Plant aquaporins: multifunctional water and solute channels with expanding roles. *Plant Cell and Environment* **25**, 173–194.

Tyerman SD, Steudle E. 1984. Determination of solute permeability in *Chara* internodes by a turgor minimum method. Effect of external pH. *Plant Physiology* **74**, 464–468.

Tyree MT, Zimmermann MH. 2002. Xylem structure and the ascent of sap, Springer-Verlag, Berlin.

Verkman AS. 1992. Water channels in cell membranes. *Annual Review of Physiology* **54**, 97–108.

Yasui M, Hazama A, Kwon TH, Nielsen S, Guggino WB, and Agre P. 1999. Rapid gating and anion permeability of an intracellular aquaporin. *Nature* **402**, 184–187.

Zhang WH, Tyerman SD. 1991. Effect of low O₂ concentration and azide on hydraulic conductivity and osmotic volume of the cortical cells of wheat roots. *Australian Journal of Plant Physiology* **18**, 603–613.

Zimmerberg J, Parsegian VA. 1986. Polymer inaccessible volume changes during opening and closing of a voltage-dependent ionic channel. *Nature* **323**, 36–39.

**3 A cohesion/tension model for the gating of aquaporins
allows estimation of water channel pore volumes in
*Chara***

Qing Ye, Jan Muhr & Ernst Steudle*

Department of Plant Ecology, Bayreuth University, D-95440 Bayreuth, Germany

Received 31 July 2004; received in revised form 1 November 2004;
accepted for publication 3 November 2004

Correspondence: Ernst Steudle. Fax: + 49 921 55 2564;
e-mail: ernst.steudle@uni-bayreuth.de

Plant, Cell & Environment (2005) 28: 525-535

DOI: 10.1111/j.1365-3040.2004.01298.x

Abstract

The water permeability (hydraulic conductivity; L_p) of turgid, intact internodes of *Chara corallina* decreased exponentially as the concentration of osmolytes applied in the medium increased. Membranes were permeable to osmolytes and, therefore, they could be applied on both sides of the plasma membrane at concentrations of up to 2.0 M (5.0 MPa of osmotic pressure). Organic solutes of different molecular size (molecular weight, MW) and reflection coefficients (σ_s) were used (heavy water HDO, MW: 19, σ_s : 0.004; acetone, MW: 58, σ_s : 0.15; dimethyl formamide [DMF], MW: 73, σ_s : 0.76; ethylene glycol monomethyl ether [EGMME], MW: 76, σ_s : 0.59; diethylene glycol monomethyl ether [DEGMME], MW: 120, σ_s : 0.78 and triethylene glycol monoethyl ether [TEGMEE], MW: 178, σ_s : 0.80). The larger the molecular size of the osmolyte, the more efficient it was in reducing cell L_p at a given concentration. The residual cell L_p decreased with increasing size of osmolytes. The findings are in agreement with a cohesion/tension model of the osmotic dehydration of water channels (aquaporins; AQPs), which predicts both reversible exponential dehydration curves and the dependence on the size of osmolytes which are more or less excluded from AQPs (Ye, Wiera & Steudle 2004). In the presence of big osmolytes, dehydration curves were best described by the sum of two exponentials (as predicted from the theory in the presence of two different types of AQPs with differing pore diameters and volumes). AQPs with big diameters could not be closed in the presence of osmolytes of small molecular size, even at very high concentrations. The cohesion/tension theory allowed pore volumes of AQPs to be evaluated, which was $2.3 \pm 0.2 \text{ nm}^3$ for the narrow pore and between 5.5 ± 0.8 and $6.1 \pm 0.8 \text{ nm}^3$ for the wider pores. The existence of different types of pores was also evident from differences in the residual L_p . Alternatively, pore volumes were estimated from ratios between osmotic (P_f) and diffusional (P_d) water flow, yielding the number of water molecules (N) in the pores. N values ranged between 35 and 60, which referred to volumes of 0.51 and $0.88 \text{ nm}^3/\text{pore}$. Values of pore volumes obtained by either method were bigger than those reported in the literature for other AQPs. Absolute values of pore volumes and differences obtained by the two methods are discussed in terms of an inclusion of mouth parts of AQPs during osmotic dehydration. It is concluded that the mouth part contributed to the absolute values of pore volumes

depending on the size of osmolytes. However, this cannot explain the finding of the existence of two different types or groups of AQPs in the plasma membrane of *Chara*.

Key words: *Chara corallina*; aquaporins; cohesion/tension; gating; hydraulic conductivity; pore volume; reflection coefficient; water channels.

Introduction

There is accumulating evidence that water channels (aquaporins; AQPs) play an important role in plant water relations at all levels of organization (cell, tissue, organ and whole plant). AQPs facilitate the rapid, passive exchange of water across cell membranes. (For reviews see: Steudle & Henzler 1995; Maurel 1997; Kjellbom *et al.* 1999; Tyerman *et al.* 1999; Steudle 2000, 2001; Maurel & Chrispeels 2001; Javot & Maurel 2002; Tyerman, Niemietz & Bramley 2002). Most (75% – 95%) of the water permeability of plasma membranes is due to AQP activity (Henzler, Ye & Steudle 2004). Since the pioneering work of Agre and co-workers, there has been much effort expended in identifying the molecular structure of water channels (Jung *et al.* 1994; Murata *et al.* 2000; Ren *et al.* 2001). This has shown that AQPs are transport proteins with a molecular weight of about 30 kDa and that they span the membrane six times thereby forming a narrow, hydrophilic pore (Verkman & Mitra 2000). Work on the transport properties of AQPs demonstrated that, in accordance with their small diameter, AQPs are highly selective for water largely by excluding bigger molecules. AQPs just allow the passage of one water molecule after the other in a single file. However, some of the AQPs identified so far have proved to be permeable to small neutral solutes as well such as glycerol or urea (Agre, Bonhivers & Borgnia 1998; Biela *et al.* 1999; Borgnia *et al.* 1999; Dean *et al.* 1999; Gerbeau *et al.* 1999; Guenther & Roberts 2000).

In the turgid, intact internodes of the green alga *Chara corallina*, it has been demonstrated that small organic solutes such as ketones, amides or monohydric alcohols

use water channels in addition to the bilayer to cross cell membranes (Henzler & Steudle 1995; Hertel & Steudle 1997; Henzler *et al.* 2004). Hence, AQPs of *Chara* are not ideally selective for water. Henzler & Steudle (2000) presented evidence that some of the *Chara* AQPs allow a rapid passage of hydrogen peroxide and may serve as ‘peroxoporins’ as well as ‘aquaporins’. The data of these authors indicated the existence of different AQPs with differing diameters and, thus, pore volumes.

Recently, Ye, Wiera & Steudle (2004) proposed a cohesion/tension (C/T) model for the gating of water channels. The model was based on the fact that osmotic solutes excluded from AQPs, should cause a tension (negative pressure) within the pores, leading to a reversible deformation or even collapse of channel protein as tensions increase (in response to increasing solute concentration). Tensions of 2.0 MPa (20 bars) or even higher have been induced by Ye *et al.* (2004). Deformation or collapse of AQPs was evident from a reversible decrease of hydraulic conductivity of the cell membrane (L_p). The larger the size (molecular weight) of the osmotic solute used, the more efficient was the reduction of L_p .

In the present paper, these experiments are continued. Further evidence for the validity of the C/T model of Ye *et al.* (2004) is presented. According to the model, different osmotic solutes should differ in their efficiency to close water channels, depending on their size in relation to the diameter of membrane pores. For example, a relatively small solute which could pass through an AQP should exert a smaller tension at a given concentration than a bigger one. According to the model, solutes have to be presented in the same concentration outside and inside the cell. So, they have to be sufficiently permeable on one hand while sufficiently large on the other. Different ethylene glycol ethers fulfil these requirements. They also vary in size. Acetone was used as a typical small organic solute which has been shown to pass across AQPs in addition to the bilayer (Henzler *et al.* 2004). The change in the activity of AQPs was measured by a pressure probe for concentration series using the different osmolytes of different degrees of exclusion from pores. Pore volumes were calculated from ‘dehydration curves’, which required the measurement of responses over large ranges of concentration. Using the extrapolation technique of Steudle & Henzler (1995),

reflection coefficients of AQPs of solutes (σ_s^a) were obtained as well. For the first time, the experiments provide estimates of the volumes of AQPs (V_c) of the plasma membrane of an intact plant cell. In alternative experiments, numbers of water molecules in water channels were estimated by comparing the osmotic (P_f) and diffusional (P_d) water permeability. According to Levitt's (1974) theory, ratios of P_f/P_d should directly yield the number of water molecules in an AQP, which is related to pore volume. Results indicate that the plasma membrane of *Chara* may contain a population of different AQPs rather than just one type, an idea previously suggested for different reasons (Henzler & Steudle 2000). Volumes of AQPs deduced from numbers of water molecules in AQPs (P_f/P_d ratios) were smaller than those calculated from dehydration curves. This suggested that either the channels are somewhat wider than just the diameter of a water molecule, or that the mouth parts of channels contributed to the overall V_c , or both.

Material and methods

Plant material

Internodes of *Chara corallina* used in the experiments were grown in artificial pond water (APW; composition in mole·m⁻³: 1.0 NaCl, 0.1 KCl, 0.1 CaCl₂ and 0.1 MgCl₂) as described previously (Ye *et al.* 2004). Internodes (length: 50 to 150 mm; diameter: 0.8 to 1.0 mm) were isolated from adjacent internodes and whorl cells and fixed in a tube (inner diameter: 3 mm) to allow rapid circulation of APW around the cells and rapid exchange of media to minimize external unstirred layers.

Determination of L_p , P_f and P_d

The water permeability of the plasma membrane of *Chara* internodes (hydraulic conductivity, L_p) was calculated from half times of water exchange ($T_{1/2}^w$) as measured with the cell pressure probe:

$$L_p = \frac{V}{A} \times \frac{\ln(2)}{T_{1/2}^w (\varepsilon + \pi^i)} \quad (1)$$

Here, V = cell volume; A = cell surface area; ε is the elastic coefficient of the cell (elastic modulus) and π^i = osmotic pressure of cell sap, which was calculated from cell turgor and external osmotic pressure. The osmotic permeability (P_f) in $\text{m}\cdot\text{s}^{-1}$ is proportional to L_p in $\text{m}\cdot\text{s}^{-1}\cdot\text{MPa}^{-1}$, and was calculated from the relation (Hertel & Steudle 1997):

$$P_f = \frac{L_p \cdot RT}{\bar{V}_w} \quad (2)$$

(R = gas constant; T = absolute temperature; \bar{V}_w = molar volume of liquid water). The diffusional permeability of solutes (P_s) and of isotopic water (P_d) was estimated from half times of solute exchange as obtained from solute phases of biphasic pressure/time curves (Henzler *et al.* 2004):

$$P_s(P_d) = \frac{V}{A} \times \frac{\ln(2)}{T_{1/2}^s} = \frac{V}{A} k_s \quad (3)$$

Here, $T_{1/2}^s$ is the half time of solute (HDO) exchange, and k_s the corresponding rate constant. For a detailed description of these equations, see earlier publications by Steudle (1993) and Henzler & Steudle (1995). The cell pressure probe (completely filled with silicone oil) was introduced across the node into the fixed *Chara* internode (Henzler & Steudle 1995; Hertel & Steudle 1997; Henzler *et al.* 2004). Using the probe, the oil/cell sap meniscus forming in the tip of the capillary, was moved forward or backward and was kept stable after each move. From the half time of pressure relaxations, L_p and P_f were calculated as a control (Eqns 1 and 2).

Effects of high solute concentration on the transport of H₂O and HDO

Heavy water (HDO; 3.8 to 4.8 M) was used for testing the diffusional water permeability (P_d) of the membrane. Control values of P_d were calculated from biphasic response curves (Steudle & Tyerman 1983; Steudle 1993; Eqn 3). To determine effects of concentration on L_p , P_f and P_d , solutes with different molecular weights were added to the medium. One solute was acetone which largely moves across the bilayer of the cell membrane. However, a limited transport of acetone across water channels is known

to occur (Henzler & Steudle 1995; Hertel & Steudle 1997; Henzler *et al.* 2004). Other solutes were dimethylformamide (DMF); ethylene glycol monomethyl ether (EGMME); diethylene glycol monomethyl ether (DEGMME); and triethylene glycol monoethyl ether (TEGMEE), all of which were expected to be excluded from water channels because of their relatively large molecular size (Table 1). To avoid plasmolysis, concentrations were increased in steps of 0.2 M and proceeding to the next was delayed until full recovery of turgor. At each step, four hydrostatic pressure relaxations were induced to measure L_p at that concentration. Maximum concentrations were 2.0 M for acetone and 1.2 M for DMF and the three glycol ethers. HDO (the same concentration as in the control) was added to the medium in the presence of 1.2 M acetone or 1.2 M TEGMEE to measure changes of P_d in response to that treatment. Whether or not the effects of acetone and TEGMEE on aquaporins were additive was determined. To do this, cell L_p was first measured in the presence of 1.0 M acetone, later adding 0.2 M TEGMEE and measuring L_p again. Alternatively, L_p was first measured in the presence of 0.8 M TEGMEE, and again later after adding 0.4 M acetone. To remove solutes taken up by the internodes, the external concentration of the medium was reduced in steps of 0.2 M until the solution was APW again. L_p , P_f and P_d were re-examined to ensure that effects were completely reversible. For a given cell, the whole time course of experiments lasted for 4 to 12 hours. During treatments, cells did not lose turgor pressure (0.6 to 0.7 MPa) within ± 0.05 MPa or ± 8 %.

The reflection coefficient of the water channel array (σ_s^a)

It has been shown that the transport properties of the plasma membrane of *Chara* may be described in terms of a composite transport model (Henzler & Steudle 1995). According to the model, the overall reflection coefficient (σ_s) is expressed in terms of a weighted mean of two different arrays (water channel array, ‘a’, and the rest of the membrane, ‘b’). Transport properties of arrays are characterized by different sets of transport coefficients (L_p^a , P_s^a , σ_s^a and L_p^b , P_s^b , σ_s^b). According to basic irreversible thermodynamics (Kedem & Katchalsky 1963), the overall σ_s is given by:

$$\sigma_s = \frac{\gamma^a L_p^a}{L_p} \sigma_s^a + \frac{\gamma^b L_p^b}{L_p} \sigma_s^b . \quad (4)$$

Here, γ^a and γ^b represent the fractional contributions in area of arrays ‘a’ and ‘b’, respectively ($\gamma^a + \gamma^b = 1$). Hence, $(\gamma^a \cdot Lp^a)/Lp$ and $(\gamma^b \cdot Lp^b)/Lp$ represent the relative contributions of arrays ‘a’ and ‘b’ to the overall hydraulic conductivity of the membrane:

$$Lp = \gamma^a Lp^a + \gamma^b Lp^b. \quad (5)$$

If we assume that the contribution of the lipid array to the overall water transport is constant (i.e. Lp^b , $\sigma_s^b = \text{constant}$) and that water channels just switch between an open and closed state, Eqns 4 and 5 can be used to evaluate the reflection coefficient of water channels (σ_s^a). For a given solute, these equations yield (Henzler & Steudle 1995):

$$\sigma_s = \sigma_s^a - \gamma^b \cdot Lp^b \cdot (\sigma_s^a - \sigma_s^b) \cdot \frac{1}{Lp}. \quad (6)$$

Thus, plotting the measured quantities σ_s and $1/Lp$ against each other should yield a straight line and the reflection coefficient of water channels (σ_s^a) from the intercept with the σ_s axis. It should be noted that, when there are different types of water channels which exhibit a different dependence on concentration, σ_s^a denotes a weighted mean of the reflection coefficients of these different channels (see Discussion). In any case, we may distinguish between an array with variable values (σ_s^a and Lp^a) and an array with constant values (σ_s^b and Lp^b ; bilayer or ‘the rest of the membrane’).

Calculation of the pore volume of water channels

Zimmerberg & Parsegian (1986) presented a model of the gating of ion channels by the osmotic pressure of the medium on both sides of the membrane. According to the model, solutes excluded from channels cause a dehydration of membrane pores. This, in turn, results in a deformation or even collapse of channel protein as tensions (negative pressures) develop within pores. Ye *et al.* (2004) extended this idea to the aquaporins of *Chara* to explain the dependence of cell Lp on solute concentration. External osmotic pressure of solutes not accessible to the pores should have caused tensions in the water in channel pores to balance the water potential between pores and medium. As for ion channels, Ye *et al.* (2004) suggested that tensions cause a reversible collapse of the AQP protein and affect the ratio between the number of open and closed states of

channels. The ratio between the number of open channels in untreated *Chara* (n_o) and the number of open channels during treatment with external permeating solutes (n) should be given by a Boltzmann distribution. This means that the ratio of n/n_o should depend on the difference in free energy between the two states (ΔG). The latter just refers to the pressure dependence of free energy (volume work: $V_c \cdot \Delta P_c$), whereby ΔP_c = hydrostatic pressure in the channel minus that in the surrounding medium, and V_c is the internal volume of the pores. In the presence of external solutes, ΔP_c is negative. It is zero in its absence. We get (see Ye *et al.* 2004):

$$\frac{n}{n_o} = \frac{Lp}{Lp_o} = \exp\left(-\frac{\Delta G}{k_B \cdot T}\right) = \exp\left(\frac{V_c \cdot \Delta P_c}{k_B \cdot T}\right). \quad (7)$$

According to this equation, the Lp of treated cells should decline exponentially as the tension created within a channel in the presence of external solutes increases. In Eqn 7, k_B = Boltzmann constant ($k_B = R/N_L$; R = gas constant; N_L = Avagadro's number = 6.023×10^{23} particles per mole); T = absolute temperature. The tension created in the channels is related to external concentration (C_m) by van't Hoff's law, i.e:

$$\Delta P_c = -RT \cdot C_m. \quad (8)$$

Hence, we predict an exponential decrease in Lp as the external concentration increases:

$$\frac{Lp}{Lp_o} = E + F \cdot \exp(-k \cdot C_m). \quad (9)$$

As compared with Eqn 7, a term ' E ' has been added in Eqn 9. It represents the residual Lp which is not affected by pore dehydration in the presence of external solutes. The parameter ' F ' refers to the component of Lp_o which is due to concentration dependent AQPs. Component ' E ' may be caused by the permeability of the bilayer or by pores (AQPs or other transporters) that are not affected by concentration. $Lp/Lp_o - C_m$ curves have been fitted exponentially with high correlation factors (see Results). Lp_o is the original hydraulic conductivity, when $C_m = 0$. Hence, $E + F = 1$. According to Eqn 9, $Lp/Lp_o - C_m$ curves should become horizontal lines when all channels responsive to external osmotic pressure are closed due to the cohesion/tension mechanism. The decline constant k is a measure of the intensity by which solutes of different sizes (molecular weights) affect Lp . According to the C/T model, one would expect that effects of solutes are less pronounced when molecules were not completely excluded from the pores, i.e. when reflection coefficients of pores (σ_s^a) were smaller than unity.

In this case, the pressures in the pores would be given by $\Delta P_c = -\sigma_s^a \cdot RT \cdot C_m$, and Eqn 7 should read:

$$\frac{Lp}{Lp_o} = E + F \cdot \exp(-\sigma_s^a \cdot 1000 \cdot N_L \cdot V_c \cdot C_m). \quad (10)$$

The factor of thousand arises from the fact that C_m should be given in $\text{mol}\cdot\text{m}^{-3}$ rather than in the usual unit $\text{mole}\cdot\text{L}^{-1}$ or M (as done here). Measurements of the concentration dependence of Lp should allow one to work out k values (in M^{-1}) and channel volume V_c , (in $10^{-27} \text{ m}^3/\text{pore} = \text{nm}^3/\text{pore} = 1000 \text{ \AA}^3/\text{pore}$) provided that the reflection coefficient of the pore (σ_s^a) is known for a given solute. From Eqns 9 and 10 we get:

$$V_c = \frac{k}{1000 \cdot \sigma_s^a \cdot N_L}. \quad (11)$$

In Eqn 9, only one type of channel of volume V_c has been assumed. However, the results of this paper suggest that there are two different types or groups of channels of different volumes V_{c1} and V_{c2} present, which may also differ in their reflection coefficients (σ_s^{a1} and σ_s^{a2}) for a given solute. In this case, Eqn 9 has to be extended to:

$$\frac{Lp}{Lp_o} = E + F \cdot \exp(-k_1 \cdot C_m) + G \cdot \exp(-k_2 \cdot C_m), \quad (12)$$

where k_1 and k_2 are defined according to Eqn 11. As in Eqn 9, the meaning of E is that of the residual water permeability, when all channels exhibiting concentration dependence are closed. The terms F and G reflect the overall contributions of channels 1 and 2 to Lp_o in the open state. Different from Eqn 9, the concentration dependence described by Eqn 12 should not be represented by a single exponential; rather, it should split into two superposed exponentials, which may be separated from each other provided that the differences in pore volumes are big enough (Fig. 2B). On the other hand, when there are channels for which the reflection coefficient of an osmolyte is virtually zero, these channels should not close in the presence of this solute, independent of its concentration as shown for acetone in this paper.

Results

Reflection coefficients of water channels (σ_s^a)

According to Eqn 6, plotting the measured overall reflection coefficients (σ_s) against the inverse of hydraulic conductivity ($1/L_p$) as measured for different concentrations yields the reflection coefficient of the water channel array (σ_s^a) from the intercept with the σ_s axis. This is shown in Fig. 1A for acetone which goes through AQPs (overall $\sigma_s^a = 0.32 \pm 0.07$; $n = 6$ cells) and in Fig. 1B for TEGMEE, which does not (overall $\sigma_s^a = 1.01 \pm 0.06$; $n = 6$ cells). For other solutes, reflection coefficients are summarized in Table 1. They vary depending on the size and on the molecules' polarity. Linear relationships between σ_s^a and $1/L_p$ such as those shown in Fig. 1 have been verified before not only for *Chara*, but also for higher plant cells (Steudle & Henzler 1995). As pointed out in the Material and Methods section, σ_s^a values would refer to a weighted mean in the presence of different AQPs.

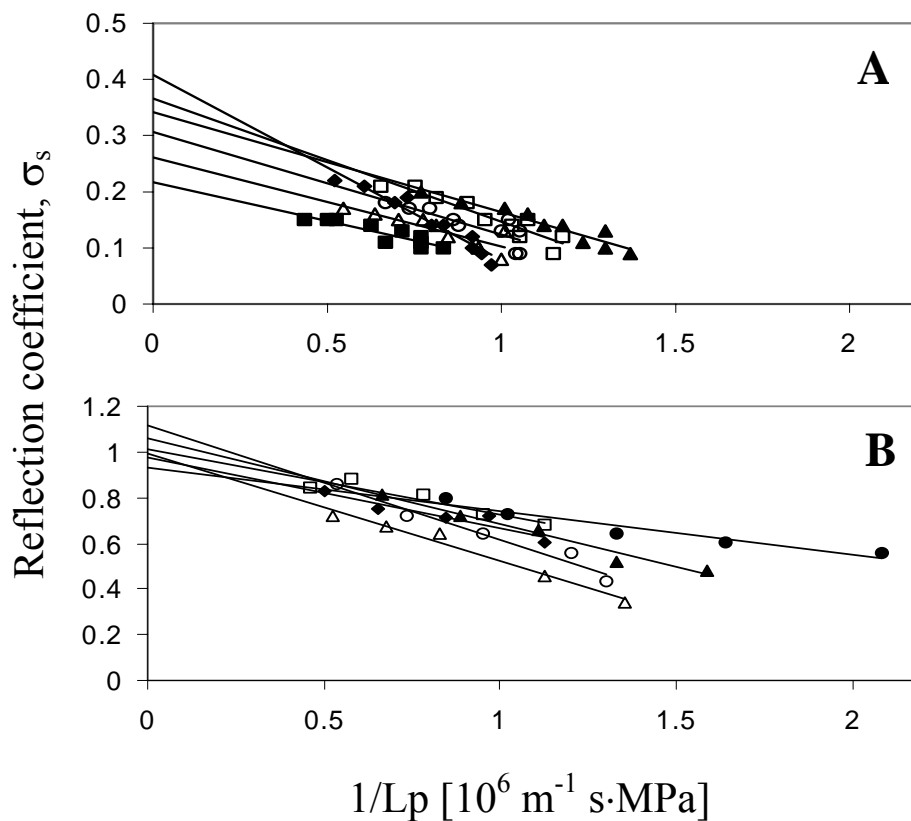


Fig. 1. Plots of the overall reflection coefficients (σ_s) of *Chara* internodes versus the inverse of hydraulic conductivities ($1/L_p$) for six individual cells of *Chara corallina* as denoted by different symbols. Internodes were treated by two different permeating solutes with increasing concentrations (A: acetone; B: TEGMEE). As expected from Eqn 6, plots yielded a straight line. From the intercept of the lines with the σ_s axis, reflection coefficients of water channel arrays (σ_s^a) were obtained for acetone (mean \pm SD: $\sigma_s^a = 0.32 \pm 0.07$) and for TEGMEE ($\sigma_s^a = 1.01 \pm 0.06$).

Residual water permeability and decline constants of $L_p/L_{p_0} - C_m$ curves

As the external osmolyte concentration increases, one would expect an exponential decrease of L_p given by a certain decline constant k and a residual water permeability E (Eqn 9). Fig. 2A shows that L_p/L_{p_0} decreased exponentially as the concentration of osmolyte increased. For all test osmolytes, single exponential fits of $L_p/L_{p_0} - C_m$ curves (Eqn 9) resulted in high correlation factors of $r^2 > 0.99$. It can be seen from Fig 2A and B that there was significant difference among residual water permeabilities for osmolytes which differed substantially in size such as acetone and TEGMEE (t-test; $P < 0.05$). Residual water permeabilities (given as a percentage of the original L_{p_0}) decreased as the size (molecular weight) of test solutes increased. For example, for acetone (the smallest solute used) $E = 52\%$; for TEGMEE (the biggest) $E = 33\%$ (Fig. 2B; Table 1). This indicated that there were bigger and smaller channels present, and the bigger channels could not be closed in the presence of even considerable

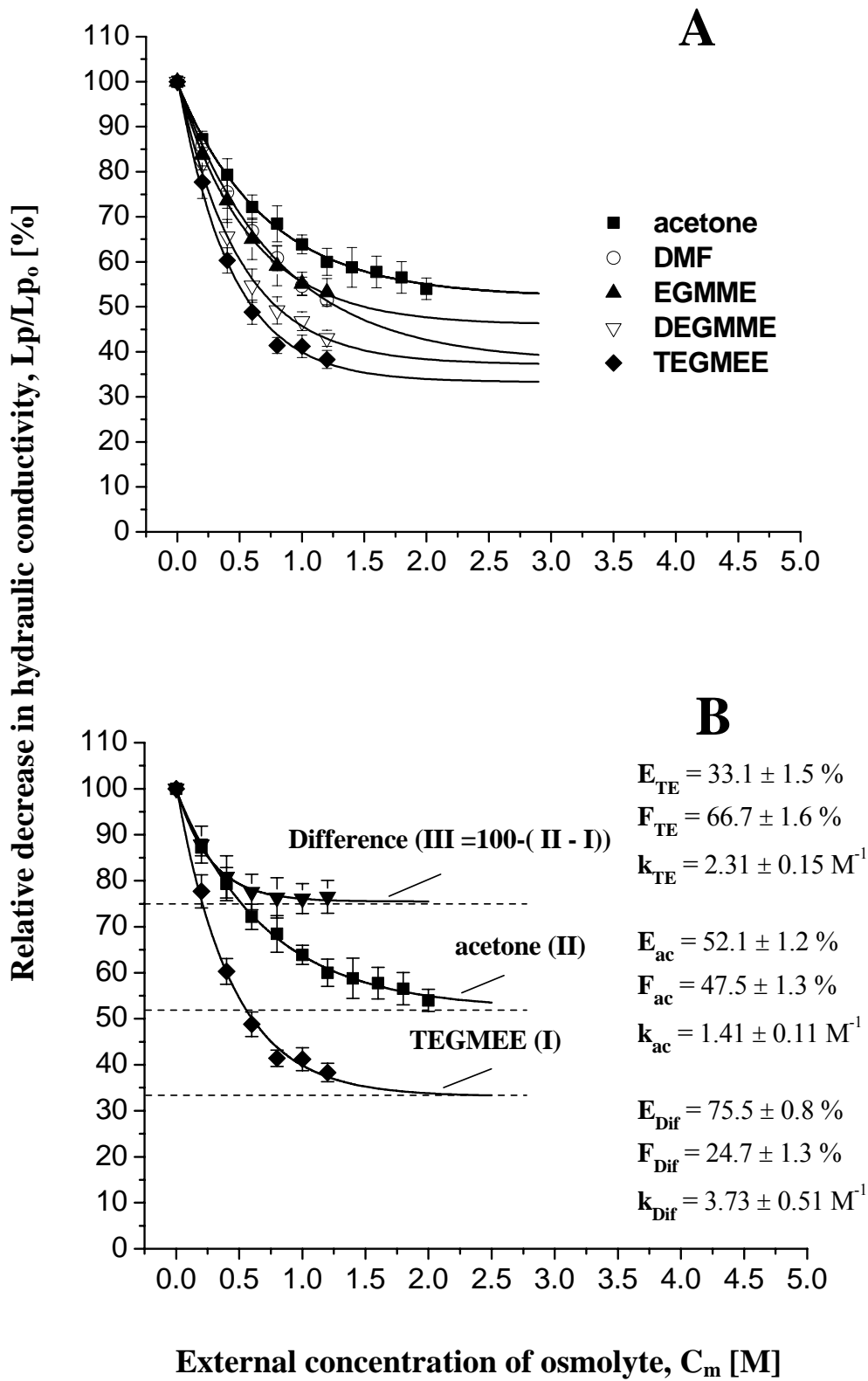


Fig. 2 (A) Effect of concentrations of five osmolytes (acetone, dimethylformamide and three glycol ethers) on bulk water permeability (L_p) of *Chara* internodes. As the concentration on both sides of the membrane increased from 0.2 M to 2 M (acetone) or to 1.2 M (DMF and glycol ethers), L_p decreased for all osmolytes ($n = 6$ cells \pm SD for each osmolyte). Points represent the mean values of relative L_p (compared with control at zero concentration, L_{p_0}) ($n = 6$ cells for each concentration). L_p/L_{p_0} curves were fitted exponentially (Eqn 9; $r^2 > 0.99$). The bigger the molecular size of the solute used, the greater was its effect in reducing L_p . In (B), it is shown for TEGMEE that the fit in (A) contained two exponentials as expected in the presence of two different groups of AQPs with different pore volumes. Subtracting results of the dehydration curve for acetone (II, representing the small channels) from that for TEGMEE (I, representing all channels) resulted in the response curve for the wide channels (III, Eqn 12). From the different decline constants k_1 and k_2 , channel volumes have been calculated (Eqn 11; Table 1). Error bars in (B) denote SD values ($n = 6$ cells), whereby the error bars in III represent the propagated errors from I and II. For each concentration and curve, mean values were significantly different from those of the other two, (t-test; $P < 0.05$), except for curves II and III at concentrations of 0.2 and 0.4 M.

concentrations of the small solute acetone, presumably because of a rather low σ_s^a of the big channels for acetone. A careful inspection of the dehydration curves for the big solutes EGMME, DEGMME, and TEGMEE showed that they would be better fitted as the sum of two exponentials according to Eqn 12 rather than by just one exponential (Eqn 9). The subtraction of the TEGMEE curve from the acetone curve of Fig. 2B showed that the TEGMEE curve contained two different components, one due to a big channel and one due to a small channel, as could be also verified from semilog plots (data not shown). Obviously, the different decline constants referred to different types of channels. Bigger channels responded to TEGMEE but not to acetone, whereas smaller channels responded to both acetone and TEGMEE. As for TEGMEE, there was also a splitting into two components for DEGMME and EGMME which resulted in two different k values and pore volumes (Table 1). However, a splitting of the DMF curve could not be done, presumably because the sizes of the acetone and DMF were too similar.

Pore volumes of water channels in *Chara*

When volumes of water channels were calculated using a single exponential (Eqn 9) and the σ_s^a values of Fig. 1, volumes ranged between 2.5 ± 0.1 and $7.3 \pm 0.2 \times 10^{-27} \text{ m}^3$

or 2.5 ± 0.1 to 7.3 ± 0.2 nm³ (data not shown), whereby the highest pore volume referred to the smallest osmolyte acetone, because of the low σ_s^a for acetone. In view of the results of Fig. 2B, this cannot be true. It is more likely that the small ('acetone') channels have a $\sigma_s^a \approx 1$ for acetone which did not affect the big channels, because they were too wide. The same should be true for the other solutes. Therefore, using the assumption of a $\sigma_s^a = 1$ for all solutes, values of V_c ranged from 2.1 ± 0.1 to 3.8 ± 0.2 nm³ tending to increase with increasing size of the solute. However, when Eqn 12 was applied to split up effects in the presence of different channels, two different types of channels could be classified. When subtracting the contribution of the small 'acetone' channel ($V_c = 2.3$ nm³) from the dehydration curves in the presence of EGMME, DEGMME and TEGMEE, the volume of the bigger channel component was found to be 5.5 ± 0.8 to 6.1 ± 0.8 nm³ (last column of Table 1). For DMF, no separation of components was possible (see above). The data strongly indicate that channels of two different sizes are present.

Table 1. Pore volumes of water channels calculated from $L_p/L_{p_0} - C_m$ dehydration curves of osmolytes of different molecular size and reflection coefficients (σ_s). Values of the decline constants, k , and of the residual L_p/L_{p_0} , E , were obtained from $L_p/L_{p_0} - C_m$ dehydration curves (Fig. 2A, B). Overall reflection coefficient of water channels (σ_s^a) for different osmolytes were estimated from the intercept with σ_s axis by plotting the measured quantities σ_s against $1/L_p$ (Fig. 1; Eqn 6). Pore volumes of water channels in the column next to the last were calculated using Eqn 9, assuming a single type of channel and a reflection coefficient of unity for all solutes including acetone. In the last column, the model of two different types of channels has been employed, whereby the acetone data refer to the small and the other data to the big channels (Eqn 12; Fig. 2B). Values are means \pm SD; $n = 6-10$ cells.

solute	Molecular weights (g/mol)	overall reflection coefficient (σ_s)	values of E in Eqn 9 (maximum change of L_p/L_{p_0} in percent)	values of decline constants, k (M^{-1}) (Eqn 9)	Overall reflection coefficients of water channel arrays (σ_s^a)	Pore volumes (nm^3) calculated assuming only one type of channel (Eqn 9)	Pore volumes (nm^3) calculated assuming two types of channels (Eqn 12). Data for acetone refer to small channels and for the other solutes to big channels (Fig. 2B)
acetone	58	0.15 ± 0.03^c	52 ± 0.8	1.41 ± 0.11	0.32 ± 0.07	2.3 ± 0.2	2.3 ± 0.2
DMF	73	0.76 ± 0.06^d	38 ± 1.8	1.25 ± 0.07	0.83 ± 0.13^d	2.1 ± 0.1	-
EGMME	76	0.59 ± 0.03^c	46 ± 1.1	1.73 ± 0.08	0.78 ± 0.05	2.9 ± 0.1	5.6 ± 1.1
DEGMME	120	0.78 ± 0.05^c	37 ± 2.4	1.99 ± 0.20	1.03 ± 0.10	3.3 ± 0.3	5.5 ± 0.8
TEGMEE	178	0.80 ± 0.07^c	33 ± 2.5	2.31 ± 0.15	1.01 ± 0.06	3.8 ± 0.2	6.1 ± 0.8

^c data from Ye *et al.* 2004, σ_s were measured at concentrations of 160 mM for acetone and 60 mM, 40 mM, 25 mM for EGMME, DEGMME, TEGMEE, respectively; ^d data from Steudle & Tyerman 1983.

Combined treatments with a small (acetone) and a large (TEGMEE) osmolyte

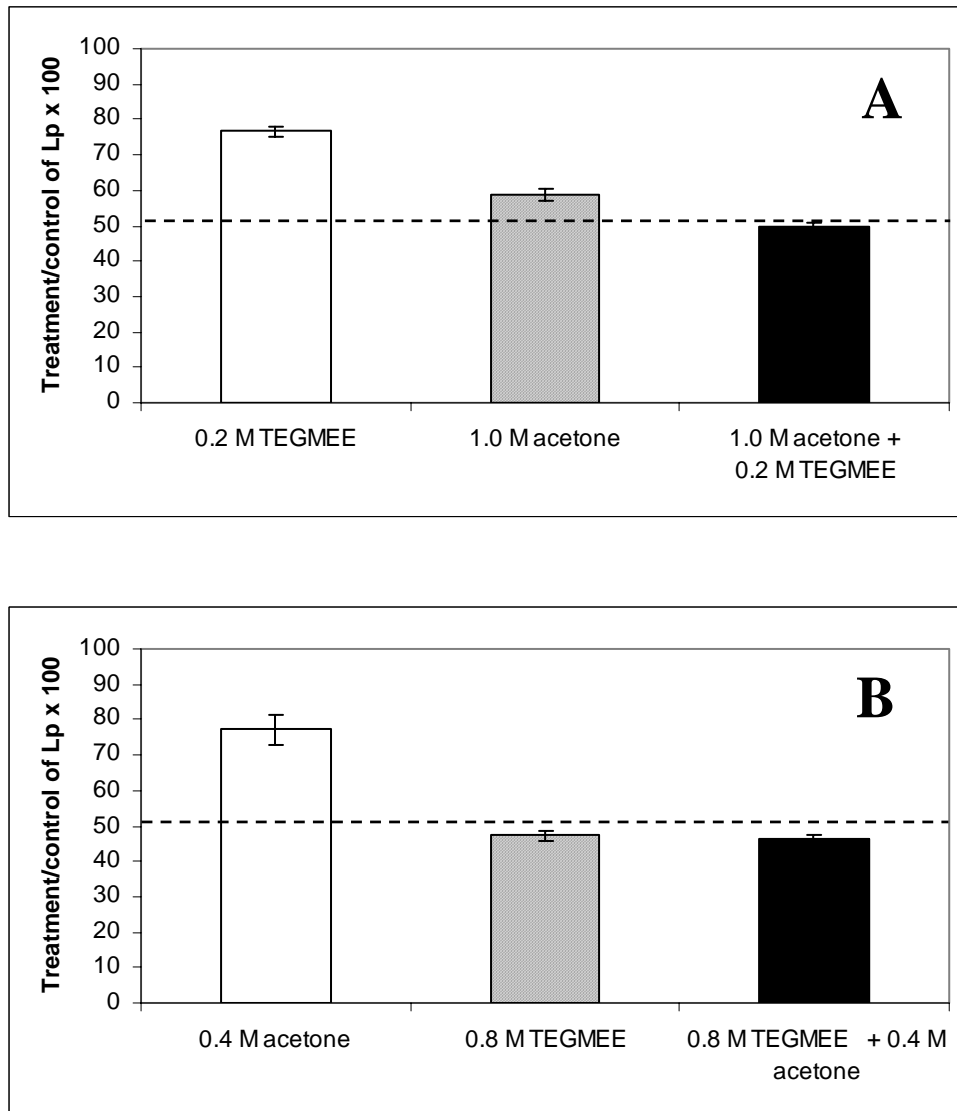


Fig. 3 (A) Treatment with either 0.2 M TEGMEE (big solute) or 1 M acetone (small solute) reduced cell Lp of *Chara* internodes down to 77% and 59% of the control, respectively. In the presence of 1 M acetone, the addition of 0.2 M TEGMEE resulted in a further significant reduction of Lp as compared with the treatment with 1 M acetone ($n = 6$ cells; $P < 0.05$). (B) When *Chara* internodes were treated first with 0.4 M acetone or 0.8 M TEGMEE, cell Lp was reduced to 77% and 47% as compared with control, respectively. In the presence of 0.8 M TEGMEE, the subsequent addition of 0.4 M acetone had no further significant effect on reducing Lp ($n = 5$ cells; $P > 0.05$). Dashed lines indicate the maximum residual value of Lp in the presence of high concentrations of acetone (52% of original Lp_0).

The striking difference in the residual L_p between acetone and the bigger osmolytes (Fig. 2) suggested that, for example, the more efficient TEGMEE closed more and, perhaps, a population of channels different from those which were affected by acetone. If true, the addition of TEGMEE should still have a substantial effect on L_p , even when the small-diameter channels had been already closed by fairly high concentrations of acetone. On the other hand, when all channels had been closed at a high concentration of TEGMEE, the addition of acetone should have no further effect. Fig. 3 demonstrates that this was the case. An internode was treated with 0.2 M TEGMEE which reduced L_p to 77% of the control value (L_{p_0}); 1.0 M of acetone decreased L_p to 59% of L_{p_0} . When a mixture of both solutes was added to the same cell (i.e. adding 0.2 M TEGMEE in the presence of 1.0 M acetone), the relative reduction of L_p was 50%; the reduction was significantly greater than that of either single treatment (means \pm SD, $n = 6$ cells, $P < 0.05$). Hence, in the presence of a rather high concentration of acetone, a relatively low concentration of TEGMEE did have an additional effect. However, when TEGMEE was present at rather high concentration, the addition of a substantial amount of acetone had no significant further effect (Fig. 3B). The results from Figs. 2B and 3B suggest that there are different water channels in *Chara* which differ in their sensitivity depending on the size of solutes.

Number of water molecules (N) within the pore

According to Levitt's (1974) theory, the number (N) of water molecules within a narrow pore where molecules move in a single file (i.e., one by one and without passing each other) is given by the ratio between the osmotic (P_f) and diffusional (P_d) water permeabilities. P_f is directly related to the hydraulic conductivity, L_p . The diffusional water permeability was determined in a separate experiment using isotopic water (HDO). We have:

$$N = \frac{P_f}{P_d} = \frac{L_p \cdot RT}{\bar{V}_w \cdot P_d} \quad (12)$$

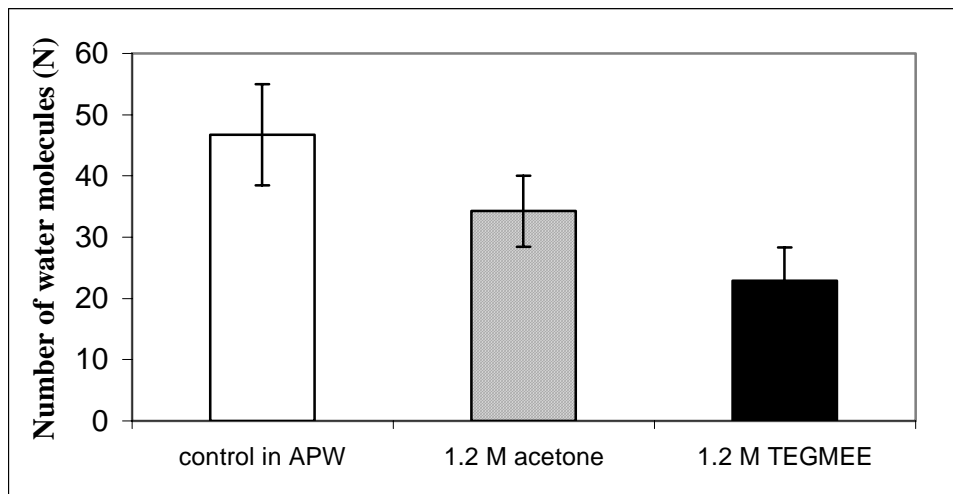


Fig. 4. The ratios between osmotic (P_f) and diffusional (P_d) water flow directly yield the number (N) of water molecules aligned in water channels. When P_f and P_d were measured in control (APW) with the aid of a cell pressure probe, N was 47 on average ($n = 12$ cells \pm SD), suggesting that there are 47 water molecules aligned in a water channel of *Chara*. Treatments with 1.2 M acetone or 1.2 M TEGMEE reduced the value of N to 34 and 23 ($n = 6$ cells for each treatment), respectively. Please, note that 6 different cells have been treated with TEGMEE and acetone, respectively, because a treatment with both solutes would not have been possible for a single cell. Nevertheless, for each cell both P_f and P_d have been measured in control and treatment.

This relation refers to the situation where all water passes across channels and there is no parallel passage across the bilayer (or rest of the membrane). This assumption is not met in the presence of a significant water flow across the bilayer (see Discussion). From the results shown in Fig. 4, we calculated that there were 47 water molecules aligned in a water channel when P_f and P_d were measured in control (APW). Treatments with 1.2 M acetone or 1.2 M TEGMEE reduced N to 34 and 23, respectively. Changes were significant (t-test; $P < 0.05$). For a non-porous pathway such as the bilayer, $N = 1$ should hold. Therefore, the results of Fig. 4 indicate a higher relative contribution of the bilayer passage as water channel activity decreased at high external concentration. The more effective solute TEGMEE had a stronger effect than the less effective acetone, as expected.

Discussion

The results support the view of a cohesion/tension mechanism operating in water channels of the green alga *Chara* as reported earlier by Ye *et al.* (2004). The mechanism is thought to be the reason for the effect of high solute concentration around the membrane on its hydraulic conductivity. This effect has been known for a long time, but had not previously been explained satisfactorily (Dainty & Ginzburg 1964; Tazawa & Kamiya 1966; Steudle & Tyerman 1983). The problem is of general interest. An inhibition of cell L_p by high solute concentration or salinity is known not only for characean species. For example, growing maize in a solution of 100 mM NaCl (with an associated build up of osmotic active substances in the cells) reduced the L_p of root cortical cells by 68 to 83% (Azaizeh, Gunse & Steudle 1992). The fact that this osmotic stress was smaller by a factor of six to ten than the stresses used in the present study suggests that AQPs of root cells may be more sensitive to mechanical stresses caused by the C/T mechanism than those of *Chara* (Wan, Steudle & Hartung 2004). Differences between species may be due to differences in the fine structure of AQPs (although the primary sequence of AQPs and the resulting structural fold should be largely conserved), or to differences in the interaction of AQPs with the bilayer into which AQPs are anchored. Because of experimental difficulties, quantitative studies of effects of osmotic stresses on water transport across plant membranes are still rare. In isolated cells of *Chara*, such effects can be studied rigorously, because both external and internal concentrations can be changed in a defined way over large ranges, provided that permeating osmolytes are used. Effects can be followed over hours on one individual cell. This is usually not possible for cells in a tissue.

We were limited in the use of osmolytes. On one hand, we wanted to cover a large range of reflection coefficients, i.e. a large range of exclusion from pores and, hence, used compounds with a rather large range of molecular weights. On the other hand, to test the C/T model solutes had to permeate into the cell to act on both sides of the membrane. Therefore, we used only uncharged solutes. Because of their low permeabilities, salts such as KCl (present in the vacuole of a *Chara* cell in high concentration) could not be used. They would have required enormous time intervals for

equilibration, if any. At the lower end, we used HDO and acetone as small, rapidly permeating substances. For larger molecules with high reflection coefficients, we employed glycol ethers and the bulky dimethyl formamide. These solutes are tolerated by the cells at high concentration and provide rather large overall reflection coefficients of up to $\sigma_s = 0.80$ in the presence of a reasonable solute permeability (Ye *et al.* 2004).

The data provide additional strong support for the C/T mechanism of a gating of water movement through AQPs in that (i) the dehydration of membrane pores in the presence of osmotic solutes depended exponentially on the concentration of osmolytes as theoretically expected in the presence of a flip-flop between different conformational states of AQPs (Eqns 9 and 12). (ii) There was a distinct effect of the size of osmolytes. It is known from other experiments that small osmolytes such as acetone and monohydric alcohols can slip through water channels whereas bigger ones do not (Henzler & Steudle 2000; Henzler *et al.* 2004). However, it had not yet been demonstrated that this might result in different residual water permeabilities as proposed by the model. The differences in the ‘osmotic efficiency’ between osmolytes as expected by the C/T theory was verified. (iii) The model predicts that the switching between different conformations of AQPs should be reversible, and this was found, too. When osmotic stresses were withdrawn, cell L_p re-attained the original L_{p0} . Membrane integrity was not affected.

The absolute values of pore volumes presented in this paper are large. Depending on the solutes used they ranged between 2.1 ± 0.1 and $3.8 \pm 0.2 \text{ nm}^3$, when using the single-channel approach of Eqn 9 and values of σ_s^a of unity. This procedure represents an oversimplification as curves should be fitted by two exponentials in the presence two types of channels (as indicated by the different values of residual L_p in Fig. 2). The results of Fig. 3 show that not all channels reacted to acetone even when it was present in high concentrations. They did react, however, to the bigger molecules of the glycol ethers. Hence, it is reasonable to assume that the overall value of σ_s^a for acetone should be separated into a low value for the wider channels and into a rather high value for the smaller channels. A relation similar to that used in Eqn 6 should hold within the population of different AQPs, whereby different types of channels would contribute to

σ_s^a according to their water permeability. Hence, the reflection coefficient of the narrow channels may be close to unity for acetone.

When considering the fact that there were two different types of channels of differing size present, the values of channel volumes (diameters) have to be split up according to Eqn 12 (Fig. 2B; Table 1). This results in absolute values of the small and big channels of $2.3 \pm 0.2 \text{ nm}^3$ and 5.5 ± 0.8 to $6.1 \pm 0.8 \text{ nm}^3/\text{channel}$, respectively. These high values may contain a contribution of the vestibules of channels. A cylindrical AQP pore of a diameter of 0.4 nm ($= 4 \text{ \AA} \approx$ diameter of water molecule) and of a length of 5 nm (\approx about half of the thickness of a plasma membrane), has a volume of 0.63 nm^3 , which is smaller by a factor of 4 to 10 than those given above. The electron diffraction studies of Ren *et al.* (2001) indicated a length of the narrow part of the AQP-1 pore of red blood cells of only 1.8 nm , which would allow the single-file alignment of about 5 water molecules with a diameter of about 0.4 nm . This would result in a pore volume of only 0.23 nm^3 . The reason for the larger value obtained for *Chara* internodes could be that either the AQPs of these cells are rather big or that the osmotic dehydration technique used to measure them produces large values by incorporating mouth parts, or both.

When osmolytes are not only excluded from the narrow, single-file part of channels but also from their mouth parts, an overestimation of channel volume (narrow part) may result. For example, when we assume that the mouth parts at both sides of narrow part are shaped as truncated cones with a diameter at the entering part of the mouth of 0.8 nm (twice the diameter of the core part), and of a length of 2 nm (as the core part), we end up with an overall volume of 1.4 nm^3 , which is closer to that measured in this work. Dimensions such as those used here for mouth parts may be realistic (Zhu, Tajkhorshid & Schulten 2004), but more precise data would be required. They are not yet available for *Chara*. A narrow inner part of the channel (such as that of AQP1) and of two additional mouth parts acting as single-file pores would increase the number of water molecules from 5 to 15. However, in the mouth parts, channels may not strictly behave as no-pass pores for water, and the figure of 15 is, hence, a lower limit. The effects of mouth parts could account for some of the differences observed. They cannot, however, account for the fact that the small osmolyte acetone could not affect the big channels

even when applied at very high concentration. This is strong indication for the presence of different types of channels.

Zimmerberg & Parsegian (1986) found large pore volumes for ion channels. Their values range between 22 and 48 nm³ (including mouth regions). This is larger by a factor of 4 to 21 than our values obtained from osmotic dehydration. Zimmerberg & Parsegian (1986) subjected their membrane preparations (mitochondrial voltage-dependent anion channels from rat liver and from *Neurospora*, reconstituted into planar phospholipid bilayers) to big osmolytes which should have been completely excluded from the channel interior including mouth parts (polyethyleneglycol, MW: 20,000; polyvinylpyrrolidone, MW: 40,000 and Dextran 1500, MW: 500,000). Membrane pores closed in the presence of osmotic pressures of only 3 bar (0.3 MPa equivalent 120 mM), i.e. at tensions of as small as 3 bar. Channel closure was measured as a decrease in the electrical conductance of ion channels. Zimmerberg & Parsegian (1986) thought that the high sensitivity to tensions of their pores was due to the rather wide diameter of the channels. They speculate that there should also be channels of smaller diameters which should resist much higher tensions, as found here for the water channels of *Chara*. For *Chara*, we could use much smaller osmolytes than Zimmerberg & Parsegian (1986), just because of the smaller diameter of AQPs.

In the present study, the fairly large volumes of pores obtained from dehydration curves coincided with rather large values of the number of water molecules in the channels (N) obtained in an alternative experiment by comparison of the osmotic (P_f) and diffusional (isotopic, P_d) permeability to water. Values ranged between $N = 35$ and $N = 60$ for untreated cells ($N = 47$ on average). These data are bigger than those obtained earlier for *Chara* from P_f/P_d ratios ($N = 27$; Henzler & Steudle 1995; $N = 31$; Hertel & Steudle 1997). Literature data for other objects also indicated smaller N values. For example, Finkelstein (1987) and Mathai *et al.* (1996) found $N = 10$ to 13 for red blood cells. In wheat root membrane vesicles, Niemietz & Tyerman (1997) reported an $N = 3$ to 7. Somewhat larger values were given for symbiosome membrane vesicles of soybean root nodules ($N = 18$; Rivers *et al.* 1997). Overall, values from different sources and for different objects range from $N = 3$ to 47 (including this paper). Using a van-der-Waals

volume of water molecules of $1.46 \times 10^{-2} \text{ nm}^3$ (14.6 \AA^3), this would be equivalent to a range of 0.04 nm^3 to $0.69 \text{ nm}^3/\text{pore}$. Hence, our data for *Chara* are at the upper edge of values reported so far. The reason may be either that *Chara* does have such big pores (perhaps, less likely in view of the fact that AQPs are highly conserved; see above) or that our method of measurement incorporated mouth parts as discussed above. Wider mouthparts lacking a single-file transport of water may explain the differences between pore volumes obtained from dehydration curves and those from P_f/P_d ratios.

It has to be noted though that N values from P_f/P_d ratios may represent overestimates because of problem with unstirred layers during the measurement of P_d . Extensive experience with the measurement of rapidly permeating solutes in *Chara* (such as HDO), however, shows that effects of internal unstirred layers are smaller than one might expect (see discussions in Henzler & Steudle 1995, 2000; Hertel & Steudle 1997; Ye *et al.* 2004). It may be reasonable to assume that effects were probably not larger than 25%. Hence, the P_f/P_d ratio of 47 would have to be corrected to 35. However, even when corrected for unstirred layers, measured ratios do not straightforwardly represent P_f/P_d ratios of aquaporins. Rather, they are overall values for the entire membrane. When we denote the $P_f(P_d)$ values of the AQP array(s) by P_{fAQP} and P_{dAQP} , respectively, and those of the rest of the membrane by $P_{f\text{rim}}$ and $P_{d\text{rim}}$, we should get P_{fAQP}/P_{dAQP} from the relation (Finkelstein 1987):

$$\frac{P_{fAQP}}{P_{dAQP}} = \frac{P_f - P_{f\text{rim}}}{P_d - P_{d\text{rim}}} \quad (13)$$

Here, P_f and P_d denote the measured overall values. When water is only moving either across the bilayer or the water channel array, $P_{f\text{rim}}$ and $P_{d\text{rim}}$ would refer to the bilayer, where $P_f = P_d$ could be assumed in the absence of pores. Bilayer values of the water permeability have been obtained for red blood cells ($P_f = 3.0 \times 10^{-5} \text{ m}\cdot\text{s}^{-1}$; Mathai *et al.* 1996). They have been used to correct for the bilayer component assuming that $P_{f\text{rim}} = P_{d\text{rim}}$ after blocking the porous passage (Finkelstein 1987; Mathai *et al.* 1996). Analogous data are difficult to obtain for *Chara*. During the most drastic closure of water channels in *Chara* in the presence of hydroxyl radicals, the residual L_p (P_f) was as small as 5-10% of the original (Henzler *et al.* 2004). In absolute terms, it was 2.2 to $8.6 \times 10^{-5} \text{ m}\cdot\text{s}^{-1}$ and is similar to that of the residual water permeability of red blood cells

(see above). However, under these conditions P_f/P_d ratios were still as large as 11. This residual figure for P_f/P_d should contain (i) effects of unstirred layers as well as (ii) other ‘porous’ transporters for water which were not affected by the AQP inhibitor, and (iii) remaining AQPs also not affected by the harsh treatment. Anyhow, when using the residual values for *Chara* (as obtained after the treatment with hydroxyl radicals) in Eqn 13, P_f/P_d ratios for AQP arrays would increase from 47 to 62. We conclude that our measured values of N , even though rather large, may represent a lower limit of the true values, because we did not correct for the rest of the membrane (Eqn 13). They may be an upper limit, because we did not correct for internal unstirred layers. At least in part, the opposing effects may cancel.

The finding of differences in residual L_p values indicates the existence of different types of channels. The small osmolyte acetone may close only relatively narrow channels. It may largely pass through wider channels which could be only closed in the presence of bigger solutes. In this way, both the striking difference in the efficiency of osmolytes as well as the trend in the differences in pore volumes may be explained. The results of measurements with mixtures of small and big solutes support this view. Support also comes from the fact that, unlike the bigger solutes, the smaller acetone had reflection coefficients of the entire AQP array substantially smaller than unity (Table 1). The results are in agreement with earlier results of Henzler & Steudle (2000). These authors used hydrogen peroxide as an osmotic solute and concluded that it could rapidly pass through some but not all of the water channels. Hence, there are ‘real’ water channels and also some which could have been termed ‘peroxoporins’. Since H_2O_2 is an important metabolite and may act as a signal substance during pathogenic attacks, this view may be of some general importance.

In conclusion, the present results indicate a dehydration of aquaporins (water channels) in the plasma membrane of *Chara* by a cohesion/tension mechanism in the presence of high osmolyte concentrations. As expected from the C/T model, osmolytes of different size (in relation to the diameter of AQPs) differently affected cell L_p , i.e. the efficiency of the osmotic dehydration of membrane pores at a given concentration of osmolyte. The results suggest that there are AQPs of bigger and smaller diameter (volume) that

may select differently between osmolytes. The small solute acetone permeated across bigger but not across the smaller, whereas bigger solutes were completely excluded from all pores. Dehydration curves obtained in the presence of big osmolytes split into two exponentials which allowed evaluation of the volumes of bigger and smaller channels. Pore volumes estimated from exponential dehydration curves according to the C/T theory suggested pore volumes substantially larger than those reported for other membranes. We think that this is due to differences in channel volumes (diameters). The effect may also incorporate an exclusion of osmotic solutes from the mouth parts of AQPs, which should increase with increasing molecular size of osmolytes, but this can not completely explain the effect. The finding of relatively big pore volumes coincided with rather high numbers of water molecules in the pore as revealed from P_f/P_d ratios which ranged between 35 and 60 water molecules per pore. Compared with other AQPs, both the volumes of small (contributing to 48 % of the overall water permeability) and big (contributing to 20 % of the overall water permeability) water channels in the plasma membrane of *Chara* internodes were relatively large. This may be due to the fact that, to some extent, the measured volumes contained volumes of mouth parts. However, there may be also differences in the fine structure of channel protein due to interactions between AQPs and the bilayer. Channel volumes were small compared with those of ion channels. In comparison to AQPs of higher plants and ion channels, AQPs from *Chara* appeared to be fairly resistant to mechanical stress. Within the frame of the C/T model, high tensional forces of up to 5.0 MPa (50 bar) were required to close AQPs depending on the size of channels and that of the solute used.

Acknowledgements

We thank Prof. Carol A. Peterson and Chris Meyer (University of Waterloo, Canada) for carefully reading the manuscript and making helpful suggestions. Thanks also go to Burkhard Stumpf (Department of Plant Ecology, University of Bayreuth) for his expert technical assistance.

References

- Agre P., Bonhivers M. & Borgnia M.J. (1998) The aquaporins, blueprints for cellular plumbing systems. *Journal of Biological Chemistry* **273**, 14659–14662.
- Azaizeh H., Gunse B., & Steudle E. (1992) Effects of NaCl and CaCl₂ on water transport across root cells of maize (*Zea mays* L.) seedlings. *Plant Physiology* **99**, 886–894.
- Biela A., Grote K., Otto B., Hoth S., Hedrich R. & Kaldenhoff R. (1999) The *Nicotiana tabacum* plasma membrane aquaporin NtAQPI is mercury-insensitive and permeable for glycerol. *The Plant Journal* **18**, 565–570.
- Borgnia M., Nielsen S., Engel A. & Agre P. (1999) Cellular and molecular biology of the aquaporin water channels. *Annual Review of Biochemistry* **68**, 425–458.
- Dainty J. & Ginzburg B.Z. (1964) The permeability of the protoplast of *Chara australis* and *Nitella translucens* to methanol, ethanol and iso-propanol. *Biochimica et Biophysica Acta* **79**, 122–128.
- Dean R.M., Rivers R.L., Zeidel M.L. & Roberts D.M. (1999) Purification and functional reconstitution of soybean nodulin 26. An aquaporin with water and glycerol transport properties. *Biochemistry* **38**, 347–353.
- Finkelstein A. (1987) Water movement through lipid bilayers, pores and plasma membranes. Theory and reality. Distinguished lecture series of the Society of General Physiologists, vol. 4. Wiley, New York.

- Gerbeau P., Guclu J., Ripoche P. & Maurel C. (1999) Aquaporin Nt-TIPa can account for the high permeability of tobacco cell vacuolar membrane to small neutral solutes. *The Plant Journal* **18**, 577–587.
- Guenther J.F. & Roberts D.M. (2000) Water-selective and multifunctional aquaporins from *Lotus japonicus* nodules. *Planta* **210**, 741–748.
- Henzler T. & Steudle E. (1995) Reversible closing of water channels in *Chara* internodes provides evidence for a composite transport model of the plasma membrane. *Journal of Experimental Botany* **46**, 199–209.
- Henzler T. & Steudle E. (2000) Transport and metabolic degradation of hydrogen peroxide: model calculations and measurements with the pressure probe suggest transport of H₂O₂ across water channels. *Journal of Experimental Botany* **51**, 2053–2066.
- Henzler T., Ye Q. & Steudle E. (2004) Oxidative gating of water channels (aquaporins) in *Chara* by hydroxyl radicals. *Plant Cell and Environment* **27**, 1184–1195.
- Hertel A. & Steudle E. (1997) The function of water channels in *Chara*: the temperature dependence of water and solute flow provides evidence for composite membrane transport and for a slippage of small organic solutes across water channels. *Planta* **202**, 324–335.
- Javot H. & Maurel C. (2002) The role of aquaporins in root water uptake. *Annals of Botany* **90**, 301–313.
- Jung J.S., Preston G.M., Smith B., Guggino W.B. & Agre P. (1994) Molecular structure of the water channel through aquaporin CHIP - The hourglass model. *Journal of Biological Chemistry* **269**, 14648–14654.
- Kedem O. & Katchalsky A. (1963) Permeability of composite membranes. Part 2. Parallel arrays of elements. *Transactions of the Faraday Society* (London) **59**, 1931–1940.
- Kjellbom P., Larsson C., Johansson I., Karlsson M. & Johansson U. (1999) Aquaporins and water homeostasis in plants. *Trends in Plant Science* **4**, 308–314.

- Levitt D.G. (1974) A new theory of transport for cell membrane pores. I. General theory and application to red cell. *Biochimica Biophysica Acta* **373**, 115–131.
- Mathai J.C., Mori S., Smith B.L., Preston G.M., Mohandas N., Collins M., van Zijl P.C., Zeidel M.L. & Agre P. (1996) Functional analysis of aquaporin-1 deficient red cells. The Colton-null phenotype. *Journal of Biological Chemistry* **271**, 1309–1313.
- Maurel C. & Chrispeels M.J. (2001) Aquaporins: a molecular entry into plant water relations. *Plant Physiology* **125**, 135–138.
- Maurel C. (1997) Aquaporins and the water permeability of plant cell membranes. *Annual Review of Plant Physiology and Plant Molecular Biology* **48**, 399–429.
- Murata K., Mitsuoka K., Hirai T., Walz T., Agre, P., Heymann J.B., Engel A. & Fujiyoshi Y. (2000) Structural determinants of water permeation through Aquaporin-1. *Nature* **407**, 599–605.
- Niemietz C.M. & Tyerman S.D. (1997) Characterization of water channels in wheat root membrane vesicles. *Plant Physiology* **115**, 561–567.
- Ren G., Reddy V.S., Cheng A., Melnyk P. & Mitra A.K. (2001) Visualization of a water-selective pore by electron crystallography in vitreous ice. *Proceedings of the National Academy of Sciences USA* **98**, 1398–1403.
- Rivers R.L., Dean R.M., Chandy G., Hall J.E., Roberts D.M. & Zeidel M.L. (1997) Functional analysis of nodulin 26, an aquaporin in soybean root nodule symbiosomes. *Journal of Biological Chemistry* **272**, 16256–16261.
- Steudle E. (1993) Pressure probe techniques: basic principles and application to studies of water and solute relations at the cell, tissue, and organ level. In: Smith JAC, Griffith H, eds. *Water deficits: plant responses from cell to community*. Oxford: BIOS Scientific Publishers, 5–36.
- Steudle E. (2000) Water uptake by roots: effects of water deficit. *Journal of Experimental Botany* **51**, 1531–1542.

- Steudle E. (2001) The cohesion/tension mechanism and the acquisition of water by plant roots. *Annual Review Plant Physiology and Plant Molecular Biology* **52**, 847–875.
- Steudle E. & Henzler T. (1995) Water channels in plants: do basic concepts of water transport change? *Journal of Experimental Botany* **46**, 1067–1076.
- Steudle E., Smith J.A.C. & Lüttge U. (1980) Water relation parameters of individual mesophyll cells of the crassulacean acid metabolism plant *Kalanchoë daigremontiana*. *Plant Physiology* **66**, 1155–1163.
- Steudle E. & Tyerman S.D. (1983) Determination of permeability coefficients, reflection coefficients and hydraulic conductivity of *Chara corallina* using the pressure probe: effects of solute concentrations. *Journal of Membrane Biology* **75**, 85–96.
- Tazawa M. & Kamiya N. (1966) Water permeability of a characean internodal cell with special reference to its polarity. *Australian Journal of Biological Sciences* **19**, 399–419.
- Tyerman S.D., Bohnert H.J., Maurel C., Steudle E. & Smith J.A. (1999) Plant aquaporins: their molecular biology, biophysics and significance for plant water relations. *Journal of Experimental Botany* **25**, 1055–1071.
- Tyerman S.D., Niemietz C.M. & Bramley H. (2002). Plant aquaporins: multifunctional water and solute channels with expanding roles. *Plant, Cell and Environment* **25**, 173–194.
- Verkman A.S. & Mitra A.K. (2000) Structure and function of aquaporin water channels. *American Journal of Physiology -Renal Physiology* **278**, F13–F28.
- Wan X.C., Steudle E. & Hartung W. (2004) Gating of water channels (aquaporins) in cortical cells of young corn roots by mechanical stimuli (pressure pulses): effects of ABA and of HgCl₂. *Journal of Experimental Botany* **55**, 411–422.
- Ye Q., Wiera B. & Steudle E. (2004) A cohesion/tension mechanism explains the gating of water channels (aquaporins) in *Chara* internodes by high concentration. *Journal of Experimental Botany* **55**, 449–461.

Zhu F.Q., Tajkhorshid E. & Schulten K. (2004) Theory and simulation of water permeation in aquaporin-1. *Biophysical Journal* **86**, 50–57.

Zimmerberg J. & Parsegian V.A. (1986) Polymer inaccessible volume changes during opening and closing of a voltage-dependent ionic channel. *Nature* **323**, 36–39.

4 Oxidative gating of water channels (aquaporins) in *Chara* by hydroxyl radicals

Tobias Henzler, Qing Ye & Ernst Steudle*

Department of Plant Ecology, Bayreuth University, D-95440 Bayreuth, Germany

Received 19 March 2004; received in revised form 28 May 2004;
accepted for publication 1 June 2004

Correspondence: Ernst Steudle. Fax: + 49 921 55 2564;
e-mail: ernst.steudle@uni-bayreuth.de

Plant, Cell & Environment (2004) 27: 1184-1195

DOI: [10.1111/j.1365-3040.2004.01226.x](https://doi.org/10.1111/j.1365-3040.2004.01226.x)

Abstract

Hydroxyl radicals (*OH) as produced in the Fenton reaction ($\text{Fe}^{2+} + \text{H}_2\text{O}_2 = \text{Fe}^{3+} + \text{OH}^- + * \text{OH}$) have been used to reversibly inhibit aquaporins in the plasma membrane of internodes of *Chara corallina*. Compared to conventional agents such as HgCl_2 , *OH proved to be more effective in blocking water channels and was less toxic to the cell. When internodes were treated for 30 min, cell hydraulic conductivity (L_p) decreased by 90% or even more. This effect was reversed within a few minutes after removing the radicals from the medium. In contrast to HgCl_2 , radical treatment reduced membrane permeability of small lipophilic organic solutes (ethanol, acetone, 1-propanol, and 2-propanol) by only 24% to 52%, indicating some continued limited movement of these solutes across aquaporins. The biggest effect of *OH treatment on solute permeability was found for isotopic water (HDO), which largely used water channels to cross the membrane. Inhibition of aquaporins reduced the diffusional water permeability (P_d) by about 70%. For the organic test solutes, which mainly use the bilayer to cross the membrane, channel closure caused anomalous (negative) osmosis, i.e. cells had negative reflection coefficients (σ_s) and were transiently swelling in a hypertonic medium. From the ratio of bulk (L_p or osmotic permeability coefficient, P_f) to diffusional (P_d) permeability of water, the number (N) of water molecules that align in water channels was estimated to be $N = P_f/P_d = 46$ (on average). Radical treatment decreased N from 46 to 11, a value still larger than unity, which would be expected for a membrane lacking pores. The gating of aquaporins by *OH radicals is discussed in terms of a direct action of the radicals when passing the pores or by an indirect action *via* the bilayer. The rapid recovery of inhibited channels may indicate an easy access of cytoplasmic antioxidants to closed water channels. Since hydrogen peroxide is a major signaling substance during different biotic and abiotic stresses, the reversible closure of water channels by *OH (as produced from H_2O_2 in the apoplast in the presence transition metals such as Fe^{2+} or Cu^+) may be downstream of the H_2O_2 signaling. This may provide appropriate adjustments in water relations (hydraulic conductivity), and a common response to different kinds of stresses.

Key words: *Chara corallina*; aquaporins; hydraulic conductivity; hydroxyl radicals; negative osmosis; oxidative gating.

Introduction

Water channels (aquaporins) play an important role in water relations. In plants, 75 to 95% of trans-membrane movement of water is across these proteins (Steudle & Henzler 1995; Maurel 1997; Kjellbom *et al.* 1999; Tyerman *et al.* 1999; Steudle 2001; Maurel & Chrispeels 2001). Current research on plant water channels is focused on the gating of aquaporins; i.e. on opening or closing mechanisms which are thought to play a key role in the adaptation of plants to different kinds of stresses and, perhaps, in the cross-linking of these stresses (Steudle 2000; Javot & Maurel 2002; Tyerman, Niemietz & Bramley 2002; Pastori & Foyer 2002). Numerous internal or external factors control the gating of water channels such as their phosphorylation, the action of the water stress hormone ABA, pH, *pCa*, osmotic pressure and salinity, heavy metals, and temperature (Steudle & Tyerman 1983; Johansson *et al.* 1996; Hose, Steudle & Hartung 2000; Wan, Steudle & Hartung 2004; Gerbeau *et al.* 2002; Ye, Wiera & Steudle 2004; Azaizeh, Gunse & Steudle 1992; Henzler & Steudle 1995; Zhang & Tyerman 1999; Niemietz & Tyerman 2002; Hertel & Steudle 1997; Lee *et al.* 2003). Low nutrients, drought, anoxia, time of day or root development may be factors as well (Clarkson *et al.* 2000; Wan & Zwiazek 1999; Martre, North & Nobel 2001; Zhang & Tyerman 1991; Henzler *et al.* 1999; Tsuda & Tyree 2000; Barrowclough, Peterson & Steudle 2000; Hukin *et al.* 2002). Recently, a mechanical gating of water channels has been proposed. In root cortical cells, Wan *et al.* (2004) initiated channel closure by pulses of turgor pressure which induced a proportional diminution in water flow. The pulses resulted in an injection of kinetic energy to the channel protein causing a conformational change and its closure. A different mechanism was proposed by Ye *et al.* (2004). These authors induced substantial tensions (negative pressures) in the water-filled pores (aquaporins) of *Chara*, which then collapsed causing a reversible interruption of water flow and a decrease of water permeability. The cohesion/tension mechanism may explain the finding that, at least in some species, water permeability is reduced in the presence of

high external solute concentration, e.g. salinity (Steudle & Tyerman 1983; Azaizeh *et al.* 1992). Mechanical gating may play a role during the adjustment of water permeability of living tissue surrounding xylem vessels that are under tension in transpiring plants. Such a mechanism has been proposed for roots (Passioura 1988; Kramer & Boyer 1995; Steudle & Peterson 1998). It has been known for a long time that root hydraulic conductivity (L_p) increases as the tension in the xylem increases due to a high demand for water by the shoot.

In this paper, we describe a new type of an effective and reversible gating of water channels by hydroxyl radicals (*OH), which may be called an 'oxidative gating'. Oxidative gating may be involved in 'cross-talks' between different stresses such as cold, drought, and high light (Xiong, Schumaker & Zhu 2002). It is also known that reactive oxygen species (ROS) such as superoxide anion radical, H_2O_2 , and *OH act as stressors (Pastori & Foyer, 2002). During an oxidative burst, they are produced to protect plants against an invasion by pathogens (Wojtaszek, 1997). ROS play a role as signaling agents as well (Pei *et al.* 2000). For the latter function, most is known for hydrogen peroxide and nitric oxide (Neill, Desikan & Hancock 2002a; Neill *et al.* 2002b). Recently, it has been shown that the green alga *Chara corallina* can tolerate levels of H_2O_2 of as high as 350 mM (Henzler & Steudle 2000). However, it turned out that *Chara* is highly sensitive to very low concentrations of hydroxyl radicals and that *OH substantially affects the water permeability of its membranes. Hence, there may be an interrelation between oxidative stress (redox state) and water relations, and this may hold for other species as well. To demonstrate the action of the highly reactive oxidant *OH, hydroxyl radicals were produced in this research by the Fenton reaction ($Fe^{2+} + H_2O_2 = Fe^{3+} + OH^- + *OH$) outside of isolated *Chara* internodes. In the presence of Fe^{2+} , internodes could tolerate H_2O_2 only at concentrations of up to a fraction of a millimole. With the aid of a cell pressure probe, effects of *OH on the water permeability (hydraulic conductivity, L_p) were measured as well as those on the permeability (P_s) and reflection coefficients (σ_s) of certain solutes which moved across the membrane rapidly (acetone, monohydric alcohols, heavy water). As with mercurials (Henzler & Steudle 1995), *OH induced anomalous (negative) osmosis in the presence of the test solutes. Effects were more pronounced than with the conventional inhibitor

mercuric chloride (HgCl_2). Among the reactive oxidative species such as hydrogen peroxide or superoxide anion radical, the hydroxyl radical is the most reactive compound. The molecule contains an unpaired electron and tends to rapidly attack and oxidize neighbouring molecules, namely organic compounds. When $\cdot\text{OH}$ takes an electron from another non-radical, that molecule becomes a radical. This may initiate a chain reaction of electron removal that will eventually result in destruction of bioactive macromolecules such as proteins, sugars, membrane lipids, nucleotides, and organic materials (Tien, Svingen & Aust 1982; Stadtman 1993; Samaha *et al.* 1999; Nakamura, La & Swenberg 2000). The action of $\cdot\text{OH}$ radicals on water channels of *Chara* was largely reversible. As with the precise mechanism by which $\cdot\text{OH}$ acts on aquaporins, the mechanism of the recovery of aquaporin activity is not yet clear. Different mechanisms are discussed such as an action of cytoplasmic antioxidants (e.g. ascorbate) directly on the aquaporin or indirectly by peroxidation of unsaturated lipids in the bilayer.

Material and methods

Plant material

Chara corallina was grown in artificial pond water (APW; composition in $\text{mole}\cdot\text{m}^{-3}$: 1.0 NaCl, 0.1 KCl, 0.1 CaCl_2 and 0.1 MgCl_2) as described previously (Henzler & Steudle 1995) in tanks that contained a layer of natural pond mud. Plants were continuously illuminated with a 15 W fluorescent lamp (Electronic, Germany) positioned 0.2 m over the water surface. *Chara* internodes freed from adjacent cells were incubated in APW for several hours before the experiments were started. Internodes used in experiments were 50 to 150 mm in length and 0.8 to 1.0 mm in diameter.

Determination of transport parameters (L_p , P_s and σ_s)

There are three important transport parameters that can be measured by cell pressure probes (Steudle 1993). The hydraulic conductivity (L_p) is a measure of water

permeability, the solute permeability coefficient (P_s) denotes the passive permeability of the cell membrane for a given solute, and the reflection coefficient (σ_s) is a quantitative measure of the ‘passive selectivity’ of the cell membrane for that solute as compared to water. Usually, plant cell membranes would have a σ_s between zero and unity. When $\sigma_s = 0$ the membrane does not distinguish between solute and water. Both pass at the same rate. When $\sigma_s = 1$ the membrane is ideally semipermeable. In this case, only water can pass through the membrane and $P_s = 0$. The respective solutes are completely ‘reflected’ by the membrane. There are also cases in which $\sigma_s < 0$ (Henzler & Steudle 1995). This refers to the striking situation that a cell does not shrink but swells in hypertonic media because, during osmosis, solutes are getting into the cell faster than the water can get out. This phenomenon, which can be observed with plant cells, is called ‘anomalous (negative) osmosis’. Equations for calculating L_p , P_s and σ_s are:

$$L_p = \frac{V}{A} \times \frac{\ln(2)}{T_{1/2}^w (\varepsilon + \pi^i)}, \quad (1)$$

$$P_s = \frac{V}{A} \times \frac{\ln(2)}{T_{1/2}^s} = \frac{V}{A} k_s, \text{ and} \quad (2)$$

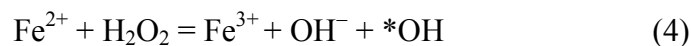
$$\sigma_s = \frac{P_o - P_{\min(\max)}}{RT \cdot \Delta C_s^o} \times \frac{\varepsilon + \pi^i}{\varepsilon} \exp(k_s \cdot t_{\min(\max)}). \quad (3)$$

Here, V = cell volume; A = cell surface area; π^i = osmotic pressure of cell sap; ε is the elastic coefficient of the cell (elastic modulus); k_s is the rate constant of solute exchange; $P_o - P_{\min(\max)}$ is the maximum change in cell turgor pressure; $RT \cdot \Delta C_s^o$ was the given change of osmotic pressure of the medium. For a detailed description of these equations, the reader is referred to earlier publications such as Steudle (1993), Henzler & Steudle (1995), or Ye *et al.* (2004).

Effects of *OH on the transport of water and solutes

As described earlier, the cell pressure probe (completely filled with silicone oil) was introduced through the protruding node adjacent to a *Chara* internode which had been placed in a glass tube of inner diameter 3 mm and fixed by a clamp (Henzler & Steudle 1995; Hertel & Steudle 1997). APW or test solutions were pumped through the other

end of the glass tube along the cell (flow rates were 0.15-0.2 m·s⁻¹), so that the solution around the cell was vigorously stirred. This minimized the thickness of external unstirred layers (Steudle & Tyerman 1983). In order to induce pressure relaxations, the oil/cell sap meniscus forming in the tip of the capillary, was moved forward or backward and was kept stable after each move. From the half time ($T_{1/2}^w$) of pressure relaxations, L_p was calculated as a control (see Eq. (1)). Solutes for testing the permeability of the membrane were heavy water (HDO at 3800 to 4750 mM; Merck, Darmstadt, Germany), acetone (134 to 173 mM), ethanol (110 to 140 mM), 1-propanol (155 to 173 mM) and 2-propanol (144 to 166 mM). Control values of P_s and σ_s were calculated from biphasic response curves (Steudle & Tyerman 1983; Steudle 1993; Eqs. 2 and 3). Hydroxyl radicals were produced by the Fenton reaction:



in the presence of 0.6 mM H₂O₂ and 3 mM FeSO₄ added to APW. This should have produced *OH at a very low concentration (see Discussion). Following the addition of H₂O₂, changes in half times of water flow ($T_{1/2}^w$) were measured during pressure relaxations which were produced every two minutes using the probe. After about 30 min, a steady half time of pressure relaxation ($T_{1/2}^w$) was attained. After reaching the maximum $T_{1/2}^w$ (minimum L_p), test solutes (HDO, acetone, ethanol, 1-propanol and 2-propanol) were added to the medium to measure changes of their P_s and σ_s in response to the radical treatment. For acetone, however, measurements of P_s and σ_s were also performed for some cells during the period of increasing of $T_{1/2}^w$.

To remove *OH, internodes were rinsed with control medium (APW). Again, using the cell pressure probe, $T_{1/2}^w$ was checked every two minutes to test for the reversibility of the effects of *OH. When control values of $T_{1/2}^w$ were re-attained, the same test solutes (HDO, acetone, ethanol, 1-propanol and 2-propanol) were used to re-examine the reversal of their effects. For a given cell, the whole time course of the experiments lasted for 2 to 4 h. During treatments, cells did not lose turgor pressure (0.6 to 0.7 MPa) within ± 0.03 MPa or ± 5 %.

Results

In the presence of $\cdot\text{OH}$, the activity of aquaporins was dramatically inhibited. Fig. 1A shows the time course of changes in $T_{1/2}^w$ ($\sim 1/L_p$) during radical treatment for a given *Chara* internode. $T_{1/2}^w$ increased continuously during treatment and attained a constant value after about 30 min. In the example shown in Fig. 1A, $T_{1/2}^w$ increased by a factor of 15. Hence, L_p was reduced by 93% in this case. Reductions in L_p varied from 90% to 95% ($n = 15$ cells). This value was significantly larger than that measured earlier in the presence of 50 μM HgCl_2 which only reduced L_p by 75% in *Chara* (Henzler & Steudle 1995). As $T_{1/2}^w$ increased, there was also an increase of the half time of permeation of the test solute acetone ($T_{1/2}^s$; Fig. 1B). $T_{1/2}^s$ was approximately doubled which resulted in a reduction of the solute permeability by a factor of two. Even though this was much less than the reduction in L_p , it was still substantial. In earlier experiments with HgCl_2 , there was no significant change in P_s for lipophilic solutes such as acetone (Table 1; Steudle & Henzler 1995). This had been interpreted by assuming a different pathway for the solutes; i.e. preferentially across the bilayer (Steudle & Henzler 1995; Hertel & Steudle 1997). The present results show that this conclusion has to be modified and that there is some movement of small uncharged solutes across water channels in *Chara* (see Discussion). As shown in Fig. 1, removal of $\cdot\text{OH}$ by washing the cell with control medium (APW), resulted in re-attaining both the original $T_{1/2}^w$ and $T_{1/2}^s$ to a good approximation (90% recovery for water and 92% for acetone).

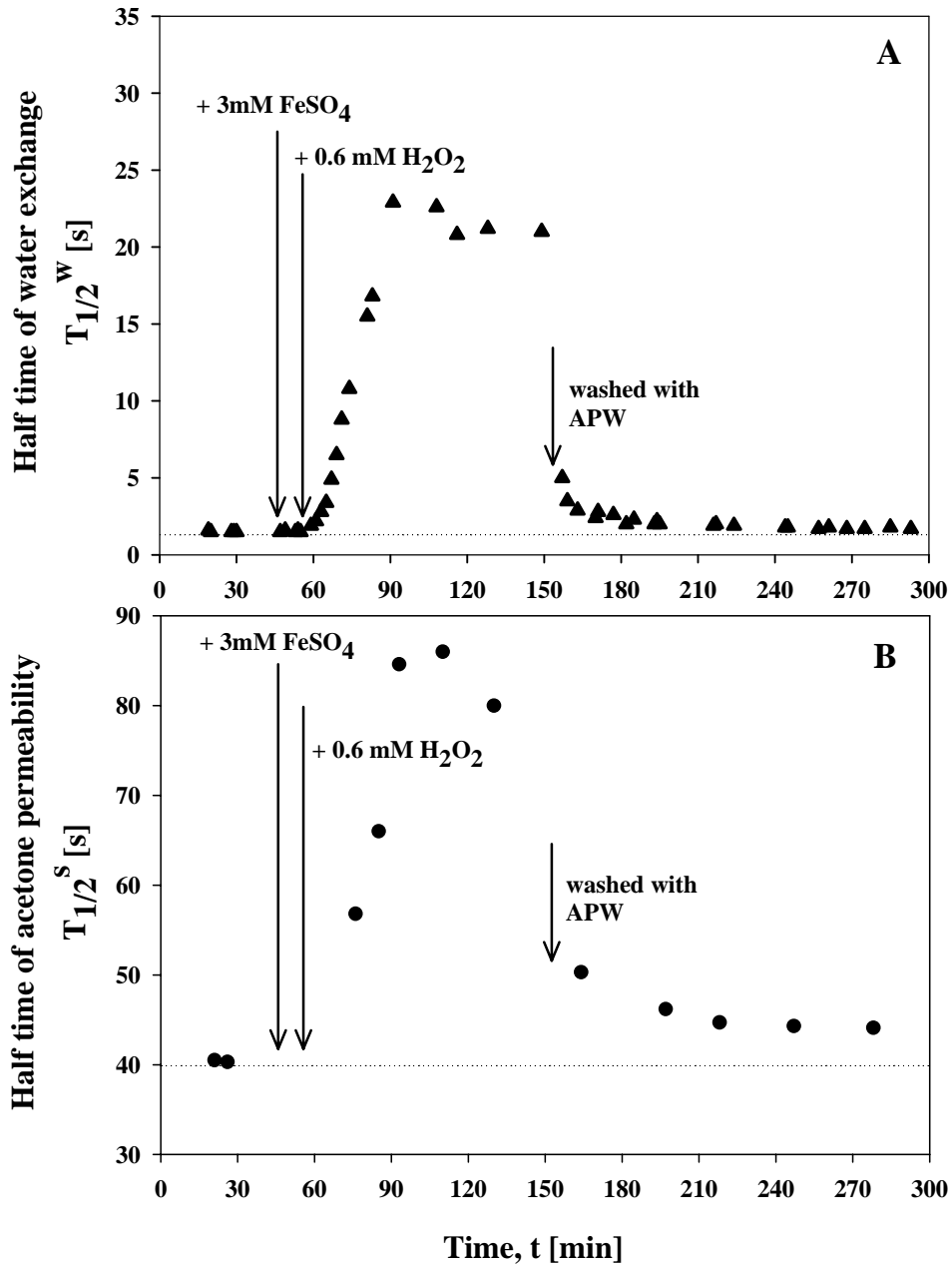


Fig. 1. Increase of half times of both water exchange ($T_{1/2}^w$; A) and acetone permeation ($T_{1/2}^s$; B) in an internode of *Chara* ($T_{1/2}^w \sim 1/L_p$; $T_{1/2}^s \sim 1/P_s$) caused by a treatment with $\cdot\text{OH}$ radicals. Closure of water channels was complete after about 30 minutes of treatment. An increase in $T_{1/2}^w$ by a factor of 15 indicates a decrease of L_p by the same factor. $T_{1/2}^s$ increased by a factor of 2 indicating that some of the solute did use aquaporins to cross the membrane. After removal of $\cdot\text{OH}$ radicals from the medium, the original $T_{1/2}^w$ was re-attained within a few minutes indicating a fast recovery of water channel activity.

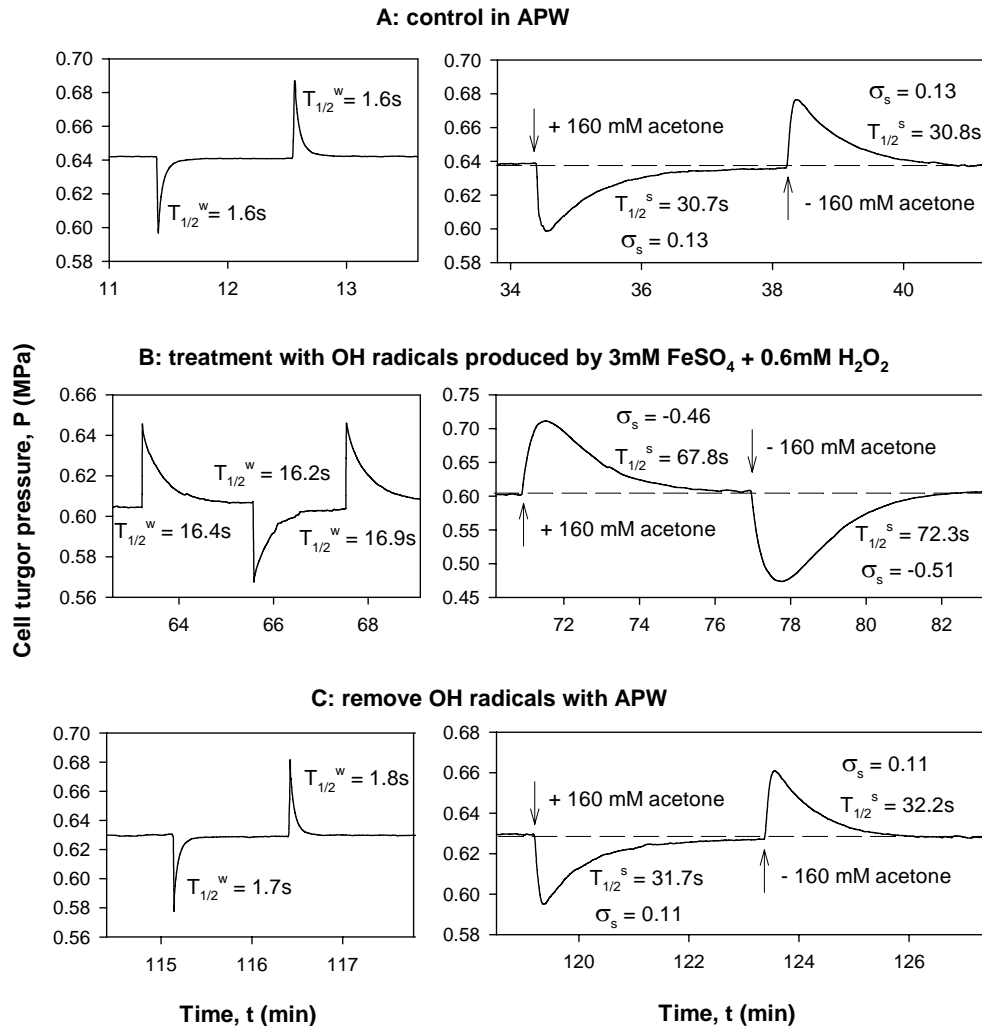


Fig. 2. Effects of $\cdot\text{OH}$ treatment on hydrostatic and osmotic pressure relaxations as measured with a pressure probe in the steady state. Compared with the control, hydrostatic half times increased by a factor of 10. With the permeating solute acetone, responses were biphasic. Reflection coefficient in the control was smaller than unity ($\sigma_s = 0.13$). Water channel closure resulted in anomalous osmosis (negative reflection coefficient, $\sigma_s = -0.46$). Because the solute entered the cell faster than the water could get out, the internode was swelling in hypertonic solution. From the second phase of responses, permeability coefficients of acetone were calculated (Eq. 2). Treatment affected solute transport much less than that of the water. A substantial amount of solute was permeating across water channels which were not completely selective for water. Removal of $\cdot\text{OH}$ from the solution resulted in a recovery of permeabilities for water and solute and of reflection coefficients by 90% (L_p), 96% (P_s) and 85% (σ_s) of the original values.

Typical relaxation curves (hydrostatic and osmotic) in response to *OH treatment are shown (steady state) in Fig. 2, again using acetone as the permeating test solute. Hydrostatic pressure relaxations are given on the left side of the figure. Usually, in the presence of a permeating solute such as acetone, osmotic response curves were biphasic (right side of the figure; Steudle & Tyerman 1983; Steudle 1993). There was an initial phase during which turgor pressure rapidly decreased or increased due to an exosmotic or an endosmotic water flow, respectively. This so-called ‘water phase’ was rapid because of the high permeability of the cell membrane to water. It was followed by a ‘solute phase’. During this second phase, turgor increased or decreased again due to the passive flow of solute into or out of the cell tending to equilibrate the concentration of permeating solutes on both sides of the membrane, and water followed the movement of the solute (Fig. 2A). As shown in Fig. 1A, blockage of water channels with *OH increased $T_{1/2}^w$ by a factor of 10 or even more (Fig. 2B). Most interestingly, upon water channel closure, the response to hypertonic solution was a transient increase in turgor (anomalous osmosis). The permeating solute (acetone) entered the cell faster than the water could get out. As a consequence, the cell did not shrink (turgor pressure decrease) but was swelling (turgor pressure increase) in hypertonic solution. The phenomenon of anomalous (negative) osmosis is described by a negative reflection coefficient. For the example given in Fig. 2B, σ_s decreased to -0.46 . Again, the figure shows a two-fold inhibition of solute permeability. When *OH was removed from the medium, the inhibition of water and solute flow was reversed within a short period of time, $T_{1/2}^w$ recovered to 90% of the original value, and the solute parameters (P_s and σ_s) recovered by 96% and 85%, respectively (Fig. 2C).

In the presence of hydrostatic or osmotic gradients of pressure, there should be a bulk water flow across aquaporins that should differ from the diffusional water flow through aquaporins as measured with isotopic water (heavy water, HDO). The ratio between the bulk (P_f ; see Eq. (5)) and diffusional (P_d) water permeability is a measure of the number of water molecules within the pores (Levitt 1974). When closing aquaporins by radical

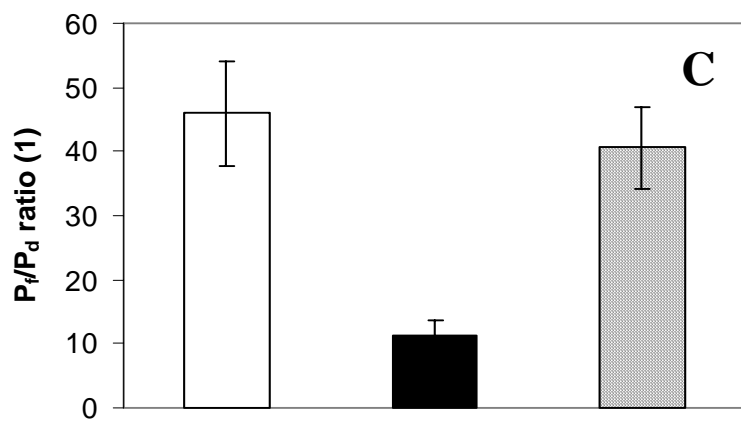
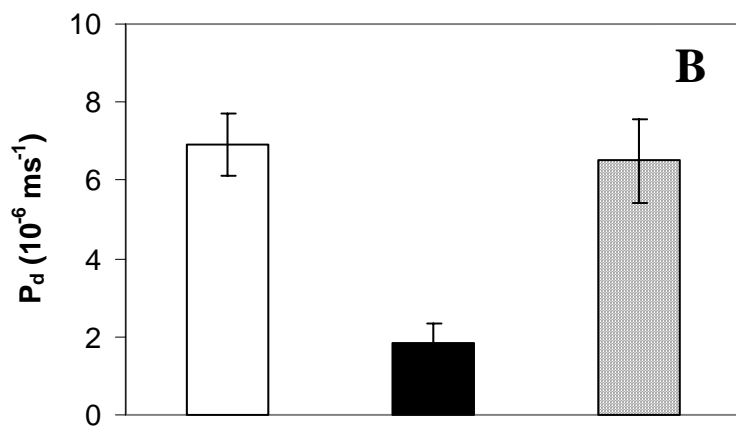
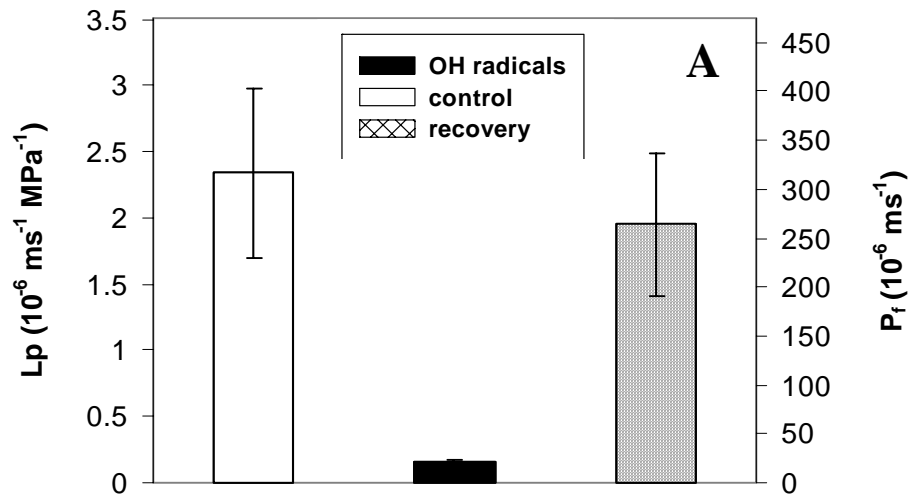


Fig. 3. Summary of the effects of *OH radical treatment on L_p and $P_f (= L_p \cdot RT / \bar{V}_w)$, and on the diffusional water permeability, P_d , as measured with heavy water (mean values \pm SD; $n = 5$ to 15 cells). (A) Closure of water channels by *OH radicals reduced L_p (P_f) to 10% of control. After removing *OH radicals from the medium, L_p (P_f) recovered to 85% of its original value. (B) Comparison between P_f and P_d shows that $P_f \gg P_d$. Inhibition of aquaporins reduced the diffusive permeability of isotopic water (HDO) to 30% of the control. This effect was reversed to 95% of the original when *OH was removed. (C) From the ratio of bulk to diffusive permeability of water (P_f/P_d), the number (N) of the water molecules that align in water channels was estimated to be $N = 35$ to 60. In the presence of closed channels, N decreased to 11.

treatment, we should thus expect to see big changes in the P_f/P_d ratio as most of the water is now using the bilayer to cross the membrane. Diffusional water flow across the bilayer should result in P_f/P_d ratio of unity. Measured changes of L_p (P_f) and P_d values are given in Fig. 3 (mean \pm SD; $n = 5$ to 15 cells). Following the inhibition of water channels by *OH, cell L_p decreased to about 1/10 of the control value indicating a closure of most of the channels. The osmotic permeability P_f shown in Fig. 3B is just proportional to L_p according to the relation:

$$P_f = \frac{L_p \cdot RT}{\bar{V}_w}. \quad (5)$$

Reductions of L_p and P_f were as large as 90% of the control (Fig. 3A). However, the reduction in P_d was 70% as compared with the control, i.e. smaller (Fig. 3B). The average value of P_f/P_d ratio was 46 in the control and 11 following the *OH treatment. The reduction of P_f/P_d ratio was significant ($P < 0.05$). *OH can be removed simply by washing *Chara* internodes with control medium APW. After the removal of *OH, water permeability L_p and P_f recovered to 85% of the controls within a few minutes (see also Fig. 1) indicating that water channels re-opened rather quickly due to the action of repair mechanisms of the cell. Ratios of P_f/P_d recovered to a large extent as well. The results indicate that *OH treatment caused a reduction of the porous channels as compared with the bilayer pathway, although ratios were still substantially bigger than unity after channel closure.

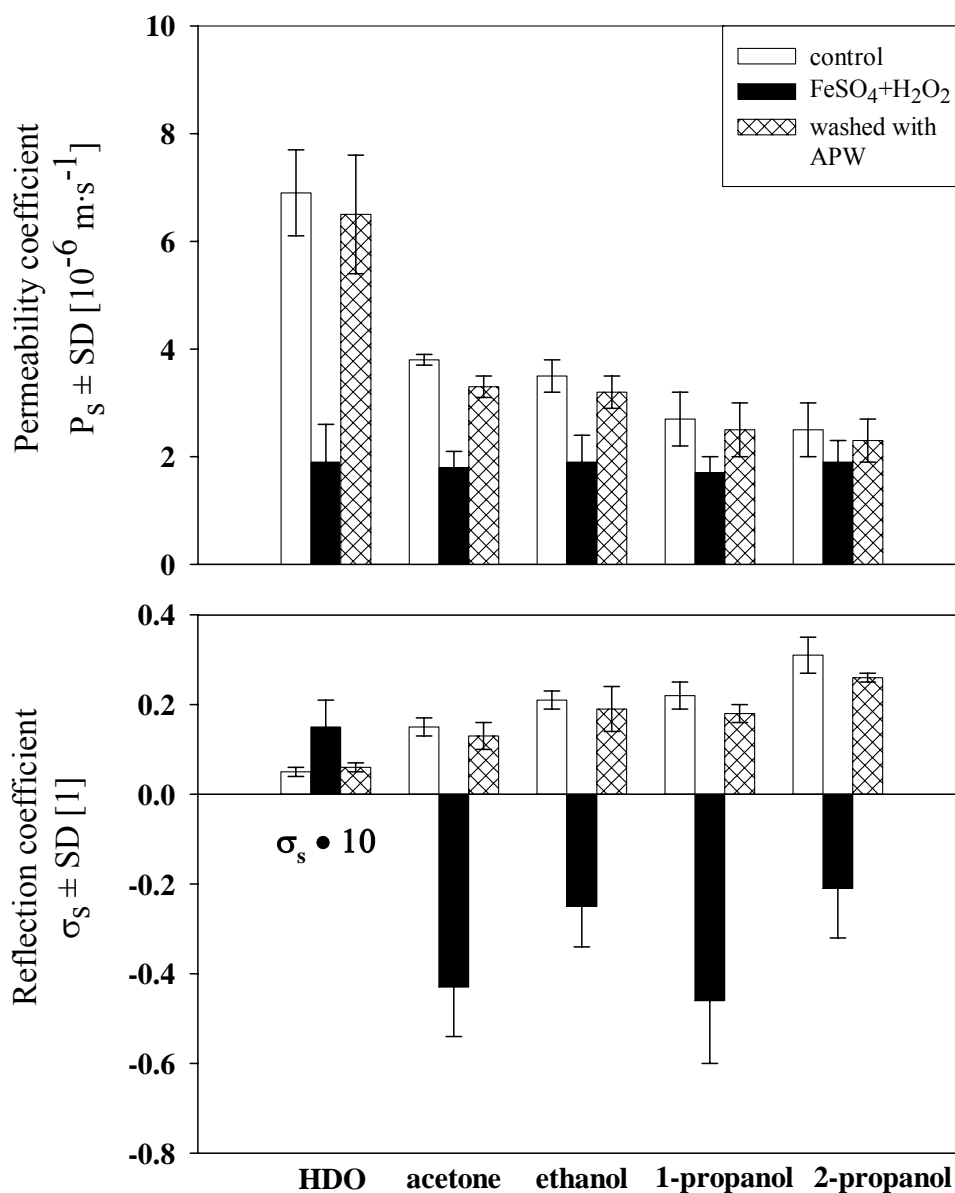


Fig. 4. Summary of diffusional permeabilities (P_s) and of reflection coefficients (σ_s) for some small, lipophilic organic solutes and heavy water as affected by $\cdot\text{OH}$ treatment (mean values \pm SD; $n = 5$ to 6 cells). To cross the membrane, organic solutes should largely use the bilayer. Heavy water should use aquaporins. Upon channel closure, there was a reduction of solute permeability which was the biggest for heavy water. The reflection coefficient of this solute, however, increased upon channel closure and did not decrease as was the case for the other solutes (acetone, ethanol, 1-propanol, and 2-propanol). Note that because of the small absolute value of the reflection coefficient of HDO, this is given as a multiple of 10. Effects nearly recovered after removal of $\cdot\text{OH}$ radicals.

Isotopic water (HDO) should be a good tracer for normal water. It should mainly use aquaporins to diffuse across cell membranes as verified in Fig. 3B. Hence, the effect of channel closure on P_d was the largest for this solute (reduction by 70%). For other test solutes, reduction of P_s ranged between 24% and 52% (acetone, 52%; ethanol, 46%; 1-propanol, 37%; 2-propanol 24%). The difference between HDO and the other solutes is evident from the fact that channel closure caused a decrease of the reflection coefficients of the latter to even negative values of down to -0.50 . However, σ_s of HDO increased, although absolute values were close to zero (Fig. 4). In terms of the composite transport model (Steudle & Henzler 1995), the result is understandable. Upon complete channel closure, reflection coefficients should assume values of the bilayer, which should be quite low or even negative for lipophilic solutes. However, for HDO, reflection coefficients of the bilayer should be bigger than those of water channels (Henzler & Steudle 1995). Hence, σ_s of HDO remained positive and increased by a factor of 3. As observed for water permeability, permeability and reflection coefficients of test solutes tended to not completely recover after removal of *OH . However, original and recovered values were not significantly different ($P > 0.05$).

Discussion

For the first time, hydroxyl radicals (*OH) have been used to reversibly inhibit the activity of water channels in internodes of *Chara* by an 'oxidative gating'. The effect was as large as one order of magnitude for water, and was much bigger than that of conventional aquaporin inhibitors such as $HgCl_2$. Mercuric chloride has the disadvantage that it is quite toxic and inhibits many cell functions. When keeping its concentration low, it appeared that toxic effects of *OH were less pronounced than those of $HgCl_2$. It should be noted that the actual concentration of *OH generated in the present study must have been quite low. In the presence of a fraction of a millimole of H_2O_2 , the actual concentration of *OH should have been in the nanomolar range due to its extremely short half-life (10^{-9} s; Caro & Puntarulo 1996; Agarwal, Saleh & Bedaiwy 2003). In the absence of Fe^{2+} , *Chara* internodes can tolerate H_2O_2 in concentrations of

up to 350 mM without affecting turgor and water transport across cell membranes (Henzler & Steudle 2000). We verified that 3 mM FeSO₄ by itself did not affect $T_{1/2}^w$ and $T_{1/2}^s$ even during long treatments. Hence, the effective agent was *OH. Cell turgor pressure was between 0.6 to 0.7 MPa. Turgor remained constant within ± 0.03 MPa during the experiments, indicating that the integrity of cell membranes was maintained.

The mechanism by which *OH acts on aquaporins is not yet understood. The highly reactive nature of *OH stems from its unpaired valence electron that causes high oxidative reactivity. *OH attacks and damages any organic matter such as nucleic acids, membrane lipids, proteins, nucleotides, and carbohydrates. The rates at which *OH reacts with organic material are extremely high. Rate constants of 10^7 to 10^{11} M⁻¹·s⁻¹ have been reported with almost every type of molecule found in living cells (Halliwell & Gutteridge 1989). Due to its high reactivity, it is unlikely that *OH produced in the medium moved across the *Chara* cell wall of 5 to 10 μ m without being completely absorbed in reactions with wall material such as during the oxidative scission of plant cell wall polysaccharides (Fry 1998). It is more likely that *OH radicals were produced close to the plasma membrane where Fe²⁺ should have been located due to negative fixed charges in the wall. Since *OH does not bear charges and is even smaller than water, it should be able to pass rapidly through the aquaporins right after its generation close to the membrane. Within the channel, it may attack cysteine or other residues as shown in the literature (Preston *et al.* 1993; Sanchez-Gongora *et al.* 1997; Caselli *et al.* 1998; Soto *et al.* 2002). Oxidation of aquaporins, in turn, may cause a change in the conformation of the protein and result in channel closure. In an alternative scenario, *OH may oxidize lipids by attacking C = C bonds and, thus, change the milieu around water channels (e.g. its polarity). Attack of the protein by lipid radicals, in turn, could result in a channel closure. To date, we can only speculate about possible mechanisms. There is no evidence regarding which of the proposed mechanisms is more likely. In the experiments it took about 30 minutes to reach the maximum effect of inhibition of channels. This could be explained by either mechanism, and a dynamic balance between damage and repair by antioxidants produced in the cytoplasm.

Plants possess very efficient scavenging antioxidant systems that protect them from destructive oxidative reactions. The fact that inhibition of water channels was reversed within a few minutes after removal of $\cdot\text{OH}$ from the medium indicated an effective repair mechanism(s) which should be related to cytoplasmic antioxidants such as ascorbate, glutathione or NADPH. Ascorbate usually acts as the reducing component which is then scavenged by glutathione and NADPH (Foyer & Lelandais 1993; Foyer, Descourvières & Kunert 1994; Schützendübel & Polle 2002). When channel closure is caused by lipid oxidation, recovery would be due to regeneration of the lipids around the channels and regeneration of oxidized protein from 'outside'. On the other hand, when the channel protein is oxidized from 'inside', the big scavenger molecules may have problems to act on the inside of the pore. However, the channel inside may become accessible during the conformational change, i.e. exposing oxidized parts to the cytoplasm.

Reversible closure of aquaporins by nanomolar concentrations of $\cdot\text{OH}$ in *Chara* are similar to those obtained in the presence of the conventional water channel blocker HgCl_2 (Chrispeels & Maurel 1994; Henzler & Steudle 1995; Tazawa, Asai & Iwasaki 1996). When *Chara* internodes were treated with 50 μM HgCl_2 for 10-15 min, cell L_p was reduced by 75%. It recovered in the presence of 5 mM of the scavenger 2-mercaptoethanol (Henzler & Steudle 1995), which removed the mercury from SH groups of the protein. However, HgCl_2 caused side effects when applied for longer periods of time. As a consequence, there was irreversible damage evidenced by a continuous decline in cell turgor pressure even when HgCl_2 was removed immediately after the experiment (Steudle & Henzler 1995; Zhang & Tyerman 1999). It was not possible to use concentrations of HgCl_2 higher than 50 μM in order to produce reductions of larger than 75%. Although there was not a complete recovery after $\cdot\text{OH}$ treatment (Fig. 3A), the present results indicate that $\cdot\text{OH}$ is much more effective and less toxic than HgCl_2 in blocking water channels in *Chara*. In longer terms, there may be a complete recovery of water and solute permeability from $\cdot\text{OH}$ treatment, an idea that is currently being tested. The fact that more water channels could be closed in the presence of $\cdot\text{OH}$ than by using HgCl_2 may be due to the existence of a population of different water channels instead of just one type. Some of the channel proteins may have SH groups and could be attacked

by HgCl_2 ; some of them do not have such groups or they are not accessible by mercurials, and are not sensitive to HgCl_2 (Daniels, Mirkov & Chrispeels 1994; Beila *et al.* 1999; Krajinski *et al.* 2000). However, these aquaporins may be accessible to $^*\text{OH}$, and more types of water channels may be affected by $^*\text{OH}$. This idea is consistent with results of molecular studies showing that plants have quite a number of putative aquaporins (Weig, Deswarte & Chrispeels 1997; Chaumont *et al.* 2001).

Unlike HgCl_2 , water channel closure by $^*\text{OH}$ also affected transport of small organic solutes such as acetone. Solute permeability was substantially reduced for monohydric alcohols as well. As one would expect, the effect was biggest for heavy water (HDO). This solute should largely use water channels to cross the membrane (Ye *et al.* 2004). The effect of $^*\text{OH}$ on solute permeability supports the earlier view of a limited passage of small organic molecules across water channels in *Chara* (Steudle & Henzler 1995; Henzler & Steudle 1995; Hertel & Steudle 1997). It is in line with results from other research on aquaporin selectivity indicating that aquaporins may allow the passage of substances such as glycerol, urea, and amino acid or even to small peptides (Kammerloher *et al.* 1994; Rivers *et al.* 1997; Agre, Bonhivers & Borgnia 1998; Borgnia *et al.* 1999; Dean *et al.* 1999; Gerbeau *et al.* 1999).

The movement of small organic solutes through water channels in *Chara* should have consequences for the overall osmotic properties of cell membranes and also to their selectivity as expressed by the reflection coefficient (σ_s). A composite transport model of the plasma membrane has been used to explain absolute overall values of reflection coefficients and how they would change upon channel closure (Henzler & Steudle 1995). According to the model, there are two different arrays (water channels and lipid bilayer) in the cell membranes which contribute to the overall reflection coefficient of a given solute. The σ_s measured with a cell pressure probe in present experiments would, thus, be a composite of water channel and lipid bilayer arrays. For HDO that should largely use the water channel path, σ_s increased by a factor of 3 upon the closure of water channels by $^*\text{OH}$ as expected from the model. The σ_s of the lipid bilayer should be small or even negative for rapidly permeating solutes like acetone, ethanol, 1-propanol, 2-propanol and so on, which mainly diffuse across cell membranes through

the bilayer. In this case, water channel closure should result in a decrease of σ_s (even to negative), as found. Changes of σ_s for HDO (increase), acetone and ethanol (decrease to negative) were more pronounced when water channels were blocked by *OH than with HgCl₂ (Table 1). The effect on σ_s can be dramatic. It is in line with the composite transport model. This is clear evidence for the role of water channels and their ability to allow the passage of uncharged small solutes besides water. As expected, passage was the biggest for HDO, but the contribution to the other solutes can be substantial as well depending on how effective the solute was fitting into the pore. Size and polarity of test solutes should have been important, and their ability to form hydrogen bonds within the pore.

At the present, we are not in a position to calculate the precise number of water molecules in the pore of a *Chara* aquaporin. According to Levitt's (1974) theory, the ratio between bulk or osmotic ($P_f \sim Lp$; Eq (5)) and diffusional (P_d) water flow directly yields the number (N) of water molecules aligned in water channels; i.e.:

$$\frac{P_f}{P_d} = \frac{Lp \cdot RT}{\bar{V}_w \cdot P_d} = N. \quad (6)$$

This assumes that water transport through water channels can be identified with the overall hydraulic conductivity (Lp), whereas P_d can be identified with the diffusional water permeability of channels. Present results shown in Fig. 3C suggest that there are 46 (on average) water molecules aligned in a water channel of *Chara*, which is larger than estimates from previous results (31 molecules/channel, Hertel & Steudle 1997; 27 molecules/channel, Henzler & Steudle 1995). It is also larger than the figure reported for red blood cells (10 molecules/channel, Finkelstein 1987). In part, the difference between *Chara* and red blood cells had been explained by the existence of unstirred layers which may have a dramatic effect on P_d but not on P_f , resulting in an overestimation of N (Steudle & Tyerman 1983; Henzler & Steudle 1995; Hertel & Steudle 1997). Using the same set-up for the internodes in a perspex tube as done here, Steudle & Tyerman (1983) measured the response in rates of transport (water, solutes) to the rate of stirring of the external medium. They concluded that, at maximum, external unstirred layers could be as thick as 50 μm . In view of diffusional exchange rates of 20 to 50 s for heavy water and for the rapidly permeating solutes, there should

have been no significant effect on P_d , P_s and σ_s (see Discussion in Henzler & Steudle 1995, and in Hertel & Steudle 1997). At a radius of internodes of ≈ 0.5 mm, internal unstirred layers could be as large as a few 100 μm , which is not negligible. However, there was some stirring by protoplasmic streaming and a substantial reduction by the cylindrical geometry of cells so that effects should have been much smaller (see Discussion in Hertel & Steudle 1997). Solute phases of HDO and of the other rapidly permeating solutes were nicely exponential throughout. This indicated that the contribution of internal unstirred layers was rather low. If unstirred layers build up, this would increase $T_{1/2}^s$ during the solute phase. Hence, effects on P_d should have been relatively small. However, the present data do not allow to really quantify the number of molecules aligned in a channel (although providing an upper limit). This would have been possible, if treatment by $\cdot\text{OH}$ would have closed all membrane pores which could allow a passage of water; i.e. all aquaporins as well as all other transporters such as pumps and ion channels. Then the assumption could be made that, after closure, $P_f = P_d$. Hence, it would be possible to work out P_f and P_d of the aquaporins themselves and its true N value as has been done for red blood cells (Mathai *et al.* 1996).

The physiological significance of the gating of water channels by $\cdot\text{OH}$ radicals needs to be addressed briefly. Hydrogen peroxide (and nitric oxide, NO) are known to be involved during signal transduction in response to many different stresses such as drought, high salinity, oxygen deprivation, chilling, and osmotic stress (Xiong *et al.* 2002). However, it is obvious, at least for *Chara*, that there is no direct effect on water transport of the systemic compound H_2O_2 . Previous results indicated that the alga tolerates concentrations of H_2O_2 as high as 350 mM. Aquaporins in *Chara* were highly permeable to this solute, which has a chemical structure similar to that of water (Henzler & Steudle 1995; 2000). Indeed, aquaporins appeared to act also as ‘peroxoporins’. In the present paper, we show that there is a strong response to locally produced, short-lived and highly reactive hydroxyl radicals which are also thought to act during ROS signaling (Neill *et al.* 2002 a, b). Hence, the apparent signaling of H_2O_2 in *Chara* is a consequence of its conversion into $\cdot\text{OH}$ radicals in the apoplast in the presence of a transition metal. This type of a downstream mechanism of the signaling of H_2O_2 may be important in higher plants. $\cdot\text{OH}$ may be produced in cell walls close to the

membranes in response to the major systemic signal substance H_2O_2 in the presence of transition metal ions such as Fe^{2+} or Cu^+ (Fry 1998). Experiments with higher plant tissues are underway to test this hypothesis. In a tissue apoplast, it is, however, more difficult than for an isolated cell to produce $\cdot\text{OH}$ radicals in a defined way close to plasma membranes.

In conclusion, the results show that the activity of water channels in the cell membranes of *Chara corallina* can be substantially and reversibly inhibited by $\cdot\text{OH}$. Compared with conventional blockers of aquaporins such as mercurials, $\cdot\text{OH}$ turned out to be more effective in blocking aquaporins and less toxic for cells. Water permeability (L_p) was reduced by more than 90 % when using $\cdot\text{OH}$ and recovered to 85 % of the control when $\cdot\text{OH}$ was removed. Unlike HgCl_2 , $\cdot\text{OH}$ reduced the permeability of small unchanged solutes indicating some transport of these solutes across the pores in addition to water. For rapidly permeating lipophilic solutes, the blockage of water channels with $\cdot\text{OH}$ resulted in negative reflection coefficients and anomalous osmosis as expected from the composite transport model. From the ratio of bulk to diffusive permeability of water, the number of water molecules that line up in channels was estimated to be $N = 46$ on average. This figure may represent an overestimate due to effects of unstirred layers, and a number of some twenty molecules/channel is, perhaps, more realistic. Treatment with $\cdot\text{OH}$ reduced N substantially as expected from the model. At present, we can only speculate about the mechanisms by which $\cdot\text{OH}$ acts on water channels. Two alternatives may be possible. One is that aquaporins were oxidized by $\cdot\text{OH}$ attacking the channel from inside the pore to cause conformational changes of the proteins and its closure. The other alternative is that $\text{C} = \text{C}$ double bonds of the plasma membrane were attacked by $\cdot\text{OH}$, resulting in the formation of aggressive radicals which attacked aquaporins from outside. Regardless of which of the mechanisms will turn to be true in the future, our results indicate a regulation of water channel activity by an oxidative signaling initiated in the presence $\cdot\text{OH}$. This may also exist in higher plants providing an interaction between the redox state (oxidative stress) and water relations (water stress).

Acknowledgements

Thanks go to Prof. Carol Peterson (University of Waterloo, Canada) and Jan Muhr (University of Bayreuth) for carefully reading the manuscript and making helpful suggestions. We are indebted to Burkhard Stumpf (Department of Plant Ecology, University of Bayreuth) for his expert technical assistance.

References

- Agarwal A., Saleh R.A. & Bedaiwy M.A. (2003) Role of reactive oxygen species in the pathophysiology of human reproduction. *Fertility Sterility* **79**, 829-843.
- Agre P., Bonhivers M. & Borgnia M.J. (1998) The aquaporins, blueprints for cellular plumbing systems. *Journal of Biological Chemistry* **273**, 14659-14662.
- Azaizeh H., Gunse B., & Steudle E. (1992) Effects of NaCl and CaCl₂ on water transport across root cells of maize (*Zea mays* L.) seedlings. *Plant Physiology* **99**, 886-894.
- Barrowclough D.E., Peterson C.A. & Steudle E. (2000) Radial hydraulic conductivity along developing onion roots. *Journal of Experimental Botany* **51**, 547-557.
- Biela A., Grote K, Otto B., Hoth S., Hedrich R. & Kaldenhoff R. (1999) The *Nicotiana tabacum* plasma membrane aquaporin NtAQP1 is mercury-insensitive and permeable for glycerol. *The Plant Journal* **18**, 565-570.
- Borgnia M., Nielsen S., Engel A. & Agre P. (1999) Cellular and molecular biology of the aquaporin water channels. *Annual Review of Biochemistry* **68**, 425-458.
- Caro A. & Puntarulo S. (1996) Effect of *in vivo* iron supplementation on oxygen radical production by soybean roots. *Biochimica et Biophysica Acta* **1291**, 245-251.

- Caselli A., Marzocchini R., Camici G., Manao G., Moneti G., Pieraccini G. & Ramponi G. (1998) The inactivation mechanism of low molecular weight phosphotyrosine-protein phosphatase by H₂O₂. *Journal of Biological Chemistry* **273**, 32554-32560.
- Chaumont F., Barrieu F., Wojcik E., Chrispeels M.J. & Jung R. (2001) Aquaporins constitute a large and highly divergent protein family in maize. *Plant Physiology* **125**, 1206-1215.
- Chrispeels M.J. & Maurel C. (1994) Aquaporins: the molecular basis of facilitated water movement through living plant cells. *Plant Physiology* **105**, 9-13.
- Clarkson D.T., Carvajal M., Henzler T., Waterhouse R.N., Smyth A.J., Cooke D.T. & Steudle E. (2000) Root hydraulic conductance: diurnal aquaporin expression and the effects of nutrient stress. *Journal of Experimental Botany* **51**, 61-70.
- Daniels M.J., Mirkov T.E. & Chrispeels M.J. (1994) The plasma membrane of *Arabidopsis thaliana* contains a mercury-insensitive aquaporin that is a homolog of the tonoplast water channel protein TIP. *Plant Physiology* **106**, 1325-1333.
- Dean R.M., Rivers R.L., Zeidel M.L. & Roberts D.M. (1999) Purification and functional reconstitution of soybean nodulin 26. An aquaporin with water and glycerol transport properties. *Biochemistry* **38**, 347-353.
- Finkelstein A. (1987) Water movement through lipid bilayers, pores and plasma membranes. Theory and reality. Distinguished lecture series of the Society of General Physiologists, vol. 4. Wiley, New York.
- Foyer C.H. & Lelandais M. (1993) The roles of ascorbate in the regulation of photosynthesis. In *Photosynthetic Responses to the Environment* (ed. H.Y. Yamamoto), pp. 88-101. American Society of Plant Physiologists, Rockville.
- Foyer C.H., Descourvières P. & Kunert K.J. (1994) Protection against oxygen radicals: an important defense mechanism studied in transgenic plants. *Plant, Cell and Environment* **17**, 507-523.
- Fry, S.C. (1998) Oxidative scission of plant cell wall polysaccharides by ascorbate-induced hydroxyl radicals. *Biochemistry Journal* **332**, 507-515.

- Gerbeau P., Amodeo G., Henzler T., Santoni V., Ripoche P. & Maurel C. (2002) The water permeability of *Arabidopsis* plasma membrane is regulated by divalent cations and pH. *The Plant Journal* **30**, 71-81.
- Gerbeau P., Guclu J., Ripoche P. & Maurel C. (1999) Aquaporin Nt-TIPa can account for the high permeability of tobacco cell vacuolar membrane to small neutral solutes. *The Plant Journal* **18**, 577-587.
- Halliwell B. & Gutteridge J.M.C. (1989) *Free Radicals in Biology and Medicine*, 2nd edn. Oxford, UK: Clarendon Press.
- Henzler T. & Steudle E. (1995) Reversible closing of water channels in *Chara* internodes provides evidence for a composite transport model of the plasma membrane. *Journal of Experimental Botany* **46**, 199-209.
- Henzler T. & Steudle E. (2000) Transport and metabolic degradation of hydrogen peroxide: model calculations and measurements with the pressure probe suggest transport of H₂O₂ across water channels. *Journal of Experimental Botany* **51**, 2053-2066.
- Henzler T., Waterhouse R.N., Smyth A.J., Carvajal M., Cooke D.T., Schäffner A.R., Steudle E. & Clarkson D.T. (1999) Diurnal variations in hydraulic conductivity and root pressure can be correlated with the expression of putative aquaporins in the roots of *Lotus Japonicus*. *Planta* **210**, 50-60.
- Hertel A. & Steudle E. (1997) The function of water channels in *Chara*: the temperature dependence of water and solute flow provides evidence for composite membrane transport and for a slippage of small organic solutes across water channels. *Planta* **202**, 324-335.
- Hose E., Steudle E. & Hartung W. (2000) Abscisic acid and hydraulic conductivity of maize roots: a root cell- and pressure probe study. *Planta* **211**, 874-882.
- Hukin D., Doering-Saad C., Thomas C.R. & Pritchard J. (2002) Sensitivity of cell hydraulic conductivity to mercury is coincident with symplasmic isolation and expression of plasmalemma aquaporin genes in growing maize roots. *Planta* **215**, 1047-1056.

- Javot H. & Maurel C. (2002) The role of aquaporins in root water uptake. *Annals of Botany* **90**, 301-313.
- Johansson I., Larsson C., Ek B. & Kjellbom P. (1996) The major integral proteins of spinach leaf plasma membranes are putative aquaporins and are phosphorylated in response to Ca^{2+} and apoplastic water potential. *The Plant Cell* **8**, 1181-1191.
- Kammerloher W., Fischer U., Piechottka G.P. & Schaffner A.R. (1994) Water channels in the plant plasma membrane cloned by immunoselection from a mammalian expression system. *The Plant Journal* **6**, 187-199.
- Kjellbom P., Larsson C., Johansson I., Karlsson M. & Johansson U. (1999) Aquaporins and water homeostasis in plants. *Trends in Plant Science* **4**, 308-314.
- Krajinski F., Biela A., Schubert D., Gianinazzi-Pearson V., Kaldenhoff R. & Franken P. (2000) Arbuscular mycorrhiza development regulates the mRNA abundance of Mtaqp1 encoding a mercury-insensitive aquaporin of *Medicago truncatula*. *Planta* **211**, 85-90.
- Kramer P.J. & Boyer J.S. (1995) *Water Relations of Plants and Soils*. Orlando: Academic.
- Lee S.H., Singh A.P., Chung G.C., Kim Y.S. & Kong I.B. (2003) Chilling root temperature causes rapid ultrastructural changes in cortical cells of cucumber (*Cucumis sativus* L.) root tips. *Journal of Experimental Botany* **53**, 2225-2237.
- Levitt D.G. (1974) A new theory of transport for cell membrane pores. I. General theory and application to red cell. *Biochimica Biophysica Acta* **373**, 115-131.
- Martre P., North G.B. & Nobel P.S. (2001) Hydraulic conductance and mercury-sensitive water transport for roots of *Opuntia acanthocarpa* in relation to soil drying and rewetting. *Plant Physiology* **126**, 352-362.
- Mathai J.C., Mori S., Smith B.L., Preston G.M., Mohandas N., Collins M., van Zijl P.C., Zeidel M.L. & Agre P. (1996) Functional analysis of aquaporin-1 deficient red cells. The Colton-null phenotype. *Journal of Biological Chemistry* **271**, 1309-1313.

- Maurel C. & Chrispeels M.J. (2001) Aquaporins: a molecular entry into plant water relations. *Plant Physiology* **125**, 135-138.
- Maurel C. (1997) Aquaporins and the water permeability of plant cell membranes. *Annual Review of Plant Physiology and Plant Molecular Biology* **48**, 399-429.
- Nakamura, J., La, D.K. & Swenberg, J.A. (2000) 5'-Nicked apurinic/aprimidinic sites are resistant to β -elimination by β -polymerase and are persistent in human cultured cells after oxidative stress. *Journal of Biological Chemistry* **275**, 5323-5328.
- Neill S.J., Desikan R. & Hancock J. (2002a) Hydrogen peroxide signalling. *Current Opinion in Plant Biology* **5**, 388-395.
- Neill S.J., Desikan R., Clarke A., Hurst R.D. & Hancock J.T. (2002b) Hydrogen peroxide and nitric oxide as signaling molecules in plants. *Journal of Experimental Botany* **53**, 1237-1247.
- Niemietz C.M. & Tyerman S.D. (2002) New potent inhibitors of aquaporins: silver and gold compounds inhibit aquaporins of plant and human origin. *FEBS Letters* **531**, 443-447.
- Passioura J.B. (1988) Water transport in and to roots. *Annual Review of Plant Physiology and Plant Molecular Biology* **39**, 245-65.
- Pastori G. & Foyer C.H. (2002) Common components, networks, and pathways of cross-tolerance to stress: the central role of "redox" and abscisic acid mediated controls. *Plant Physiology* **129**, 460-468.
- Pei Z.M., Murata Y., Benning G., Thomine S., Klusener B., Allen G.J., Grill E. & Schroeder J.I. (2000) Calcium channels activated by hydrogen peroxide mediate abscisic acid signalling in guard cells. *Nature* **406**, 731-734.
- Preston G.M., Jung J.S., Guggino, W.B. & Agre P. (1993) The mercury-sensitive residue at cysteine-189 in the CHIP28 water channel. *Journal of Biological Chemistry* **268**, 17-20.

- Rivers R.L., Dean R.M., Chandy G., Hall J.E., Roberts D.M. & Zeidel M.L. (1997) Functional analysis of nodulin 26, an aquaporin in soybean root nodule symbiosomes. *Journal of Biological Chemistry* **272**, 16256-16261.
- Samaha R.R., Joseph S., O'Brien B., O'Brien T.W. & Noller H.F. (1999) Site-directed hydroxyl radical probing of 30S ribosomal subunits by using Fe (II) tethered to an interruption in the 16S rRNA chain. *Proceedings of the National Academy Science USA* **96**, 366-370.
- Sanchez-Gongora E., Ruiz F., Mingorance J., An W., Corrales F.J. & Mato J.M. (1997) Interaction of liver methionine adenosyltransferase with hydroxyl radical. *The FASEB Journal* **11**, 1013-1019.
- Schützendübel A. & Polle A. (2002) Plant responses to abiotic stresses: heavy metal-induced oxidative stress and protection by mycorrhization. *Journal of Experimental Botany* **53**, 1351- 1365.
- Soto M.A., González C., Lissi E., Vergara C. & Latorre R. (2002) Ca²⁺-activated K⁺ channel inhibition by reactive oxygen species. *American Journal of Physiology Cell Physiology* **282**, C461-C471.
- Stadtman, E.R. (1993) Oxidation of free amino acids and amino acid residues in proteins by radiolysis and by metal-catalyzed reactions. *Annual Review of Biochemistry* **62**, 797-821.
- Stedle E. & Henzler T. (1995) Water channels in plants: do basic concepts of water transport change? *Journal of Experimental Botany* **46**, 1067-1076.
- Stedle E. & Peterson C.A. (1998) How does water get through roots? *Journal of Experimental Botany* **49**, 775-788.
- Stedle E. & Tyerman S.D. (1983) Determination of permeability coefficients, reflection coefficients and hydraulic conductivity of *Chara corallina* using the pressure probe: effects of solute concentrations. *Journal of Membrane Biology* **75**, 85-96.
- Stedle E. (1993) Pressure probe techniques: basic principles and application to studies of water and solute relations at the cell, tissue, and organ level. In: Smith JAC,

- Griffith H, eds. *Water deficits: plant responses from cell to community*. Oxford: BIOS Scientific Publishers, 5-36.
- Steudle E. (2000) Water uptake by roots: effects of water deficit. *Journal of Experimental Botany* **51**, 1531-1542
- Steudle E. (2001) The cohesion/tension mechanism and the acquisition of water by plant roots. *Annual Review Plant Physiology and Plant Molecular Biology* **52**, 847-875.
- Tazawa M., Asai K. & Iwasaki N. (1996) Characteristics of Hg- and Zn-sensitive water channels in the plasma membrane of *Chara corallina*. *Botanica Acta* **105**, 388-3986
- Tien M., Svingen B.A. & Aust S.D. (1982) An investigation into the role of hydroxyl radical in xanthine oxidase-dependent lipid peroxidation. *Archives of Biochemistry and Biophysics* **216**, 142-151.
- Tsuda M. & Tyree M.T. (2000) Plant hydraulic conductance measured by the high pressure flow meter in crop plants. *Journal of Experimental Botany* **51**, 823-828.
- Tyerman S.D., Bohnert H.J., Maurel C., Steudle E. & Smith J.A. (1999) Plant aquaporins: their molecular biology, biophysics and significance for plant water relations. *Journal of Experimental Botany* **25**, 1055-1071.
- Tyerman S.D., Niemietz C.M. & Bramley H. (2002). Plant aquaporins: multifunctional water and solute channels with expanding roles. *Plant, Cell and Environment* **25**, 173-194.
- Wan X. & Zwiazek J.J. (1999) Mercuric chloride effects on root water transport in aspen seedlings. *Plant Physiology* **121**, 939-946.
- Wan X.C., Steudle E. & Hartung W. (2004) Gating of water channels (aquaporins) in cortical cells of young corn roots by mechanical stimuli (pressure pulses): effects of ABA and of HgCl₂. *Journal of Experimental Botany* **55**, 411-422.
- Weig A., Deswarte C. & Chrispeels M.J. (1997) The major intrinsic protein family of *Arabidopsis* has 23 members that form three distinct groups with functional aquaporins in each group. *Plant Physiology* **114**, 1347-1357.

- Wojtaszek P. (1997) Oxidative burst: an early plant response to pathogen infection. *Biochemical Journal* **322**, 681-692.
- Xiong L., Schumaker K.S. & Zhu, J.K. (2002) Cell signaling during cold, drought and salt stress. *Plant Cell* **14** (suppl.), S165-S183.
- Ye Q., Wiera B. & Steudle E. (2004) A cohesion/tension mechanism explains the gating of water channels (aquaporins) in *Chara* internodes by high concentration. *Journal of Experimental Botany* **55**, 449-461.
- Zhang W.H. & Tyerman S.D. (1991) Effect of low O₂ concentration and azide on hydraulic conductivity and osmotic volume of cortical cells of wheat roots. *Australian Journal of Plant Physiology* **18**, 603-613.
- Zhang W.H. & Tyerman S.D. (1999) Inhibition of water channels by HgCl₂ in intact wheat root cells. *Plant Physiology* **120**, 849-858.

5 Oxidative gating of water channels (aquaporins) in corn roots

Qing Ye & Ernst Steudle*

Department of Plant Ecology, Bayreuth University, D-95440 Bayreuth, Germany

Received 4 April 2005; received in revised form 15 June 2005;
accepted for publication 20 July 2005

Correspondence: Ernst Steudle. Fax: + 49 921 55 2564;
e-mail: ernst.steudle@uni-bayreuth.de

Plant, Cell & Environment (2005) 28: in press

Doi: 10.1111/j.1365-3040.2005.01423

Abstract

An oxidative gating of water channels (aquaporins: AQPs) was observed in roots of corn seedlings as already found in the green alga *Chara corallina* (Henzler, Ye & Steudle 2004). In the presence of 35 mM hydrogen peroxide (H_2O_2) – a precursor of hydroxyl radicals (*OH) – half times of water flows (as measured with the aid of pressure probes) increased at the level of both entire roots and individual cortical cells by factors of 3 and 9, respectively. This indicated decreases of the hydrostatic hydraulic conductivity of roots ($L_{p_{hr}}$) and of cells (L_{p_h}) by the same factors. Different from other stresses, the plant hormone ABA had no ameliorative effect neither on root $L_{p_{hr}}$ nor on cell L_{p_h} , when AQPs were inhibited by oxidative stress. Closure of AQPs reduced permeability of acetone by factors of 2 in roots and of 1.5 in cells. This indicated that AQPs were not ideally selective for water, but allowed the passage of the small organic solute acetone. In the presence of H_2O_2 , channel closure caused anomalous (negative) osmosis at both the root and cell level. This was interpreted by the fact that, in case of the rapidly permeating solute acetone, channel closure caused a situation in which the solute moved faster than the water and the reflection coefficient (σ_s) reversed its sign. When H_2O_2 was removed from the medium, effects were reversible, again at both the root and cell level. The results provide evidence for an oxidative gating of AQPs and thus inhibiting water uptake by roots. Possible mechanisms of the oxidative gating of AQPs induced by H_2O_2 (*OH) are discussed.

Key words: hydraulic conductivity; hydrogen peroxide; hydroxyl radicals; negative osmosis; oxidative stress.

Introduction

The gating (opening and closing) of water channels (aquaporins: AQPs) is thought to be of key importance in the regulation of water transport across plant cell membranes. There are numerous internal or external factors that cause a gating of AQPs such as high concentration or salinity, pH, pCa and heavy metals (Steudle & Tyerman 1983; Azaizeh, Gunse & Steudle 1992; Henzler & Steudle 1995; Gerbeau *et al.* 2002; Niemietz & Tyerman 2002; Ye, Wiera & Steudle 2004; Ye, Muhr & Steudle 2005). The activity of AQPs can also be affected by temperature, nutrient deprivation or hypoxia (Hertel & Steudle 1997; Zhang & Tyerman 1999; Clarkson *et al.* 2000; Lee, Chung & Steudle 2005a, b). It has been shown that protein phosphorylation can provide a metabolic control of AQP activity (Johansson *et al.* 1996). The plant stress hormone ABA has an ameliorative effect tending to either keep AQPs open or cause a rapid transition from the closed to the open state (Freundl, Steudle & Hartung 1998, 2000; Hose, Steudle & Hartung 2000; Wan, Steudle & Hartung 2004; Lee, Chung & Steudle 2005b). Other experiments have shown that there may be a diurnal rhythm in AQP activity which is related to diurnal synthesis and degradation of channel proteins (Henzler *et al.* 1999). Recent results of Wan *et al.* (2004) indicated a mechanical inhibition of AQPs, which may be important during rapid changes in cell turgor as they occur during osmotic stress or rapid changes in transpiration. The list of factors may get longer in the future. In most of the cases, the precise mechanism by which stresses or other factors affect the open/closed states of AQPs is not known.

Recently, Henzler, Ye & Steudle (2004) described a new type of an oxidative gating of AQPs in the green alga *Chara corallina*. Hydroxyl radicals (*OH) as produced during the Fenton reaction ($Fe^{2+} + H_2O_2 = Fe^{3+} + OH^- + *OH$) had been used to inhibit AQP activity in the plasma membrane of *Chara* internodes. When cells were treated with *OH radicals for about 0.5 h, cell hydraulic conductivity (L_p) decreased by 90 % or even more. The effect was reversed within a few minutes after removal of the radicals from the medium. Aroca *et al.* (2005) found that treatment with 100 μM hydrogen peroxide decreased root hydraulic conductance of a chilling-sensitive maize genotype, but had no effect on a chilling-tolerant genotype. These authors referred the changes to

a membrane damage caused by H₂O₂ accumulation during chilling treatment to the chilling-sensitive genotype which did not recover upon the increase of AQP abundance and activity. Since hydrogen peroxide is a major signaling substance during different biotic and abiotic stresses (Xiong, Schumaker & Zhu 2002; Pastori & Foyer 2002), Henzler *et al.* (2004) speculated that the reversible closure of water channels by *OH as produced from H₂O₂ in the apoplast in the presence of transition metals such as Fe²⁺ or Cu⁺ (Fry 1998), may be a downstream reaction during H₂O₂ signaling. It may provide appropriate adjustments in water relations and a common response to different kinds of stresses from which plants may suffer during their life.

In the present paper, the idea of an oxidative gating of AQPs is pursued further in experiments with young roots of corn (*Zea mays* L.). Because the nutrient solution already contained FeNaEDTA as Fe³⁺, Fe²⁺ should also be present as a result of the reaction with the superoxide anion (O₂⁻) such as follows: Fe³⁺ + O₂⁻ = Fe²⁺ + O₂ or other reactions either within cells or in the root apoplast (Chen & Schopfer 1999; Liskay, Zalm & Schopfer 2004). Therefore, we used just hydrogen peroxide at a concentration of 35 mM instead of a mixture of H₂O₂ and Fe²⁺ to produce *OH radicals (as during the *Chara* experiments of Henzler *et al.* (2004), where mixture of 3 mM Fe²⁺ and 0.6 mM H₂O₂ were used). The relatively high concentrations of H₂O₂ were not harmful to the roots, which reversibly tolerated them when applied for 2 – 3 h. Pressure probes were used to measure effects on cell (in the outer cortex) and entire root hydraulic conductivity. Anomalous osmosis could be reversibly induced in the presence of the lipophilic solute acetone at both the root and cell level. The phenomena have been interpreted in terms of the composite structure of cell membrane and of roots (Steudle & Henzler 1995; Steudle & Peterson 1998). The stress hormone ABA had ameliorative effect during the inhibition of root Lp_r and cell Lp by treatment like mechanical stimuli or low temperature (Freundl *et al.* 2000; Hose *et al.* 2000; Wan *et al.* 2004; Lee *et al.* 2005b). In the present paper, this effect has been tested as well during the ‘oxidative’ gating of AQPs.

Material and methods

Plant material

Seeds of corn (*Zea mays* L. cv. Helix, Kleinwanzlebener Saatzucht AG, Einbeck, Germany) were germinated on filter paper soaked in 0.5 mM CaSO₄ for 3 d at 25 °C in the dark. When seminal roots were 30 to 50 mm long, seedlings were transferred to 7-L containers which accommodated 20 seedlings each. For detailed information of growing conditions, the reader is referred to earlier publications such as Freundl *et al.* (1998), Hose *et al.* (2000), and Wan *et al.* (2004). Roots of 8 to 10 days old seedlings (including time required for germination) were used in the experiments. At that time roots were 250 to 400 mm long.

Root pressure probe experiments

End segments of roots were placed in a glass tube (inner diameter: 6 mm) with the basal cut end protruding, which were connected to a root pressure probe. Segments (80 to 120 mm long) were fixed to the probe by silicone seals (Zhu & Steudle 1991). Root medium was flowing along the roots by gravity from a reservoir sitting about 0.5 m above the glass tube (0.2 m long) at a rate of 0.30 – 0.50 m/s, and circulated back to the reservoir by a peristaltic pump. The flexible silicone rubber tubes connecting reservoir and glass tube also had an inner diameter of 6 mm. According to Poiseuille's law, this should have resulted in an average flow rate of 4 m/s or to a peak value in the center of the tubing of 8 m/s. This rate was much too high. It would have caused leakages in the roots or would even break them. Hence, the speed was reduced by a two-way stopcock between the reservoir and the glass tube which also allowed to change solutions using two different reservoirs (see Fig. 1 in Hertel & Steudle 1997; Azaizeh & Steudle 1991). Average rates of water flow were regulated to 0.30 – 0.50 m/s which did not cause too much shaking of the roots or even damages, but reduced unstirred layers to a minimum (Steudle & Tyerman 1983). Water flow within the rubber tubing and the glass pipe was turbulent as the water stream was injected into the tubing through borings in the stopcock which had a diameter of 2 mm and were arranged at an angle of about 30°.

Turbulences within the system could be seen from the movement of little air bubbles which occasionally passed through (namely, when changing solutions). In tests, they were made visible using finely suspended matter (murky solution obtained by shaking sand for gardening with the root medium). Turbulences were largely created by the fact that there were changes in diameter and that flow was forced to deviate from straight direction (see above and below). Also, the Reynolds number (Re) was already close to the critical value of 2000, where laminar flow tends to become turbulence (Re = 1800 to 3000). During its travel along the tubing (0.5 m), turbulences tended to even out, but were reinforced by a constriction (3 mm in diameter) at the entrance to the glass tube which caused an increase in the rate of the water stream (Bernoulli) before releasing it into the wider glass tube. The breaking of the water stream at the root should have caused turbulences as well. At high rates of water flow, roots tended to tremble depending on their length and mechanical rigidity. Trembling or even shaking was quite intensive with the softer wheat roots (14 d old and raised hydroponically) rather than with the tougher corn roots (S.Q. Zhang, personal communication). Roots were approximately centered in the glass tube. Often, their shape deviated from that of a straight cylinder by slight curvatures. Due to the turbulences in the glass tube, rates of water flow in its center should have been close to the measured average value rather than to the higher rates which one could calculate assuming an ideal laminar streaming (Poiseuille's law). The set-up allowed to quickly push out the solution from the glass tube. When changing solutions, the mixing area between old and new solution should have been no longer than 50 mm. At a root length of 100 mm, this would relate to a time of 0.4 s for a complete exchange of media around a root. This was small compared to the rate of water exchange across roots in osmotic experiments (around 30 s). Hence, the time required for an exchange of media was not rate limiting during these experiments.

After tightening the silicone seals in steps with the aid of a screw, root pressure (P_r) began to increase and became steady within 1 to 3 h (Hose *et al.* 2000). In hydrostatic experiments, pressure relaxations were induced with the aid of the probe to measure the hydrostatic half time ($T_{hr1/2}^w$) of radial water exchange across the root ($T_{hr1/2}^w \propto 1/Lp_{hr}$; Lp_{hr} = hydrostatic root hydraulic conductivity). As described by Hose *et al.* (2000),

hydrostatic relaxation curves were composed of two exponential phases brought about by different rates of changes of P_r with time: the initial rapid phase covered about 80 % of the entire pressure (volume) change, and was followed by a slow reversible phase (about 20 % of the entire change) which is related to concentration polarization effects at the endodermis (Steudle & Frensch 1989). In the present study, the initial phase of the hydrostatic relaxation curve was used to measure $T_{hr1/2}^w$. In osmotic experiments, the original root medium was rapidly exchanged by a solution which contained 320 mM acetone (0.8 MPa of osmotic pressure) in the root medium in addition to the other contents. From the first phase (water phase) of the biphasic pressure responses, osmotic root hydraulic conductivity was calculated from the osmotic half time ($T_{or1/2}^w \propto 1/Lp_{or}$; Lp_{or} = osmotic root hydraulic conductivity). In order to work out $T_{or1/2}^w$, the portion around the minimum (maximum) was not incorporated (about 10 % of the overall pressure change). This portion contains significant interactions between water and solute flows tending to increase the rate (Steudle & Tyerman 1983; Tyerman & Steudle 1984). It was not used to work out $T_{or1/2}^w$. From the second phase (solute phase), the permeability of acetone across root (P_{sr}) was calculated from the half time of acetone flow ($T_{r1/2}^s \propto 1/P_{sr}$). From the biphasic curves, the reflection coefficient of roots (σ_{sr}) was worked out. For the calculation of Lp_r , P_{sr} and σ_{sr} , the reader is referred to earlier publications such as Henzler *et al.* (1999) and Hose *et al.* (2000). After re-attaining a stable root pressure, the acetone solution was replaced by the original root medium. Then the root was treated for 0.5 h with 35 mM H_2O_2 applied to the root medium. Following this treatment, again hydrostatic and osmotic experiments were performed to observe the effects. In the presence of 35 mM H_2O_2 , ABA [(±)-*cis-trans*-] was added to the medium at a concentration of 1 μ M and hydrostatic $T_{hr1/2}^w$ was observed for 0.5 to 1 h. Eventually, the medium was exchanged for the original root medium to check whether or not effects were reversible. After experiments with a given root, it was cut at a position close to the seal. When root pressure decreased immediately to close to zero, and half times of pressure relaxations became short as compared with the original values (less than 1 s as compared to 4 to 12 s observed for the intact system in hydrostatic and 20 to 60 s in osmotic experiments), this indicated that root xylem within the seal remained open. If there was no or a delayed effect upon cutting, this indicated

that root xylem was interrupted during tightening or later. Results from these experiments were discarded (Peterson & Steudle 1993). For a given root, the whole time course of the experiments lasted for 8 to 10 h (including time to get steady root pressure). Root pressure (0.1 to 0.2 MPa) changed within ± 0.03 MPa during the experiments.

Cell pressure probe experiments

The same type of cell pressure probe was employed as that used by Henzler *et al.* (1999) or Wan *et al.* (2004). A root segment (length: 80 to 120 mm) was fixed by magnetic bars on a metal sledge which was arranged at an angle of 45° . It was covered by one layer of paper tissue at the top and at the bottom to keep the root wet. The center part of the root was lying open at a length of 10 mm and solution was running down along the root and at the edges of the metal plate. An average rate of solution flow was calculated dividing the overall water flow of around $800 \text{ mm}^3/\text{s}$ (0.8 ml/s) by the estimated cross section of solution flow along the root (most of the flow that was running down the metal sledge) and along the edges of the sledge, which was 4 to 5 mm^2 . Hence, the flow rate along the root was at least 0.16 to 0.20 m/s, and the flow turbulent displaying some flickering in shape. Higher rates of solution flow were not possible because higher turbulences at the root surface would have interfered with measurements with the cell pressure probe tending to cause leakages due to vibrations of the root and/or the tip of the micro-capillary of the probe.

Using the probe, cortical cells from the 2nd to 4th layer were punctured at a distance of about 50 mm from the root tip. In the oil-filled micro-capillary of the probe, a meniscus formed between cell sap and oil. Cell turgor was rebuilt by gently pushing the meniscus to a position close to the surface of the root. In hydrostatic experiments, pressure relaxations were applied to measure the hydrostatic half time ($T_{h1/2}^w$) of water flow across the cell membrane which is inversely proportional to the hydraulic conductivity of the cell membrane ($T_{h1/2}^w \propto 1/Lp_h$; Lp_h = hydrostatic cell hydraulic conductivity). To avoid a mechanical inhibition of AQPs, peak sizes of pressure change were less than 0.1 MPa (Wan *et al.* 2004). As during the experiments at the root level, osmotic

experiments were conducted by adding acetone to the circulating medium at a final concentration of 200 mM. Even at the high rates of solution flow along the root segments, there may have been reductions in the osmotic concentration of the volatile solute during its passage down the sledge. This was regularly checked using an osmometer (Gonotec, Berlin, Germany). The osmotic half times ($T_{o1/2}^w \propto 1/Lp_o$; Lp_o = osmotic 'cell' hydraulic conductivity) were measured from the water phase of responses. Different from the hydrostatic cell experiments, half time of water exchange from cell osmotic experiments referred to a complex barrier which was not as well-defined as that during the experiments with the root pressure probe. The tissue barrier was less thick (cell pressure probe in the second to fourth layer) than that during root experiments. It was somewhat variable depending on which layer was punctured. Hence, only relative changes in Lp_o ($T_{o1/2}^w$) could be worked out rather than absolute values, as in the cell experiments using hydrostatic gradients (see above).

Half times of acetone transport ($T_{1/2}^s$) were measured from the solute phase which referred to the inverse of solute permeability of the same complex barrier between cell and medium rather than just to the membrane of the cell punctured ($T_{1/2}^s$). As for Lp_o , relative changes in P_s ($T_{1/2}^s$) rather than absolute values could be given because of the variability of the thickness of the tissue layer. After treating the root with 35 mM H_2O_2 , the same experiments as in the control were performed to observe effects of H_2O_2 on water and acetone transport. In some experiments, ABA [(±)-*cis-trans*-] was added to the medium in the presence of H_2O_2 resulting in a final concentration of 1 μ M of ABA. Following this addition, $T_{h1/2}^w$ was observed for 0.5 to 1 h. To check whether or not effects were reversible, the same experiments as in the control were repeated after changing back to the original root medium. Cell turgor was between 0.4 to 0.6 MPa. Within ± 0.04 MPa, turgor remained constant during the experiments for a given cell which lasted for 2 to 4 h.

Results

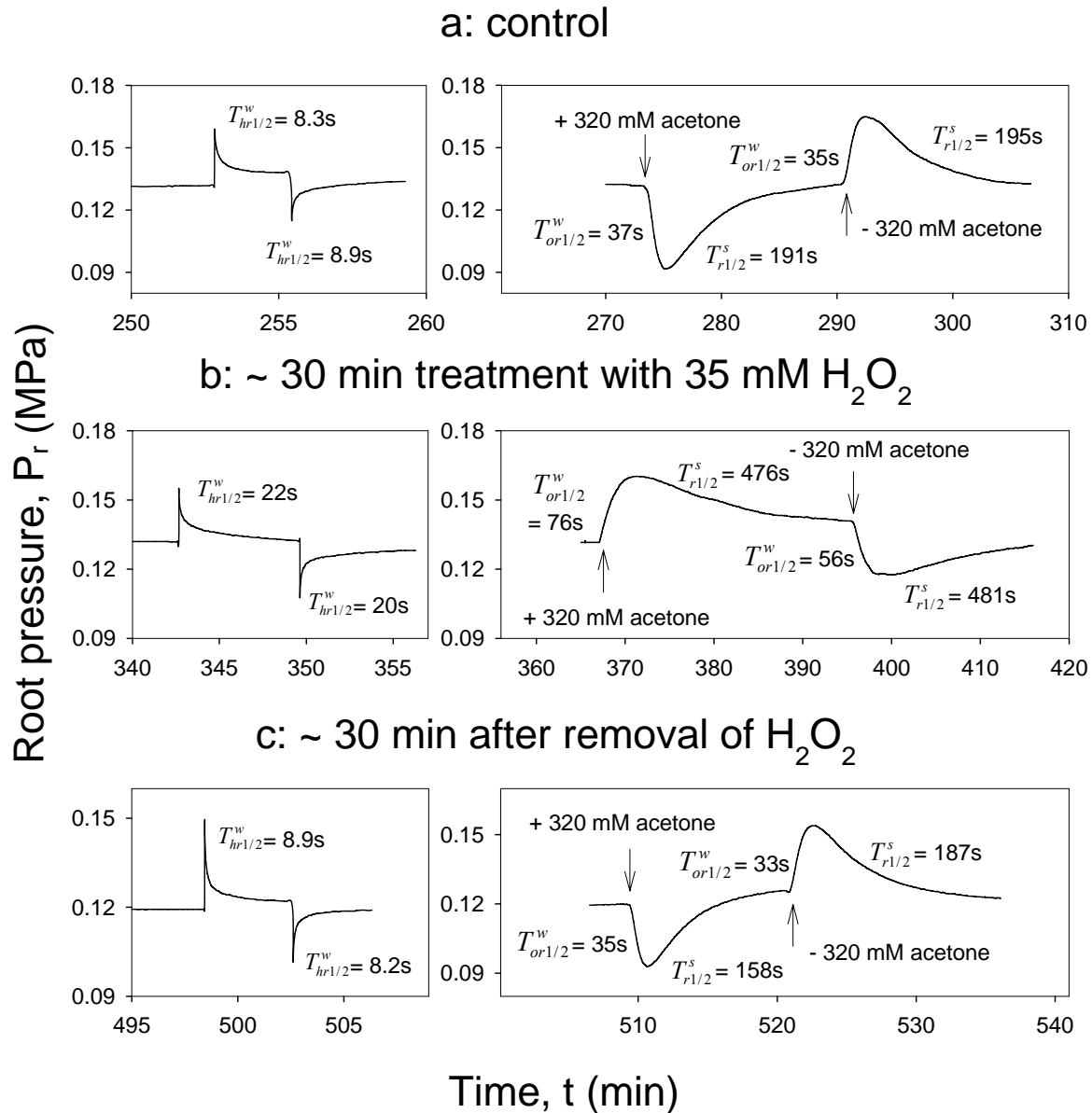


Fig. 1 (a) Typical hydrostatic relaxations of root pressure and biphasic osmotic response curves as measured by a root pressure probe in a root excised from a corn seedling and treated with 35 mM H₂O₂. Compared with the control, hydrostatic half times ($T_{r1/2}^w$) increased by a factor of 2.5. In osmotic experiments with the permeating solute acetone responses were biphasic. (b) Treatment with 35 mM H₂O₂ caused anomalous (negative) osmosis (root was swelling in hypertonic solution, because the solute

entered the root faster than the water could get out). Also, it increased half times ($T_{r1/2}^s$) of acetone permeability (P_{sr}) from 190 s to 480 s (on average). (c) Removal of H_2O_2 from the medium resulted in a restoration of Lp_r , P_{sr} and of normal osmosis as in the control.

In the presence of 35 mM H_2O_2 , the radial permeability of water across corn roots (hydrostatic root Lp_{hr}) was substantially inhibited. As for *Chara* internodes, we refer this to the existence of reactive oxygen species (ROS), namely of $*OH$, which should have been generated in the presence of Fe^{2+} in the root (see Introduction). As can be seen from Fig. 1, hydrostatic half times of root water permeability ($T_{hr1/2}^w$) increased from 8.6 s to 21 s (on average) in the presence of 35 mM H_2O_2 , i.e. root Lp_{hr} decreased by a factor of 2.5. When removing H_2O_2 from the medium, the original $T_{hr1/2}^w$ recovered within 0.5 to 1 h. In the presence of acetone which rapidly permeated the root, osmotic response curves were biphasic as shown in Fig. 1A (Frensch & Steudle 1989; Steudle 1993). This is so, because roots behave like osmometers permeable to both water and solutes (Steudle & Brinckmann 1989). The first phase during which root pressure decreased or increased with a half time of between 20 and 60 s due to an exosmotic/endosmotic volume flow, is dominated by water and is called ‘water phase’ (Steudle & Jeschke 1983; Steudle 1993). During the ‘solute phase’, root pressure increased/decreased again due to the passive flow of solute tending to equilibrate the concentration of permeating solutes on both sides of the barrier (medium and xylem), and water follows. Osmotic half times ($T_{or1/2}^w$) measured from the water phase were longer than hydrostatic $T_{hr1/2}^w$ by a factor of four. This indicated that osmotic root hydraulic conductivity (Lp_{or}) was smaller than hydrostatic root hydraulic conductivity (Lp_{hr}) by the same factor. As $T_{hr1/2}^w$, H_2O_2 treatment increased $T_{or1/2}^w$ by a factor of two. The effects were reversible as can be seen from Fig. 1c.

Since acetone was rather permeable for root cell membranes, its reflection coefficient in roots was close to zero ($\sigma_{sr} = 0.04 \pm 0.02$; $n = 5$ roots). However, in the presence of H_2O_2 , the osmotic response of the root to the permeating solute reverted its direction. The reflection coefficient of acetone changed from 0.04 ± 0.02 to -0.04 ± 0.01 . Although absolute values of the reflection coefficients were small, anomalous osmosis

was clearly observed: acetone entered the root faster than the water could get out, and root pressure was increasing instead of decreasing (see Discussion). This meant that the root was not shrinking but was swelling in the presence of the hypertonic solution (Fig. 1b). Removal of H_2O_2 from the medium again resulted in normal osmosis as in the control (Fig. 1c). Hence, H_2O_2 caused a substantial decrease in the water permeability of the root. H_2O_2 also reduced the permeability of the root for acetone as half time of acetone permeation increased from 190 s to 480 s (on average).

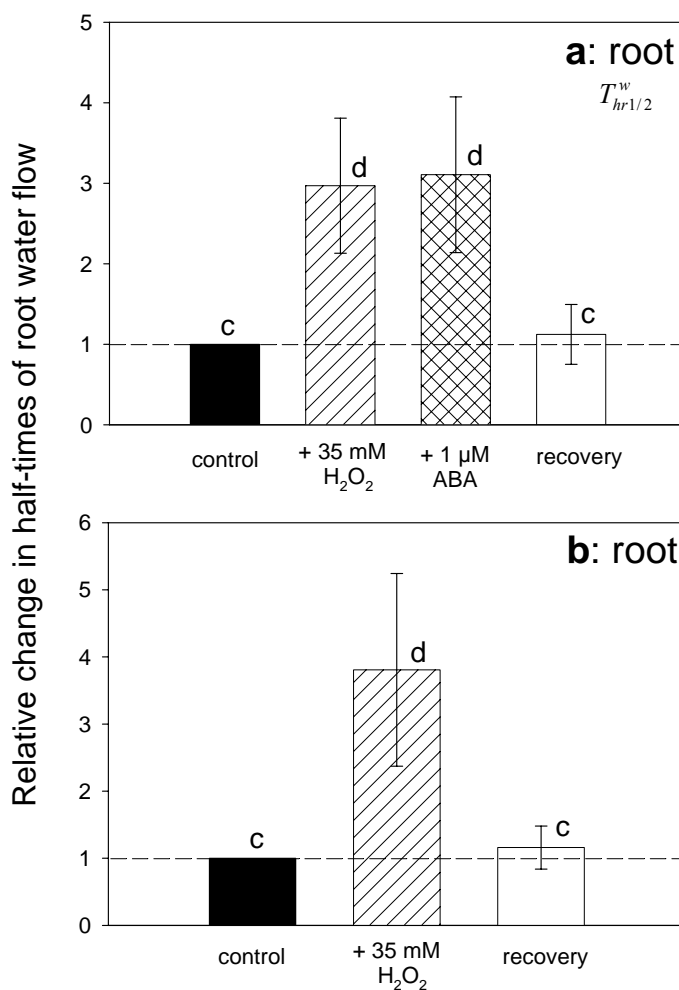


Fig. 2 Summary of the effects of 35 mM H_2O_2 and of 1 μM ABA on half times (a: $T_{hr/2}^w \propto 1/Lp_{hr}$; b: $T_{or/2}^w \propto 1/Lp_{or}$) of root hydraulic conductivity ($n = 6$ roots \pm SD). Relative changes are given rather than absolute values to avoid the variability between roots. Treatment of H_2O_2 increased $T_{hr/2}^w$ and $T_{or/2}^w$ by

factors of 3 and 3.8, respectively ($L_{p_{hr}}$ or $L_{p_{or}}$ decreased by the same factor). The addition of ABA in the presence of H_2O_2 had no significant effect on $T_{hr1/2}^w$. Removal of H_2O_2 from the medium resulted in a recovery of both $T_{hr1/2}^w$ and $T_{or1/2}^w$. Different symbols on the top of each column denote significant differences between results. (t-test; $p < 0.01$).

Relative changes of half times of water flows in response to H_2O_2 treatment are summarized in Fig. 2 for the root level. It can be seen from the figure that increases in hydrostatic $T_{hr1/2}^w$ (a) and osmotic $T_{or1/2}^w$ (b) were similar. On average, $T_{hr1/2}^w$ increased by a factor of three, i.e. $L_{p_{hr}}$ should have decreased by the same factor. The stress hormone ABA, which has been found to transiently increase root hydraulic conductivity (Hose *et al.* 2000), had no positive effect on water permeability of the roots in the presence of H_2O_2 . The osmotic half time, $T_{or1/2}^w$, increased by a factor of 3.8, when roots were treated with H_2O_2 . After the removal of H_2O_2 from the medium and washing the root with control medium, the original half times restored within 0.5 to 1 h in both types of experiments.

Results from the root level, paralleled those found at the level of individual cortical cells. However, at the cell level, effects on water flow were more pronounced than those at the root level. Treatment with 35 mM H_2O_2 dramatically inhibited AQP activity and increased half times of water permeability across cell membranes (hydrostatic $T_{h1/2}^w$). In the example given in Fig. 3, hydrostatic $T_{h1/2}^w$ increased from 0.8 s to 8.0 s (on average), i.e. by one order of magnitude. When removing H_2O_2 from the medium, the effect was completely reversible. As at the root level, closure of water channels by treatment of 35 mM H_2O_2 resulted in anomalous osmosis and increased half times for water and acetone permeation (Fig. 3b). Again, removal of H_2O_2 from the medium resulted in a reversal to normal osmosis (as in the control; Fig. 3c). As for $T_{h1/2}^w$, a similar effect on osmotic half time ($T_{o1/2}^w$) was found. It is clear that H_2O_2 treatment was effective in reversibly closing water channels in cortical cells of corn roots, though the function-repair mechanisms are not yet known.

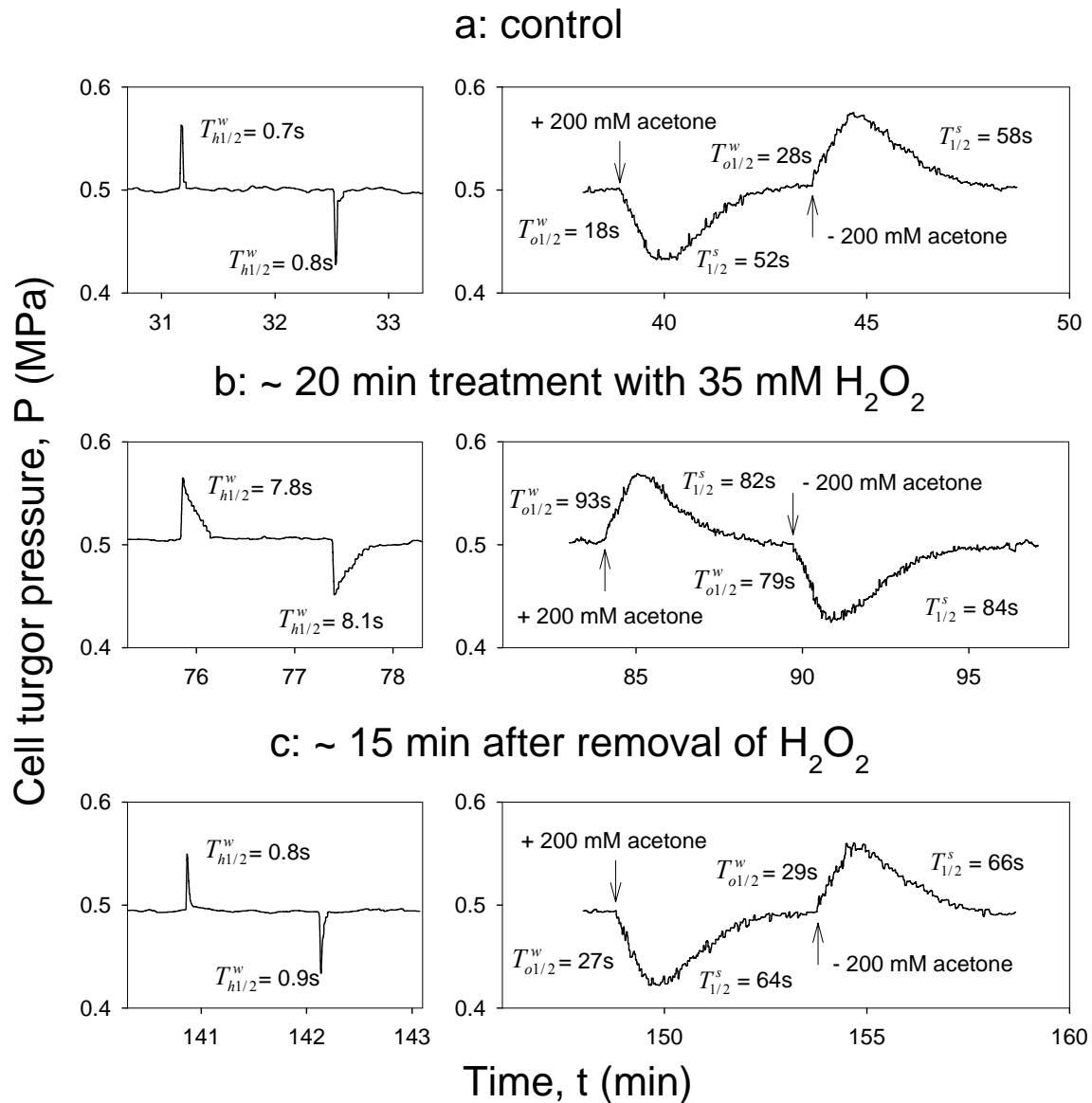


Fig. 3 Typical curves of hydrostatic and osmotic pressure relaxations as measured with a cell pressure probe in an individual cortical cell of corn root as affected by H₂O₂ treatment. (a) With the permeating solute acetone, responses were biphasic in osmotic experiments. (b) Half times ($T_{h/2}^w$) of water flow increased by a factor of 10 as compared with the control indicating that water channel activity was substantially inhibited. As at the root level, the cell was swelling in a hypertonic acetone solution (anomalous osmosis) in the presence of 35 mM H₂O₂. Half times ($T_{1/2}^s$) of acetone permeability increased from 55 s to 83 s (on average). (c) Removal of H₂O₂ from the medium resulted in restoration of L_p , P_s to a good approximation and of normal osmosis, as in the control.

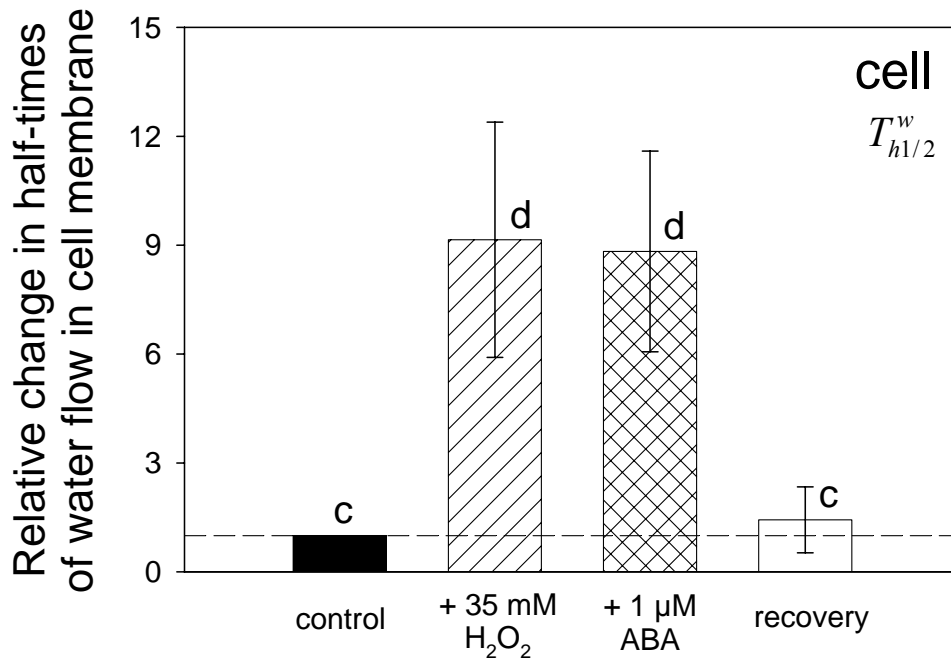


Fig. 4 Summary of the effects of 35 mM H_2O_2 and of 1 μ M ABA on half times ($T_{hl/2}^w \propto 1/Lp_h$) of cell hydraulic conductivity ($n = 6$ cells \pm SD). As in Fig. 2, relative changes are given to avoid the variability between cells. Half time ($T_{hl/2}^w$) of cell hydraulic conductivity (Lp_h) increased by a factor of nine as compared with the control indicated that the activity of aquaporins was substantially inhibited by the treatment with H_2O_2 . In the presence of H_2O_2 , addition of ABA had no effect on $T_{hl/2}^w$. Removal of H_2O_2 from the medium resulted in a recovery of $T_{hl/2}^w$. Different symbols on the top of each column denote significant differences between results. (t-test; $p < 0.01$).

Relative changes in half times of cell hydraulic conductivity as found during treatment with H_2O_2 are summarized in Fig. 4 (hydrostatic experiments). During water channel closure in the presence of H_2O_2 , $T_{hl/2}^w$ increased by a factor of 9 indicating that hydrostatic cell hydraulic conductivity decreased by the same factor. As at the root level, ABA had no positive effect on water permeability across cell membranes in the presence of H_2O_2 . Cell hydraulic conductivity was recovered within 15 to 30 min after the removal of H_2O_2 from the medium. As roots recovered, results indicated that H_2O_2

treatment did not simply cause an overall damage of membranes (Aroca *et al.* 2005). Also, in case of an unspecific damage, there should have been an increase of L_p and P_s upon treatment rather than a decrease.

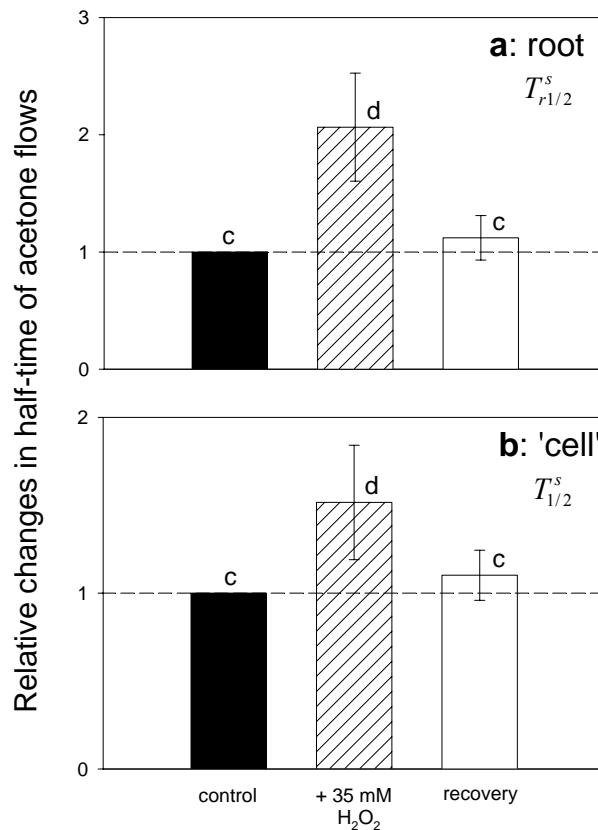


Fig. 5 Summary of the effects of 35 mM H₂O₂ on half times ($T_{r1/2}^s \propto 1/P_{sr}$; $T_{1/2}^s \propto 1/P_s$) of acetone permeability across roots (a) and 'cells' (b) ($n = 6$ roots or cells \pm SD). Relative changes are given to avoid the variability between roots or cells. Treatment with H₂O₂ doubled $T_{r1/2}^s$ (P_{sr} decreased by a factor of two) and increased $T_{1/2}^s$ of acetone permeability by 50 % as compared with the control indicated a substantial amount of acetone was permeating across AQPs which were not completely selective for water. Both $T_{r1/2}^s$ and $T_{1/2}^s$ were recovered after the removal of H₂O₂ from the medium. Different symbols on the top of each column denote significant differences between results. (t-test; $p < 0.05$).

Hydrogen peroxide increased half times of acetone permeability at the level of both cortical cells (Fig. 5a) and entire roots (Fig. 5b) by factors of 1.5 and 2, respectively, as compared with control. This meant that permeabilities of acetone were reduced by the

same factors. When H₂O₂ was removed from the medium, the original permeabilities were recovered. These results resemble previous findings that AQPs in *Chara* are not ideally selective for water, but allow the passage of small organic solutes as well, at least to some extent (Hertel & Steudle 1997; Henzler *et al.* 2004).

Discussion

The results indicate an ‘oxidative gating’ of aquaporins in the membranes of root cells of young corn seedlings which, in turn, caused a reversible reduction of the overall water permeability of roots. At least qualitatively, the effects are similar to those obtained recently for the plasma membrane of *Chara corallina* (Henzler *et al.* 2004). As for the isolated internodes of *Chara*, channel closure in root cell membranes caused anomalous osmosis in the presence of a rapidly permeating solute acetone, i.e. closure of AQPs resulted in the curious situation that the solute moved faster than the water and the reflection coefficient became negative ($\sigma_{sr} = -0.04$ as compared to values of $\sigma_s = -0.50$ for *Chara*; Henzler *et al.* 2004). Responses demonstrated at the cell level were more pronounced than at the root level. Overall, the results suggest an oxidative gating of AQPs in corn roots similar to that already found for *Chara*.

It may be argued that during the experiments at the cell and root level, external unstirred layers play an important role or were even dominant during water and solute movement. However, the high rates of solution flow around roots in both types of experiments (cell and root pressure probes) guaranteed that effects of external unstirred layers should have been small. Water around roots and root sections was in turbulent motion (see MM section). Hence, the thickness of unstirred layers should have been no bigger than 50 μm (Steudle & Tyerman 1983). According to the Einstein-Smoluchowski relation for a plane sheet, this would refer to a half time of 0.6 s for the complete equilibration with the external solute acetone ($D = 1.1 \times 10^{-9} \text{ m}^2 \cdot \text{s}^{-1}$; $t_{1/2} = 0.281 \cdot (5 \cdot 10^{-5})^2 / (1.1 \cdot 10^{-9})$; Jost 1960). Rates of water exchange across the unstirred layer should have been much faster than those across the root in the osmotic experiments ($T_{or1/2}^w = 20$ to 60 s in the untreated root). A thickness of 50 μm would refer to a acetone permeability of $2.2 \times 10^{-5} \text{ m} \cdot \text{s}^{-1}$,

which is much larger than that measured for cell membranes (Steudle & Tyerman 1983; Henzler *et al.* 2004). Hence, the unstirred layer still adhering to the root even in the presence of vigorous stirring should not contribute much during the experiments with the root pressure probe. In the hydrostatic experiments with individual cortical cells, unstirred layer effects should have been even smaller. In these experiments, only a small amount of water is moved across the membrane forming a layer of only a fraction of a micron (sweep-away effect; Dainty 1963; Steudle, Smith & Lüttge 1980; Steudle & Tyerman 1983; Steudle 1993).

In *Chara* internodes, treatment with hydroxyl radicals (*OH as produced by the Fenton reaction in the presence of a fraction of a millimole of H₂O₂), reversibly reduced cell Lp by more than 90 % (Henzler *et al.* 2004). It has been verified that *OH rather than H₂O₂ was the inhibiting agent. In the absence of Fe²⁺ in the medium, *Chara* cells tolerated H₂O₂ at concentrations of up to 350 mM without affecting cell Lp (Henzler & Steudle 2000). In the present study, the equivalent test could not be made because the roots should have contained sufficient Fe²⁺ or cations from other transition metals (see Introduction and Chen & Schopfer 1999). In the presence of 18 μM of FeNaEDTA (much less than that in the experiments with *Chara*), a concentration of as large as 35 mM H₂O₂ was required to cause effects similar to those in *Chara*. This may point to the fact that *OH radicals produced in roots were also used in reactions other than the inhibition of AQPs or that AQPs of roots were less sensitive to *OH radicals than those of *Chara* internodes, or both. For *Chara* and root cells, changes in hydraulic conductivity were reversible. For *Chara*, it has been proposed that, because of the high reactivity of radicals, *OH radicals were most likely produced close to the cell membranes (see Henzler *et al.* 2004 for details). This may be also true for corn roots. Besides the idea that AQPs were directly attacked by *OH radicals, there may be another mechanism in which C = C double bonds of the plasma membrane were attacked by *OH resulting in the formation of aggressive radicals which attacked aquaporins laterally from inside the bilayer. Both types of chemical attacks may have resulted in conformational changes of the water channel proteins and their reversible closure. Which type of mechanism is valid cannot be decided from the present results. However, there may have been a similar mechanism by which chemical alterations were

removed, most likely by the reduction of oxidized groups of AQPs (Henzler *et al.* 2004). Alternatively, H₂O₂ is thought to be a messenger molecule involved in signal transductions, when plants suffer biotic or abiotic stresses (Xiong, Schumaker & Zhu 2002; Pastori & Foyer 2002). Hence, the regulation of water channel activity by an oxidative signaling in the presence of reactive oxygen species (ROS) could play a role as part of a downstream reaction to stresses such as during a response to low temperature, drought or high light intensity stress or during a pathogen attack (Wojtaszek 1997; Pei *et al.* 2000; Neill, Desikan & Hancock 2002), probably, by eliciting the activation of Ca²⁺ permeable channels in cell membranes, which in turn, block water channels *via* intracellular Ca²⁺ signaling (Gerbeau *et al.* 2002; Mori & Schroeder 2004).

The addition of a rapidly permeating solute to the root medium resulted in biphasic osmotic response curves (Steudle 1993). This type of response has been demonstrated in the past for different roots and quite a number of solutes including those which rapidly permeate membranes (e.g. Steudle, Oren & Schulze 1987; Steudle & Brinckmann 1989). In the biphasic responses, there is a 'water phase' due to an exosmotic volume flow (largely water) which causes a pressure decrease. This is followed by a 'solute phase' due to the passive flow of the solute and water is again taken up (pressure increase). Responses of roots are analogous to those of isolated cells, though not completely identical (Steudle *et al.* 1987). At the cell level, there are cases in which turgor pressure increases in the presence of a hypertonic solution (anomalous osmosis; Steudle & Henzler 1995; Henzler *et al.* 2004). To date, anomalous osmosis could be only induced in the presence of rather 'exotic' solutes which exhibit a permeability which is already similar to that of water (such as acetone). The phenomenon refers to the striking situation that a cell does not shrink but swells in the hypertonic medium. Here, we present evidence that anomalous osmosis may be also demonstrated in roots, i.e. for an entire organ and in the presence of a rather complicated osmotic barrier. At a first glance, anomalous osmosis takes place, when solutes (osmolytes) are getting faster into the cell or root than the water can get out (see above), namely, when AQPs are closed and osmolytes are more rapidly permeating the membrane or barrier. However, this simple interpretation in terms of a change in the ranking between water and solute

permeability cannot completely explain the story. The biphasic pressure/time curves (or volume/time curves) in the presence of a permeating solute can be described by (cell or root level; Steudle & Tyerman 1983; Steudle *et al.* 1987):

$$\frac{V(t) - V_0}{V_0} = \frac{P(t) - P_0}{\varepsilon} = \frac{\frac{A}{V} \cdot \sigma_s \cdot \Delta\pi_s^o \cdot Lp}{k_w - k_s} [\exp(-k_w \cdot t) - \exp(-k_s \cdot t)]. \quad (1)$$

Here, $V(t)$ = cell volume; V_0 = cell volume at $t = 0$; $P(t)$ = cell turgor pressure; P_0 = cell turgor pressure at $t = 0$; A = cell surface area; $\Delta\pi_s^o$ = change in the external osmotic pressure; $k_w = Lp \cdot A(\varepsilon + \pi_o^i)/V$ = rate constant of water flow; $k_s = P_s \cdot A/V$ = rate constant of solute flow. Due to the presence of AQPs, water movement across membranes/roots is usually much faster than that of solutes, i.e. $k_w > k_s$ holds. If solute transport is relatively faster than that of water, i.e. $k_s > k_w$, this will change the sign of the term within the brackets in Eqn 1. However, $k_s > k_w$ will also change the sign of the denominator on the right side of Eqn 1, i.e. the effect of a change from $k_w > k_s$ to $k_s > k_w$ will cancel. Hence, the explanation of the anomalous osmosis is not due to the relative of k_w vs. k_s . According to Eqn 1, it is due to a change in the reflection coefficient (σ_s) from positive to negative values. Although often correlated with the permeabilities of water and solutes (P_s and Lp ; see below), σ_s is an independent parameter required to describe osmosis besides Lp and P_s .

In a homogenous membrane lacking pores (which provide the only way of a direct interaction between water and solute flow), the reflection coefficient should be related to the water and solute permeability by (e.g. Dainty 1963; Steudle & Henzler 1995):

$$\sigma_s = 1 - \frac{\bar{V}_s \cdot P_s}{Lp \cdot RT} = 1 - \frac{\bar{V}_s \cdot P_s}{P_d \cdot \bar{V}_w}. \quad (2)$$

Here, \bar{V}_s is the partial molar volume of the solute; P_d is the diffusional water permeability and \bar{V}_w the molar volume of liquid water. The physical meaning of the second term on the right side of the equation is that it represents the contribution of solute flow to the overall volume flow. A comparison of measured and calculated values of reflection coefficients shows that measured values are usually substantially smaller than those calculated from P_s and Lp (e.g. Table 1 of Steudle & Tyerman 1983).

In the past, this has been referred to the existence of water-filled pores and to a frictional interaction between water and solute as they cross the membrane (Dainty 1963; Steudle & Tyerman 1983):

$$\sigma_s = 1 - \frac{\bar{V}_s \cdot P_s}{Lp \cdot RT} - \frac{K_s^c \cdot f_{sw}^c}{f_{sw}^c + f_{sm}^c}. \quad (3)$$

In this classical equation, the last term on the right side denotes the frictional interaction; K_s^c is the partition coefficient of solute 's' between membrane pores and the membrane; f_{sw}^c represents the frictional interaction between solute and water in the pores and f_{sm}^c the interaction between solutes and the wall of the pores. The frictional term, f_{sw}^c , describes the per mole force which acts on water and solute molecules, when they pass the pore in opposite directions during an osmotic experiment in the presence of a permeating solute. The model assumes rather wide pores where water and solutes may pass each other. However, recent evidence showed that most of the water uses narrow and rather selective AQP pores, where the water is aligned in single files (no-pass pores; e.g. Jung 1994; Maurel 1997; Ren *et al.* 2001). It turned out that AQPs allowed the passage of small uncharged solutes (such as acetone and a limited amount of other solutes; Steudle & Henzler 1995; Henzler *et al.* 2004). The coupling in single-file pores tends to reduce reflection coefficients, but effects should be small according to the limited stoichiometric coupling between solutes and water during their passage across the membrane (Finkelstein 1987; Hertel & Steudle 1997). How do we then get to negative reflection coefficients and anomalous osmosis? According to Eqns 2 and 3, the membrane is looked at as a homogenous structure, i.e. water and solutes are just passing through the pores, and the passage across the parallel bilayer (or other structures) is not taken into account explicitly. This model cannot explain negative reflection coefficients for lipophilic solutes upon channel closure ($f_{sw}^c = 0$). The finding is, however, explained when the composite structure of membranes is taken into account (composite transport model of membrane; Steudle & Henzler 1995). In terms of this model, channel closure could result in a negative reflection coefficient according to Eqn 2 provided that $\bar{V}_s \cdot P_s > \bar{V}_w \cdot P_d$ holds for a lipophilic solute such as acetone. When the porous passage (AQPs) is closed, the overall transport properties of the membrane should assume those of the

bilayer (or of the rest of the membrane), i.e. overall reflection coefficients could be negative for these solutes, as found (Henzler & Steudle 1995; Henzler *et al.* 2004). Hence, the water/solute movement across the membrane is explained in terms of the composite nature of membrane transport following the basic treatment of Kedem & Katchalsky (1963a) for parallel transport elements.

In tissues, such as corn roots, the KK concept should apply as well (Steudle *et al.* 1987; Steudle & Peterson 1998; Tyerman *et al.* 1999). Different from the membrane, series arrays would have to be considered in roots besides the parallel such as different tissues (rhizodermis, cortex, stele) or special barriers such as the exo- and endodermis with its Casparian bands. Again, basic concepts should apply both for the parallel and series arrangement (Kedem & Katchalsky 1963a, b; House 1974). With respect to the parallel elements, the apoplast has to be considered besides the other two pathways. One would expect a reflection coefficient of close to zero for acetone in the apoplast and a relatively high diffusional permeability along this structure. In untreated cells of the root cortex, the reflection coefficient should be small but positive (for *Chara* the σ_s of acetone was 0.15; Ye *et al.* 2004). According to the parallel arrangement of pathways, the basic theory predicts that the overall reflection coefficient should have been between zero (apoplast) and 0.15 (cell-to-cell passage), as found. Reflection coefficients of different pathways should have contributed according to their individual conductances, which, however, are not known. When channels were closed in root cells, this should have caused a negative reflection coefficient (in *Chara*, this resulted in a substantially negative reflection coefficient for acetone of $\sigma_s = -0.50$). In the root, one would expect an overall value of between zero and this value, as found too. Hence, the measured switching between normal and anomalous osmosis is explained by the composite transport model, as are the rather low absolute values of σ_{sr} . The same refers to the osmotic experiments with cortical cells which differed from those of entire roots just by the somewhat variable thickness of the layer of tissue around them.

According to the composite transport model for the radial transport of water across the root cylinder (Steudle 2000; 2001), root L_{pr} very much depends on how intensively the two parallel pathways across the root are used, i.e. the apoplastic and the cell-to-cell

path. The latter rather than the former would be very much determined by AQP activity. It has been shown readily that the relative contribution of the two components is highly variable depending on the nature of driving force (osmotic *vs.* hydrostatic) and root anatomy (e.g. Steudle & Peterson 1998; Lee *et al.* 2005a). In the presence of hydrostatic pressure gradients, water flow should be largely around protoplasts, i.e. apoplastic, because this path represents a low hydraulic resistance (high L_p). On the other hand, water flow in the presence of osmotic gradients is low in that osmotic driving forces cause water movement largely across membranes, i.e. an osmotic water flow across the root has to pass many membranes, which then results in $L_{p_{or}}$ smaller than $L_{p_{hr}}$ (Zhu & Steudle 1991; Steudle & Frensch 1996). Under conditions of salinity stress that inhibits AQP activity of corn root cells, effects on cell L_p were substantially bigger than those on root L_{p_r} , as shown here, too (Azaizeh *et al.* 1992). However, the results of Azaizeh *et al.* (1992) also showed that inhibition of cell L_p also affected hydrostatic root $L_{p_{hr}}$ indicating a contribution of membranes along the path, too (see below and Steudle 1992). On longer terms, the apoplastic path may be affected by anatomical changes such as the formation of barriers (Zimmermann *et al.* 2000; Lee *et al.* 2005a). In the short-term treatment with H_2O_2 , it is most likely that the transport step at the endodermis included a bigger membrane component than in the rest of the root (see below and Zimmermann & Steudle 1998). Nevertheless, effects in response to the oxidative gating were much bigger at the cell (reduction by a factor of 9) than at the root or tissue level (reduction by a factor of 3).

At a first sight, the finding that the fold change of osmotic $L_{p_{or}}$ caused by treatment was similar to the fold change in hydrostatic $L_{p_{hr}}$ (3.8 fold *vs.* 3 fold) seems to contradict the interpretation in terms of the composite structures, which is usually in terms of parallel transport elements. During the hydrostatic experiment, water flow should largely bypass protoplasts along the apoplast, which should not be affected by the H_2O_2 treatment. During the osmotic experiment, however, it should be largely along the cell-to-cell path. If the latter is true, we may calculate $L_{p_{or}}$, assuming that all the water moved across cell membranes arranged in concentric cylinders and not in the apoplast. Per cell layer, two membranes would have to be crossed. The overall root osmotic hydraulic conductivity

($L_{p_{or}}$) would relate to individual cell hydraulic conductivity (L_p) by (Steudle & Brinckmann 1989):

$$\frac{1}{L_{p_{or}}} = \frac{1}{L_p} \cdot \sum_{i=1}^n \frac{r_o}{r_i} \quad (4)$$

Here, n is the number of membrane layers which would have to be crossed by the water (twice as many as cell layers); r_o is the radius of the root and r_i the radius of the i^{th} membrane layer. For a typical corn root of 1 mm in diameter (such as those used in the present study), 12 – 14 cell layers would have to be crossed by the water. Taking average diameters of cells in different layers from an earlier paper (Table II of Zhu & Steudle 1991), $\sum_{i=1}^n \frac{r_o}{r_i}$ was calculated to be 74. Using a typical cell L_{p_h} of $L_{p_h} = 6.0 \times 10^{-6} \text{ m}\cdot\text{s}^{-1}\cdot\text{MPa}^{-1}$ (equivalent to a $T_{hl/2}^w = 0.8 \text{ s}$), this should have resulted in a $L_{p_{or}} = 8.0 \times 10^{-8} \text{ m}\cdot\text{s}^{-1}\cdot\text{MPa}^{-1}$. This value is close to that measured with root pressure probe ($L_{p_{or}} = 7.0 \times 10^{-8} \text{ m}\cdot\text{s}^{-1}\cdot\text{MPa}^{-1}$; equivalent to a $T_{or1/2}^w = 35 \text{ s}$). The estimate supports the view of a largely cell-to-cell movement of water in osmotic experiments.

On the other hand, the passage of water during a hydrostatic root experiment is not completely free of membrane components, namely, in the endo- or exodermis where Casparian bands tend to interrupt the apoplastic flow (see above; Steudle & Peterson 1998; Zimmermann & Steudle 1998; Zimmermann *et al.* 2000). The present findings agree with this view. When it holds that endodermal cell L_p can be identified with that of other cortical cells, we would expect a reduction by a factor of nine (Fig. 3) of root $L_{p_{or}}$ provided that the endodermis represents the dominating hydraulic resistance and Casparian bands completely interrupt water flow (in the classical view of the function of the bands). However, the latter is not true, and the finding of a reduction of ‘only’ 3.8 (instead of nine fold) is understandable. The similar fold change in hydrostatic and osmotic root L_{p_r} , does not mean that, in both types of experiments, water flow was predominantly from cell to cell and that the hydrostatic root L_{p_r} of untreated roots was larger by a factor of four because of unstirred layers in the apoplast. If this were true, apoplastic unstirred layers would have been by-passed by the high cell-to-cell permeability. A rigorous treatment of apoplastic diffusional unstirred layers has shown that they would contribute to less than expected to the overall root L_{p_r} (Steudle &

Frensch 1989). These authors assumed thickness of unstirred layers of as large as the entire cortex (300 μm) and a stellar unstirred layer of as large as 50 μm . Assuming a reduction of solute diffusibility within the root apoplast by a factor of 5 to 20, they arrived at the conclusion that the contribution of unstirred layers was as small as 7 %. Apoplastic diffusive mobility should be similar for the solutes used by Steudle & Frensch (1989) as for the acetone used here. Hence, it should have been similar, too. Also, it has to be kept in mind that, during composite transport, the parallel pathways interact with each other, e.g., by a rapid equilibration of water ('local equilibrium'; Steudle 1992). Hence, treating the apoplast on both sides of the endodermis as an ordinary diffusional unstirred layer would be premature.

In plant roots, the stress hormone abscisic acid (ABA) is produced under unfavourable conditions such as water shortage (Zhang, Schurr & Davies 1987). It is transported to the shoot as a signal which induces closure of stomata in leaves. It has been reported that in corn roots, ABA increased root and cell hydraulic conductivity (Freundl *et al.* 1998; 2000; Hose *et al.* 2000; 2001). Recently, it was found that ABA has a positive effect on AQP activity, when channels were closed by mechanical stimuli or at low temperature (Wan *et al.* 2004; Lee *et al.* 2005b). It was concluded that ABA tended to restore the original open state of channel proteins by a mechanism which is not yet known. However, ABA had no such effect in the present study, when AQPs were blocked by an oxidative gating. This may be due to the fact that the gating mechanism of AQPs by oxidation is different from that by mechanical stimuli or low temperature. We hypothesize that ABA could not recover chemical modifications of AQPs during the treatment with H_2O_2 or $\cdot\text{OH}$. This may require a biochemical (reduction of oxidized AQPs) rather than just a physical action (change of activation energy of the transition between different conformational states to re-open closed channels).

In conclusion, the closure of AQPs of young corn roots caused responses in cell L_p and root L_{p_r} which were similar to those found in *Chara* internodes. Water permeabilities at the root and cell level were substantially and reversibly reduced indicating an inhibition of AQP activity by oxidative stress ($\cdot\text{OH}$ radicals and/or H_2O_2). As in earlier root experiments, the inhibition of AQPs at the cell level resulted in a decrease of cell L_{p_h}

which was bigger than that of the root or tissue $L_{p_{hr}}$. Unlike *Chara*, a much higher H_2O_2 concentration was required in corn roots, which may be due to the fact that either AQP responsiveness in roots was smaller or that $*OH$ radicals were also used in other processes, or both. As for the *Chara* system, anomalous osmosis (negative reflection coefficients) could be reversibly induced during oxidative stress in the presence of the rapidly permeating solute acetone which should have largely used the bilayer to pass through the root cylinder. Oxidative stress inhibited cell L_{p_h} by a factor of nine, which was larger than the inhibition at the root level (factor of three). Differences in the inhibition are readily explained in terms of the composite transport model of the root, which also explains the switching between normal and anomalous osmosis in the presence of the rapidly permeating solute. As during the application of other stresses, hydrostatic root $L_{p_{hr}}$ was also affected by oxidative treatment. This indicated that the apoplastic passage was partially interrupted, most likely at the endodermis. Unlike the gating by mechanical stimuli (Wan *et al.* 2004) or by low temperature (Lee *et al.* 2005 a, b), the stress hormone ABA had no ameliorative effect on restoring the original conformation of channel proteins and re-opening closed channels, possibly, because the oxidative gating in the presence of $*OH$ radicals caused a chemical modification of AQPs. The precise mechanism of the oxidative gating of AQPs in the presence of the ROS ($*OH$ or H_2O_2) is not yet understood. Three alternatives may be possible: AQPs were (i) directly attacked (oxidized) by $*OH$, or (ii) oxidized by other aggressive radicals which were subsequently produced by $*OH$. (iii) Alternatively, H_2O_2 may have elicited changes in cytoplasmic Ca^{2+} concentration *via* cell signaling cascades resulting in channel closure. In either case, AQP activity could be regulated by an oxidative gating or signaling initiated by the presence of H_2O_2 or $*OH$ radicals. There may be a common interaction between the redox state (oxidative stress) and water relations (water stress) during the life of plants.

Acknowledgements

Thanks go to Burkhard Stumpf (Department of Plant Ecology, University of Bayreuth) for his expert technical assistance.

References

- Aroca R., Amodeo G., Fernandez-Illescas S., Herman E.M., Chaumont F. & Chrispeels M.J. (2005) The role of aquaporins and membrane damage in chilling and hydrogen peroxide induced changes in the hydraulic conductance of maize roots. *Plant Physiology* **137**, 341-353.
- Azaizeh H., Gunse B., & Steudle E. (1992) Effects of NaCl and CaCl₂ on water transport across root cells of maize (*Zea mays* L.) seedlings. *Plant Physiology* **99**, 886-894.
- Azaizeh H, Steudle E (1991) Effects of salinity on water transport of excised maize (*Zea mays* L.) roots. *Plant Physiology* **97**, 1136-1145.
- Chen S.X. & Schopfer P. (1999) Hydroxyl-radical production in physiological reactions. *European Journal of Biochemistry* **260**, 726-735.
- Clarkson D.T., Carvajal M., Henzler T., Waterhouse R.N., Smyth A.J., Cooke D.T. & Steudle E. (2000) Root hydraulic conductance: diurnal aquaporin expression and the effects of nutrient stress. *Journal of Experimental Botany* **51**, 61-70.
- Dainty J. (1963) Water relations of plant cells. *Advances in Botanical Research* **1**, 279-326.
- Finkelstein A. (1987) Water movement through lipid bilayers, pores and plasma membranes. Theory and reality. Distinguished lecture series of the Society of General Physiologists, vol. 4. Wiley, New York.
- Frensch J. & Steudle E. (1989) Axial and radial hydraulic resistance to roots of maize (*Zea mays* L.). *Plant Physiology* **91**, 719-726.
- Freundl E., Steudle E. & Hartung W. (1998) Water uptake by roots of maize and sunflower affects the radial transport of abscisic acid and the ABA concentration in the xylem. *Planta* **207**, 8-19.
- Freundl E., Steudle E. & Hartung W. (2000). Apoplastic transport of abscisic acid through roots of maize: effect of the exodermis. *Planta* **210**, 222-231.
- Fry, S.C. (1998) Oxidative scission of plant cell wall polysaccharides by ascorbate-induced hydroxyl radicals. *Biochemistry Journal* **332**, 507-515.

- Gerbeau P., Amodeo G., Henzler T., Santoni V., Ripoché P. & Maurel C. (2002) The water permeability of *Arabidopsis* plasma membrane is regulated by divalent cations and pH. *The Plant Journal* **30**, 71-81.
- Henzler T. & Steudle E. (1995) Reversible closing of water channels in *Chara* internodes provides evidence for a composite transport model of the plasma membrane. *Journal of Experimental Botany* **46**, 199-209.
- Henzler T. & Steudle E. (2000) Transport and metabolic degradation of hydrogen peroxide: model calculations and measurements with the pressure probe suggest transport of H₂O₂ across water channels. *Journal of Experimental Botany* **51**, 2053-2066.
- Henzler T., Waterhouse R.N., Smyth A.J., Carvajal M., Cooke D.T., Schäffner A.R., Steudle E. & Clarkson D.T. (1999) Diurnal variations in hydraulic conductivity and root pressure can be correlated with the expression of putative aquaporins in the roots of *Lotus Japonicus*. *Planta* **210**, 50-60.
- Henzler T., Ye Q. & Steudle E. (2004) Oxidative gating of water channels (aquaporins) in *Chara* by hydroxyl radicals. *Plant Cell and Environment* **27**, 1184-1195.
- Hertel A. & Steudle E. (1997) The function of water channels in *Chara*: the temperature dependence of water and solute flow provides evidence for composite membrane transport and for a slippage of small organic solutes across water channels. *Planta* **202**, 324-335.
- Hose E., Clarkson D.T., Steudle E., Schreiber L. & Hartung W. (2001) The exodermis – a variable apoplastic barrier. *Journal of Experimental Botany* **52**, 2245-2264.
- Hose E., Steudle E. & Hartung W. (2000) Abscisic acid and hydraulic conductivity of maize roots: a study using cell- and root-pressure probes. *Planta* **211**, 874-882.
- House C.R. (1974) Water transport in cells and tissues. London: Edward Arnold.
- Johansson I., Larsson C., Ek B. & Kjellbom P. (1996) The major integral proteins of spinach leaf plasma membranes are putative aquaporins and are phosphorylated in response to Ca²⁺ and apoplastic water potential. *The Plant Cell* **8**, 1181-1191.
- Jost W. (1960) Diffusion in solids, liquids, gases. In *Physical Chemistry a series of monographs* (eds E. Hutchinson & P. van Rysselberghe), pp. 1-488. Academic press, New York.

- Jung J.S., Preston G.M., Smith B., Guggino W.B. & Agre P. (1994) Molecular structure of the water channel through aquaporin CHIP - The hourglass model. *Journal of Biological Chemistry* **269**, 14648-14654.
- Kedem O. & Katchalsky A. (1963a) Permeability of composite membranes. Part 2. Parallel arrays of elements. *Transactions of the Faraday Society* (London) **59**, 1931-1940.
- Kedem O. & Katchalsky A. (1963b) Permeability of composite membranes. Part 3. Series arrays of elements. *Transactions of the Faraday Society* (London) **59**, 1941-1953.
- Lee S.H., Chung G.C. & Steudle E. (2005a) Gating of aquaporins by low temperature in roots of chilling-sensitive cucumber and chilling-tolerant figleaf gourd. *Journal of Experimental Botany* **56**, 985-995.
- Lee S.H., Chung G.C. & Steudle E. (2005b) Low temperature and mechanical stresses differently gate aquaporins of root cortical cells of chilling-sensitive cucumber and chilling-resistant figleaf gourd. *Plant Cell and Environment* **28**, (in press).
- Liszskay A., Zalm van der E. & Schopfer P. (2004) Production of reactive oxygen intermediates (O_2^- , H_2O_2 and $\cdot OH$) by maize roots and their role in wall loosening and elongation growth. *Plant Physiology* **136**, 3114-3123.
- Maurel C. (1997) Aquaporins and the water permeability of plant cell membranes. *Annual Review of Plant Physiology and Plant Molecular Biology* **48**, 399-429.
- Mori I.C. & Schroeder J.I. (2004) Reactive oxygen species activation of plant Ca^{2+} channels. A signaling mechanism in polar growth, hormone transduction, stress signaling, and hypothetically mechanotransduction. *Plant Physiology* **135**, 702-708.
- Neill S.J., Desikan R. & Hancock J. (2002) Hydrogen peroxide signalling. *Current Opinion in Plant Biology* **5**, 388-395.
- Niemietz C.M. & Tyerman S.D. (2002) New potent inhibitors of aquaporins: silver and gold compounds inhibit aquaporins of plant and human origin. *FEBS Letters* **531**, 443-447.
- Pastori G. & Foyer C.H. (2002) Common components, networks, and pathways of cross-tolerance to stress: the central role of "redox" and abscissic acid mediated controls. *Plant Physiology* **129**, 460-468.

- Pei Z.M., Murata Y., Benning G., Thomine S., Klusener B., Allen G.J., Grill E. & Schroeder J.I. (2000) Calcium channels activated by hydrogen peroxide mediate abscisic acid signalling in guard cells. *Nature* **406**, 731-734.
- Peterson C.A. & Steudle E. (1993) Lateral hydraulic conductivity of early metaxylem vessels in *Zea mays* L. roots. *Planta* **189**, 288-297.
- Ren G., Reddy V.S., Cheng A., Melnyk P. & Mitra A.K. (2001) Visualization of a water-selective pore by electron crystallography in vitreous ice. *Proceedings of the National Academy of Sciences USA* **98**, 1398-1403.
- Steudle E. & Brinckmann E. (1989) The osmometer model of the root: water and solute relations of *Phaseolus coccineus*. *Botanica Acta* **102**, 85-95.
- Steudle E. & Frensch J. (1989) Osmotic responses of maize roots. Water and solute relations. *Planta* **177**, 281-295.
- Steudle E. & Frensch J. (1996) Water transport in plants: role of the apoplast. *Plant Soil* **187**, 67-79.
- Steudle E. & Henzler T. (1995) Water channels in plants: do basic concepts of water transport change? *Journal of Experimental Botany* **46**, 1067-1076.
- Steudle E. & Jeschke W.D. (1983) Water transport in barley roots. *Planta* **158**, 237-248.
- Steudle E. & Peterson C.A. (1998) How does water get through roots? *Journal of Experimental Botany* **49**, 775-788.
- Steudle E. & Tyerman S.D. (1983) Determination of permeability coefficients, reflection coefficients and hydraulic conductivity of *Chara corallina* using the pressure probe: effects of solute concentrations. *Journal of Membrane Biology* **75**, 85-96.
- Steudle E. (1992) The biophysics of plant water: compartmentation, coupling with metabolic processes, and water flow in plant roots. In: *Water and life: comparative analysis of water relationships at the organismic, cellular, and molecular levels*. Eds.: G.N. Somero, C.B. Osmond, and C.L. Bolis, Springer-Verlag, Berlin, pp. 173-204.
- Steudle E. (1993) Pressure probe techniques: basic principles and application to studies of water and solute relations at the cell, tissue, and organ level. In: Smith JAC, Griffith H, eds. *Water deficits: plant responses from cell to community*. Oxford: BIOS Scientific Publishers, pp. 5-36.

- Steudle E. (2000) Water uptake by roots: effects of water deficit. *Journal of Experimental Botany* **51**, 1531–1542.
- Steudle E. (2001) The cohesion/tension mechanism and the acquisition of water by plant roots. *Annual Review Plant Physiology and Plant Molecular Biology* **52**, 847-875.
- Steudle E., Oren R. & Schulze E.D. (1987) Water transport in maize roots. *Plant Physiology* **84**, 1220-1232.
- Steudle E., Smith J.A.C. & Lüttge U. (1980) Water relation parameters of individual mesophyll cells of the crassulacean acid metabolism plant *Kalanchoe daigremontiana*. *Plant Physiology* **66**, 1155-1163.
- Tyerman S.D. & Steudle E. (1984) Determination of solute permeability in *Chara* internodes by a turgor minimum method. Effect of external pH. *Plant Physiology* **74**, 464-468.
- Tyerman S.D., Bohnert H.J., Maurel C., Steudle E. & Smith J.A. (1999) Plant aquaporins: their molecular biology, biophysics and significance for plant water relations. *Journal of Experimental Botany* **25**, 1055-1071.
- Wan X.C., Steudle E. & Hartung W. (2004) Gating of water channels (aquaporins) in cortical cells of young corn roots by mechanical stimuli (pressure pulses): effects of ABA and of HgCl₂. *Journal of Experimental Botany* **55**, 411-422.
- Wojtaszek P. (1997) Oxidative burst: an early plant response to pathogen infection. *Biochemical Journal* **322**, 681-692.
- Xiong L., Schumaker K.S. & Zhu, J.K. (2002) Cell signaling during cold, drought and salt stress. *Plant Cell* **14** (suppl.), S165-S183.
- Ye Q., Muhr J. & Steudle E. (2005) A cohesion/tension model for the gating of aquaporins allows estimation of water channel pore volumes in *Chara*. *Plant Cell and Environment* **28**, 525-535.
- Ye Q., Wiera B. & Steudle E. (2004) A cohesion/tension mechanism explains the gating of water channels (aquaporins) in *Chara* internodes by high concentration. *Journal of Experimental Botany* **55**, 449-461.
- Zhang W.H. & Tyerman S.D. (1999) Inhibition of water channels by HgCl₂ in intact wheat root cells. *Plant Physiology* **120**, 849-858.

- Zhang, J., Schurr U. & Davies W.J. (1987) Control of stomatal behavior by abscisic acid which apparently originates in the roots. *Journal of Experimental Botany* **38**, 1174-1181.
- Zhu G.L. & Steudle E. (1991) Water transport across maize roots. *Plant Physiology* **95**, 305-315.
- Zimmermann H.M. & Steudle E. (1998) Apoplastic transport across young maize roots: effect of the exodermis. *Planta* **206**, 7-19.
- Zimmermann H.M., Hartmann K., Schreiber L. & Steudle E. (2000) Chemical composition of apoplastic transport barriers in relation to radial hydraulic conductivity of corn roots (*Zea mays* L.). *Planta* **210**, 302-311.

6 A re-examination of the minor role of unstirred layers during the measurement of transport coefficients of *Chara* internodes with the cell pressure probe

Qing Ye, Yangmin Kim & Ernst Steudle*

Department of Plant Ecology, Bayreuth University, D-95440 Bayreuth, Germany

Correspondence: Ernst Steudle. Fax: + 49 921 55 2564
e-mail: ernst.steudle@uni-bayreuth.de

Plant, Cell & Environment (in press)

Manuscript No.: 05-417

Abstract

The impact of unstirred layers (USLs) during cell pressure probe experiments with *Chara* internodes has been quantified. The results show that the hydraulic conductivity (L_p) measured in hydrostatic relaxations was not significantly affected by USLs even in the presence of high water flow intensities ('sweep-away effect'). During pressure clamp, there was a reversible reduction in L_p by 20 %, which was explained by the constriction of water to aquaporins in the *Chara* membrane and a rapid diffusional equilibration of solutes in arrays where water protruded across aquaporins. In osmotic experiments, L_p , and permeability (P_s) and reflection (σ_s) coefficients increased as external flow rate of medium increased indicating some effect of external USLs. However, the effect was levelling off at 'usual' flow rates of 0.20 to 0.30 $\text{m}\cdot\text{s}^{-1}$ and in the presence of vigorous stirring by air bubbles suggesting a maximum thickness of external USLs of around 30 μm including the cell wall. Since diameters of internodes were around 1 mm, internal USLs could have played a significant or even dominating role, at least in the presence of the rapidly permeating solutes used (acetone, 2-propanol and dimethylformamide). Comparison of calculated (diffusion kinetics) and of measured permeabilities indicated an upper limit of the contribution of internal USLs for the rapidly moving solute acetone of 29 % and of 15 % for the less rapidly permeating dimethylformamide. The results throw some doubt on recent claims of Tyree *et al.* (2005) that, in *Chara*, USLs rather than the cell membrane dominate solute uptake, at least for the most rapidly moving solute acetone.

Key words: aquaporin, cell pressure probe, *Chara corallina*, hydraulic conductivity, permeability coefficient, reflection coefficient, unstirred layers

Introduction

The solute concentrations that govern the permeation of solutes and water across cell membranes are the concentrations adjacent to the membrane/solution interfaces, which are usually not measurable. Due to ‘unstirred layers (USLs)’, these concentrations differ from the concentration in the bulk solutions which are usually measured. When bulk concentrations are used to quantify the driving forces such as an osmotic pressure difference driving a water flow (J_v) or a concentration difference driving a solute flow (J_s), the ‘real’ forces may be overestimated due to the existence of USLs. As a consequence, transport parameters such as the hydraulic conductivity (L_p), the permeability (P_s) and reflection (σ_s) coefficient are underestimated.

Concentration changes at the membrane surface may be either caused by a volume flow (induced by either hydrostatic or osmotic gradients) or they are caused by solute transfer. The first type of a diffusion vs. convection is referred to as a ‘sweep-away effect’ (Dainty 1963). The second type in the presence of purely diffusional USLs, has been denoted as a ‘gradient-dissipation effect’ tending to increase as solute permeability increases (Barry & Diamond 1984). For tissue cells, sweep-away can be studied using the cell pressure probe (Steudle, Smith & Lüttge 1980), but the evaluation of gradient-dissipation is difficult, as the entire tissue around a cell will act as an USL. Rather than the plasma membrane, the latter should usually dominate the exchange of water and solutes (Steudle & Frensch 1989; Ye & Steudle 2005). Isolated, giant cells of algae have been used in the past and recently to study USLs using different techniques such as isotopic exchange of solutes, transcellular osmosis, or the cell pressure probe (Dainty & Ginzburg 1964a; Steudle & Tyerman 1983; Steudle 1993; Hertel & Steudle 1997; Henzler & Steudle 2000; Ye, Wiera & Steudle 2004). Most of these data refer to internodes of *Chara corallina*. USLs of isolated cells can be treated as additional permeation resistances in series to the cell membrane. They add to the overall transport resistance. It has been shown that the contribution of sweep-away is usually small and that of gradient-dissipation more significant although not dominating, even in the presence of rapidly permeating solutes such as monohydric alcohols, acetone, formamide, dimethylformamide or isotopic water (heavy water; HDO). For the most

rapidly permeating solute HDO, a value of 25 % of underestimation was recently given (Ye, Muhr & Steudle 2005). In isolated giant cells or suspensions of small cells or vesicles, the thickness of external USLs can be efficiently reduced by stirring. However, the cell interior cannot be stirred. For small cells or vesicles, dimensions of a few μm provide a small upper limit of USLs (Finkelstein 1987; Niemietz & Tyerman 1997), but for giant cells this is not the case. For example, for the cylindrical internodes of *Chara* with a diameter of around 1.0 mm, the thickness of internal USL could, in principle, be identical with the radius, i.e. the thickness could be 500 μm in the worst case. However, it has been shown that it is substantially smaller than the radius (Hertel & Steudle 1997; Henzler & Steudle 2000). Hence, transport coefficients (L_p , P_s (P_d), and σ_s) measured with the probe are usually dominated by the membrane rather than by internal USLs. At least for isotopic water and the most rapidly permeating test solutes used so far, the system behaves like two compartments. This is in agreement with older findings that removal of the tonoplast did not affect cell L_p in *Chara* (Kiyosawa & Tazawa 1977), and with more recent data that indicate a much higher L_p of the tonoplast than of the plasmalemma (Maurel *et al.* 1997). Recent measurements demonstrated that there are different AQPs in the plasma membrane of *Chara*, which, in part, transport small organic solutes besides the water (Hertel & Steudle 1997; Henzler & Steudle 2000; Henzler, Ye & Steudle 2004; Ye & Steudle 2005). The comparison of the osmotic ($P_f = L_p \cdot RT/V_w$; V_w is the molar volume of liquid water) with the diffusional water permeability (P_d) allowed conclusions about the amounts of water molecules aligned in AQPs which relate to P_f/P_d ratios. However, when P_d was underestimated due to a substantial contribution of USLs, ratios would be overestimated. Hence, it is important to know the contribution of USLs, namely, when discussing basic mechanisms of water and solute flow across membranes (Hertel & Steudle 1997; Henzler *et al.* 2004; Ye *et al.* 2005).

Recently, Tyree, Koh & Sands (2005) argued that transport coefficients measured with the probe in *Chara* are subject to substantial or even dominating effects of USLs. In part, this should be due to the experimental arrangement of characean internodes fixed in tubes which are perfused with solution at a certain rate to minimize thicknesses of external USLs (Steudle & Zimmermann 1974; Steudle & Tyerman 1983). Tyree *et al.*

(2005) used results from a simulation model to support their view. These authors tested USLs ranging from 0 to 120 μm and from 0 to 350 μm for external and internal layers, respectively. They concluded that the permeation resistance of external and internal USLs may be larger by a factor of five than that of the plasma membrane and should, therefore, dominate the overall rate of permeation. According to Tyree *et al.* (2005), no conclusions can be drawn from the pressure probe experiments with *Chara* about the true permeation properties of membranes in the presence of rapidly permeating solutes.

In this paper, we present a rigorous re-examination of the role of external and internal USLs using rapidly permeating solutes (as in Tyree *et al.* 2005). We consider the roles of sweep-away and of gradient-dissipation on measurements of cell L_p , P_s , and σ_s . We provide quantitative evidence that (i) the thicknesses of USLs claimed by Tyree *et al.* (2005) have no basis. (ii) We show that Tyree *et al.* (2005) are wrong in their conclusions about the vigorous stirring in the experimental set-up used so far in experiments with *Chara*. (iii) We demonstrate that the analysis of pressure relaxations by Tyree *et al.* (2005) is based on false assumptions about the resolution of the pressure probe. (iv) Our data strongly support the view that the conventional sweep-away does not play a role during pressure relaxations. (v) New evidence is presented that during pressure clamp, there is a reversible reduction of cell L_p by 20 %. This is explained by a combined action of a constriction of water flow in the membrane to arrays containing AQPs and a local effect of elevated concentration on the open/closed state AQPs. (vi) When there is an efficient stirring of the medium, the upper limit of the thickness of external USLs was estimated as 30 μm . (vii) The theoretical comparison of the rates of uptake (loss) into a cell cylinder either lacking a plasma membrane or containing it with measured rates revealed an upper limit of 50 μm for the thickness of internal USLs. Hence, for rapidly permeating solutes, this may cause an underestimation of P_s and σ_s by less than 25 ~ 30 %. (viii) It was concluded that most of the points raised by Tyree *et al.* (2005) lack a sound physical basis or are based on wrong assumptions, largely, because no original experimental data were presented to support the conclusions.

Theory

At any permeation of water and solutes, there are, in principal, errors due to unstirred layers (USLs) caused by the fact that concentrations right at the membrane surfaces change. A lack or surplus of solutes has to be levelled off by an equilibration with the bulk media on both sides of the membrane. Equilibration may be rapid or slow compared to membrane permeation tending to make the effect of USLs either small or substantial. The ‘sweep-away effect’ refers to the action of a net water flow (J_V). At a steady J_V , there is a balance between convective and diffusive solute flow at the membrane. As a result, the solute concentration right at the membrane is increased on the side, to which bulk solution is swept. It is decreased on the other side from which solutes are swept away (Fig. 1B). Consequently, the osmotic component of the overall driving force for water is overestimated. An underestimation of the bulk water permeability (hydraulic conductivity; L_p) is caused. The ‘gradient-dissipation effect’ refers to relative rates of diffusion of solutes across membranes and its supply from the bulk solution. When permeation is relatively rapid as compared with the supply, the latter could affect the overall solute transport between compartments or may even dominate it. In this case, the actual concentration gradient driving permeation across the membrane is smaller than that between the bulk solutions. There are three resistances in series, the permeation resistance of the membrane ($1/P_s$) and the two diffusional resistances related to USLs.

In the presence of a steady water flow, the amount of solutes moved to the membrane or moved away from it by convection would be equilibrated by a diffusional counter flow of the solutes. The effect of changes of concentrations at the membrane surface (C_s^m) may be calculated as a function water flow (Dainty 1963; Steudle & Tyerman 1983):

$$C_s^m = C_s^b \cdot \exp\left(-\frac{J_V \cdot \delta}{D_s}\right), \quad (1)$$

for just one side of the membrane. Here, C_s^b is the concentration in the bulk solution; δ is the thickness of the USL, and D_s the diffusion coefficient of the solute. The effects on the two sides of the membrane would be additive, but both D_s and δ may be different. For example, the external solution may be stirred while the internal is stagnant and δ

different. D_s may be smaller in the cell wall than in bulk medium or cytoplasm. According to Eqn 1, the effect increases with an increasing J_V as well as with an increasing thickness of the USL, but decreases with an increasing diffusional mobility of the solute. Often, thicknesses of USLs are hard to access experimentally. They are subject to external stirring, but this cannot completely remove them. During hydrostatic experiments with the probe, an upper limit of the thickness of USLs may be worked out for the hydrostatic type of experiment. In these experiments, cell volume is changed by a ΔV inducing a change of pressure (ΔP). According to the definition of the cell elasticity (elastic modulus; ε), we have:

$$\varepsilon = V \frac{dP}{dV} \approx V \frac{\Delta P}{\Delta V}. \quad (2)$$

Here V is volume of the cell. Assuming that all of the water is extruded instantaneously during a relaxation building up an USL, the maximum value of the thickness (δ_{\max}) can be worked out (Steudle *et al.* 1980; Steudle & Tyerman 1983). For a cylindrical cell such as a *Chara* internode, we have:

$$\delta_{\max} = \frac{\Delta V}{A} = \frac{V \cdot \Delta P}{A \cdot \varepsilon} = \frac{R}{2} \cdot \frac{\Delta P}{\varepsilon}, \quad (3)$$

where A is the cell surface area and R its radius. It can be seen that for typical experimental values of $R = 0.40$ mm, $\Delta P = 0.05$ MPa and $\varepsilon = 30$ MPa, the δ_{\max} would be as small as $0.3 \mu\text{m}$. Using realistic values of J_V and D_s (Eqn 1), this results in a rather small sweep-away, even in the presence high external solute concentrations, C_s^b (see Results section). However, the above treatment may underestimate the role of sweep-away. It assumes that water flow is even throughout the entire cell surface. This may not be true. Water flow should be largely constricted to certain arrays in the membrane such as aquaporins (AQPs). In the literature, constrictions of water flow have been discussed on the tissue scale such as for epithelia (Barry & Diamond 1984), but not yet for membranes in the presence of AQPs, where the concept should apply as well. When water flow across a membrane is largely across AQPs, the water flow density in these arrays should be higher than in the rest of the membrane tending to increase sweep-away in these arrays. In order to correct for the channelling of water, a flow-constriction factor, ϕ , has been used, which denotes the fraction of the conducting area to the overall area ($\phi < 1$; Barry & Diamond 1984). The actual flow density across the conducting

array would be then J_V/ϕ . There should be also an effect of flow constriction on the actual thickness of USLs in the arrays where AQPs are located tending to increase the δ . However, effects of flow constriction are, perhaps, substantially smaller than expected, because the water layers built up on parts of the cell surface should rapidly even out (see Discussion).

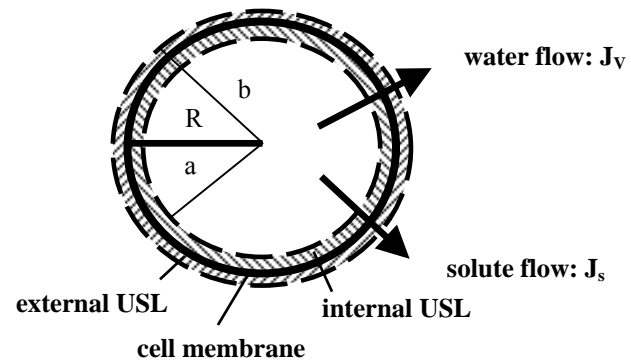
In the presence of rapidly permeating solutes such as HDO or acetone, gradient dissipation should contribute to the absolute values of P_s and σ_s as measured with the pressure probe from biphasic pressure relaxations. As outlined in the Introduction, gradient dissipation tends to level off gradients of solute concentration across the membrane resulting in a local depletion of solutes on one side of the membrane and its enrichment on the other (Fig. 1). The overall measured ‘permeation resistance’ per unit area of the solute ($1/P_s^{meas}$) contains the true diffusional resistances for the membrane ($1/P_s$) and that of the two USLs on both side of the membrane δ^o/D_s^o and δ^i/D_s^i , respectively (δ^o and δ^i = equivalent thicknesses of USLs on the two sides of the membrane; D_s^o and D_s^i = diffusion coefficients of the solute which may be different on both sides):

$$\frac{1}{P_s^{meas}} = \frac{1}{P_s} + \frac{\delta^o}{D_s^o} + \frac{\delta^i}{D_s^i}. \quad (4)$$

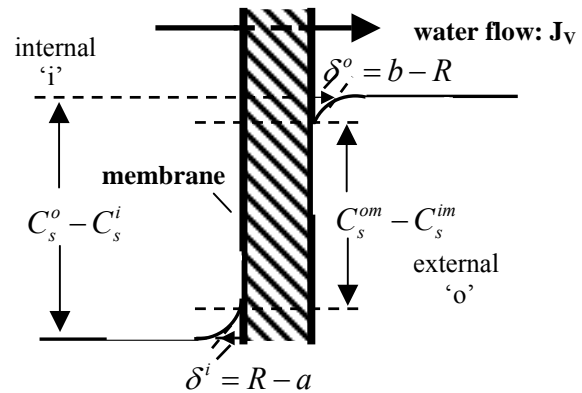
Again, this assumes steady state, a planar, homogenous membrane, and linear concentration profiles within the layers. For the cylindrical *Chara* internodes used in this paper, we may denote the radial distances from the center of the cell to the boundaries of USLs by ‘a’ (internal) and ‘b’ (external) (Fig 1A). Hence, the thicknesses of the external USL (δ^o) and of the internal USL (δ^i) would be $\delta^o = (b - R)$ and $\delta^i = (R - a)$, respectively (Fig 1B and C). In the steady state, assuming $D_s^o = D_s^i = D_s$, the overall measured permeation resistance $1/P_s^{meas}$ can be written as:

$$\frac{1}{P_s^{meas}} = \frac{1}{P_s} + \frac{R}{D_s} \cdot \ln \frac{b}{a}. \quad (5)$$

A: unstirred layers in a cylindrical cell (schematic)



B: sweep away (planar membrane)



C: gradient dissipation (planar membrane)

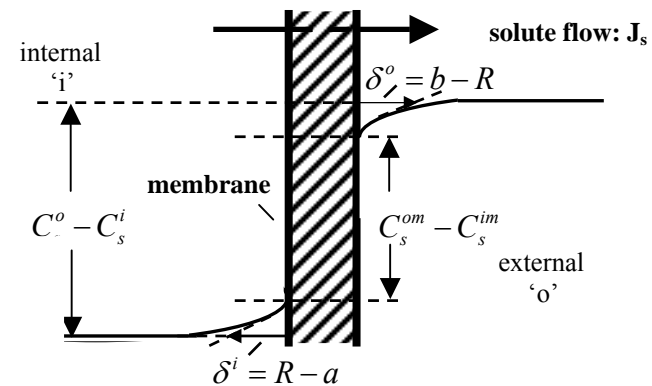


Figure 1. (A) Schematic picture of external and internal USLs in a cylindrical cell. (B, C) Concentration profiles of a solute 's' at a planar membrane separating two compartments with different concentrations (schematic; 'o' = external and 'i' = internal, respectively). δ^o and δ^i are the thicknesses of USLs on the two sides of the membrane (for further explanations, see text).

Steudle & Frensch (1989) give this equation, which they extensively discuss with respect to the role of USLs during solute permeation across roots with the endodermis being the main barrier ($R = E$) and, the cortex and stele the USLs, across which solutes have to diffuse, preferentially in the apoplast. It should be noted that, as Eqn 4, Eqn 5 relates to linear concentration profiles within the USLs. In the presence of USLs at both sides of the plasma membrane of a *Chara* cell, for $D_s^o = D_s^i = D_s$, the measured value of reflection coefficient (σ_s^{meas}) would be given as (Steudle & Frensch 1989):

$$\sigma_s^{meas} = \frac{1/P_s}{1/P_s + R/D_s \cdot (\ln(b/a))} \cdot \sigma_s \quad (6)$$

By the first factor on the right side of Eqn 6, the measured coefficient would be smaller than the true one (σ_s). If D_s would be different in the medium/cell wall from that in the cytoplasm, a more extended expression may be used (Steudle & Frensch 1989). Eqn 5 may be re-written to separate external from internal USLs, i.e.:

$$\underbrace{\frac{1}{P_s^{meas}}}_{\text{measured resistance}} = \underbrace{\frac{1}{P_s}}_{\text{true membrane resistance}} + \underbrace{\frac{R}{D_s} \cdot \ln \frac{b}{R}}_{\text{resistance of external USL}} + \underbrace{\frac{R}{D_s} \cdot \ln \frac{R}{a}}_{\text{resistance of internal USL}} \quad (7)$$

In Eqns 5 to 7, the natural logs of ratios appear because of the cylindrical geometry of cells. It is easily verified from the equations that, for $b \approx a$ or $(R-a)$, $(b-R) \ll R$, Eqn 7 reduces to the situation of the planar membrane (Eqn 4).

In a typical permeation experiment, solutes are added to the stirred medium and pass the membrane. Within the cell, mixing is largely by diffusion, which may take some time. Depending on the relative rate of the internal mixing as compared with that required for solute transfer across the membrane, internal diffusion may rate-limit the overall process as suggested by Tyree *et al.* (2005) for the rapidly permeating solute acetone. An analytical solution in the presence of a membrane surrounding a cylindrical *Chara* cell may be found when considering just internal and no external USLs. In this case (Crank 1975),

$$\frac{M_t}{M_\infty} = 1 - \sum_{n=1}^{\infty} \frac{4L^2}{\beta_n^2 \cdot (\beta_n^2 + L^2)} \cdot \exp\left[-\beta_n^2 \cdot \left(\frac{D_s \cdot t}{R^2}\right)\right] \quad (8)$$

is valid during the uptake of solute into the cylindrical cell, whereby M_t denotes the amount of solute in gram or mole in the cell at time t and M_∞ the amount when uptake is completed and $M_t/M_\infty = 1$. The β_n are the roots of $\beta \cdot J_1(\beta) - L \cdot J_0(\beta) = 0$, where J_1 and J_0 are Bessel functions and $L = P_s \cdot R / D_s$. It should be noted that, unlike Eqns 4 to 7, Eqn 8 refers to the unsteady state. Re-writing Eqn 8 in terms of the mean concentration in the cell, $\langle C_t \rangle$, rather than amounts, one gets:

$$\frac{C_m - \langle C_t \rangle}{C_m} = \sum_{n=1}^{\infty} \frac{4L^2}{\beta_n^2 \cdot (\beta_n^2 + L^2)} \cdot \exp\left[-\beta_n^2 \cdot \left(\frac{D_s \cdot t}{R^2}\right)\right], \quad (9)$$

where C_m is the concentration of the medium. The equivalent relation describing the elution of solute from a cylindrical cell previously loaded with solute, is given by:

$$\frac{M_t}{M_{or}} = \frac{\langle C_t \rangle}{C_{or}} = \sum_{n=1}^{\infty} \frac{4L^2}{\beta_n^2 \cdot (\beta_n^2 + L^2)} \cdot \exp\left[-\beta_n^2 \cdot \left(\frac{D_s \cdot t}{R^2}\right)\right]. \quad (10)$$

M_{or} (C_{or}) denotes the original content (concentration) of the cell prior to elution by a medium which does not contain the solute. For given experimental values of L , the β_n of Eqn 9 are tabulated (see, for example, Table 5.2 of Crank 1975). The absolute amounts of the exponential terms in the series on the right sides of Eqns 9 and 10 rapidly decline with time. After a sufficiently long period of time, only the first term (β_1) has to be taken into account. The physical background for this is that for small t values diffusion across the internal USL will be rapid. However, as this diffusive USL develops within the cylinder, the rate is slowing down. The USL tends to reach a certain quasi-steady thickness, and the overall permeability of the barrier (membrane plus internal USL) tends to become constant in this quasi-steady state. In this case, we have:

$$\frac{C_m - \langle C_t \rangle}{C_m} = \frac{4L^2}{\beta_1^2 \cdot (\beta_1^2 + L^2)} \cdot \exp\left[-\beta_1^2 \cdot \left(\frac{D_s \cdot t}{R^2}\right)\right], \quad (11)$$

during an uptake experiment. For a typical experimental value of $L = 2.36$ (acetone; $P_s^{meas} = 4.2 \times 10^{-6} \text{ m} \cdot \text{s}^{-1}$; $R = 0.40 \text{ mm}$), $\beta_1 = 1.68$ may hold. Under these conditions, Eqn 11 indicates an upper limit of around 40 % for the contribution of internal mixing for the rapidly permeating solute acetone (see Discussion). This is in

agreement with numerical solutions (data not shown). When considering the uptake or loss of less permeating solutes such as 2-propanol or DMF, the contribution of internal mixing is less (Fig. 8). This is a consequence of the series arrangement of permeation barriers (membrane and internal USL; see Discussion). In the absence of a membrane, i.e., when $P_s \rightarrow \infty$ and USLs dominate permeation (as claimed by Tyree *et al.* 2005), the equation corresponding to Eqn 8 is (Crank 1975):

$$\frac{M_t}{M_\infty} = 1 - \sum_{n=1}^{\infty} \frac{4}{\xi_n^2} \cdot \exp\left[-\xi_n^2 \cdot \left(\frac{D_s \cdot t}{R^2}\right)\right], \quad (12)$$

where the ξ_n are roots of a zeroth order Bessel function, and $\xi_n = 2.405, 5.520, 8.654, 11.792, 14.931, 18.071$, etc. (Jost 1960). Neglecting roots of higher order, we get:

$$\frac{M_t}{M_\infty} = 1 - \frac{4}{2.405^2} \cdot \exp\left[-2.405^2 \cdot \left(\frac{D_s \cdot t}{R^2}\right)\right], \quad (13)$$

analogous to Eqn 11.

Material and methods

Plant material

Chara corallina was grown in artificial pond water (APW; composition in mM: 1.0 NaCl, 0.1 KCl, 0.1 CaCl₂ and 0.1 MgCl₂) as described in earlier publications such as Henzler *et al.* (2004) and Ye *et al.* (2005). *Chara* internodes used in experiments were 40 to 100 mm long and 0.7 to 1.0 mm in diameter.

Determination of cell wall elasticity (ε) and transport parameters (L_p , P_s and σ_s)

Using a cell pressure probe, three transport parameters were measured (Steudle 1993): (i) the hydraulic conductivity (L_p) is a measure of water permeability across the cell membrane; (ii) the permeability coefficient (P_s) denotes the passive permeability of the cell membrane for a given solute; (iii) the reflection coefficient (σ_s) is a quantitative measure of the ‘passive selectivity’ of the cell membrane for a solute as compared to

that for the water. Cell L_p was evaluated from both hydrostatic ($\rightarrow L_{ph}$) and osmotic ($\rightarrow L_{po}$) pressure relaxations and calculated from half times (rate constants) of such relaxations and cell geometry (V = volume, A = surface area) and the elastic modulus (ε) of the cell which was determined separately (Eqn 2):

$$L_p = \frac{V}{A} \times \frac{\ln(2)}{T_{1/2}^w (\varepsilon + \pi^i)} \quad (14)$$

In the osmotic experiments with rapidly permeating solutes (acetone), the permeation of the solute contributed to the water phase of relaxations, namely close to the minima (maxima) of biphasic curves (Steudle & Tyerman 1983; Tyerman & Steudle 1984; Ye & Steudle 2005). Using semi-log plots, these ranges were omitted when determining $T_{1/2}^w$, as well as the short period in the beginning of curves which was due to the time required for the exchange of solutions in the tube which contained the *Chara* internodes. Pressure signals coming from the pressure transducer (Honeywell; type 26PCGFA6D) were continuously recorded, amplified and digitized using the sensor interface from Burster, D-96593 Gernsbach, Germany (types 92101 & 92101-Z001; RS232/RS485), which also contained the starter set with the software. Relaxations (water & solutes) were analyzed using exponential fits which also allowed semi-log plots and statistics.

Permeability (P_s) and reflection (σ_s) coefficients, were determined from the biphasic pressure (volume) relaxations according to the theory of Steudle & Tyerman (1983):

$$\frac{V(t) - V_0}{V_0} = \frac{P(t) - P_0}{\varepsilon} = \frac{\sigma_s \cdot \Delta\pi_s^o \cdot Lp}{(\varepsilon + \pi^i)Lp - P_s} [\exp(-k_w \cdot t) - \exp(-k_s \cdot t)]. \quad (15)$$

From the half time (rate constant) of the solute phase, $T_{1/2}^s$ ($\propto 1/k_s$), P_s was given by:

$$P_s = \frac{V}{A} \times \frac{\ln(2)}{T_{1/2}^s} = \frac{V}{A} k_s. \quad (16)$$

As for the water, ranges around extrema in pressure were not included in the analysis.

From the minimum (maximum) changes in pressure ($P_{\min(\max)}$), σ_s was derived according to (Steudle & Tyerman 1983):

$$\sigma_s = \frac{P_o - P_{\min(\max)}}{RT \cdot \Delta C_s^o} \times \frac{\varepsilon + \pi^i}{\varepsilon} \exp(k_s \cdot t_{\min(\max)}). \quad (17)$$

Here $t_{\min(\max)}$ is the time required to reach $P_{\min(\max)}$. Values of osmotic Lp_o , P_s and σ_s may contain contributions of USLs which would tend to underestimate the real coefficients as discussed in the Theory section (see also Steudle & Tyerman 1983; Steudle & Frensch 1989; Henzler & Steudle 2000; Ye *et al.* 2005; Ye & Steudle 2005). USLs may develop during experiments in which transient flows of water and solutes are induced to measure transport coefficients. One would expect effects of external stirring on the measurement of coefficients (see Results). However, Eqns 15 to 17 either hold only in the absence of USLs or in a steady state, when thicknesses of USLs are constant.

Hydrostatic experiments with small or big pressure pulses and pressure ‘clamp’

Pressure pulses (ΔP) of different sizes were used to induce transient water flows across the membrane (J_V) of different intensity ($\Delta P \propto J_V$). With the aid of the probe, the oil/cell sap meniscus was moved forward or backward and was kept in a constant position after each move. This resulted in pressure relaxations. According to Eqn 14, hydrostatic Lp_h was calculated from half times ($T_{1/2}^w$) of pressure relaxations. In control experiments, conventional small peak sizes of pressure pulse ($\Delta P \approx \pm 0.04$ MPa) and big peak size of pressure pulse ($\Delta P \approx \pm 0.4$ MPa) were performed to measure $T_{1/2}^w$ of water flows across the cell membrane. According to Eqn 3, different ΔP (J_V) should result in different δ_{\max} , i.e., the effects of sweep-away were varied. Experiments were repeated in the presence of high concentrations of osmotic solute presented at both sides of the membrane (1.0 M acetone and 1.0 M 2-propanol). This should have increased the effect which was expected to be bigger at high ΔP than at lower one (Eqn 3). The biggest sweep-way effects may be expected during pressure clamp, when turgor pressure was clamped at a reasonable $\Delta P \approx \pm 0.2$ MPa for about 5 seconds to move larger amounts of water across the membrane tending to build up an USL. The ΔP was limited to about 0.2 MPa in these experiments, due to the rather small diameter of the capillary in the tip region. Following pressure clamps, $T_{1/2}^w$ of water flows were measured from pressure relaxations by fixing the meniscus right at the end of the clamp. When the original turgor was re-attained, pressure relaxations were repeated at a time of between 10 and 20 s after the termination of the clamp. These experiments should show how USLs built

up during the clamp affected $T_{1/2}^w$ (Lp_h) and of how rapid USLs would dissipate away by diffusion following its build-up.

Effects of external flow rate (v_{med}) on P_s , σ_s , and Lp_o

In order to induce turbulent water flow within the glass tube that contained the cells (internal diameter: 3 mm; length: 250 mm), solutions were injected across a stopcock and a constriction (Ye & Steudle 2005). To vary the intensity of turbulent flow within the pipe, the average flow of solution (v_{med}) was varied between $0.02 \text{ m}\cdot\text{s}^{-1}$ (nearly stagnant) and $0.55 \text{ m}\cdot\text{s}^{-1}$ by adjusting the stopcock in the experimental set-up (see Fig. 1 of Hertel & Steudle 1997). Average flow rates were calculated by dividing the volume passing through the tube in a given time by the cross-sectional area of the tube containing the *Chara* internode. Depending on the flow rate, it took 2.0 to 0.1 s to completely replace the solution around the shortest (40 mm long) and 5.0 to 0.2 s to replace it around the longest (100 mm) internodes used. At high rates, the turbulent water flow should have minimized the thickness of USLs attached to the cell surface. To test whether or not the stirring by the speed of the external solution was sufficient to minimize the thickness of USLs, an additional stirring was provided in some experiments by injecting air bubbles into the pipe which were flushing across the tube at a frequency of 160 to 200 bubbles per minute. Effects of stirring of the turbulent solution around the internodes were measured for the osmotic hydraulic conductivity (Lp_o), and permeability (P_s) and reflection (σ_s) coefficients. Three different osmolytes of different permeability were employed at different concentrations: acetone (300 mM), 2-propanol (120 mM), and DMF (60 mM). Values of osmotic Lp_o , P_s and σ_s were derived from biphasic pressure (volume)/time curves (Eqn 15).

Results

Figure 2 shows typical pressure relaxations obtained during hydrostatic experiments with an individual *Chara* internode. To test for effects of USLs due to ‘sweep-away’, half times of water flow across the cell membrane ($T_{1/2}^w$) were measured with small ($\Delta P \approx \pm 0.04$ MPa) or big ($\Delta P \approx \pm 0.4$ MPa) peak sizes of pressure pulses. Since the intensities of water flow across the cell membrane were proportional to the size of pulses (Eqn 3), the J_V induced by big pulses should have been larger by an order of magnitude than that in the presence of small pulses.

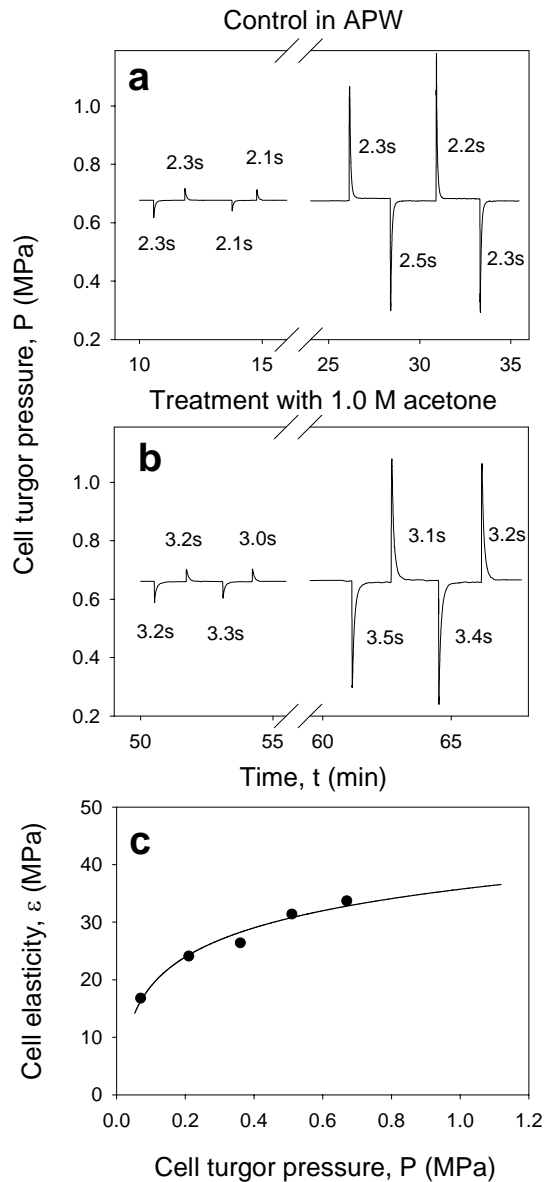


Figure 2. Effects of pressure pulses of different peak sizes on $T_{1/2}^w$ during hydrostatic pressure relaxations induced in a *Chara* internode. Rates of water flow across the membrane (J_v) were increased by increasing the size of pulses by about an order of magnitude. This, however, did not increase $T_{1/2}^w$ (decrease L_{ph} ; $L_{ph} \propto 1/T_{1/2}^w$). (a) It is concluded that USLs due to sweep away do not play a significant role during relaxations. (b) There was also no effect of increases in peak size on $T_{1/2}^w$ in the presence of a solute such as 1.0 M acetone on both sides of the membrane, although high concentration should have increased sweep away according to Eqn 3. However, due to the gating of AQPs in the presence of high concentration, $T_{1/2}^w$ increased (L_{ph} decreased) by a factor of about 1.5, when cells were treated with 1.0 M acetone (Ye *et al.* 2004). (c) Effects of the cell elastic modulus (ϵ) around the steady state turgor (0.65 MPa) were too small in the presence of the small pulses ($\Delta P \approx \pm 0.04$ MPa) and had no effect in the presence of big positive pulses ($\Delta P \approx + 0.4$ MPa). They may have caused a tendency in $T_{1/2}^w$ to increase in the presence of the negative pulses ($\Delta P \approx - 0.4$ MPa). The latter effect, however, was not caused by a change in L_{ph} (see text).

The thickness of USLs built up by sweep-away during big pulses should have had a bigger effect on $T_{1/2}^w$ than during the small ones. However, there was no significant difference in $T_{1/2}^w$ when comparing the results both in the presence of just APW (Fig. 2a) or of 1.0 M acetone (Fig. 2b). The reason is that in either case thicknesses of USLs were too small to cause significant effects, even in the presence of a flow constriction (Table 1). For the cell used in Fig. 2, $\epsilon = 34$ MPa, $R = 0.40$ mm, and δ_{max} was calculated to be 0.24 and 2.4 μm for small and big pulses, respectively (Eqn 3; without considering flow constriction by AQPs). It may be argued that cell elasticity (ϵ) could have changed with cell turgor pressure during the peaks and this could have compensated for the effect, at least for positive ΔP (Eqn 3). However, it can be seen from Fig. 2c that changes of ϵ around the steady state turgor of 0.65 MPa were too small both in the presence of small ($\Delta P \approx \pm 0.04$ MPa) or big positive pulses ($\Delta P \approx + 0.4$ MPa). It may have caused the slight increase of $T_{1/2}^w$ in the presence of the big negative pulses ($\Delta P \approx - 0.4$ MPa), but the L_{ph} should have remained constant due to the compensating decrease of ϵ with decrease of cell turgor pressure (Eqn 14). Results suggested that hydraulic conductivity ($L_{ph} \propto 1/T_{1/2}^w$) as measured by pressure relaxations

should be rather free of effects of USLs (see Discussion). There was no difference, when cells were subjected to 1.0 M acetone or 2-propanol. This treatment should have increased absolute values of $(C_s^b - C_s^m)$ and, therefore reduced J_v and L_{ph} . It should be noted that in Fig. 2b, $T_{1/2}^w$ increased (L_{ph} decreased) by a factor of about 1.5, when cells were treated with 1.0 M acetone. This was due to a gating of AQPs in the presence of high concentration (Ye *et al.* 2004; 2005).

Table 1. Half-times ($T_{1/2}^w$) of hydrostatic water flow across cell membranes of *Chara* as measured either in APW and in the presence of 1.0 M acetone or 1.0 M 2-propanol. $T_{1/2}^w$ increased due to the gating of AQPs by high concentration. $T_{1/2}^w$ measured with small pressure pulses ($\Delta P \approx \pm 0.04$ MPa) were not significantly different from those measured in the presence of big pressure pulses ($\Delta P \approx \pm 0.4$ MPa) both in APW and at high external concentration. Relative changes of the mean of $T_{1/2}^w$ are given as mean \pm SD (n = 6 cells).

cell No.	Half-times ($T_{1/2}^w$) of hydrostatic water flows across cell membranes of <i>Chara</i> (s)					
	experiments in APW			treatment with 1.0 M acetone (cell 1 to 3) or 1.0 M 2-propanol (cell 4 to 6)		
	$\Delta P \approx \pm 0.04$ MPa	$\Delta P \approx \pm 0.4$ MPa	relative change of the mean (%)	$\Delta P \approx \pm 0.04$ MPa	$\Delta P \approx \pm 0.4$ MPa	relative change of the mean (%)
1	2.4 \pm 0.2	2.5 \pm 0.2	4	3.3 \pm 0.3	3.7 \pm 0.2	12
2	2.2 \pm 0.1	2.3 \pm 0.1	5	3.2 \pm 0.1	3.3 \pm 0.2	3
3	1.7 \pm 0.1	2.0 \pm 0.2	18	3.6 \pm 0.2	4.1 \pm 0.4	14
4	2.5 \pm 0.2	2.6 \pm 0.1	4	5.1 \pm 0.4	5.2 \pm 0.9	2
5	2.8 \pm 0.3	3.0 \pm 0.4	7	5.0 \pm 0.3	5.5 \pm 0.6	10
6	2.5 \pm 0.2	2.6 \pm 0.1	4	4.3 \pm 0.2	4.4 \pm 0.4	2
			mean: 7 SD: \pm 5			mean: 7 SD: \pm 5

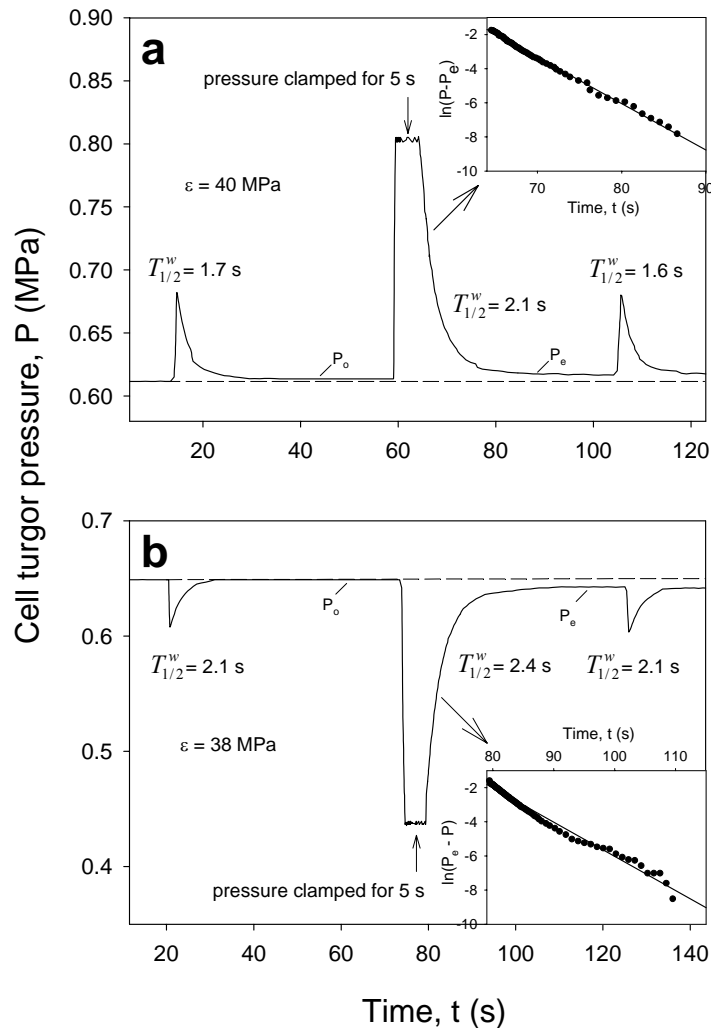


Figure 3. Effects of ‘sweep-away’ during a pressure-clamp experiment. In order to increase amounts of water moving across the membrane, a steady-state pressure clamp was used, where the pressure was clamped at a ΔP of ± 0.2 MPa for 5 s. Immediately following this treatment, half times ($T_{1/2}^w$) increased by 24 % at a $\Delta P \approx +0.2$ MPa ($\epsilon = 40$ MPa) and by 14 % at a $\Delta P \approx -0.2$ MPa ($\epsilon = 38$ MPa). The insets in (a) and (b) provide semi-long plots of either $(P - P_e)$ or $(P_e - P)$ vs. time showing that, during hydrostatic pressure relaxations, there were no significant changes in the USLs, i.e., a tendency of $T_{1/2}^w$ to decrease as J_v decreased during the relaxations. $T_{1/2}^w$ reached the original values after about 20 s after termination of relaxations indicating that the USLs or other polarization effects rapidly dissipated away by diffusion after that time. There were slight differences between the original values of cell turgor pressure (P_o) and the steady pressure following the pressure clamp which was due to either a concentration (exosmotic water flow; a) or dilution of cell sap (endosmotic water flow; b). For further explanation, see text.

Table 2. Half-times ($T_{1/2}^w$) of water flows across cell membranes of *Chara* as measured during hydrostatic pressure relaxation and following a pressure clamp for 5 seconds at $\Delta P \approx \pm 0.2$ MPa. It can be seen that the clamp increased $T_{1/2}^w$ by 20 % as compared with the control ($\Delta P \approx \pm 0.04$ MPa). Relative changes of the mean of $T_{1/2}^w$ are given as mean \pm SD (n = 6 cells).

cell No.	Half-time ($T_{1/2}^w$) of hydrostatic water flows across cell membranes of <i>Chara</i> (s)		
	Control ($\Delta P \approx \pm 0.04$ MPa)	pressure clamp for 5 sec ($\Delta P \approx \pm 0.2$ MPa)	relative change of the mean (%)
1	2.5 \pm 0.2	3.1 \pm 0.2	24
2	1.7 \pm 0.1	2.0 \pm 0.2	18
3	2.2 \pm 0.2	2.4 \pm 0.1	9
4	4.8 \pm 0.3	5.7 \pm 0.4	19
5	2.7 \pm 0.1	3.3 \pm 0.2	22
6	2.9 \pm 0.2	3.4 \pm 0.3	17
			mean: 18
			SD: \pm 5

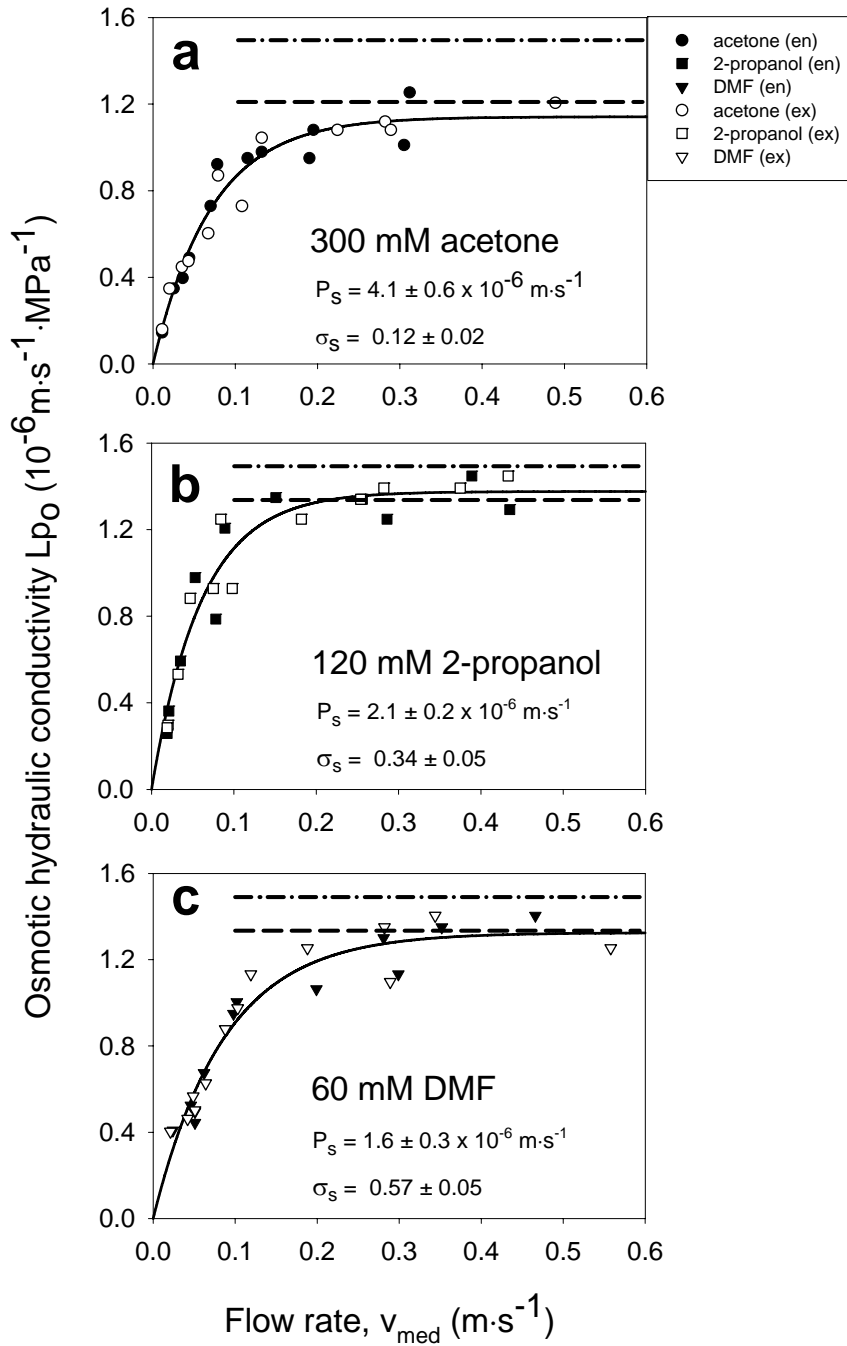
In order to increase the amounts of water flowing across the cell membrane ($J_V \times t$), a pressure-clamp was used to produce a steady water flow or nearly so. In Fig. 3, the pressure was clamped for 5 s at a ΔP of ± 0.2 MPa causing an amount of water flowing across the membrane larger than that in the relaxation experiments of Fig. 2 in the presence of small pulses. Effects of sweep away during pressure-clamp experiments were tested by directly going from the clamp to the relaxation mode. It can be seen that clamping resulted in an increase of $T_{1/2}^w$ by about 20 % as compared with the control (for statistics, see Table 2). The effect vanished rapidly (within less than 20 s). When the original turgor pressure was re-attained, subsequent pressure relaxations following the clamp showed $T_{1/2}^w$ values which were not different from the original (Fig. 2a and b). The slight increase of steady turgor during pressure clamp was caused by the displacement of water from the cell during exosmotic water flow resulting in an

increase of its osmotic concentration. There was a slight decrease of turgor, when water was taken up by the cell. These changes remained during subsequent relaxations. Relative changes of steady turgor of $\pm 2\%$ agreed with the estimated relative changes of cell volume. The changes in the overall thickness of USLs during pressure clamp were $2.4 - 3.2\ \mu\text{m}$ in the absence of flow constriction of AQPs (see Theory and Discussion sections). The relaxation back to steady-state pressure could be fitted by a single exponential (see insets of Fig. 2). The results indicate that ‘sweep-away-effects’ in the presence of a pressure clamp may have caused transient increases of $T_{1/2}^w$ (decreases of L_{p_h}) which could have been affected by flow constriction or concentration polarization effects (see Discussion).

Fig. 4 indicates that L_{p_o} increased with increasing external stirring (mean external flow rates) tending to reach saturation at rates of between 0.20 and $0.30\ \text{m}\cdot\text{s}^{-1}$ (depending on solute used). This is similar to results of Steudle & Tyerman (1983), who used mannitol as the osmolyte. At saturation, L_{p_o} values were identical with the L_{p_h} values measured in the presence of the same solutes at the given concentration. Changing the direction of water flow (endosmotic; en (closed symbols) vs. exosmotic; ex (open symbols)) did not change the dependence of L_{p_o} on v_{med} .

Figure 4. Effects of external stirring on $T_{1/2}^w$ (L_{p_o}) in osmotic experiments. In order to vary thicknesses of external USLs and solution exchange along *Chara* internodes during osmotic experiments, external stirring was varied by changing mean flow rates along tubes (v_{med} in $\text{m}\cdot\text{s}^{-1}$). Three different concentrations and osmolytes of different permeability (P_s) and reflection (σ_s) coefficients were used: (a) 300 mM acetone, $\sigma_s = 0.12$; (b) 120 mM 2-propanol, $\sigma_s = 0.34$; and (c) 60 mM dimethylformamide (DMF), $\sigma_s = 0.57$. It can be seen that L_{p_o} ($T_{1/2}^w$) was quite low in nearly stagnant solution tending to increase with increasing flow rates. Depending on the solutes used, saturation of L_{p_o} was reached at flow rates between 0.20 and $0.30\ \text{m}\cdot\text{s}^{-1}$, the latter range being the standard flow rate usually used in earlier experiments. The data in the figure refer to three different internodes (a to c). Horizontal lines denote values of hydrostatic L_{p_h} determined in the absence of the solute (i.e. in APW - - - -) or in its presence (----). It can be seen that, at saturation, L_{p_o} values were identical with the L_{p_h} values measured in the presence of solute. It should be noted that the response of L_{p_o} to v_{med} should incorporate (i) the reduction of the thickness of USLs as turbulences increase, (ii) effects of progressive coverage of cells following exchanges of solution, and (iii) effects of the concentration dependence of L_{p_o} as coverage proceeds. The latter two points may

dominate at low flow rates. The data show that changing the direction of water flows (endosmotic (closed symbols) vs. exosmotic (open symbols)) did not change the dependence of Lp_o on v_{med} .



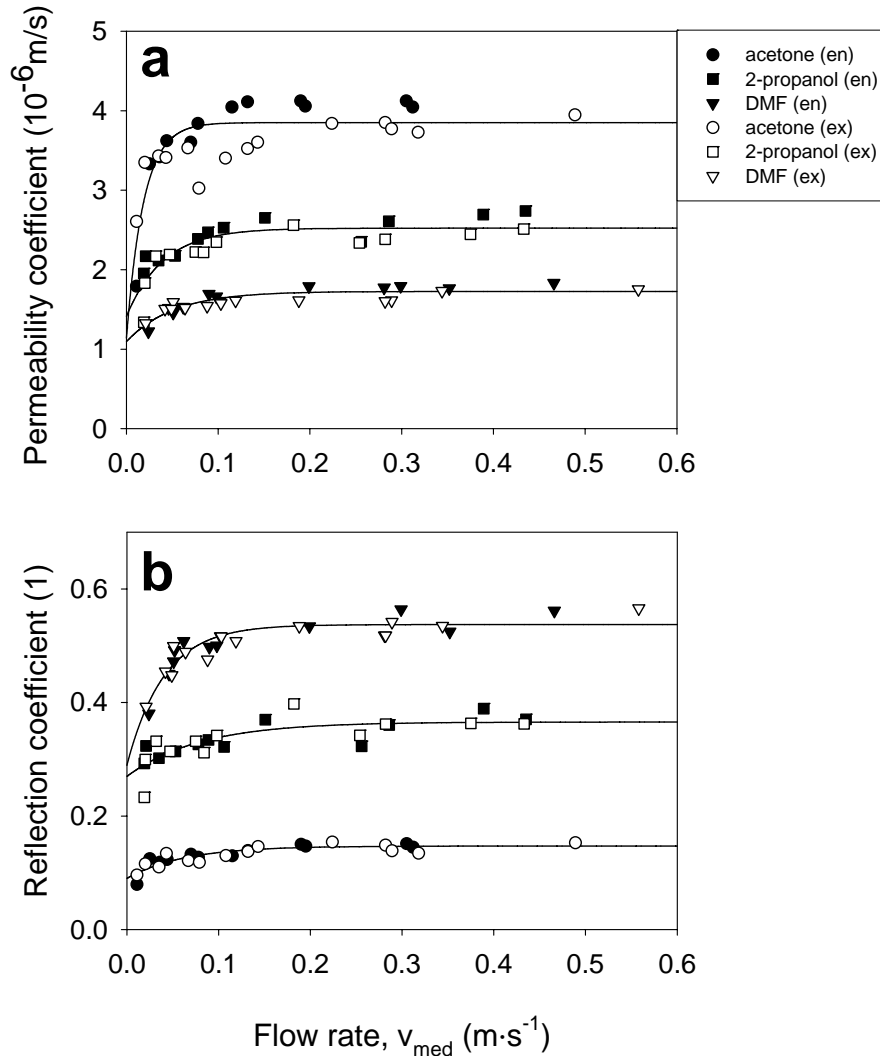


Figure 5. Effects of external stirring (flow rates) on (a) permeability coefficient (P_s) and (b) reflection coefficient (σ_s) of *Chara* internodes for the three osmolytes and cells of Fig. 4 (300 mM acetone, circles; 120 mM 2-propanol, squares; 60 mM DMF, triangles). Both P_s and σ_s were reduced in nearly stagnant solution ($v_{med} < 0.02 m \cdot s^{-1}$). Saturation was reached at a $v_{med} \geq 0.1 m \cdot s^{-1}$, which was smaller than the rates required for reaching a saturation value of osmotic Lp_o (Fig. 4). This indicated that external stirring had less effect on P_s and σ_s than on osmotic Lp_o .

In Fig. 5, typical effects of external stirring on permeability (P_s) and reflection (σ_s) coefficients are shown as worked out from biphasic osmotic relaxation curves for three different osmolytes and cells. It can be seen that in a nearly stagnant solution, where replacement of the solution around the internodes should have been rate limiting, P_s and σ_s were rather small. Both P_s (a) and σ_s (b) increased as v_{med} increased. Saturation

values were attained at smaller rates ($v_{\text{med}} \approx 0.10 \text{ m}\cdot\text{s}^{-1}$) than during the measurement of L_{p_0} ($v_{\text{med}} \approx 0.20 \text{ m}\cdot\text{s}^{-1}$). This would be expected considering the different half times of water and solute transport across the membrane (see Discussion).



Figure 6. (a) Vigorous stirring of external solution by injecting air bubbles into the water stream along the pipe. Air bubbles (red arrows) were rapidly flushed through at frequencies of between 160 and 200 air bubbles per minute, which caused a tremendous stirring by sweeping away the solution around the *Chara* internodes. For the sake of a clearer view on the air bubbles, (b) was taken under conditions of a slow motion of air bubbles.

In some experiments, the stirring in the presence of high rates of v_{med} was enhanced by injecting air bubbles into the water flow along the pipe. This caused a tremendous sweeping away of the solution along the internodes as can be seen in Fig. 6 and on a video at <http://www.homepage.steudle.uni-bayreuth.de>. The effect of the stirring by air bubbles did not further increase the osmotic L_{p_0} .

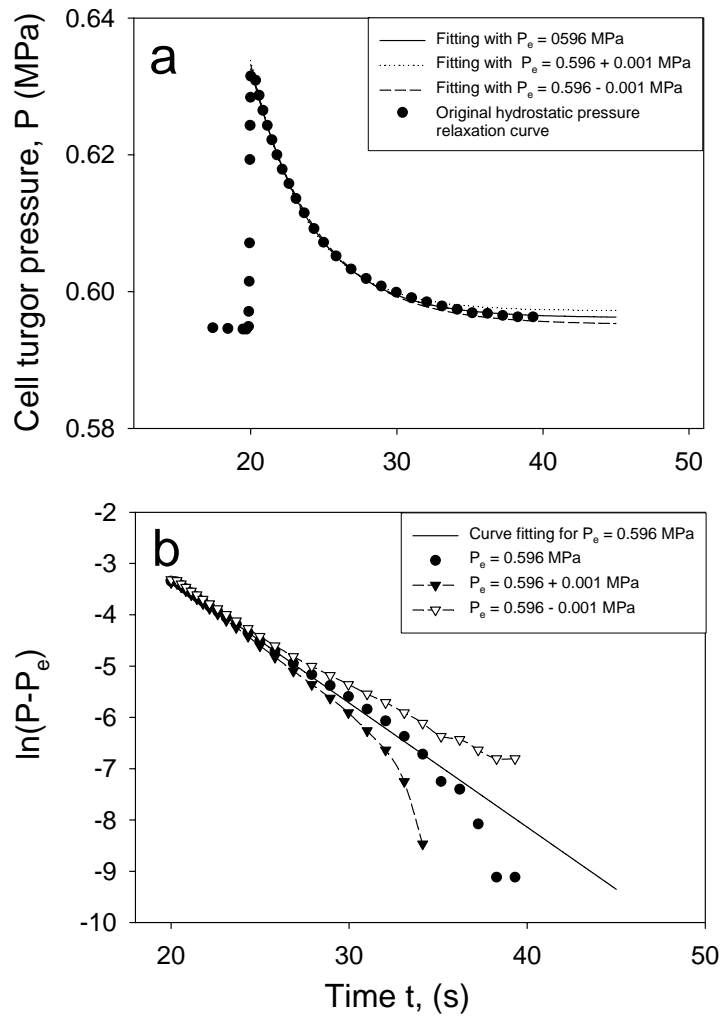


Figure 7. Analysis of a typical hydrostatic relaxation of cell turgor pressure as measured by a cell pressure probe. Lines (a) are fits of the data using $P = P_e + \Delta P \cdot \exp(-\ln(2) \cdot t / T_{1/2}^w)$. The solid line is the best fit with the P_e value of 0.596 MPa. Dashed lines are fits with P_e values fixed either at 0.596 + 0.001 MPa or at 0.596 - 0.001 MPa. Closed circles are the original data of hydrostatic relaxation. (b) Natural logarithm of $(P - P_e)$ versus time for the pressure relaxation data from (a). The circles and triangles represent the logs of $(P - P_e)$, when P_e is 0.596 MPa (closed circles), 0.596 + 0.001 MPa (closed triangles), and 0.596 - 0.001 MPa (open triangles). The solid line is the fit of natural logarithm of $(P - P_e)$ with $P_e = 0.596$ MPa. The results show that small variations of P_e of an order similar to the resolution of the pressure probe (± 1 kPa) caused a bending of log plots upward or downward. Hence, a wrong choice of P_e within the limits of accuracy may suggest that pressure relaxations have more than one exponential phase. This type of systematic errors should be avoided by cutting off the pressure range where $P - P_e$ gets close to the resolution of the probe.

Usually, the hydrostatic relaxations measured with the pressure probe could be nicely fitted by a single exponential. The same was true for the solute phases of biphasic responses in the presence of permeating solutes, provided that analyses are not made just around the minima or maxima of $P(t)$ curves (Tyerman & Steudle 1984). However, when relaxations approached the final value of turgor pressure (P_e), semi-log plots of the differences of $(P - P_e)$ vs. time tended to become scattered, when $(P - P_e)$ got close to the resolution of the probe (around 0.002 MPa; Steudle & Tyerman 1983). When the fitted P_e value slightly differed from the real one, there could be either a bending up or down in the plots (Fig. 7). As discussed by Steudle & Tyerman (1983) and others, this is due to a systematic error, which results from the facts that, under these conditions, $(P - P_e)$ represents a small difference of two rather big figures. As $P \rightarrow P_e$, errors get fairly large. Data from this part of relaxations should not be used for analysis. Bending of semi-long plots in one way or the other in this range of relaxations are artefacts. In Fig. 7, the effect is demonstrated by varying the P_e in steps of ± 0.001 MPa which is close to the resolution of the transducer in the probe.

To work out upper limits of thicknesses of USLs during experiments with permeating solutes, both ordinary steady state diffusion (Eqns 4 to 7) and unsteady state diffusion kinetics in the presence of a membrane were employed (Eqns 8 to 11). During steady state, the maximum thickness of an internal USL was estimated assuming that the measured P_s^{meas} just reflects the permeation across internal USLs rather than across the membrane, i.e., USLs dominated permeation. Neglecting the external USL, we then get for acetone ($P_s^{meas} = 4.2 \times 10^{-6} \text{ m}\cdot\text{s}^{-1}$; $D_s = 1.2 \times 10^{-9} \text{ m}^2\cdot\text{s}^{-1}$; $R = 0.40 \text{ mm}$) a $\delta_{max}^i = 204 \text{ }\mu\text{m}$. In the presence of an additional external USL of $30 \text{ }\mu\text{m}$, this value is reduced to $189 \text{ }\mu\text{m}$. In terms of unsteady state diffusion, we first made the approach that the membrane was not rate limiting at all ($P_s \rightarrow \infty$), i.e., there was free diffusion across the boundary of a cylinder having the same diameter as a cell ($R = 0.40 \text{ mm}$; Eqn 13; in the absence of an external USL). This result was then compared with the uptake into a cylinder bounded by a membrane (Eqn 11). Eventually, results were compared with data measured with an intact *Chara* internode using the probe. Fig. 8 provides typical results for the rapidly permeating acetone and the less permeating DMF ($D_s = 1.0 \times 10^{-9}$

$\text{m}^2\cdot\text{s}^{-1}$; Poling, Prausnitz & O'Connell 2001). Natural logs for solute uptake into a cylinder bounded by a membrane and free diffusion within the stagnant inside of a cylinder are plotted against time according to Eqns 9 and 12, respectively. It can be seen from the figure that during free diffusion, uptake was rather rapid during the first 10 s as already discussed in the Theory section. During later stages, the process could be described by a single exponential, when the internal USLs formed rate-limited further uptake (quasi-steady state). Hence, a straight line was obtained in the semi-log plot of the relative uptake/loss versus time. From the rate constant (slope k_D) during this phase, an equivalent thickness of the USL could be obtained which was 117 μm ($R = 0.40$ mm) and 108 μm ($R = 0.37$ mm), respectively. In the presence of a membrane with measured $P_s^{\text{meas}} = 4.2 \times 10^{-6} \text{ m}\cdot\text{s}^{-1}$ containing resistance of membrane and USL ($R = 0.40$ mm in the example), the maximum thickness of the internal USL reduced to 97 μm (Eqns 5 and 11). The maximum values of 117 and 97 μm are substantially smaller than the steady state value of 204 μm given above. Results indicate that for the most rapidly permeating acetone ($P_s^{\text{meas}} = 4.2 \times 10^{-6} \text{ m}\cdot\text{s}^{-1}$), the contribution of internal USLs was maximally 40 %. The equivalent calculation for the less permeating DMF ($P_s^{\text{meas}} = 1.8 \times 10^{-6} \text{ m}\cdot\text{s}^{-1}$) resulted in a steady state equivalent thickness of 124 μm and maximum thicknesses of 108 and 95 μm , respectively ($R = 0.37$ mm), and the contribution of internal USLs was maximally 18 %. This means that the effect caused by internal USLs substantially decreased as P_s decreased (see Discussion). Accordingly, internal USLs contributed to 40 % (acetone) or 18 % (DMF) of the measured permeability.

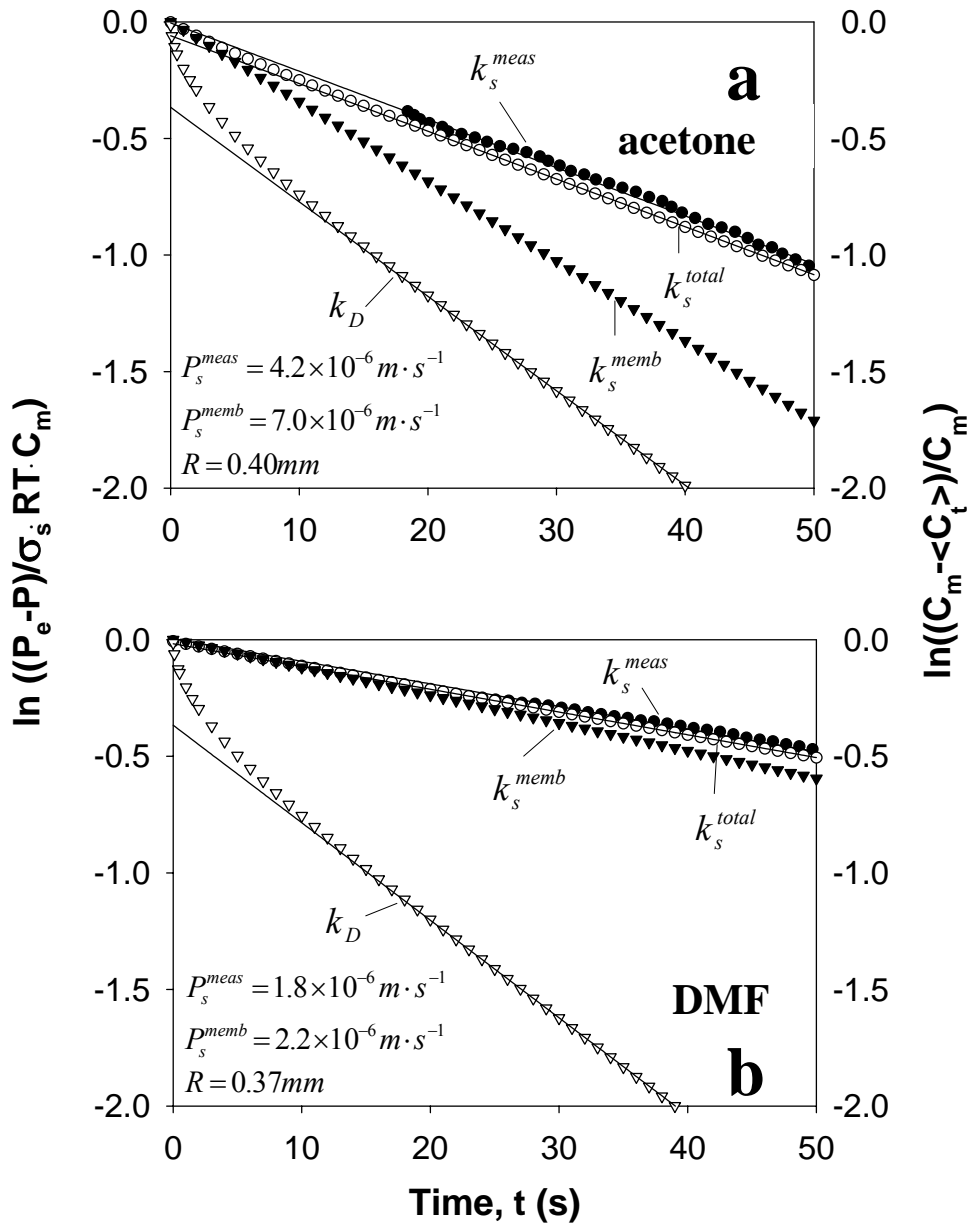


Figure 8. Kinetics of the uptake of a rapid (acetone: overall $P_s^{meas} = 4.2 \times 10^{-6} \text{ m} \cdot \text{s}^{-1}$) and a slow (DMF: overall $P_s^{meas} = 1.8 \times 10^{-6} \text{ m} \cdot \text{s}^{-1}$) solute into two typical *Chara* internodes as measured with the pressure probe (slope: k_s^{meas}). Semi-log plots of relative amounts of solute taken up by the cells are given, i.e., $\ln[(P_e - P(t))/(\sigma_s \cdot RT \cdot C_m)]$ as a function of time t (P_e = final value of cell turgor pressure; C_m = concentration of solute in the medium). They are compared with the calculated diffusion into cylinders with the same diameter (i) either lacking a plasma membrane (open triangles; rate constant k_D ; Eqn 12) or (ii) containing it in series to internal USLs (open circles; k_s^{total} ; Eqn 9). Furthermore, the uptake in the

presence of just the membrane in the absence of USLs is given ($P_s^{memb} = 7.0 \times 10^{-6} \text{ m}\cdot\text{s}^{-1}$ and $2.2 \times 10^{-6} \text{ m}\cdot\text{s}^{-1}$ for acetone and DMF, respectively). It can be seen from the figure that the effect of the internal USL was larger for the rapidly permeating acetone than for the less permeating DMF. For diffusion into the cylinders, relative amounts were given by $(C_m - \langle C_t \rangle)/C_m$, where $\langle C_t \rangle$ denotes the average concentration in the cylinder (Eqn 9). Diffusion kinetics of acetone uptake (open triangles in (a); $D_s = 1.2 \times 10^{-9} \text{ m}^2\cdot\text{s}^{-1}$) is given for a cylinder lacking a membrane of the same diameter of 0.80 mm as the cell. For DMF (open triangles in (b); $D_s = 1.0 \times 10^{-9} \text{ m}^2\cdot\text{s}^{-1}$) and the diameter was 0.74 mm. The calculation of k_s^{memb} (closed triangles) from k_s^{meas} was based on the procedure given by Stevenson (1974), which assumed completely stagnant conditions in the cells. k_s^{total} was produced from the analytical solution in the presence of the estimated k_s^{memb} (P_s^{memb}) and the inner USL arranged in series (Eqn 9). The data show that the measured curves (closed circles) differ from those of calculated in the absence of a membrane (open triangles) in that bended parts close to $t = 0$ are missing or can not be resolved in the presence of the membrane. Bended parts during diffusion kinetics relate to the building up of a diffusional USL in the outer part of cylinders. When this layer is quasi-steady, the process can be described by a single exponential, i.e., the layer acts like a membrane. In the absence of membranes, bended parts close to $t = 0$ result in intercepts with the ordinate which are significantly smaller than zero. Comparing the measured values of k_s^{meas} with calculated values of k_s^{memb} , the maximum contribution of internal USLs to the overall measured permeability coefficients were estimated to be 40 % for acetone and 18 % for DMF. For further explanation, see text.

The semi-log plots of Fig. 8 demonstrate the effects of USLs in terms of slopes which represent rates of uptake. Slopes were biggest in the absence of membranes (slope: k_D) followed by slopes in just the presence of the membrane without any USL (slope: k_s^{memb}). The combined effect of USLs and membrane resistances resulted in the smallest slopes (slope: k_s^{total}). Using calculations based on measured data, the figure shows that, in this case, calculated curves (slope: k_s^{total}) and measured values (slope: k_s^{meas}) were nearly identical. However, measured values resulted in intercepts often > 0 , which was, of course, not the case for calculated data. When diffusive USLs were rate-limiting (as assumed by Tyree *et al.* 2005), the curve with the measured data points in Fig. 8 (k_s^{meas}) should have been close to the uptake curve in the absence of a membrane (k_D) rather than to k_s^{total} . Also, the intercept with the ordinate should have differed significantly from zero. This was not the case. It should be noted that all calculation were based on

the assumption of a completely stagnant and homogenous internal compartment which may be questioned (see Discussion).

Discussion

(A) Present results

During hydrostatic relaxations, L_{ph} was not significantly affected by sweep-away, even in the presence of water flows across the membrane (J_v), which were bigger than usual by a factor of ten. Sweep-away did not play a role because maximum thicknesses of USLs (δ_{max}) remained as small as fractions of a micrometer, i.e., they were substantially smaller than the thickness of the cell wall (5 to 10 μm) or of the cytoplasmic layer (a few μm). Calculations assumed a maximum (peak) J_v during the entire relaxation and are, therefore, pessimistic with respect to the effects of USLs. Sweep-away also remained small in the presence of high external concentration which should have increased the effect. However, all these estimates did not incorporate the constriction of water flow across AQPs, which could have been crucial. The effect should refer to both J_v and δ . The estimation of flow constriction would require the knowledge of the density of AQPs and of the hydraulic conductivity of individual subunits (l_p). At present, there are no data of the density of AQPs of *Chara* and of their l_p . However, there are data for the water channels of red blood cells (AQP1). The l_p of a single water channel subunit of AQP1 is $l_p = 4.0 \times 10^{-22} \text{ m}^3 \text{ H}_2\text{O} \cdot \text{s}^{-1} \cdot \text{MPa}^{-1} \cdot (\text{AQP subunit})^{-1}$ (Walz *et al.* 1994; see also Wan, Steudle & Hartung 2004). This may be used for a rough estimate of the effect of flow constriction neglecting the contribution of the bilayer which is only 5 to 10 % of the overall L_p (Henzler *et al.* 2004). A typical value of cell L_p of *Chara* is $1.6 \times 10^{-6} \text{ m}^3 \cdot \text{m}^{-2} \cdot \text{s}^{-1} \cdot \text{MPa}^{-1}$. Hence, we get an AQP density of $L_p/l_p = 4.0 \times 10^{15} (\text{AQP subunits}) \cdot \text{m}^{-2}$. Given a cross section of about 10 nm^2 for an AQP subunit (Walz *et al.* 1994), this results in a value for ϕ of 0.04. Hence, J_v and δ should be each corrected by a factor of as large as 25. However, the measured effect was small if any. One reason could be that, as the water protrudes out of AQPs, it may be rapidly evened out by creeping along the hydrophilic membrane surface surrounding the pores.

It is, perhaps, more likely that, as columns of distilled water protrude either into the cytoplasm or wall space, they are rapidly evened out by lateral diffusion of solutes into them. According to Eqn 12, the time constant required for this diffusional equilibration should be as short as 4 ns (using a radius of 1.8 nm of the columns (equivalent to a cross sectional area of AQP subunits of 10 nm^2 , see above); and a diffusion coefficient of $1.0 \times 10^{-10} \text{ m}^2 \cdot \text{s}^{-1}$ of the solutes). This time constant is much shorter than that of water flow equilibration. As a consequence, changes of the local concentration by sweep-away or concentration polarization should be substantially smaller than expected from the overall enhancement by constriction by a factor of 625 (25×25). Accordingly, there was no effect of sweep away during hydrostatic relaxations, even in the presence of big peak sizes. Only during pressure clamp, when rather large amounts of water were continuously moved across AQPs, the effect was measurable, i.e., there was a significant dilution/concentrating effect around the vestibules of AQPs. In addition, we may think that there could have been effects of concentration polarization and dilution within the non-selective mouth parts (vestibules) of channels. There is evidence that at least some of the AQPs of *Chara* have a rather large internal volume suggesting that volumes of vestibules may be substantial (Ye *et al.* 2004, 2005). It is also known that *Chara* exhibits a reversible inhibition of AQP activity in response to elevated concentration (Kiyosawa & Tazawa 1972; Steudle & Tyerman 1983). The latter has been interpreted in terms of a cohesion/tension mechanism (Ye *et al.* 2004, 2005). Hence, high concentrations created on one side of the membrane could result in a channel closure. Experiments are underway to test the different hypotheses by varying both the size of osmolytes and its chemical nature (electrolytes *vs.* non-electrolytes; polar *vs.* non-polar). For these experiments, pressure probes have been modified in order to extend the range of water flow intensity and of its duration. The AQP activity of *Chara* did not change in response to considerable water flow densities, i.e., substantial inputs of kinetic energy into AQPs do not seem cause conformational changes of AQPs as found in other systems (Wan *et al.* 2004; Lee, Chung & Steudle 2005). Therefore, *Chara* should be a suitable object to test the idea of concentration polarization effects close to or within the vestibules of AQPs during extreme rates of J_V .

Different from L_{p_h} , the osmotic L_{p_o} depended on external stirring in accordance with the earlier findings of Steudle & Tyerman (1983). This has been referred to the existence of external USLs. For low v_{med} and nearly stagnant conditions, the effect was rather big, and L_{p_o} small. However, it would be premature to assume that, in this case, it was just the diffusion of solute from bulk solution to the membrane surface across an extended external USL which was rate limiting. As already mentioned in the Results, there are two other factors, which should be even more important at low flow rates. One is the fact that, during a slow exchange of solution, there will be no ‘instantaneous’ replacement of solution around the internodes. At low rates of stirring and relatively long lengths of internodes, complete exchange of solution will require up to 5 s (see MM section), which is longer than $T_{1/2}^w$. The other factor is the fact that the L_p of *Chara* decreases with increasing external concentration, which may also happen with a certain delay and proceed as solution is exchanged along the cell. Hence, at low flow rates, values of low osmotic L_{p_o} cannot be directly referred to increases in the thickness of external USLs.

The fact that L_{p_h} and L_{p_o} were close at high rates of stirring, enabled Steudle & Tyerman (1983) to estimate the thickness of external USLs (as measured in a set-up similar to the present and at high stirring) to be less than 50 μm . The present data support this view, that due to vigorous stirring, external layer thickness was minimized. This view was strongly supported by the experiments in which air bubbles were introduced into the system at high frequency that efficiently swept away solution from around the cylindrical cells except for a thin boundary layer at their surface. This vigorous external stirring did not furthermore increase L_{p_o} . Overall, the results show that the conclusions of Tyree *et al.* (2005) about the stirring and in earlier experiments with the probe are premature. Because of possible complications by external USLs and by the effect of elevated concentration, the L_p of *Chara* was usually measured in the past hydrostatically such as in the paper by Henzler *et al.* (2004). Tyree *et al.* (2005) ignored this important point.

(B) Rebuttal to Tyree *et al.* (2005)

Tyree *et al.* (2005) stressed that hydrostatic relaxations could not entirely be described by a single exponential and were bending off at their very ends in semi-log plots. They criticized the ‘usual procedure’ of Steudle & Tyerman (1983) and others for not analyzing this part and just cutting it off. However, Tyree *et al.* (2005) overlooked that the reason for the cut off is that in a range where measured pressure differences ($P(t) - P_e$) get close to the sensitivity of the pressure measurement. Hence, errors in the differences are quite big in these ranges. Systematic errors may be produced which may result in either a bending upwards and downwards of semi-log plots. In the pressure probe literature, the point has been stressed several times (e.g., Steudle & Tyerman 1983; Henzler & Steudle 2000). The literature also provides the reason for the cut off. It is touching to realize that Tyree *et al.* (2005), rather than accepting the physical limit of the resolution of the probe, think that the output from the transducer given as accurate as 0.1 kPa (0.0001 MPa) can be taken as the resolution of the pressure measurement. As a consequence, curves were bending for Tyree *et al.* (2005) as $P(t)$ approached P_e . The authors interpreted their artifact as an effect of a ‘membrane movement’ which is strange.

Tyree *et al.* (2005) claim that during the osmotic experiments of Henzler *et al.* (2004), stirring was not sufficient. They think that the flow of solution around the internodes fixed in a glass tube of an inner diameter of 3 mm was not turbulent and stirring not vigorous. On p. 3, para 4, of their paper, Tyree *et al.* (2005) state that the flow in the tube was laminar at all rates used. Hence, there should have been USLs of substantial thickness. The claims of Tyree *et al.* (2005) have no physical basis. In the experiments of Henzler *et al.* (2004) and of others, cylindrical *Chara* internodes (lengths of 40 to 150 mm; thickness of around 1 mm) were centered in a tube of an inner diameter of 3 mm and of a length of 250 mm and fixed at one end in a slid (see, for example, Fig. 1 of Hertel & Steudle 1997). From the other end of the tube, solutions were applied *via* a tube across a stopcock which reduced the speed from a few $\text{m}\cdot\text{s}^{-1}$ to a speed that would be tolerated during the experiments without causing leakages of the cell due to an intense trembling of the internode (Ye & Steudle 2005). There was also a constriction (teflon tube of an inner diameter of 2 mm that was fitted into the entrance of the glass

tube over a length of 80 mm). Flow was turbulent at the entrance because of the stopcock, and it was furthermore stirred when it left the constriction to reach the internode after a passage of 70 to 130 mm. According to basic fluid dynamics, this path is not sufficient to make the turbulent flow laminar. This length (l_e) would be (see textbooks of fluid dynamics, e.g., White 1999):

$$l_e = 0.06 \times \text{Re} \cdot d . \quad (18)$$

Here, d is the diameter of the tube and Re the Reynolds number, which is around 750 for a cylindrical pipe having a $d = 3$ mm (viscosity of water $\eta = 1.002 \times 10^{-3}$ Pa·s at 20 °C and flow rate of $0.25 \text{ m}\cdot\text{s}^{-1}$). Hence, we may estimate a distance of $l_e = 135$ mm for a laminar flow to develop which was not available. Even if basic fluid dynamics would not apply for Tyree *et al.* (2005) and there were a laminar Poiseuillian flow profile arriving at the internode, the existence of the latter would tend to disturb the parabolic flow pattern making it turbulent again. After a sufficiently long distance along the annulus of solution around the *Chara* internode, flow would tend to become laminar again. The maximum flow rate should establish close to the center of the annulus, whereby the velocity profile should be that of a parabola wrapped around the *Chara* like a doughnut. However, this will not happen over distances of as short as 40 to 150 mm, and flow should remain turbulent. The question is just how thick the remaining laminar boundary layer adjacent to the cell is, which is not affected by turbulence. This question is difficult to address theoretically. Therefore, we used two different approaches to test it, i.e., we varied v_{med} and we flushed air bubbles around the cell at high frequency, which displaced most of the solution tending to even enhance the vigorous stirring (see video). The result of both procedures was that we could not further reduce thicknesses of USLs, which adhered as thin films close to the cell surface. Hence, we may conservatively estimate the thickness of external USLs to be around 30 μm (including the cell wall) at sufficient rates of stirring. The value of Tyree *et al.* (2005) of 100 μm in the experiments of Henzler *et al.* (2004) clearly overestimated δ^o . It would have been adequate for Tyree *et al.* (2005) to provide some own data and experience on the subject prior to judging about the experiments of Henzler *et al.* (2004).

On p. 3 (left column), para 3, and on p. 4 (left column), para 5, of Tyree *et al.* (2005), state that in their simulations, the system of two USLs and a membrane soon assumed

conditions of steady state, where the Steudle/Tyerman theory applied (which they seem to accept; Eqn 15). According to Tyree *et al* (2005), this happened at times of substantially smaller than the time required to reach the extrema of pressure during biphasic responses (around 10 s for acetone). The finding is not new. Tyerman & Steudle (1984) used a turgor-minimum technique to analyze the $k_s (P_s)$ obtained around the maxima (minima) for different solutes. The result was that the $k_s (P_s)$ measured around the minimum was similar to that obtained from solute phases. Because the solute flow is buried within the water phase at time periods of close to zero, it is not possible to use the pressure probe to directly measure $k_s (P_s)$ at times close to zero. However, there are P_s values from isotopic measurements where P_s was worked out from the initial uptake for some of the solutes studied (Dainty & Ginzburg 1964b). These data are rather free of USLs and agree with those measured with the pressure probe. We do agree with Tyree *et al.* (2005) that the system very soon becomes steady with constant thicknesses of USLs. However, this just indicates that USLs developed fast and that their thickness should have been relatively small.

Tyree *et al.* (2005) did not realize that their simulations contained the solvent drag which was neglected in the Steudle/Tyerman theory (1983). In simulations of biphasic responses, Rüdinger, Hierling & Steudle (1992) showed that the solvent drag had no significant effect on the shape of curves. From their simulations, these latter authors concluded that Eqn 15 could be used to describe the entire course of $P(t)$ during biphasic pressure relaxations. In principal, there could be another type of interaction between solutes and water which was not considered by Rüdinger *et al.* (1992) and is not incorporated in Eqn 15. This is active solute (ion) transport which may change during osmotic treatments. However, this effect should be quite small for *Chara*, but should be considered during biphasic responses of roots measured with the root pressure probe, as shown in the simulations of Steudle & Brinckmann (1989).

Unlike osmotic Lp_o , values of both P_s and σ_s were only slightly smaller at low flow rates and tended to saturate earlier. This is expected because of the longer half-times of solute exchange which would reduce effects of external USLs. Assuming an external USL of a thickness of $\approx 30 \mu\text{m}$, a half time of 0.2 s would be required for the filling of this layer with solute (acetone; $D_s = 1.2 \times 10^{-9} \text{ m}^2 \cdot \text{s}^{-1}$; Jost 1960; Ye & Steudle 2005).

This can be neglected at values of $T_{1/2}^s \geq 30$ s (Ye & Steudle 2005). Nevertheless, effects of USLs on permeability coefficient (P_s) and reflection coefficient (σ_s) were very much dependent on the property of solutes. USLs could more likely act as rate-limiting diffusion barriers for rapidly than for slowly permeating solutes (Barry & Diamond 1984). This was found in the present paper. Three different solutes were used with a sequence of the P_s as $P_{s(\text{acetone})} > P_{s(2\text{-propanol})} > P_{s(\text{DMF})}$. A tendency sequence of USLs effects on P_s and σ_s was (acetone) > (2-propanol) > (DMF).

Tyree *et al.* (2005) argue that values of P_s and σ_s of acetone measured with a CPP were considerably underestimated. Assuming external and internal USLs of as large as 100 μm and 350 μm , respectively, they arrived at the conclusion that true values of P_s and σ_s of acetone of Henzler *et al.* (2004) could have been underestimated by a factor of as large as five (see p. 4, right column of Tyree *et al.* 2005). This meant that USLs instead of the cell membrane represent the rate-limiting resistance of acetone permeation through *Chara* internodes. The argument of Tyree *et al.* (2005) fails. They assumed steady state diffusion during most of the biphasic responses measured with the pressure probe. Hence, there will be a series arrangement of permeation resistances (2 USLs plus membrane) according to Eqn 7 of the Theory section. Since this is true and agrees with Tyree *et al.* (2005), Eqn 5 may be used to evaluate maximum thicknesses of USLs, when $1/P_s$ can be neglected as compared to the diffusional resistances, i.e. when $P_s \rightarrow \infty$. In the example used in Table 1 of Tyree *et al.* (2005) ($P_s^{meas} = 4.2 \times 10^{-6} \text{ m}\cdot\text{s}^{-1}$; $D_s = 1.2 \times 10^{-9} \text{ m}^2\cdot\text{s}^{-1}$; $R = 0.40 \text{ mm}$), one gets a limiting ratio of b/a of 2.1 from Eqn 5. For 6 out of 9 combinations of the table the b/a ratio was bigger indicating a negative P_s , which is not possible. Hence, there is either something wrong with the values given in Table 1 of Tyree *et al.* (2005) or the table does not refer to steady state as does the rest of their paper.

The conclusions of Tyree *et al.* (2005) are contradictive in view of the comparison between free unsteady state diffusion into a cylinder and the values measured with the probe (Fig. 8). If Tyree *et al.* (2005) were right, the uptake kinetics measured with the probe should be similar to the type of kinetics obtained in the absence of a membrane

which shows two distinct phases. However, this was not observed in the experiments. No building up of an internal USL was observed. When uptake curves were extrapolated back to $t = 0$ in the semi-log plots of Fig.8, their intercepts with the ordinate were close to zero. Hence, these layers should have had a rather small impact on the measurement of transport coefficients.

According to Tyree *et al.* (2005), changes in membrane properties such as the closure of AQPs should have had little if any effect on the P_s^{meas} of rapidly permeating solutes such as acetone ($P_s = 4.2 \times 10^{-6} \text{ m}\cdot\text{s}^{-1}$) or HDO ($P_d = 7.0 \times 10^{-6} \text{ m}\cdot\text{s}^{-1}$) as demonstrated by Henzler *et al.* (2004). This is so because membrane treatment should not affect USLs. However, this was not the case in the experiments of Henzler *et al.* (2004) and others. For example, when using hydroxyl radicals (*OH) to inhibit AQP activity, there was a substantial decrease of the P_d of HDO by a factor of 3 and of the P_s of acetone (in part, also using AQPs to cross the membrane) by a factor of 2. When Tyree *et al.* (2005) were right and USLs had permeation resistances of larger by a factor of five than those of membranes, this would result in a decline of the real membrane P_s (P_d) by factors of 6 and 11 for acetone and HDO, respectively. This would mean that there were a tremendous permeability of acetone across water channels. Absolute values are unlikely to be true in view of other findings of changes in P_s and P_d upon channel closure (Henzler & Steudle 1995; Mathai *et al.* 1996). Similarly, the re-examination of reflection coefficients (negative for acetone upon channel closure) would result in extreme values. Tyree *et al.* (2005) avoid to discuss these consequences although the effects of a closure of AQPs on permeability and reflection coefficients are dealt with in the paper of Henzler *et al.* (2004).

Tyree *et al.* (2005) claim that they obtained the estimated thicknesses of USLs of up to 350 μm (Henzler *et al.* 2004; see also Henzler & Steudle 2000). This is a misquote. Henzler *et al.* (2004) discuss the possibility that internal USLs of the solute HDO may, in principle, be as large as the radius of the cells, which sets a geometric upper limit (see Introduction). However, they conclude that the idea that USLs extend across the entire cell has to be rejected for different reasons. The most important, perhaps, is that a rate-limitation by internal USL could not explain that the experiments clearly showed a rate

limitation by membrane transport (see Discussion on p. 333 of Hertel *et al.* 1997). Henzler & Steudle (2000) conclude that, ‘although there may be some influence of internal USLs, on the absolute values of the P_s and σ_s of H_2O_2 ($D_s = 1.3 \times 10^{-9} \text{ m}^2 \cdot \text{s}^{-1}$), membrane permeation and the subsequent degradation of the substrate in the cell should have dominated the process measured’. For the rapidly permeating solute HDO, Ye *et al.* (2005) estimate the contribution of internal USLs in P_d as 25 %. The earlier statements about the thickness of internal USLs have been overlooked by Tyree *et al.* (2005).

In the present paper, we show that, under conditions of vigorous external stirring, external USL may have a thickness of 30 μm , at maximum (including the reduction of D_s in wall pores and the tortuosity during the passage of solutes within wall pores). The contribution of internal USLs was estimated by the data presented in Fig. 8 (see last para of Results). According to these data, the overall measured permeability of a *Chara* cell for acetone was equivalent to a thickness of an internal USL of 204 μm . In the presence of the membrane plus an internal USL, the thickness of the latter was reduced to 97 μm (at maximum), which was equivalent to 40 % of the entire permeation resistance. It should be noted this estimation refers to a completely stagnant and homogenous internal compartment. However, this was not the case. There is some internal mixing by cytoplasmic streaming and by the shaking of the cell during the experiments (see discussion in Stevenson *et al.* 1975). Hence, the underestimation by 40 % has to be taken as an upper limit. Preliminary results in which the concentration of solute right at the surface of the inner side of the plasma membrane was followed during permeation experiments, indicated an actual underestimation of around 20 % for acetone and of around 2 % for DMF, which may turn out to be more realistic (Ye, Kim & Steudle, unpublished results). Hence, we may end up with an internal USL of a thickness of around 50 μm . It has to be stressed that the effects of USLs which have been worked out here for acetone should be similar to those for HDO. Permeability of this solute is bigger by a factor of two than that of acetone, but this should be compensated for by a bigger diffusion coefficient ($D_s = 2.4 \times 10^{-9} \text{ m}^2 \cdot \text{s}^{-1}$; Reid & Sherwood 1966). Values of the diffusional permeability of isotopic water have been often compared with those of the bulk permeability ($P_f \propto L_p$) to work out the internal

size of aquaporins (see Introduction; Ye *et al.* 2005). In an analysis similar to the present study, Sehy *et al.* (2002) provide evidence that the contribution of internal mixing by diffusion to the overall rate of uptake of HDO by spherical oocytes of *Xenopus laevis* (R = 0.6 mm) was 30 % (39 % were actually reported in the paper for the ratio of P_s^{memb} / P_s^{meas} , i.e., $2.7 \times 10^{-6} \text{ m}\cdot\text{s}^{-1} / 1.9 \times 10^{-6} \text{ m}\cdot\text{s}^{-1} = 1.39$). This percentage is smaller than that given here for acetone in *Chara*. However, the oocytes used by Sehy *et al.* (2002) had a spherical geometry so that the contribution of internal mixing should have been smaller at the same radius. Stevenson *et al.* (1975) used cylindrical tubes of collagen and cellulose acetate (as used during the purification of blood in kidney machines; R = 0.14 to 0.35 mm) to work out the contribution of unsteady experimental condition to the overall permeability. Using Eqn 11, they worked out a membrane permeabilities of urea of around $P_s^{meas} = 6.0 \times 10^{-6} \text{ m}\cdot\text{s}^{-1}$ from isotopic experiments. They then compared these values of P_s^{memb} , which they calculated from empirical relation between P_s^{meas} and P_s^{memb} . When the external solution was vigorously stirred, the difference was found to be between 10 and 15 % for urea for both types of tubular membranes. Considering the smaller diameter of the tubes used by Stevenson *et al.* (1975), this is similar to the result obtained here for acetone. Stevenson *et al.* (1975) concluded that unsteady experimental conditions do not significantly affect the measurement of membrane permeability.

In conclusion, the re-examination of the role of USLs during pressure probe experiments with isolated internodes of *Chara* showed that effects of internal and external USLs do not play a significant role when hydrostatic pressure pulses are applied to induce monophasic pressure relaxations. Careful consideration of the limitations of the pressure probe to resolve relaxations indicated that the claim of Tyree *et al.* (2005) of an additional phase in relaxations is due to an artifact. Tyree *et al.* (2005) overlooked limitations in the resolution of the probe. During hydrostatically driven water flow, an effect of high flow rates was only observed in the present paper during pressure clamp when using substantial step changes in turgor pressure. Effects could not completely be explained by conventional sweep away where the water flow density is evenly distributed within the cell membrane, but may be due to a sweep away

in the presence of a considerable constriction of water flow through AQPs including a concentration polarization of solutes within the vestibules of AQPs. A rigorous examination of the stirring of the solution surrounding the internodes during osmotic experiments indicated that external USLs had a small thickness of less than 30 μm . The conclusions drawn by Tyree *et al.* (2005) that, in standard pressure probe experiments, water flow around the internodes is laminar, lacks a physical basis. The earlier conclusion that flow is turbulent and the medium vigorously stirred was strongly supported by experiments in which air bubbles were flushed through the tubes containing *Chara* internodes. The additional stirring caused complete replacements of solution around the cells which did not result in a further increase of measured transport coefficient in osmotic experiments. By applying unsteady-state diffusion kinetics, upper limits of equivalent thicknesses of internal USLs were provided for cylindrical compartments lacking or containing a membrane. These were 117 or 97 μm , respectively (for acetone; $R = 0.40$ mm). This is smaller than the maximum figure of 350 μm erroneously assumed by Tyree *et al.* (2005). The real equivalent thickness of USLs was estimated to be smaller by at least a factor of 2 to 3 than the upper limits. This in turn would provide an upper limit of around 50 μm for the most rapidly permeating solutes (acetone, HDO). It should be smaller for other solutes having a more favourable ratio of D_s/P_s (e.g., monohydric alcohols, H_2O_2 , or DMF). The quantitative estimates are in line with earlier findings, which showed that closure of water channels massively affected overall L_p , P_s , and σ_s . These results are hard to explain in the presence of a dominating effect of USLs.

Acknowledgements

We thank Prof. Jack Dainty for discussing the manuscript and Burkhard Stumpf (Department of Plant Ecology, University of Bayreuth) for his expert technical assistance. YMK thanks for a research grant for doctoral candidates and young academics and scientists from the Deutscher Akademischer Austauschdienst (DAAD).

References

- Barry P.H. & Diamond J.M. (1984) Effects of unstirred layers on membrane phenomena. *Physiological reviews* 64, 763–872.
- Crank J. (1975) The mathematics of diffusion (second edition of the original 1956 print). University Press Oxford, UK.
- Dainty J. & Ginzburg B.Z. (1964a) The measurement of hydraulic conductivity (osmotic permeability to water) of internodal characean cells by means of transcellular osmosis. *Biochimica et Biophysica Acta* 79, 102–111.
- Dainty J. & Ginzburg B.Z. (1964b) The permeability of the protoplast of *Chara australis* and *Nitella translucens* to methanol, ethanol and iso-propanol. *Biochimica et Biophysica Acta* 79, 122–128.
- Dainty J. (1963) Water relations of plant cells. *Advances in Botanical Research* 1, 279–326.
- Finkelstein A. (1987) Water movement through lipid bilayers, pores and plasma membranes. Theory and reality. Distinguished lecture series of the Society of General Physiologists, vol. 4. Wiley, New York.
- Henzler T. & Steudle E. (1995) Reversible closing of water channels in *Chara* internodes provides evidence for a composite transport model of the plasma membrane. *Journal of Experimental Botany* 46, 199–209.
- Henzler T. & Steudle E. (2000) Transport and metabolic degradation of hydrogen peroxide: model calculations and measurements with the pressure probe suggest transport of H₂O₂ across water channels. *Journal of Experimental Botany* 51, 2053–2066.
- Henzler T., Ye Q. & Steudle E. (2004) Oxidative gating of water channels (aquaporins) in *Chara* by hydroxyl radicals. *Plant Cell and Environment* 27, 1184–1195.
- Hertel A. & Steudle E. (1997) The function of water channels in *Chara*: the temperature dependence of water and solute flows provides evidence for composite membrane transport and for a slippage of small organic solutes across water channels. *Planta* 202, 324–335.

- Jost W. (1960) Diffusion in solids, liquids, gases. In *Physical Chemistry a series of monographs* (eds E. Hutchinson & van P. Rysselberghe), Academic Press, New York, USA.
- Kiyosawa K. & Tazawa M. (1972) Influence of intracellular and extracellular tonicities on water permeability in characean cells. *Protoplasma* 74, 257–270.
- Kiyosawa K. & Tazawa M. (1977) Hydraulic conductivity of tonoplast free *Chara* cells. *Journal of Membrane Biology* 37, 157–166.
- Lee S.H., Chung G.C. & Steudle E. (2005) Low temperature and mechanical stresses differently gate aquaporins of root cortical cells of chilling-sensitive cucumber and chilling-resistant figleaf gourd. *Plant Cell and Environment* 28, 1191–1202.
- Mathai J.C., Mori S., Smith B.L., Preston G.M., Mohandas N., Collins M., van Zijl P.C., Zeidel M.L. & Agre P. (1996) Functional analysis of aquaporin-1 deficient red cells. The Colton-null phenotype. *Journal of Biological Chemistry* 271, 1309–1313.
- Maurel C., Tacnet F., Güclü J., Guern J. & Ripoche P. (1997) Purified vesicles of tobacco cell vacuolar and plasma membranes exhibit dramatically different water permeability and water channel activity. *Proceedings of the National Academy of Sciences USA* 94, 7103–7108
- Niemietz C.M. & Tyerman S.D. (1997) Characterization of water channels in wheat root membrane vesicles. *Plant Physiology* 115, 561–567.
- Poling B.E., Prausnitz J.M. & O'Connell J.P. (2001) *The properties of gases and liquids* (fourth edition). McGraw-Hill, New York, USA.
- Reid R.C. & Sherwood T.K. (1966) *The properties of gases and liquids*. McGraw-Hill, New York, USA.
- Rüdinger M., Hierling P. & Steudle E. (1992) Osmotic biosensors. How to use a characean internode for measuring the alcohol content of beer. *Botanica Acta* 105, 3–12.
- Sehy J.V., Banks A.A., Ackerman J.J.H. & Neil J.J. (2002) Importance of intracellular water apparent diffusion to the measurement of membrane permeability. *Biophysical Journal* 83, 2856–2863.
- Steudle E. & Brinckmann E. (1989) The osmometer model of the root: water and solute relations of *Phaseolus coccineus*. *Botanica Acta* 102, 85–95.

- Steudle E. & Frensch J. (1989) Osmotic responses of maize roots. Water and solute relations. *Planta* 177, 281–295.
- Steudle E. & Tyerman S.D. (1983) Determination of permeability coefficients, reflection coefficients and hydraulic conductivity of *Chara corallina* using the pressure probe: effects of solute concentrations. *Journal of Membrane Biology* 75, 85–96.
- Steudle E. & Zimmermann U. (1974) Determination of the hydraulic conductivity and of reflection coefficients in *Nitella flexilis* by means of direct cell-turgor pressure measurements. *Biochimica et Biophysica Acta* 322, 399–412.
- Steudle E. (1993) Pressure probe techniques: basic principles and application to studies of water and solute relations at the cell, tissue, and organ level. In *Water Deficits: Plant Responses from Cell to Community* (eds J.A.C. Smith & H. Griffith), pp. 5–36. BIOS. Scientific Publishers, Oxford, UK.
- Steudle E., Smith J.A.C. & Lüttge U. (1980) Water relation parameters of individual mesophyll cells of the crassulacean acid metabolism plant *Kalanchoe daigremontiana*. *Plant Physiology* 66, 1155–1163.
- Stevenson J.F. (1974) Unsteady mass transfer in a long composite cylinder with interfacial resistances. *AIChE Journal* 20, 461–466.
- Stevenson J.F., Von Deak M.A., Weinberg M. & Schuette R.W. (1975) An unsteady state method for measuring the permeability of small tubular membranes. *AIChE Journal* 21, 1192–1199.
- Tyerman S.D. & Steudle E. (1984) Determination of solute permeability in *Chara* internodes by a turgor minimum method. Effect of external pH. *Plant Physiology* 74, 464–468.
- Tyree M.T., Koh S. & Sands P. (2005) The determination of membrane transport parameters with the cell pressure probe: theory suggests that unstirred layers have significant impact. *Plant Cell and Environment* 28, (in press). doi: 10.1111/j.1365-3040.2005.01384.x
- Walz T., Smith B.L., Zeidel M.L., Engel A. & Agre P. (1994) Biologically active two-dimensional crystals of aquaporin CHIP. *Journal of Biological Chemistry* 269, 1583–1586.

- Wan X.C., Steudle E. & Hartung W. (2004) Gating of water channels (aquaporins) in cortical cells of young corn roots by mechanical stimuli (pressure pulses): effects of ABA and of HgCl₂. *Journal of Experimental Botany* 55, 411–422.
- White F.M. (1999) Fluid mechanics (fourth edition). McGraw-Hill, Boston, USA.
- Ye Q. & Steudle E. (2005) Oxidative gating of water channels (aquaporins) in corn roots. *Plant Cell and Environment* 28, (in press) doi: 10.1111/j.1365-3040.2005.01423.
- Ye Q., Muhr J. & Steudle E. (2005) A cohesion/tension model for the gating of aquaporins allows estimation of water channel pore volumes in *Chara*. *Plant Cell and Environment* 28, 525–535.
- Ye Q., Wiera B. & Steudle E. (2004) A cohesion/tension mechanism explains the gating of water channels (aquaporins) in *Chara* internodes by high concentration. *Journal of Experimental Botany* 55, 449–461.

7 Advances in the Studies on Water Uptake by Plant Roots

Chang-Xing Zhao¹, Xi-Ping Deng^{1*}, Sui-Qi Zhang¹, Qing Ye²,
Ernst Steudle² & Lun Shan¹

1. State Key Laboratory of Soil Erosion and Dryland Farming on Loess Plateau, Institute of Soil and Water Conservation, Chinese Academy of Sciences and Ministry of Water Resource, Yangling Shaanxi, 712100, China
2. Department of Plant Ecology, Bayreuth University, D-95440 Bayreuth, Germany

Received 22 October 2003; accepted for publication 9 January 2004

Correspondence: Xi-Ping Deng. E-mail: dengxp@ms.iswc.ac.cn

Acta Botanica Sinica (2004) 46: 505-514

Abstract

In the past decade, our understanding of the mechanisms of water uptake by plant roots at the cell, tissue, and whole-plant levels rapidly progressed due to the introduction of new techniques and concepts. Some aspects of this work are reviewed, mainly including the composite structure of roots and effects of the distribution of roots in the soil. The nature of water flow in plant roots is discussed. A link is provided between root hydraulics and the expression and function of aquaporins. This relates to the regulation of water transport and to the signalling between roots and shoots. The composite transport model of root is mentioned which represents a physical model of water uptake. This is part of a comprehensive analysis of recent findings of studies on water uptake by plant roots and contributes to our current understanding of the basic mechanisms that govern the water uptake by roots.

Key words: aquaporins; water uptake; root anatomy; water channel; composite transport model; soil-plant-atmosphere continuum.

Introduction

Water uptake by plant roots is controlled or is even regulated by different physical and physiological processes. Water supplied to plants by its roots has a major influence on the shoot water status, and, in turn, on plant growth and development. Water moves from the surface of a root to the root xylem through a series of tissues. Each of these tissues represents a hydraulic conductance that changes during root development and in response to environmental factors (Steudle, 1994; 2000; 2001). In different root habitats, root anatomy has to adapt to specific physical and water constraints. Water transport properties of roots are adjusted to the physiological demand of the whole plant (Javot and Maurel, 2002). In recent years, our understanding of water uptake by and transport within plant roots has been substantially improved by new tools, which operate at the molecular, cell, tissue, organ, plant, and ecosystem levels. Techniques such as cell and root pressure probes, stopped flow, the use of transgenic plants, and of

stable isotopes provided a fast progress in water transport research (Steudle, 1993; 2001; Kramer and Boyer, 1995; Maurel, 1997; Steudle and Peterson, 1998; Tyerman et al., 1999; 2002;). A better understanding of the mechanisms of water uptake by plant roots should be vital for improving water use efficiency (WUE) in agriculture. The present article reviews the progress in recent years for people who want to update their understanding of basic mechanisms of root hydraulics and plant water relations.

Distribution of root systems in soil

The spatial distribution of roots in soil determines the ability of plants to take up soil water and nutrients in order to sustain plant growth and development. A large number of studies confirm that deeper root systems enable plants to access water not available to shallow rooted plants, and to balance rather high rates of transpiration during periods of water deficit (Zhu et al., 2002). Usually, plants in drier environment develop deeper root systems. A survey of global patterns of root distribution and depth was given by Jackson et al. (1996) and Canadell et al. (1996). On a global average, desert vegetation reaches a maximum root depth of 13.4 m, with 31% of the total root biomass below 0.3 m soil depth, Temperate forests have a maximum rooting depth of 3.7 m, with 35% of the root biomass below the 0.3 m soil depth. The root systems of temperate grassland reach a maximum depth of only 2.4 m, and root biomass accounts for 17% of the total. Differences in rooting depths and ability of plants to extract soil water are likely to influence survival and productivity in the natural or artificial ecosystem. However, large varieties of root distribution in soil profile prevented the establishment of any definitive model for crops, irrespective of the soil environment (Liedgens and Richer, 2001). The effects of many parameters such as root growth rate, soil water, fertilizer, soil compaction, and root system structure are not yet well defined. For example, root extension characteristics are significantly inhibited by soil compaction and limited by the distribution of water. Soil compaction affects plant growth in many ways. Roots do not develop well or penetrate well in compacted soil. Often, shallow root systems and malformed (tight, small etc.) roots are symptoms of compacted soil. Plants are generally stunted, and moisture and nutrient stresses may occur. However, under certain

conditions soil compaction may contribute to root water uptake and improve WUE in dry land farming (Liu et al., 2001). Usually, drought tolerant crops have deep explorative root systems (Counor and Sadras, 1992). Many researchers think that better adaptability of cultivars to dry growing conditions was attributed to deeper rooting. Deng et al. (2003) think that improving root growth to use deeper soil water may promote the efficiency of the use of water supplied to plants in the field. However, during the development of wheat, root growth had an adverse effect on water use efficiency (Zhang et al., 2002). The latter authors think that the increase of the ability of roots to take up water may compensate for the decrease in the size of root systems. The general principle of relating the distribution of root systems to water uptake patterns may hold. However, there are not many studies which actually confirm or disprove it. The reason for this is that there is, for technical reasons, not much data which show the true distribution of roots in soil. In the future, the situation may be improved by the use of ingenious methods or advanced instruments such as underground reflecting technology and root tracker (automatic detecting implement of root growth) (Zhang et al., 1997).

Effects of root anatomy/morphology on water uptake

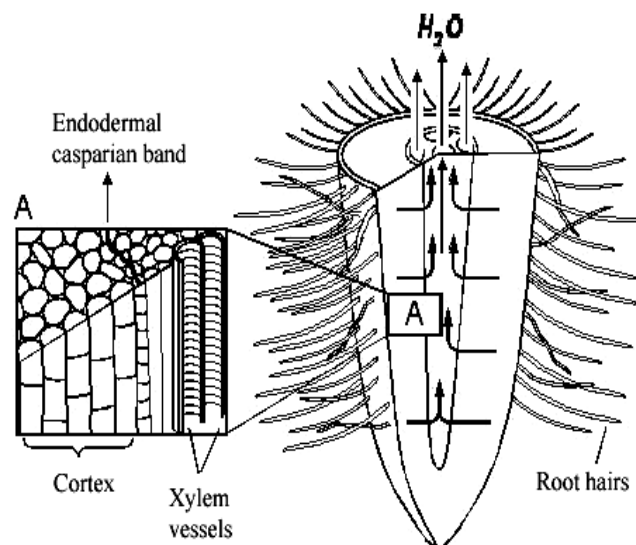


Fig. 1 Radial and axial water flow across a young root. Usually, the radial rather than the axial hydraulic resistance limits water flow (for further explanation, see text).

Single root functioning during water uptake is based on root structure and anatomy. There is no way to understand root water uptake without knowing root structure and anatomy in sufficient detail. Most individual roots have a central vascular cylinder surrounded by the cortex which usually makes up the bulk of the root (Fig. 1). To pass from the soil solution into vascular tissues, water has to flow radially across a series of concentric cell layers. These layers include the epidermis, exodermis, several layers of cortex, endodermis, pericycle, xylem parenchyma cells and finally the vessel (Steudle and Peterson, 1998). The cell walls of exo- and endodermal cells have particular structures, Casparian bands, which mean effective barriers to water uptake as do suberin lamellae (Zimmermann and Steudle, 1998). It is generally accepted that endodermal Casparian bands represent tight apoplastic barriers to solutes and prevent their backflow from the stele (Tester and Leigh, 2001). Due to the hydrophobic properties of suberins, suberization substantially reduces the water permeability of roots, whereby the aliphatic rather than the aromatic suberin is more effective in making the apoplast impervious for water (Schreiber et al., 1999; Zimmermann et al., 2000; Hose et al., 2001). Suberization of roots increases with increasing plant age and during stress (drought, high salinity, etc). This decreases the root hydraulic conductivity (hydraulic conductance per unit root surface area in $\text{m}\cdot\text{s}^{-1}\cdot\text{MPa}^{-1}$, Steudle, 2000). Some researchers studied how changes in root structure caused by environmental stress are reflected into changes of root water-transport properties (Peyrano et al, 1997). For technical reasons, it is still difficult to quantify water uptake or hydraulic conductivity of different root zones (Frensch et al., 1996). Compared to shoots, much less is known about the ‘hydraulic architecture’ of roots (Steudle, 2000). Following the differentiation of cells and tissues along developing roots, profound changes in the hydraulic properties of both the axial and radial path have been observed (Melchior and Steudle, 1993). There are many differences among species, habitats and even individual root. The complexity of water transport across plant roots relates to the structural variability of roots during their growth and development. The relation between the function and structure/anatomy of roots should be further studied.

Pathways for water, driving forces, and hydraulic resistances of roots

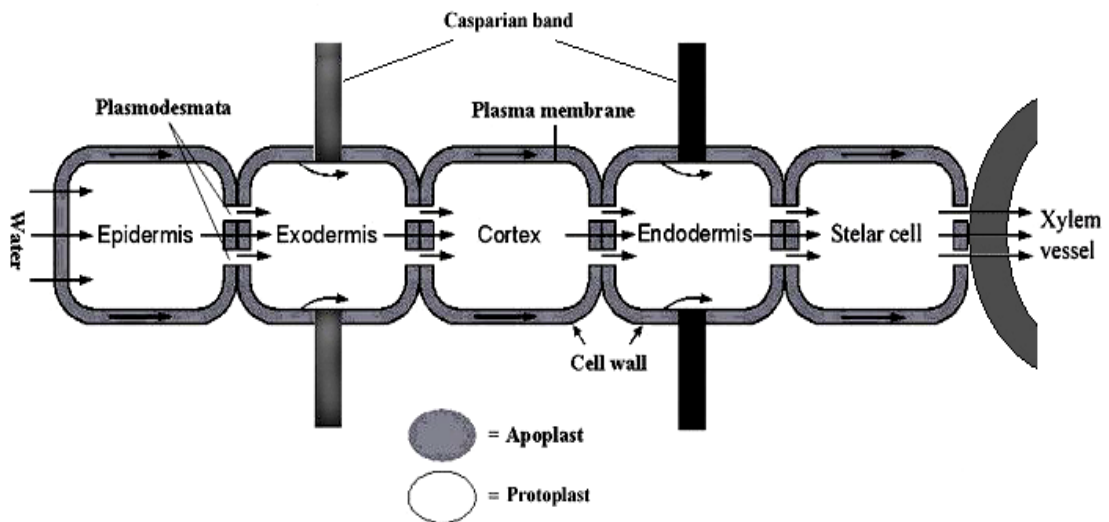


Fig. 2 Radial water flow across the root cylinder (schematic). For the sake of simplicity, the cortex and stellar tissue are indicated by just one cell. Across the protoplast, there are two parallel passages, i.e. the symplastic and apoplastic passage. They are usually summarized as a cell-to-cell component. The apoplastic component is more or less interrupted at apoplastic barriers such as the Casparian bands of exo- and endodermis.

Under natural conditions, water uptake by roots and loss from leaves are driven by variable forces. Nevertheless, plants keep a proper balance of water by continuously adjusting the water conductance of roots (Weatherley, 1982). There are three pathways of water transport which co-exist in living root tissue (Fig.2): apoplastic, symplastic and transcellular paths (Steudle, 1989). To date, the symplastic and transcellular components cannot be separated experimentally. Therefore, they are summarized as a cell-to-cell component. During the radial transport of water across the root cylinder, there could be combinations of the three pathways, which may make allowance for a rapid exchange of water between pathways (Steudle, 2000). Different pathways may dominate in response to changes of the physical nature of the forces that drive the water across roots (Steudle and Peterson, 1998). For technical reasons, the relative contribution of the different pathways to the overall water uptake has not yet been studied in sufficient detail. However, there are some quantitative data around from

comparative measurements of root hydraulics at the cell and root level (Steudle 1994; 2000; 2001; Steudle and Peterson, 1998).

Biophysical analyses have established that, in plant tissue, water moves passively along water potential gradients (Steudle, 1994; Schultz, 2001). When plants transpire, evaporation of water vapor from the stomatal cavity results in highly negative pressures (tensions) in xylem vessels, which draw water from the roots up into the aerial parts (Wei et al., 1999; Steudle, 2001; Tyree and Zimmermann, 2002). In the absence of transpiration, i.e., when stomata are closed during the night or during periods of water stress, residual water movement is driven by the active pumping of solutes (nutrient ions) into the root. This creates an osmotic driving force that results in a positive, hydrostatic root pressure. Root pressure pushes the sap up along the xylem (Javot and Maurel, 2002). Because of its lack of selectivity with respect to water and solutes, the apoplast can not maintain osmotic driving forces (Steudle, 1994). Water transport in the apoplast is essentially driven just by hydrostatic forces. External pressure can change root hydraulic conductance. For example, the root hydraulic conductivity measured at high pressure differences or water flows is usually remarkably larger (the hydraulic resistance smaller) than that measured at low pressure differences. The possible cause of the non-linear pressure/flow characteristics may be that the water content in intercellular spaces increases with increasing hydrostatic pressure difference between soil solution and root xylem, hence, increasing the apoplast water flow (Liu et al., 2002). Alternatively, water flow may change osmotic driving forces ('dilution model' of Fiscus) (Fiscus, 1975), or may affect the hydraulic conductivity of cell membranes (aquaporins). In the composite transport model of the root (see below), the effect is due to a switching of water flow between pathways.

In contrast to the apoplast, cell membranes allow to establish and maintain osmotic gradients along the cell-to-cell path. In addition to hydrostatic forces, these gradients will drive water flow (Steudle, 1994; Steudle and Peterson, 1998). In the past, the movement of water across cell membranes in roots has been often described as an osmotic process (Kramer and Boyer, 1995). Recent evidence, however, indicated that this view has to be modified (Steudle, 2000). This is so, because the hydraulic

conductivity of root should differ depending on specific conditions, namely, in the presence or absence of hydrostatic pressure.

Water transport from root to shoot involves both axial and radial hydraulic resistance in plants. Vascular plants have evolved two types of highly modified cells, tracheids and vessel members, strands of which provide an axial pathway with an exceedingly low resistance to water flow. The importance of the removal of the protoplasts for reduction of the axial resistance to water flow can be demonstrated both theoretically and experimentally (Steudle and Peterson, 1998). According to Poiseuille's law, axial resistances can be worked out. They can be measured as well (Steudle, 2001; Tyree and Zimmermann, 2002). Many researches indicated that effects of vessel maturation on the axial resistance were enormous (Steudle and Peterson, 1998). Usually, axial resistances of roots are much smaller than radial. However, this may change at high rates of transpiration which may cause cavitations (embolism) of water in vessels. Cavitations interrupt water flow and reduce axial hydraulic conductivity of roots substantially (Peterson et al., 1993; Holbrook et al., 1999).

In roots with mature vessels, it is the radial rather than the axial resistance which limits water uptake (see above). For the early metaxylem of young maize root, axial resistance is smaller by 1-2 orders of magnitude than that for the radial flow (Steudle and Peterson, 1998). Overall, radial resistances result from a series of smaller resistances in plant roots. Experimental results obtained with young roots of maize, indicated that, the major resistance to water flow was evenly spread over the living tissues of the root, which is in contrast to the usual concept that in roots the major resistance to water flow is in the endodermis. However, the situation may change during later development of roots and in different species (Miyamoto et al., 2001). To date, there are only a few results of hydraulic properties of individual parts in roots to water uptake (such as in rice: Ranathunge et al., 2003). Novel methods are required to quantify the specific effects of different root tissue such as the role of the exo- and endodermis (North and Nobel, 1996; Zimmermann and Steudle, 1998; Zimmermann et al., 2000; Miyamoto et al., 2001; Ranathunge et al., 2003). Changes in the hydraulic resistance at the tissue level

may be derived from the propagation of changes in water potential across the root cylinder, and during root growth and development (Westgate and Steudle, 1985).

Water balance and movement in plants is driven by gradients in water potential. Catenary models have been proposed for the movement of water between soil and atmosphere in analogy to the flow of electricity in electric circuits (soil-plant-air-continuum, SPAC: van den Honert, 1948). At steady water flow across a plant, we have in analogy to basic laws of electricity (Ohm's law):

$$\begin{aligned} \text{water flow} &= (\Psi_{\text{soil}} - \Psi_{\text{root surface}}) / R_{\text{soil}} \\ &= (\Psi_{\text{root surface}} - \Psi_{\text{xylem}}) / R_{\text{root}} \\ &= (\psi_{\text{xylem}}^{\text{root}} - \psi_{\text{xylem}}^{\text{leaf}}) / R_{\text{xylem}} \\ &= (\Psi_{\text{leaf}} - \Psi_{\text{air}}) / R_{\text{leaf}}. \end{aligned}$$

Water flow = total water potential gradient / total resistance (Tyree, 1997; Steudle and Peterson, 1998). In the root cylinder, water potential will drop along the different tissues which are arranged in series (epidermis, exodermis, cortex, etc). The analogy with electrical circuits holds both on the 'microscopic scale' (e.g., when comparing pathways for water across cells within tissue), and at a macroscopic level (e.g., when comparing different zones along roots: Steudle and Peterson, 1998).

Water transport at the level of root membranes

The flow of water in and out of plant cells is largely regulated by water channels or aquaporins sitting in plasma membranes (Fig. 3). Plant water relations and water flow in plant tissues have been well characterized, but the presence of aquaporins not established until the early 1990s. The first aquaporin was identified in human erythrocytes in Peter Agre's lab who received the Nobel Prize for the "discovery of water channels" earlier this year (Preston et al., 1992; Zeidel et al., 1992; Walz et al., 1994). Aquaporins (water channel proteins) are major intrinsic proteins (MIPs) of a molar weight of around 30 kDa (Maurel and Chrispeels, 1994; Maurel, 1997; Murata et

al., 2000). They are found in vacuolar and plasma membranes of plants. Aquaporins facilitate the transport of water across cell membranes (Fig. 3), and 75%-95% of the water permeation of plasma membranes is due to aquaporin activity (Steudle and Henzler, 1995).

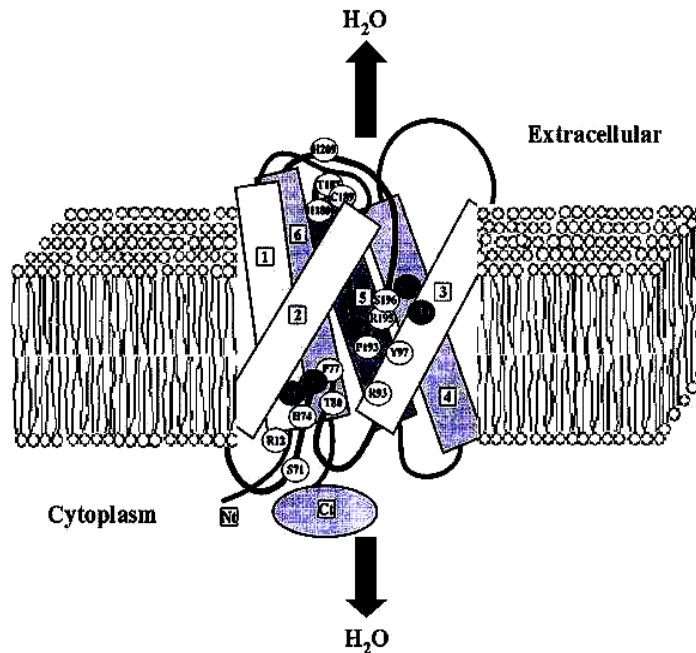


Fig. 3 Structure of an aquaporin (water channel of AQP1 adapted from Heymann et al., 1998). 75% to 95% of the water permeability (hydraulic conductivity) of plant cell membranes due to the existence of aquaporins. There are six main transmembrane helical rods and two short ones (the latter not marked as such) which form the channel in the center of the protein. Four of the functional subunits such as that shown in the figure are arranged in the membrane as a stable tetramer.

Aquaporins are highly selective membrane-spanning pores that facilitate the rapid, passive exchange of water across membrane (Walz et al., 1997; Johansson et al., 2000). Water flow through cells has been observed to be with direction, with the flow probably due to distinct types of water channels at either pole of the cell (Maurel, 1997), that is to say, one type represents a distinct group within the ubiquitous membrane intrinsic protein family. Direct correlations between membrane water permeability and expression of aquaporin mRNA have been shown (Steudle and Henzler, 1995; Henzler et al., 1999; Javot et al., 2003). Usually, water transport across water channels is a bulk flow driven by either osmotic or hydrostatic forces. It is not diffusional in nature. It is possible to inhibit water channel activity by chemical reagents such as mercurials

(HgCl₂), which bind to SH-groups of cysteine residues and change the conformation of AQPs. Other heavy metals have been used as well (Javot and Maurel, 2002). Wang et al. (2003) used a pressure-flux approach to measure the effect of drought stress on the water transport across roots of tomato in the field. In these experiments, HgCl₂ served as an inhibitor of aquaporins. The results indicated that aquaporins was in drought stressed roots and mediated water transport. A pressure-flux approach was used to evaluate the effects of HgCl₂ on water transport in tomato roots. Addition of HgCl₂ to a root-bathing solution caused a large and rapid reduction in pressure-induced root water flux, and root system hydraulic conductivity was reduced by 57% (Maggio and Joly, 1995). Mercury-sensitive processes in aspen roots play a significant role in regulating plant water balance by their effects on root hydraulic conductivity (Wan and Zwiazek, 1999).

The diurnal variation in root hydraulic conductivity mentioned above was found to be closely correlated with aquaporin gene expression (Clarkson et al., 2000). A link has been established between rapid changes in root Lp (hydraulic conductivity) and the expression and function of aquaporins. The activity of aquaporins may provide a tight coupling between root uptake and water physiology of whole plant (Javot et al., 2002). However, the possible functional redundancy of close aquaporin homologues may limit the detection of phenotypes. Accurate biophysical measurements are badly required to reveal the function of single aquaporins during water uptake both at the cell and root level. The study of aquaporins provides a solid molecular basis to physiological and biophysical investigations of root water transport. An integrative knowledge of cell-specific expression, localization and functioning of root aquaporins is still lacking (Javot et al., 2002). This should be done both at transcript and at the protein level, such as by comparing constitutively expressed and inducible aquaporins. Nevertheless, a better understanding of the roles of aquaporins in water uptake can be expected in the near future.

Regulation of water transport in roots

Fast and reversible regulation of trans-membrane water transport relates to the activity of aquaporins. In plant roots, water channel activity may be controlled by metabolism (Johansson, 2000). It may be triggered or even gated by environmental factors (Steudle and Henzler, 1995). The growth-inducing signals of light and the hormones abscisic acid and gibberellic acid affect aquaporins and putative aquaporin genes in *Arabidopsis* (Kaldenhoff et al., 1993). Thus, water channels may be looked at as a tool to provide some 'fine regulation' of water uptake in tissues, when the apoplastic path cannot be used in the absence of transpiration or when roots are heavily suberized (Steudle and Peterson, 1998; Steudle, 2000). Regulation along the cell-to-cell path may be affected by external factors such as drought, high salinity, nutrient deprivation and temperature (Carvajal et al., 1996; Henzler et al., 1999; Steudle, 2000). With regard to the possible upstream signal transduction pathways responsible for regulating the opening and closing of aquaporins it is probable that specific membrane proteins monitor the water potential difference across the membrane, and either directly interact and regulate aquaporins (by phosphorylation and dephosphorylation) or regulate aquaporins indirectly, such as by regulating protein kinases and phosphatases, or gating by a cohesion/tension mechanism (Johansson et al., 2000; Ye et al., 2004). In cortical cells of corn, high rates of water flow across aquaporins caused a reversible deformation of channel protein and a closure of channels. The intensity of water flow affected the extent of deformation and the time required for a relaxation back to the native (ground) state (Wan et al., 2004). The effect was independent of the direction of the change of turgor which induced the water flow. It has been interpreted as an effect of the kinetic energy injected into the pores which was largely transmitted to the aquaporin (Wan et al., 2004). Despite this progress, the molecular mechanisms that link hormone action, or stress stimuli of different kind to the activity of aquaporins in root cell membranes are still poorly understood.

Fine regulation of the water balance may also include alternatives such as osmotic adjustment, photosynthesis, respiration, and changes of key gene expression. However,

these mechanisms do not necessarily imply a regulation of water balance at the level of cell hydraulic conductivity.

Coarse regulation may co-exist with fine regulation. While coarse regulation is physical in nature, and strongly depends on root structure, water channel activity is under metabolic control as well. When regulated by physical means, water channel activity may be rapidly adjusted in response to adverse conditions. This would tend to avoid tissue dehydration, while maintaining tissue water potential as high as possible, or by tolerating low tissue water potential. Plant water status and uptake are associated with a lot of adaptive traits. These coarse regulations mainly involve minimizing water loss and maximizing water uptake. Water loss is minimized by closing stomata or stomatal limitation, by reducing light absorbance through rolled leaves (Ehleringer and Cooper, 1992), a dense trichome layer increasing reflectance (Larcher, 2000), or by other means. Water uptake, on the other hand, is maximized by adjusting the allocation pattern, namely increasing investment in the roots, enhancing root depth or extending root system distribution.

In order to keep water in balance, plants can regulate water transport in roots or shoots by sensing the water status in plant or in soil (Yang et al., 2001). Thus, root/shoot communication is being increasingly studied at the molecular level. The return of root pressure after water stress was associated with the complete recovery of leaf diffusive conductance, leaf-specific photosynthetic rate, and soil-leaf hydraulic conductance (Stiller et al., 2003). Altering speed of changes of water status (potential) in plant or soil may result in totally different responses in terms of a regulation or adaptation to stress. The time is an important factor in shaping plant responses according to genotype and environment. Root-to-shoot signaling requires that chemical or physical (hydraulic) signals travel through the plant in response to stresses sensed in roots. The nature of the primary mediators of cellular process—water status, turgor, ratio of bound and free water, hormones, alteration in cell membranes and others—are still under debate (Chaves et al., 2003). After the first stress reorganization events, cell to organ responses diverge in different pathways, such as during the involvement of ABA (ABA-dependent and ABA-independent pathways) (Zhu, 2002). ABA is a major regulator of plant water

balance. It acts as a stress hormone involved in the adaptation to various environmental conditions (Gazzarrini and McCourt, 2001). ABA affects the hydraulic conductivity of roots and cells, that is, ABA facilitates water uptake by roots and the cell-to-cell component of transport of water across the root cylinder when soil starts drying, especially under non-transpiration conditions, when the apoplastic path of water transport is largely excluded (Hose et al., 2000). There is a considerable overlap between abiotic stress signaling pathways with specificity to water conditions in or outside of plants present. For example, this occurs at the level of initial stress perception (Knight and Knight, 2001). Signaling pathways may contribute to a complex network, interconnected at many different levels. A revived interest in hydraulic components of signaling is apparent. However, little is still known as to how chemical and hydraulic signals are integrated into the overall regulation of plant water.

Composite transport model of root: physical model of water uptake

The composite transport model mentioned above (Fig. 2) explains the variable uptake of water by roots and the response of root hydraulics to different factors. In the model, the cohesion-tension mechanism of ascent of sap plays an important role (Steudle, 2001). It is based on detailed measurement of root hydraulics both at the level of excised roots (root hydraulic conductivity, L_{pr}) and root cells (membrane level, cell L_p) using pressure probes and other techniques (Azaizeh et al., 1992; Melchior and Steudle, 1993). The composite transport model integrates apoplastic and cellular components of radial water flow across the root cylinder. It well explains why the hydraulic conductivity of roots changes in response to the nature and intensity of water flow (Steudle, 2000). In fact, the composite transport model is based on the composite structure of root. The variability of root hydraulic properties in terms of changes in forces is used which cause a switching between the pathways. The model tends to optimize the water balance by adjusting root hydraulics according to the demand from the shoot. Thus, the composite transport model provides some kind of an integration of views to explain the variability of water uptake.

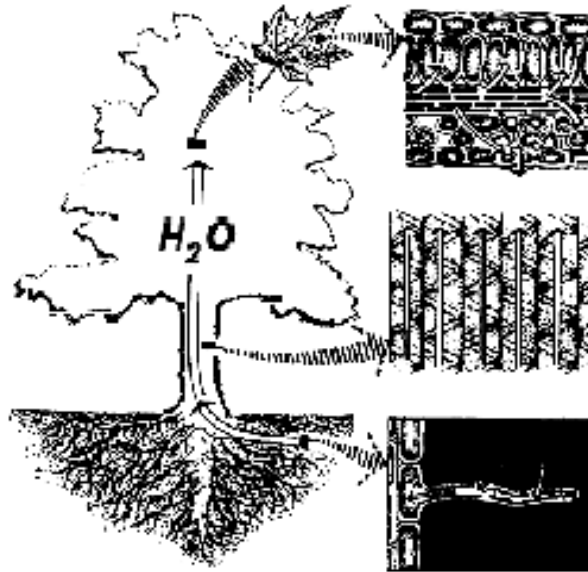


Fig. 4 Soil-Plant-Air-Continuum (SPAC). Water is transferred from the soil through the plant to the atmosphere. The force driving the water across the SPAC is the gradient in water potential which is in the direction from soil towards the atmosphere.

The basic assumption is that the force driving water from the soil through the plant to the atmosphere (Fig. 4) is the gradient in the energy level of the water along this pathway. In the soil, this level is expressed by the water potential of the soil around the root. The vapor pressure of the air is a measure of the level of free energy of water in the atmosphere which is almost always lower than that of the water in the soil. Hence, the driving force is in the direction from soil towards the atmosphere. The pathway from the soil up to the evaporating surfaces in the leaves is assumed to consist of a continuum of liquid water where the strong cohesive forces between water molecules provide a strong chain that can sustain the strong driving forces (tensions). Therefore, Philip (1966) proposed a more integrated physical model of the Soil Plant Atmosphere Continuum (SPAC). The concept of SPAC resulted in the introduction of mathematical models of water uptake by root systems. SPAC involves some aspects of water movement in the soil such as unsaturated hydraulic conductivity and water diffusivity as well as water uptake by plant roots, water movement in plant roots as described by hydraulic resistances and capacities (Shao and Huang, 2000). The water transport rate

(J_v) can be calculated from the follow equation: $J_v = L_p \cdot (\Delta\psi_w)$, Where J_v is the volume flow of water across the membrane per unit area of membrane and per unit time ($m^3 \cdot m^{-2} \cdot s^{-1}$). Water movement through the root system is a very important component of the SPAC. Dynamic hydraulic properties of roots differ between species and between different parts of the same roots (depending on age). To some extent, mathematical models can be used to account for a quantitative description of water uptake by roots. Such models of water uptake by roots can be looked at as a basis of agricultural moisture management of dryland farming used to optimize irrigation systems. However, in the future, present physical models need to be extended to incorporate detailed plant anatomy (such as apoplastic barriers), root biochemistry and the gating of water channels.

Conclusions

A higher WUE at a given water uptake is a desirable trait for plants. Improving the water use efficiency (WUE) of plants has been always an important goal during plant breeding and for cultivation practices. The effective use of precipitation and optimization of WUE are critical for promoting crop productivity of dry land farming systems (Shan, 1998; Shan and Chen, 1998; Shan, 2002). The focus should be on whole-plant processes that enhance or maintain water uptake by roots, increase the plant's capacity to retain water in a desiccating environment, or maintain a positive carbon balance during prolonged periods of water shortage. Avoidance of severe water deficit requires coordination at the whole level between the control of water loss from transpiring shoots and water absorption through root systems. Thus, it is important to understand the regulation of water transport in plants and the basic mechanisms of water uptake by roots. Only in this way it is possible to combine the present knowledge of plant adaptation and water use with available technology to control the efficient use of limited water resources. So far, relatively little is known about the processes that govern or even regulate root water uptake. From transport and anatomical studies it is clear that the composite structure of roots and the distribution conditions of roots play a key role during the regulation of water uptake by roots. With new regulatory mechanisms to be

discovered in plants, the water transport properties of membranes now appear as a new and important focus in modern plant physiology and agronomy.

During variable periods of water supply, roots are optimized in their abilities to use water resources in the soil. Future work should concentrate on a more detailed mapping of hydraulic resistance in the root cylinder and how this would change in response to water and other stresses. There are only a few alternatives to the composite transport model to explain the finding of variable root water uptake (Fiscus, 1975; Wheatherley, 1982; Boyer, 1995), which is crucial for our understanding of overall plant water relations. Although a link has been established between root hydraulics and expression and function of aquaporins, the knowledge of cell-specific expression, specified location and function of root aquaporins is largely lacking, mainly due to the high diversity of aquaporin isoforms in plants. In the future, analysis of single knock-out aquaporin mutants will hopefully provide evidence for the multiple functions of aquaporins in the growth and development of plants and in their adaptive response to stresses. Further investigations are necessary to determine the molecular structure of the water pores and the mechanisms of its selectivity and gating. There are, to date, no novel approaches to estimate the relative contribution of the three water transport pathways to the overall uptake on hydraulic conductivity of roots. With respect to water stress signaling, we are still far from having a clear picture. Models of water uptake by root systems are still only semi-quantitative and require completion. In order to set up good quantitative (physical) models, we must combine mathematical principles and computer technology with biological principles, including some biophysics and biochemistry. Studies of root physiology and of key genes that regulate water transport, should complement traditional studies of shoot physiology and stomatal control of water loss, are fundamental for the understanding of plant water balance.

Many researchers have contributed a large amount of valid work in the mechanisms of water uptake by roots. Yet there are still a lot of aspects, which need perfection and improvement. Intense research is underway in different labs to clarify mechanisms. Therefore, the future promises to see a much clearer picture of the basic mechanisms for water uptake by plant roots.

Acknowledgements

We thank Mrs. Libuse Badewitz, University of Bayreuth, Germany, for preparing some of the drawings for the manuscript.

References

- Azaizeh H, Gunse B, Steudle E. 1992. Effects of NaCl and CaCl₂ on water transport across root cells of maize (*Zea mays* L.) seedlings. *Plant Physiology*, **99**: 886-894.
- Boyer J S. 1995. Measuring the Water Status of Plants and Soils. Academic Press: San Diego.
- Canadell J, Jackson, R B, Ehleringer J R. 1996. Maximum rooting depth of vegetation types at global scale. *Oecologia*, **108**: 583-595.
- Carvajal M, Cooke D T, Clarkson D T. 1996. Responses of wheat plants to nutrition deprivation may involve the regulation of water-channel function. *Planta*, **199**: 372-381.
- Chaves M M, Maroco J, Pereira J S. 2003. Understanding plant responses to drought — from genes to the whole plant. *Functional Plant Biology*, **30**: 239-264.
- Chrispeels M J, Maurel C. 1994. Aquaporins: the molecular basis of facilitated water movement through living plant cells. *Plant Physiology*, **105**: 9-15.
- Counor D J, Sadras V O. 1992. Physiology of yield expression in sunflower. *Field Crops Research*, **30**: 383-389.
- Clarkson D T, Carvajal M, Henzler T, Waterhouse R N, Smith A J, Cooke D T, Steudle E. 2000. Root hydraulic conductance: diurnal aquaporin expression and the effects of nutrient stress. *Journal of Experimental Botany*, **51**: 61-70.
- Deng X-P, Shan L, Kang S-Z, Inanaga S, Mohammed E K. 2003. Improvement of wheat water use efficiency in semiarid area of China. *Agricultural Science in China*, **2**: 35-44.

- Ehleringer J R, Cooper T A. 1992. On the role of orientation in reducing photoinhibitory damage in photosynthetic-twig desert shrubs. *Plant Cell and Environment*, **15**: 301-306.
- Fiscus E L. 1975. The interaction between osmotic- and pressure-induced water flow in plant roots. *Plant Physiology*, **55**: 917-922.
- Frensch J, Hsiao T C, Steudle E (1996) Water and solute transport along developing maize roots. *Planta*, **198**: 348-355.
- Gazzarrini S, McCourt P. 2001. Genetic interactions between ABA, ethylene and sugar signaling pathways. *Current Opinion of Plant Biology*, **4**: 387-391.
- Henzler T, Waterhouse R N, Smyth A J, Carvajal M, Cooke D T, Schaffner A R, Steudle E, Clarkson D T. 1999. Diurnal variations in hydraulic conductivity and root pressure can be correlated with the expression of putative aquaporins in root in *Lotus japonicus*. *Planta*, **210**: 50-60.
- Heymann J B, Agre P, Engel A. Progress on the structure and function of aquaporin 1. *Journal of Structural Biology*, 1998, **121**: 191-206.
- Holbrook N M, Zwieniecki M A. 1999. Embolism repair and xylem tension: do we need a miracle? *Plant Physiology*, **120**: 7-10.
- Hose E, Steudle E, Hartung W. 2000. Abscisic acid and hydraulic conductivity of maize roots: a study using cell- and root-pressure probes. *Planta*, **211**: 874-882.
- Hose, E, Clarkson D T, Steudle E, Schreiber L, Hartung W. 2001. The exodermis: a variable apoplastic barrier. *Journal of Experimental Botany*, **52**: 2245-2264.
- Jackson R B, Canadell J, Ehleringer J R, Mooney H A, Sala O E, Schulze E D. 1996. A global analysis of root distributions for terrestrial biomes. *Oecologia*, **108**: 389-411.
- Javot H, Maurel C. 2002. The role of aquaporins in root water uptake. *Annals of Botany*, **90**: 301-312.
- Javot H, Lauvergeat V, Santoni V, Laurent M, Güçlü J, Vinh J, Heyes J, Franck K I, Schäffner A R, Bouchez D, Maurel C. 2003. Role of a single aquaporin isoform in root water uptake. *Plant Cell*, **15**: 509-522.
- Johansson I, Karlsson M, Johanson U. 2000. The role of aquaporins in cellular and whole plant water balance. *Biochim et Biophys Acta*, **1465**: 324-342.

- Kaldenhoff R, Kolling A, Richter G. 1993. A novel blue light- and abscisic acid-inducible gene of *Arabidopsis thaliana* encoding an intrinsic membrane protein. *Plant Molecular Biology*, **23**: 1187-1198.
- Knight H, Knight M. 2001. Abiotic stress signaling pathways: specificity and cross-talk. *Trends Plant Science*, **6**: 262-267.
- Kramer P J, Boyer J S. 1995. Water relations of plants and soils. Academic Press, Orlando.
- Larcher W. 2000. Temperature stress and survival ability of Mediterranean sclerophyllous plants. *Plant Biosystem*, **134**: 279-295.
- Liedgens M, Richer W. 2001. Minirhizotron observations of the spatial distribution of the Maize root system. *Agronomy Journal*, **93**: 1097-1104.
- Liu W-G, Deng X-P, Shan L. 2001. Responses of plant to soil compaction. *Plant Physiol Communication*, **37**: 254-259.
- Liu W-G, Shan L, Deng X-P. 2002. Water transport in maize root system in the process of ascending and descending pressure. *Journal of Hydraulic Engineering*, **8**: 118-120.
- Maggio A, Joly R J. 1995. Effects of mercuric chloride on the hydraulic conductivity of tomato root systems (evidence for a channel-mediated water pathway). *Plant Physiology*, **109**: 331-335.
- Maurel C. 1997. Aquaporins and water permeability of plant membranes. *Annual Review of Plant Physiology and Plant Molecular Biology*, **49**: 199-222.
- Maurel C, Chrispeels M J. 2001. Aquaporins: a molecular entry into plant water relations. *Plant Physiology*, **125**: 135-138.
- Maurel C, Javot H, Lauvergeat V. 2002. Molecular physiology of aquaporins in plants. *International Review Cytol*, **215**: 105-118.
- Melchior W, Steudle, E. 1993. Water transport in onion (*Allium cepa* L.) roots. Changes of axial and radial hydraulic conductivities during root development. *Plant Physiology*, **101**: 1305-1315.
- Miyamoto N, Steudle E, Hirasawa T, Lafitte R. 2001. Hydraulic conductivity of rice roots. *Journal of Experimental Botany*, **52**: 1835-1846.

- Murata K, Mitsuoka K, Hirai T, Walz T, Agre P, Heymann J B, Engel A, Fujiyoshi Y. 2000. Structural determinants of water permeation through aquaporin-1. *Nature*, **407**: 599-605.
- North G B, Nobel P S. 1996. Radial hydraulic conductivity of individual root tissues of *Opuntia ficus-indica* (L.) Miller as soil moisture varies. *Annals of Botany*, **77**: 133-142.
- Peterson C A, Murrmann M, Steudle E. 1993. Location of major barriers to water and ion movement in young roots of *Zea mays* L. *Planta*, **190**: 127-136.
- Peyrano G, Taleisnik E, Quiroga M, de Forchetti S M, Tigier H. 1997. Salinity effects on hydraulic conductance, lignin content and peroxidase activity in tomato roots. *Plant Physiology Biochemistry*, **35**: 387-393.
- Philip J R. 1966. Plant water relations: some physical aspects. *Annual Review of Plant Physiology*, **17**: 245-268.
- Preston G M, Carroll T P, Guillemot J C, Agre P. 1992. Appearance of water channels in *Xenopus* oocytes expressing red cell CHIP28 protein. *Science*, **256**: 385-387.
- Ranathunge K, Steudle E, Lafitee R. 2003. Control of water uptake by rice (*Oryza sativa* L.): role of the outer part of the root. *Planta*, **217**: 193-205.
- Schultz S G. 2001. Epithelial water absorption: osmosis or cotransport? *Proceedings of the National Academy of Sciences USA*, **98**: 3628-3630.
- Shan L, Chen P-Y. 1998. Eco-physiological bases of dryland farming. Beijing: Chinese Academic Press.
- Shan L. 1998. Research and practice of water-saving agriculture. *Bulletin of the Chinese Academy of Science*, **112**: 42-49.
- Shan L. 2002. Developmental tendency of dryland farming technologies. *Agricultural Sciences in China*, **1**: 934-944.
- Shao M-A, Huang M-B. 2000. Soil-root system hydraulics. Xi'an: Shaanxi Academy Press. 131-155.
- Steudle E. 1989. Water flow in plants and its coupling to other processes: an overview. *Method of Enzymology*, **174**: 183-225.
- Steudle E. 1993. Pressure probe techniques: basic principles and application to studies of water and solute relations at the cell, tissue, and organ level. In: Water deficits: plant responses from cell to community. Oxford: BIOS sci, pp. 5-36.

- Steudle E. 1994. Water transport across roots. *Plant Soil*, **167**: 79-90.
- Steudle E, Henzler T. 1995. Water channels in plants: do basic concepts of water transport change? *Journal of Experimental Botany*, **46**: 1067-1076.
- Steudle E, Peterson C A. 1998. How does water get through roots? *Journal of Experimental Botany*, **49**: 775-788.
- Steudle E. 2000. Water uptake by plant root: a integration of views. *Plant Soil*, **226**: 45-45.
- Steudle E. 2001. The cohesion-tension mechanism and acquisition of water by plant roots. *Annual Review of Plant Physiology and Plant Molecular Biology*, **52**: 847-875.
- Stiller V, Lafitte H R, Sperry J S. 2003. Hydraulic properties of rice and the response of gas exchange to water stress. *Plant Physiology*, **132**: 1698-1706.
- Tester M, Leigh R A. 2001. Partitioning of nutrient transport process in roots. *Journal of Experimental Botany*, **52**: 445-457.
- Tyerman S D, Bohnert H J, Maurel C, Steudle E, Smith J A C. 1999. Plant aquaporins: their molecular biology, biophysics and significance for plant water relations. *Journal of Experimental Botany*, **50**: 1055-1071.
- Tyree M T. 1997. The cohesion-tension theory of sap ascent current controversies. *Journal of Experimental Botany*, **48**: 1753-1765.
- Tyree M T, Zimmermann M H. 2002. Xylem structure and the ascent of sap. 2nd edition. Springer-Verlag, Berlin.
- Van den Honert T H. 1948. Water transport in plants as a catenary process. *Discuss. Faraday Society*, **3**: 146-153.
- Walz T, Hirai T, Murata K. 1997. The three-dimensional structure of aquaporin-1. *Nature*, **387**: 624-627.
- Wan X, Zwiazek J J. 1999. Mercuric chloride effects on root water transport in aspen seedlings. *Plant Physiology*, **121**: 939-946.
- Wan X, Steudle E, Hartung W. 2004. Gating of water channels (aquaporins) in cortical cells of young corn roots by mechanical stimuli (pressure pulses): effects of ABA and of HgCl₂. *Journal of Experimental Botany*, **55**: 411-422.

- Wang S-Y, Deng X-P, Xue S, Xue S-L. 2003. Comparison research on water transportation of non-drought and drought-stressed tomato root systems. *Journal of Northwest Sci-Tech Univ of Agriculture and Forestry*, **31**: 105-108.
- Weatherley P E. 1982. Water uptake and flow into roots. In: Lange O L, Nobel P S, Osmond C B, Ziegler H. *Encyclopedia of Plant Physiology*, Vol 12B. Springer, Berlin Heidelberg New York, pp 79-109.
- Wei C, Steudle E, Tyree M T. 1999. Water ascent in plants: do ongoing controversies have a sound basis. *Trends Plant Science*, **4**: 372-375.
- Yang H-Q, Zhang L-Z, Li L-G, Li J. 2001. Perception of drought signal and the production and transport of stress messenger in plant. *Research of Soil and Water Conservation*, **8**: 72-76.
- Ye Q, Wiera B, Steudle E. 2004. A cohesion/tension mechanism explains the gating of water channels in *Chara* internodes by high concentration. *Journal of Experimental Botany*, **55**: 449-461.
- Zeidel M L, Ambudkar S V, Smith B L, Agre P. 1992. Reconstitution of functional water channels in liposomes containing purified red cell CHIP28 protein. *Biochemistry*, **31**: 7436-7440.
- Zhang A-L, Miao G-Y, Wang J-P. 1997. Crop root systems and soil water. *Crop Research*, **2**: 4-6.
- Zhang S-Q, Shan L, Deng X-P. 2002. Change of water use efficiency and its relation with root system growth in wheat evolution. *Chinese Science Bulletin*, **47**: 1879-1883.
- Zhu J K. 2002. Salt and drought stress signal transduction in plants. *Annual Review of Plant Biology*, **53**: 247-273.
- Zhu W-Q, Wu L-H, Tao Q-N. 2002. Advances in the studies on crop root against drought stress. *Soil and Environmental Science*, **11**: 430-433.
- Zimmermann H M, Steudle E. 1998. Apoplastic transport across young maize root: effect of the exodermis. *Planta*, **206**: 7-19.

8 Summary

The dissertation focuses on studies of the gating of water channel activity (aquaporin; AQP) in plants by different stresses. Pressure probe techniques have been employed to study water and solute flows across cell membranes (internodes of giant green alga *Chara* and of cortical cells of corn root) and across an entire organ (roots of young corn seedlings). Based on detailed information on the function of AQPs, two new gating mechanisms of AQPs have been proposed. One is the ‘cohesion/tension (C/T) mechanism’ for the gating of AQPs, which is used to interpret the effect of high concentration on cell hydraulic conductivity (L_p) during osmotic stress. The other one is the ‘oxidative gating mechanism’ of AQPs in the presence of hydroxyl radicals (*OH) or of hydrogen peroxide (H_2O_2).

Gating of AQPs by osmotic stress

Evidence for an osmotic gating of AQPs was provided from measurements of effects of high concentration on cell L_p in *Chara* internodes. The osmotic dehydration is thought to be caused by the fact that the exclusion of solutes from AQPs creates tensions (negative pressures) within the water channel pores, when the osmolyte is present on both sides of the membrane (as in the experiments). This should have affected the open/closed state by changing the free energy between states favouring a reversible distorted/collapsed state rather than the open. The contribution of different states should be governed by a Boltzmann distribution as already indicated in results with ion channels by Zimmerberg & Parsegian (1986). These authors studied the reversible closure of ion channels in the presence of fairly big osmolytes (MW: 20,000 to 500,000 Da), and deduced volumes of the pores from these studies. Inhibition of water channel activity in *Chara* was affected by much smaller osmolytes (MW: 58 to 178 Da), but required much higher concentrations. As expected from the C/T model, effects increased with increasing size of osmolytes besides the concentration. The bigger the reflection coefficient (σ_s) of the solute, the lower was the concentration required to induce a reversible closure of AQPs. As cell L_p decreased, solute permeability coefficients (P_s) increased and reflection coefficients decreased. This indicated that

water and solutes used different passages across cell membrane, i.e., water mainly used AQPs, while solutes were largely diffusing through the bilayer.

The C/T model of osmotic dehydration of AQPs predicted that cell L_p should decrease exponentially with increasing the osmolyte concentration as found. According to the theory of Zimmerberg & Parsegian (1986), pore volumes of AQPs (V_c) in the plasma membrane of *Chara* internodes were estimated from ‘dehydration curves’. The analysis of osmotic responses showed that there were narrow pores with a volume of $2.3 \pm 0.2 \text{ nm}^3$, which could be closed in the presence of the small solute acetone, and bigger ones with a volume of between 5.5 ± 0.8 and $6.1 \pm 0.8 \text{ nm}^3$. The latter could not be affected by the small solute, even when presented at very high concentrations. The existence of different types of pores was also evident from differences in the residual L_p obtained at high concentrations. The residual cell L_p decreased with increasing size of osmolytes.

Alternatively, pore volumes were estimated from ratios between osmotic ($P_f = L_p \cdot RT / \bar{V}_w$) and diffusional (P_d) water flow as derived from measurements of hydraulic and isotopic water flows. According to Levitt’s theory (1974), which is based on Einstein’s (1905) theory of diffusion in liquids, P_f/P_d should represent the number of water molecules (N) in a single-file pore transporting water. Values of N ranged between 35 and 60, which referred to volumes of 0.51 and 0.88 nm^3/pore . This value was substantially smaller than that obtained during osmotic dehydration (see above), but bigger than values from literature which range between $N = 3$ to 7 (Niemietz & Tyerman 1997) and $N = 27$ to 31 (Henzler & Steudle 1995; Hertel & Steudle 1997). The difference may be due to an underestimation caused by unstirred layers, which would affect P_d rather than P_f (L_p). These effects have therefore been examined (see below) showing that, in *Chara*, unstirred layers may underestimate P_d by up to 25 %, and have virtually no effect on cell L_p (P_f). Hence, it was concluded that most of the pore volumes determined by either method was real. This may be due to (i) the fact that water channels in *Chara* are somewhat wider than just the diameter of a water molecule, and/or (ii) that mouth parts of channels contributed to the overall pore volume, when using the dehydration technique.

Gating of AQPs by oxidative stress

Evidence for a new type of ‘oxidative gating’ of AQPs was derived from experiments with *Chara* internodes, which was then tested for higher plant tissue cells as well (root cortical cells of corn). *Chara* internodes tolerated H₂O₂ in the medium of up to 350 mM for up to 2 hours without obvious damages. However, in the presence of millimolar concentrations Fe²⁺ in the medium, only a fraction of one mM of H₂O₂ could be tolerated, and there were substantial, reversible reductions of cell Lp under these conditions. Changes have been referred to the presence of hydroxyl radicals (*OH) as produced during the Fenton reaction ($\text{Fe}^{2+} + \text{H}_2\text{O}_2 = \text{Fe}^{3+} + \text{OH}^- + *\text{OH}$). Compared to conventional agents used to inhibit AQP activity such as mercuric chloride (HgCl₂), *OH proved to be more effective in blocking water channels, and was less toxic to the cell.

In experiments with young corn roots, in the presence of hydrogen peroxide (H₂O₂), half times of water flows increased at the level of both entire roots and individual cortical cells by factors of 3 and 9, respectively, i.e., hydraulic conductivity decreased by the same factors. The effect was referred to reversible inhibition on AQP activity suggesting an oxidative gating mechanism similar to that found for *Chara*. There may be a common interaction between the redox state (oxidative stress) and water relations (water stress) in plants.

Anomalous (negative) osmosis

For solutes rapidly permeating through cell membranes, closure of water channel resulted in anomalous osmosis (negative reflection coefficients), i.e., in the striking situation that a cell did not shrink but swelled in a hypertonic medium. For the first time, anomalous osmosis has been demonstrated in roots as well, i.e., for an entire organ and in the presence of a rather complicated osmotic barrier. The phenomenon has been interpreted in terms of the composite transport structure of both the cell membrane and the root. In the presence of a rapidly permeating solute like acetone, channel closure resulted in a situation that the solute moved faster than the water, and the reflection coefficient (σ_s) reversed its sign. Upon water channel closure, the permeability coefficients (P_s) of lipophilic solutes were also reduced indicating that AQPs are not

ideally selective for water. AQPs should allow small organic lipophilic solutes to pass through in addition to the water.

The plant stress hormone ABA had no ameliorative effect during the ‘oxidative gating’ of AQPs to re-open the closed channels as found earlier in the lab with other stresses like mechanical stimuli or low temperature (Wan *et al.* 2004; Lee *et al.* 2005b). This may be due to reason that the chemical modification of AQPs in the presence of oxidative stress required a biochemical (reduction of oxidized AQPs) rather than just a physical action (change of activation energy of transition between conformational states) to re-open closed channels.

Unstirred layers

When measuring the permeation of water and solutes, there are inevitable errors due to unstirred layers (USLs) caused by the fact that concentrations right at the membrane surface change. There are two types of USLs, one is called ‘sweep-away effect’, which refers to the action of a net water flow; the other type is termed ‘gradient-dissipation effect’ referring to relative rates of diffusion of solutes across membranes and its supply from the bulk solution. As a consequence, transport parameters such as the hydraulic conductivity (L_p), the permeability (P_s) and reflection (σ_s) coefficient are underestimated. During the experiments with giant cells of green algae *Chara corallina*, a quantitative re-examination indicated a minor role of USLs for the measurement of transport coefficients for water and solutes with the cell pressure probe. The results show that cell L_{ph} measured in hydrostatic pressure-relaxation experiments was not significantly affected by the ‘sweep-away effect’, even when peak sizes of pressure pulses ($\pm \Delta P$) were increased by one order of magnitude above normal. During pressure clamp at high $\pm \Delta P$, there was a reduction in L_{ph} by 20 %, which was reversible within 20 s. This may be explained by the constriction of water to aquaporins (AQPs) in the *Chara* membrane and a rapid diffusional equilibration of solutes in arrays where water protruded across AQPs. As the rate of stirring of the medium (flow rate, v_{med}) increased, the osmotic hydraulic conductivity L_{po} increased as well. Saturation of L_{po} occurred at $v_{med} = 0.20 - 0.30 \text{ m}\cdot\text{s}^{-1}$, when absolute values of L_{po} reached a values of close to L_{ph} , which has proven to be rather free of effects of USLs. Substantially smaller values of

v_{med} were required to saturate P_s and σ_s ($v_{\text{med}} \approx 0.10 \text{ m}\cdot\text{s}^{-1}$). There was no further increase of Lp_o , P_s and σ_s , when the vigorous external stirring was furthermore increased by flushing air bubbles through the system at high rates suggesting a maximum thickness of external USLs of around $30 \mu\text{m}$ including the cell wall. During osmotic experiments, the cell membrane of *Chara* internodes acts as a rate-limiting resistance allowing substantial time for an internal mixing of solutes by diffusion. Even for the most rapidly permeating solute acetone, USLs should have resulted in an underestimation of P_s and σ_s by $\leq 30 \%$. For the less permeating solute dimethylformamide (DMF), it reduced to 15% . Based on analytical solutions from diffusion kinetics and measured experimental results, upper limits of the ‘equivalent thicknesses’ of diffusive internal USLs were estimated to be 117 and $97 \mu\text{m}$ for a cylindrical cell lacking and containing a membrane, respectively (cell radius $R = 0.4 \text{ mm}$; test solute: acetone). For DMF, upper limits of the ‘equivalent thicknesses’ are estimated to be 108 and $95 \mu\text{m}$, respectively. It was concluded that the ‘real equivalent thicknesses’ of internal USLs was substantially smaller than the upper limits estimated. It is probably safe to assume thickness of internal USL of around $50 \mu\text{m}$ in the presence of rapidly permeating solutes.

9 Zusammenfassung

Die Dissertation befasst sich mit der Steuerung der Aktivität von Wasserkanälen in Pflanzen (Aquaporine; AQP). Druckmesssondentechniken wurden eingesetzt, um Wasser- und Teilchenflüsse durch Zellmembranen (Internodien der Armleuchteralge *Chara* und Zellen in der Wurzelrinde von Mais) und durch ganze Organe zu messen (Wurzeln von Mais-Keimlingen). Aufbauend auf detaillierten Informationen über die Funktion der AQPs, werden zwei neue Steuermechanismen von AQPs vorgeschlagen. Der eine ist der "Kohäsionsmechanismus" (C/T) für die Steuerung von AQPs, welcher die Abhängigkeit der hydraulischen Leitfähigkeit (L_p) von der Konzentration erklärt. Der andere ist der "oxidative Steuermechanismus" von AQPs in der Gegenwart von Hydroxylradikalen ($\cdot\text{OH}$) oder von Wasserstoffperoxid (H_2O_2).

Steuerung von AQPs durch osmotischen Stress

Evidenz für ein osmotisches "Gating" von AQPs ergab sich aus Messungen der Konzentrationsabhängigkeit der hydraulischen Leitfähigkeit (L_p) von *Chara*-Internodien. Nach dem C/T-Modell für die Steuerung der Aktivität der AQPs, entwickeln sich Spannungen (negative Drücke) innerhalb der Wasserkanäle, weil die hohe Osmolytkonzentration zu beiden Seiten der Membran das Wasser aus den Kanälen herauszieht. Dieses sollte einen Effekt auf den Offen oder Geschlossen-Zustand haben, indem sich die freie Energie zwischen beiden Zuständen ändert, was den Geschlossen-Zustand (kollabierte Kanäle) gegenüber dem Offen-Zustand bevorzugt. Der Beitrag der verschiedenen Zustände sollten sich nach Art einer Boltzmann-Verteilung ergeben, wie es bereits die Ergebnisse von Zimmerberg und Parsegian (1986) an Ionenkanälen zeigen. Diese Autoren untersuchten den reversiblen Verschluss von Ionenkanälen in Gegenwart von relativ großen Osmolyten (MW: 20,000 bis 500,000 Da) und berechneten Porenvolumina aus den Ergebnissen ihrer Untersuchungen. Bei *Chara* war die Inhibierung der Wasserkanalaktivität bereits durch wesentlich kleinere Osmolyte beeinflusst. Sie erforderte allerdings wesentlich höhere Konzentrationen. Wie nach dem C/T-Modell zu erwarten war, nahm die Inhibierung nicht nur mit zunehmender Konzentration sondern auch mit zunehmender Größe der eingesetzten Osmolyte in der erwarteten Weise zu, d.h. mit zunehmendem Reflexionskoeffizienten (σ_s) der

Substanzen. Je größer die Osmolyte waren, desto niedriger war die Konzentration, welche zu einem reversiblen Schließen der AQPs führte. In Gegenwart hoher Osmolytkonzentrationen nimmt die hydraulische Leitfähigkeit (L_p) ab, während der Permeabilitätskoeffizient (P_s) zunimmt. Das zeigt, dass Wasser und Teilchen die Zellmembran auf verschiedenen Wegen passieren; das Wasser nutzte hauptsächlich die AQPs, während Teilchen größtenteils durch die Lipiddoppelschicht diffundierten.

Das C/T-Modell der osmotischen Dehydratation der AQPs sagt voraus, dass die hydraulische Leitfähigkeit (L_p) mit steigender Konzentration der Osmotika im Medium exponentiell abnimmt, was auch experimentell gefunden wurde. Nach der Theorie von Zimmerberg und Parsegian (1986) wurden Porenvolumina der AQPs in der Plasmamembran von *Chara* aus den Dehydratationskurven bestimmt. Die Analyse der osmotischen Antworten ergab neben engen Poren mit einem Volumen von $2.3 \pm 0.2 \text{ nm}^3$ auch größere Poren mit Volumina zwischen 5.5 ± 0.8 and $6.1 \pm 0.8 \text{ nm}^3$. Selbst in Gegenwart hoher Osmolytkonzentrationen konnten großporige AQPs nicht durch kleine Osmotika geschlossen werden. Die Existenz verschiedener Porentypen zeigte sich auch in Unterschieden in den Restwerten von L_p bei hoher Konzentration: die Restwerte nahmen mit der Größe der eingesetzten Osmotika ab.

Alternativ zur osmotischen Dehydratation wurde das Porenvolumen auch über das Verhältnis zwischen dem osmotischem (P_f) und Diffusions-Wasserfluss (P_d) bestimmt. Nach der Levittschen (1974) Theorie, die auf Einstein's (1905) Theorie der Diffusion in Flüssigkeiten zurückgeht, repräsentiert P_f/P_d die Anzahl der Wassermoleküle (N) in einer Single-file-Pore, d.h. in einem AQP. Die Werte für N lagen zwischen 35 und 60, was einem Porenvolumen von 0.51 und $0.88 \text{ nm}^3/\text{Pore}$ entspricht. Dieser Wert war deutlich kleiner als der mithilfe der osmotischen Dehydratation bestimmte Wert (s. o.), aber immer noch größer als Literaturwerte, die zwischen $N = 3$ bis 7 (Niemitz & Tyerman, 1997) und $N = 27$ bis 31 liegen (Henzler & Steudle 1995; Hertel & Steudle 1997). Der Unterschied mag auf die Unterschätzung von P_d durch ungerührte Schichten zurückzuführen sein. Dieser Effekt wurde deshalb im Detail untersucht und auf bis zu 25 % bei P_d abgeschätzt. Da P_f (L_p) praktisch nicht durch USLs beeinflusst war, reicht dies nicht aus um die Unterschiede zu erklären. Die Gründe für die Unterschiede

könnten sein, dass (i) die Wasserkanäle in *Chara* etwas größer im Durchmesser sind als ein Wassermolekül, oder dass (ii) die Vorhöfe der eigentlichen Kanäle während der osmotischen Dehydratation zu den berechneten Gesamtvolumina beitragen oder beides.

Steuerung von AQPs durch oxidativen Stress

Die Experimente mit den Internodien von *Chara* ergaben Hinweise auf einen neue Typ eines Gating durch oxidativen Stress, der dann auch bei den Wuzelrindenzellen von Mais gefunden werden konnte. *Chara*-Internodien tolerierten H_2O_2 im Medium in Konzentrationen von bis zu 350 mM (2 Stunden) ohne messbare Schäden. Dagegen tolerierten die Zellen in Gegenwart millimolarer Konzentrationen von Fe^{2+} nur Bruchteile eines mM H_2O_2 . Sie reagierten mit drastischen Reduktionen der hydraulischen Leitfähigkeit unter diesen Bedingungen. Die Änderungen im L_p der Zellen wurden der Gegenwart von Hydroxyl-Radikalen (OH^*) zugeschrieben, die unter diesen Bedingungen entstehen (Fenton-Reaktion: $\text{Fe}^{2+} + \text{H}_2\text{O}_2 = \text{Fe}^{3+} + \text{OH}^- + \text{*OH}$). Das Zell- L_p wurde um einen Faktor von mehr als 10 reversibel reduziert. Verglichen mit konventionellen Mitteln wie HgCl_2 , erwies sich *OH als ein effektiverer Blocker der Wasserkanäle, der darüberhinaus weniger toxisch für die Zellen war. In Experimenten mit jungen Maiswurzeln nahmen die Halbwertszeiten des Wasserflusses in der Gegenwart von Wasserstoffperoxid (H_2O_2) auf dem Level einzelner Zellen der Wurzelrinde und der ganzen Wurzel um von Faktoren 9 bzw. 3 zu, d.h., die hydraulische Leitfähigkeit nahm um denselben Faktor ab. Die Ergebnisse zeigen ein oxidatives Gating ähnlich dem bei *Chara*. Sie lassen Interaktionen zwischen dem Redoxstatus (oxidativer Stress) und der Wasserverfügbarkeit (Wasserstress) vermuten.

Anomale (negative) Osmose

Für schnell durch die Zellmembranen permeierende Teilchen führte ein Schließen der Wasserkanäle zu anomaler Osmose (negativer Reflexionskoeffizient), d.h. zu der merkwürdigen Situation, dass eine Zelle in einem hypertonen Medium nicht schrumpft sondern anschwillt. In der vorliegenden Arbeit konnte die anomale Osmose auch in Wurzeln gezeigt werden, dass heißt für ein ganzes Organ und in Gegenwart einer ziemlich komplizierten osmotischen Barriere. Das Phänomen wird anhand der “zusammengesetzten” Struktur von Zellmembranen und Wurzeln erklärt (“composite transport”). In der Gegenwart eines schnell permeierenden Stoffes wie Aceton

verursacht das Schließen der Wasserkanäle eine Situation, in welcher die Teilchen schneller durch die Zellmembran (den Bilayer) wandern als das Wasser, und der Reflexionskoeffizient (σ_s) ändert sein Vorzeichen. Beim Schließen der Wasserkanäle wurde der Permeabilitätskoeffizient (P_s) von lipophilen, kleinen Teilchen darüberhinaus abgesenkt, was zeigt, dass die AQPs nicht ideal selektiv für Wasser sind. AQPs sollten auch für kleine organische Moleküle permeabel sein, wie dies von anderen Systemen her bereits bekannt ist.

Das Pflanzenstresshormon ABA hatte keinen positiven Effekt auf Status der AQPs nach oxidativem Stress, wie dies etwa mechanischem Stress oder bei Kältestress gefunden worden ist (Wan *et al.* 2004; Lee *et al.* 2005). Der Grund ist möglicherweise daran zu suchen, dass die chemische Modifizierung der AQPs bei oxidativem Stress eine biochemische (Reduktion von oxidierten AQPs) anstatt einer physikalischen Aktion (Änderung der Aktivierungsenergie des Übergangs zwischen zwei Konformationen) erfordert, um geschlossene Kanäle wieder zu öffnen.

Ungerührte Schichten

Wenn Wasser und darin gelöste Stoffe durch Membranen permeieren, sind Fehler durch ungerührte Schichten (Unstirred Layers; USLs) unvermeidlich, weil die Konzentrationen direkt an der Membran von denen in den freien Lösungen abweichen. Es gibt zwei verschiedene Typen von USLs. Der "Sweep-Away-Effekt" ist das Resultat eines Netto-Wasserflusses. Der "Gradient-Dissipation-Effekt" auf die relative Diffusionsrate eines gelösten Stoffes über eine Membran und dessen Nachlieferung aus der Lösung Lösung zurückzuführen. Als Folge von USLs werden für die Transportparameter wie die hydraulische Leitfähigkeit (L_p), die Permeabilität (P_s) und den Reflexionskoeffizienten (σ_s) zu geringe Werte ermittelt. Bei der Untersuchung von Internodialzellen von *Chara* mit Hilfe der Zelldruckmesssonde konnte durch eine quantitative Überprüfung eine relativ geringe Rolle der USLs auf die Transportkoeffizienten nachgewiesen werden. Die osmotische hydraulische Leitfähigkeit L_{p_0} erhöht sich mit steigender Geschwindigkeit, mit der das Medium an den Zellen vorbeigeführt wird (v_{med}). L_{p_0} wird bei $v_{med} = 0.20 - 0.30 \text{ m}\cdot\text{s}^{-1}$ gesättigt und erreicht fast den Wert für L_{p_h} , welches mit Hilfe von hydrostatischen Druck-Impulsen

(monophasische Druckrelaxationen) bestimmt wird und sich als unabhängig von USLs zeigt. In den osmotischen Experimenten erweist sich die Zellmembran der *Chara*-Internodien als limitierender Widerstand, welcher die notwendige Zeit für ein Mischen der gelösten Salze innerhalb der Zelle liefert. Sogar für sehr schnell permeierende Stoffe wie schweres Wasser (HDO) oder Aceton sollten P_s und σ_s um lediglich 25 ~ 30 % unterschätzt werden. Auf Grund der Diffusions-Kinetik-Theorie wurde die Dicke der diffusiven inneren USLs für eine zylindrische Zelle mit einem Radius $R = 0.4$ mm mit 120 μm abgeschätzt werden. Die wirkliche Dicken der inneren USLs wesentlich kleiner als die angenommenen 120 μm sein sollten; bei intensiver Rührung dürfte die Dicke der äußeren USL dürfte nicht größer als 30 μm und die der inneren nicht größer als 50 μm sein.

10 Erklärung

Hiermit erkläre ich, dass ich die Arbeit selbständig verfasst und keine anderen als die von mir angegebenen Quellen und Hilfsmittel benutzt habe.

Ferner erkläre ich, dass ich anderweitig mit oder ohne Erfolg nicht versucht habe, diese Dissertation einzureichen. Ich habe keine gleichartige Doktorprüfung an einer anderen Hochschule endgültig nicht bestanden.

Bayreuth, den 16. November 2005

(Qing Ye)